AN ABSTRACT OF THE DISSERTATION OF

Harold S. J. Zald for the degree of Doctor of Philosophy in Forest Science presented on March 9, 2010.

Title: Patterns of Tree Establishment and Vegetation Composition in Relation to Climate and Topography of a Subalpine Meadow Landscape, Jefferson Park, Oregon, USA.

Abstract approved:

Thomas A. Spies

The forest alpine tundra ecotone (FTE, also known as alpine treeline or subalpine parkland), is a conspicuous feature of mountain landscapes throughout the world. Climate change-driven increases in temperature are believed to result in FTE movement and tree invasion of subalpine meadows, which have been documented throughout the Northern Hemisphere across a wide range of geographic locations, climatic regimes, forest types, land use histories, and disturbance regimes. Climate-driven FTE movement may have numerous ecological effects such as: positive temperature feedbacks, increased net primary productivity and carbon storage, and declines of plant populations and species. The magnitude of these ecological effects is highly uncertain, but will be largely determined by the rates and spatial extent of FTE movement and meadow invasion. FTE movement and meadow invasion are often considered at global or regional spatial scales in relation to climate, yet they are fundamentally driven by tree regeneration processes that are influenced by a variety of climatic and biophysical factors at micro site, landscape, and regional scales. Much of the research on the FTE has not taken a landscape approach incorporating multi-scale processes. For example, species distribution models used to project climate change effects on future species distributions and plant biodiversity in mountainous landscapes rely on species distribution data that is often sparse and incomplete across FTE landscapes.

This dissertation attempts to overcome many of the limitations in FTE research by taking a landscape approach to develop a greater understanding of past spatiotemporal patterns of tree invasion, current spatial patterns of vegetation composition and structure, and potential future patterns of climate-driven tree invasion in the FTE. The setting for this research is Jefferson Park, a 260 ha subalpine parkland landscape in the Oregon High Cascades, USA.

This study uses field plots, remotely sensed imagery, airborne Light Detection and Ranging (LiDAR), and simulation modeling to: 1) predictively map current fine-scale species distributions, vegetation structure, and tree ages; 2) reconstruct patterns of tree invasion over the last fifty years in subalpine meadows in relation to climatic conditions, landforms, microtopography, and seed dispersal limitations; and 3) develop a statistical model that projects future patterns of tree invasion into subalpine meadows under different climate scenarios in Jefferson Park.

In chapter two, I generated fine-scale spatially-explicit predictions of current vegetation composition, structure, and tree ages in the Jefferson Park study area. Objectives of this chapter were threefold: 1) to characterize spatial patterns of tree ages, vegetation composition, and vegetation structure in a FTE landscape in the Oregon Cascades using predictive mapping; 2) determine how vegetation composition and structure were associated with gradients of environmental factors derived from multispectral satellite imagery and Light Detection and Ranging (LiDAR) data; and 3) determine if predictive mapping characterizations of tree age, vegetation composition, and vegetation structure were improved by the inclusion of LiDAR data. Predictive mapping of vegetation attributes was accomplished using gradient analysis with nearest neighbor imputation; integrating field plots, multispectral SPOT 5 satellite imagery, and LiDAR data. Vegetation composition was best described by SPOT 5 imagery and LiDAR-derived topography, while vegetation structure was best described by LiDAR-derived vegetation heights. Predictions of species occurrence were most accurate for tree species, moderate for shrub species and vegetation groups, and highly variable for graminoid species. Tree age, which was the most accurately predicted vegetation structure variable, indicates the study area was largely un-forested in 1600, gradually invaded by trees from 1600 to the 1920’s, and rapidly invaded from the 1920’s to 1980. Predictive mapping of vegetation structure variables such as basal area and stand density were subject to large amounts of error, possibly resulting from scale incompatibilities between vegetation patterns and plot size, and/or heterogeneous FTE landscapes where forest structure does not develop along consistent trajectories with stand age. This study suggests integrating multispectral satellite imagery, LiDAR data, and field plots can accurately predict fine-scale spatial characterizations of species distributions and tree invasion in the FTE. This study also indicates that sample design can influence spatial patterns of model uncertainty, which needs to be considered if predictive mapping of vegetation and sensitive ecosystems is a component of inventory and monitoring programs.

In chapter three, I focused on quantifying spatiotemporal patterns of subalpine parkland tree invasion in Jefferson Park over the past five decades in relation multi-scale climatic and biophysical controls. LiDAR data provided previously unavailable fine-scale spatial characterizations of microtopography and vegetation structure. I utilized LiDAR, geo-referenced field plots, and tree establishment reconstructions to quantify spatiotemporal patterns of tree invasion in relation to late season snow persistence, landform types, fine-scale topographic variability, distances from potential seed sources, and climate variation within 130 ha of the subalpine parkland landscape of Jefferson Park. Tree occurrence (i.e. tree presence in 2 m plots and grid cells) occurred in 7.75% of study area meadows in 1950 and increased to 34.7% in 2007. Landform types and finer-scale patterns of topography and vegetation structure influenced summer snow depth, which influenced temporal and spatial patterns of tree establishment. Tree invasion rates were higher on debris flow landforms, which had lower summer snow depth than glacial landforms, suggesting potentially rapid treeline responses to disturbance events. Tree invasion rates were strongly associated with reduced annual snow fall on glacial landforms, but not on debris flows. Tree establishment was spatially constrained to micro sites with high topographic positions and close proximity to overstory canopy, site conditions associated with low summer snow depth. Seed source limitations placed an additional species-specific spatial constraint on where trees invaded meadows. Climate and topography had an interactive effect, with trees establishing on higher topographic positions during both high snow/low temperature and low snow/high temperature periods, but had greater than expected establishment on lower topographic positions during low snow/high temperature periods. Within the context of larger landform types, topography and proximity to overstory trees constrained where trees established in the meadows, even during climate periods with higher temperatures and lower snowfall. Results of this study suggest large scale climate-driven models of vegetation change may overestimate treeline movement and meadow invasion, because they do not account for biophysical controls limiting tree establishment at multiple spatial scales.

In chapter four, I used field data and analyses from chapter 3 to parameterize a spatially and temporally explicit statistical model of fine-scale tree invasion within 130 ha of the Jefferson Park study area. The model incorporated both the climatic and biophysical controls found in chapter 3 to influence tree invasion. The model was used in two ways: (1) to spatially project patterns of tree invasion from 1950 to 2007 in response to historical climate; and (2) to project future tree invasion of the study area from 2007 to 2064 under six different

annual snowfall scenarios. Modeling addressed the following questions: (1) Can fine-scale (2 m pixel size) patterns of historical tree invasion be accurately predicted? (2) How sensitive is future tree invasion (and therefore meadow persistence) to different future snowfall scenarios? (3) Are non-climatic factors such as landforms and biotic interactions associated with different spatial patterns of tree invasion? From 1950 to 2007, simulated historical meadow area declined from 82% to 65% of the study area. Model outputs of historical area, spatial distributions, and spatial clustering of tree invasion generally agreed with independent validation, and suggest biotic interactions due to young tree establishment facilitation are important on glacial landforms but not debris flows. Simulations of future scenarios indicated meadow declined to 36 to 43% of the study area by 2064. Projected meadow area declined with reduced annual snow fall, but not under prolonged high and low snow fall periods. Meadows persisted under all future scenarios in 2064. This model suggests subalpine meadows may significantly decline under climate warming, but will still persist in 2064. Micro sites and recruitment limitation may be equally or more important factors than climate change in influencing subalpine landscape change, suggesting local high-elevation persistence of subalpine meadows under future climate warming.

Patterns of Tree Establishment and Vegetation Composition in Relation to Climate and Topography of a Subalpine Meadow Landscape, Jefferson Park, Oregon, USA

by

Harold S. J. Zald

A DISSERTATION

submitted to

Oregon State University

in partial fulfillment of
the requirements for the
degree of

Doctor of Philosophy

Presented March 9, 2010

Commencement June 2010

Doctor of Philosophy dissertation of Harold S. J. Zald presented on March 9, 2010.

APPROVED:

Major Professor, representing Forest Science

Head of the Department of Forest Ecosystems and Society

Dean of the Graduate School

I understand that my dissertation will become part of the permanent collection of Oregon State University libraries. My signature below authorizes release of my dissertation to any reader upon request.

Harold S. J. Zald, Author

ACKNOWLEDGEMENTS

Primary funding for this research was provided by the USDA Forest Service, Pacific Northwest Research Station, Forest Inventory and Analysis Program. Additional funding came from the USDA Forest Service, Pacific Northwest Research Station; the Leighton Ho Memorial Field Botany Award from the Oregon Native Plant Society; the Dorothy D. Hoener Memorial Fellowship from the College of Forestry, and the Richard and Doris Waring Forest Science Student Travel Award. Tuition support was provided by the Department of Forest Ecosystems and Society, Oregon State University. Access to the Jefferson Park study area was provided by the Willamette National Forest, Detroit Ranger District.

Many people made this research possible. Tom Spies, my major professor, provided positive criticism, enthusiasm, and support which enabled this project to succeed. I also thank Tom for providing a long enough rope for me to explore new research avenues and ideas, but not long enough to hang myself with. I thank my committee members, Andy Gray, Bruce McCune, Michael Wing, and Arthur Sleight. Andy deserves special thanks, in many ways serving as an unofficial co-major professor, and being instrumental in obtaining the primary funding support for this project. Andy and Demetrios Gatziolis of the USDA Forest Service procured and provided access to LiDAR data for the Jefferson Park study area, which improved my research immeasurably. Field work would not have been possible without Dan Irvine and Alex Gonsiewski, whose hard work and humor were greatly appreciated. Keith Olsen, Matt Gregory, Jonathan Thompson, and Robert Kennedy provided excellent advice regarding GIS and remote sensing. Emile Grossman and Nick Som deserve thanks for my indoctrination into the R computing language. Manuela Huso provided invaluable statistical advice, and Rob Pabst was always willing to be a sounding board for concepts and analytical approaches. Barb Lachenbruch, John Bailey, Fred Swanson, and Julia Jones graciously provided lab space and funding for tree-ring analysis equipment. For their advice, support, and friendship I am grateful to: Alan Tepley, Claire Philips, Steve Voelker, Matt Hurteau, Garrett Meigs, Chris Dunn, Rebecca Kennedy, Janet Ohmann, Lisa Ganio, and Barb Bond. I also wish to thank the College of Forestry Computing Helpdesk, and the excellent faculty, staff, and students of the College of Forestry and the Department of Forest Ecosystems and Society.

At one point in my life going to college, let alone completing a doctorate, would have invoked a good laugh or open jawed stare of disbelief. I thank my parents Joan and Mayer Zald for their many years of support to make this possible, even when their support was unwarranted. Last but not least I thank Erin Thompson. During the last four years Erin has provided constant support, encouragement, and tolerance. Most importantly, Erin has always reminded me of the excellent a life I have outside of “dissertation world”.

CONTRIBUTION OF AUTHORS

Harold Zald was primarily responsible for all aspects of this dissertation. Tom Spies assisted with the study design and writing of chapters 2-4. Demetrios Gatziolis and Andrew Gray provided airborne Light Detection and Ranging (LiDAR) data used in chapters 2-4. Emily Grossman provided computer code used in data analysis of chapter 2. Manuela Huso assisted with the study design and data analysis of chapter 3.

TABLE OF CONTENTS

LIST OF FIGURES

LIST OF FIGURES (CONTINUED)

LIST OF TABLES

LIST OF TABLES (CONTINUED)

Patterns of Tree Establishment and Vegetation Composition in Relation to Climate and Topography of a Subalpine Meadow Landscape, Jefferson Park, Oregon, USA

CHAPTER 1: INTRODUCTION

The boundary between forests and alpine/arctic vegetation (referred to as treeline, subalpine parklands, or the forest-tundra ecotone, FTE), is a conspicuous feature of mountain and high latitude landscapes throughout the world. The FTEs and alpine areas above them are globally popular areas for outdoor recreation. The boundary between forests and tundra is also of ecological significance; alpine areas are found at almost all latitudes and have high overall species diversity, yet alpine vegetation only comprises about three percent of global terrestrial surface area (Troll 1961, Körner 1995, Körner and Spehn 2002). FTE positions are associated with thermal deficiencies limiting plant growth (Körner 1998, Jobbágy and Jackson 2000), and FTE movement may be a sensitive ecosystem response to climate change (Neilson 1993, Grace et al. 2002). Varying degrees of climate-driven FTE movement have been documented across a wide range of climatic regimes, forest types, and land use histories (Harsch et al. 2009). In the future, climate change is projected to be most pronounced in mountain and high latitude regions (Beniston et al. 1997, Liu and Chen 2000, Christensen, et al. 2007), suggesting increased FTE movement and invasion of alpine vegetation in the future. Climate-driven FTE movement may have numerous ecological effects including: temperature feedbacks resulting from altered surface energy balances (Bonan et al. 1992, Beringer et al. 2005), changes in ecosystem carbon storage (Prichard et al. 2000, Wilmking et al. 2006), and the loss of alpine biodiversity (Dirnbock et al. 2003, Halloy and Mark 2003). The magnitude of ecological effects resulting from FTE movement will largely be determined by the spatial extent and temporal rates of FTE movement.

FTE research has a long history in North America, focusing on detecting evidence of FTE movement in response to climate, and describing plant communities in relation to environmental gradients (Griggs 1934, Brink 1959, Franklin et al. 1971, Douglas 1972, Lloyd and Graumlich 1997). However, our understanding of climate-driven FTE movement across landscapes is surprisingly limited. FTE research has focused on pattern detection, but has tended to not estimate populations (in this context I am loosely defining population estimation to include land cover extent and land cover change). The choice of pattern detection versus population estimates is important, because it strongly influences sampling design, statistical analysis, and scope of inference (Kenkel et al. 1989). Because of well recognized global relationships between FTE position and climate (Hermes 1955, Körner 1998, Jobbágy and Jackson 2000, Harsch et al. 2009) pattern detection has been the norm in FTE research. The lack of focus on population estimates in FTE research has resulted in a poor understanding of how FTE movement, and vegetation composition and structure are distributed across landscapes, both currently, and over time. The question of pattern detection versus population or landscape level estimates is ubiquitous in ecology, but may be especially problematic in FTE research. FTE positions may have global explanations, but FTE positions and sensitivity to climate can be dependent on numerous non-climatic biophysical factors (i.e. topography, seed sources, disturbance, etc.) important at multiple spatial scales, making it difficult to generalize and downscale FTE movement and associated ecological effects in response to climate change (Miller and Halpern 1998, Daniels and Veblen 2004, Holtmeier and Broll 2005).

Another significant limitation to understanding past, current, and potential future changes in FTE vegetation composition and structure is the lack of field data. Vegetation data in the FTE is often sparse and incomplete due to: under sampling of the small FTE land area; sampling that does not address fine-scale patterns of FTE vegetation in relation to steep environment gradients; subjective sampling in relation to a limited number of environmental gradients perceived as most important; and the cost and logistic difficulties in sampling often remote FTE landscapes. The scarcity and incompleteness of vegetation composition and structure data is important because historical changes in plant biodiversity and species distributions in the FTE and alpine tundra are typically quantified using long-term time series of field plots (Cannone et al. 2007, Pauli et al. 2007), while potential future changes are typically based on species distribution models that rely on bioclimatic envelope approaches (Thuiller et al. 2005). Without a more complete picture of species composition and structure across landscapes, documented changes over time attributed to climate change may not be representative of larger areas and regions, baseline reference conditions for inventory and monitoring may not be representative landscapes, while potential future changes in species distributions may be based on inaccurate or oversimplified characterizations of current species habitat.

This dissertation attempts to overcome many of the above mentioned limitations in FTE research by taking a landscape approach to develop a greater understanding of past spatiotemporal patterns of tree invasion, current spatial patterns of vegetation composition and structure, and potential future patterns of climate-driven tree invasion. The setting for this research is Jefferson Park, an approximately 260 ha subalpine parkland landscape in the Oregon High Cascades, USA. This dissertation focuses on three different temporal components of FTE movement: (1) quantifying long-term (centuries) and short-term (decades) histories of tree establishment; (2) spatially characterizing current tree and non-tree species distributions; (3) and spatially projecting potential future tree invasion over the next five decades, which also serves as a proxy for potential future non-tree meadow habitat. Within these three time periods of investigation, there are three general themes in this dissertation which emerge in different but interconnected ways in Chapters 2-4. The first theme is to integrate pattern detection and landscape estimation approaches of ecological inquiry, to determine if tree invasion is occurring within the subalpine meadows of Jefferson Park, while also quantifying temporal rates and spatial extent of tree invasion across the Jefferson Park Landscape. The second theme is how climatic and non-climatic factors have interacted to shape patterns of tree invasion over time (e.g. how have climate and biophysical features in the landscape influenced FTE movement, do these factors operate at different spatial scales and in are they a function of landscape context, and how they may interactively control tree invasion). The third theme is the incorporation of advanced remote sensing tools to improve our understanding of past, current, and future FTE dynamics. Historically, FTE research has been based exclusively on field data collection, or remote sensing data such as aerial photographs or satellite imagery. New technologies such as Light Detection and Ranging (LiDAR) can generate synoptic characterizations of topography and vegetation structure at unprecedented data resolutions (Lefsky et al. 2002). However, I do not just use a new technology such as LiDAR to view the FTE from above. I also use LiDAR to formulate research questions and sampling methodologies to combine pattern detection and population estimate driven avenues of scientific inquiry, while also integrating LiDAR with field data collection and other remote sensing data types to generate more detail landscape based characterizations of past, current, and potential future FTE dynamics.

Chapter 2 had three objectives: (1) characterize spatial patterns of tree ages, vegetation composition, and vegetation structure in a FTE landscape in the Oregon Cascades; (2) determine how vegetation composition and structure were associated with gradients of environmental factors derived from multispectral satellite imagery and LiDAR data; and (3) determine if predictive mapping characterizations of tree age, vegetation composition, and vegetation structure were improved by the inclusion of LiDAR data. If successful, this approach would make it possible to characterize vegetation composition and retrospective tree invasion at fine scales; create new monitoring protocols, and establish reference conditions distributions in patchy FTE landscapes. Current vegetation composition, structure, and tree ages were spatially characterized (predictively mapped) by integrating vegetation composition, structure, and tree age data collected in 2006 and 2007 on 98 circular plots (7.32 m radius) located in a randomized clustered design with topographic and vegetation indices derived from Light Detection and Ranging (LiDAR), and SPOT 5 HRG multispectral satellite imagery. Predictive mapping of vegetation composition, structure, and tree ages was accomplished using the gradient nearest neighbor with imputation approach (Ohmann and Gregory 2002); field vegetation data was related to mapped explanatory variables using gradient analysis (i.e. canonical correspondence analysis); and field vegetation attributes were then projected onto the landscape by calculating gradient analysis axes scores for mapped explanatory variables, determining nearest neighbor plots in gradient space, and imputing nearest neighbor plot data into mapped space.

In chapter 2 I used predictive mapping to estimate current area and spatial distributions of species composition, structure, and tree ages. Chapter 2 does not directly address how tree invasion is related to climate conditions, or non-climate factors such as topography or seed sources. In chapter 3, I determined how climate and biophysical (topography and vegetation structure) variables have interactively controlled temporal and spatial patterns of tree invasion in the meadows of Jefferson Park over the 1950 to 2007 time period. In addition, I estimated landscape-level areal extent of tree establishment in subalpine meadows of the study area over time. The specific objectives of chapter 3 were to: (1) determine how climate and biophysical variables interactively control the temporal and spatial patterns of tree establishment in the subalpine parkland landscape of Jefferson Park; and (2) estimate landscape-level areal extent of tree establishment in subalpine meadows of the study area over time. FTE research has traditionally been based on transect sampling methods. However, transect sampling in the FTE can result in spatial autocorrelation between explanatory variables, confounding attempts to untangle the relative influences of different controls on FTE dynamics. Transects are also rarely representative or explicitly linked to landscape patterns as a whole, prohibiting accurate estimation of the extent and rates of FTE movement across landscapes. To overcome these problems, I used LiDAR data collected in September of 2007 to map micro site (1 m pixel size) topography and vegetation structure (distance from overstory canopy) throughout the Jefferson Park basin. Maps of LiDAR-derived microtopography and distance to overstory canopy were entered into a Geographic Information System (GIS) to select plot locations in a spatially constrained stratified random sampling design. By stratifying in relation to microtopography and distance from overstory canopy, the individual and interactive variable effects could be assessed, while also allowing for landscape-level estimates of tree establishment, since the proportional distribution of each strata within the study area was known. Five hundred GIS-selected sites were located within 132 ha of Jefferson Park with a sub-meter global positioning system (GPS). One circular plot (1 m radius) was established at each site, and July snow depth, tree abundance and size, tree ages (via. increment coring), non-tree vegetation heights, and substrate cover were measured on each plot. Chapter 3 reports on the rates and extent of tree invasion over time in relation to annual climate (particularly annual snowfall), how larger landform types alter variation in the biophysical controls nested within them, and how landform types and nested biophysical controls influence summer snow depth which spatially constrains where tree invade meadows. Chapter 3 also reports on how seed source limitations may place additional species-specific constraints of tree invasion of meadows, and how topographic conditions may interact with climate to produce complex spatiotemporal patterns of tree invasion over time.

In chapter 4 I asked the how might tree invasion occur in the future in response to climate change? My primary objective was to spatially project historical and near-term future (1950 to 2064) tree invasion within 132 ha of meadows in Jefferson Park. Specifically, this chapter addressed three questions: (1) can fine-scale patterns of historical tree invasion be accurately predicted? (2) how sensitive is future tree invasion (and therefore meadow persistence) to different future snowfall scenarios? and (3) how important are non-climatic factors such as landforms and biotic interactions in influencing the extent and spatial patterns of tree invasion? To answer these questions I developed an empirically-derived statistical model to quantify tree invasion in relation to deterministic spatial patterns of tree invasion controlled by biophysical factors (microtopography, seed sources, overstory and young tree interactions, larger-scale landform types), and probabilistic temporal patterns of tree establishment in relation to climate (specifically snowfall). Spatial and temporal patterns of tree invasion were quantified based on the results from chapter 3. Modeling focused on two time periods, historical (1950 to 2007) and near-term future (2007 to 2064). During the historical time period, the model drives tree invasion using regional climate data. For the near-term future time period, six different climate scenarios were developed crossing three levels of change from historical mean annual snow fall (no change, 25%, and 50% reductions in snowfall) with two levels of persistent extreme snow fall (same as historical record, and extreme high or low snow fall persistently for three consecutive years).

Chapter 5 synthesizes the results of chapters 2-4, relating results of each chapter to the three emergent themes of: pattern dectection versus population/landscape estimation, the importance of climatic and non-climate controls of FTE dynamics at multiple spatial scales, and how integration of field data with remotely sensed data can greatly improve our understanding of FTE dynamics, current conditions, and potential future changes across landscapes.

CHAPTER 2: INTEGRATING LIDAR, SATELLITE IMAGERY, AND FOREST INVENTORY DATA TO SPATIALLY CHARACTERIZE TREE INVASION, VEGETATION COMPOSITION, AND VEGETATION STRUCTURE IN A SUBALPINE MEADOW LANDSCAPE, OREGON CASCADES, USA.

ABSTRACT

The forest tundra ecotone (FTE) is the transitional area between forest and tundra ecosystems. FTE positions are sensitive to climate change, and FTE movement may have numerous ecological impacts at multiple spatial and temporal scales. Spatial patterns of vegetation composition and structure can affect future ecosystem dynamics, and characterizing the spatial of vegetation composition, structure, and tree invasion are needed to assess landscape level change. Study objectives were to: (1) characterize spatial patterns of tree invasion via tree ages, vegetation composition, and vegetation structure in a FTE landscape using predictive mapping, (2) determine how vegetation composition and structure were associated with gradients of environmental factors derived from multispectral satellite imagery and LiDAR, and (3) determine if predictive mapping characterizations of tree ages, vegetation composition, and vegetation structure were improved by the inclusion of LiDAR data. A gradient analysis with nearest neighbor imputation was used to generate spatial predictions; integrating forest inventory field plots, SPOT 5 satellite imagery, and LiDAR data. Vegetation composition was best described by SPOT 5 imagery and LiDAR-derived topography, while vegetation structure was best described by LiDAR-derived vegetation heights. Species occurrence predictions were most accurate for tree species, moderate for shrub species and vegetation groups, and highly variable for graminoid species. Tree age was the most accurately predicted vegetation structure variable, and indicates the study area was largely un-forested in 1600, gradually invaded by trees from 1600 to the 1920's, and then rapidly invaded until 1980. Many vegetation structure variables (e.g. stand and regeneration density) had large prediction errors, possibly a function of scale incompatibilities between data sources, and heterogeneous FTE landscapes where forest structure does not develop along consistent trajectories as stands age. Vegetation composition and structure predictions had greater uncertainty with increased geographic distance from field plots, suggesting spatial distribution of field plots needs to be considered if predictive mapping of vegetation is a goal of inventory and monitoring programs.

INTRODUCTION

Subalpine parklands and alpine treeline communities (also referred to as the alpine forest-tundra ecotone, or FTE) are transitional areas between forested and alpine ecosystems. FTE positions are often associated with thermal deficiencies limiting plant growth, implying that increased temperatures will result in FTE movement (Grace 1989, Körner 1998, Jobbágy and Jackson 2000). Contemporary movement of alpine treeline and declines in subalpine and alpine meadow extent vary, but have been documented across a diverse range of geographic locations, climatic zones, and tree species, suggesting a global ecological response to climate change (Harsch et al. 2009). Besides being highly desirable areas for outdoor recreation (Dearden and Sewell 1983, Price 1985, Tolvanen 2005), FTE movement may have numerous ecological effects at multiple spatial scales, including: positive temperature feedbacks due to decreased surface albedo (Bonan et al. 1992, Foley et al. 2000), increased NPP and carbon storage (Solomon et al. 1997, Prichard et al. 2000, Lafleur et al. 2001), and declines of plant and animal populations and species (Halloy and Mark 2003, Dirnböck et al. 2003, Cannone et al. 2007, Roland and Matter 2007).

The magnitude of these ecological effects will be largely driven by the rates and spatial extent of FTE movement. Current FTE vegetation composition and structure are important drivers of future FTE movement via modification of: snow persistence, available soil moisture, soil development, nutrient availability, inter-specific competition, and seed quantity (Tranquillini 1979, Holtmeier 2003, Didier 2001, Germino et al. 2002, Bekker 2005, Maher and Germino 2006). Although the FTE is often referred to as a “line”, it is typically a transitional area of variable width whose spatial complexity increases from global to local scales, where it forms complex mosaics of forest and non-forest components (Holtmeier and Broll 2005). In the FTE (and spatially heterogeneous ecosystems in general), spatial patterns of existing trees and vegetation may affect current and future dynamics of the entire landscape (Hardt and Foreman 1989, Turner et al. 1998, Bekker 2005, Malanson et al 2007). Consequently, understanding current FTE dynamics and how these systems may respond in the future to climate change requires an understanding of the current spatial patterns of FTE vegetation composition and structure. This would suggest developing spatially explicit characterizations (i.e. maps) of vegetation composition and structure would be an important component in monitoring change in the FTE.

Spatially-explicit characterizations of current FTE vegetation composition and structure have rarely been generated, and have not included tree age structure (Brown 1994, Wallentin et al. 2008). This is likely due to the objectives typical of FTE research. Field-based FTE research typically attempts to detect patterns of change, quantifying temporal changes in FTE position in relation to climate, or characterizing vegetation composition and structure in relation to a limited number of underlying environmental gradients (Kuramoto and Bliss 1970, Woodward et al. 1995, Rochefort and Peterson 1996, Lloyd and Graumlich 1997, Miller and Halpern 1998). However, spatial patterns of vegetation composition and structure are often shaped by multiple drivers and their interactions at varying spatial and temporal scales (Turner et al 1998, Urban et al. 2002, Daniels and Veblen 2004). FTE field research collected along a low number of environmental gradients is also unlikely to characterize the full range of environmental gradients that occur in complex landscapes, and consequently this research cannot be simply “scaled-up” to accurately characterize spatial patterns or make landscape-level estimates of vegetation composition, structure, and age distributions.

Unlike field research, FTE research based on remotely sensed data is well suited to spatially characterizing and estimating FTE land cover and land cover change at multiple spatial scales (Masek 2001, Mihai et al. 2007, Zald 2008). However, for numerous reasons, FTE research based on remote sensing alone has low ecological resolution. Typical land cover derived from remote sensing data is large scale mapping projects with relatively large minimum mapped units of 30 to 100 m, and are not optimized to accurately characterize the proportionately small and heterogeneous FTE (CEC 1994, Vogelmann et al. 2001, Homer et al. 2004). Pixels in remote sensing based land cover classifications can typically be occupied by only one land cover type (i.e. hard classification). Mixed within-pixel land cover composition is common in ecotones, but hard classification approaches inadequately characterize ecotones as either pixel boundaries between vegetation classes or finely delineated vegetation types found only within the ecotone (Johnston and Bonde 1989, Allen and Walsh 1996, but see Hill et al. 2007). Land cover classifications based solely on remotely sensed data do not contain vegetation composition and structure information, so they lack the ecological resolution to characterize important attributes of FTE vegetation conditions. Finally, changes in image quality, short time periods of existing imagery, and limited sample dates (typically two dates) over time restrict the temporal extent, resolution, and quality of remote sensing based estimates of FTE conditions and change.

Fine-scale maps of the FTE are needed to answer questions of ecological effects of climate change on ecosystems and feedbacks between ecosystem patterns, processes, and climate change. Characterizing spatial patterns of FTE age structure would provide accurate estimates of landscape-level tree invasion. Additionally, quantifying species occurrences and distributions across landscapes could improve species distribution models used to project plant migration and biodiversity in response to climate change, since performance of these models is often influenced by incomplete biological data (Kadmon et al. 2003, Martínez-Meyer 2005, Araújo and Guisan 2006). One approach to generating such information (referred to as predictive mapping), combines field data, remotely sensed imagery, and additional spatially explicit datasets (i.e. digital elevation models, topographic moisture indices, solar radiation indices, etc.), utilizing the strengths of both field and remotely sensed data types to generate spatially explicit predictions of vegetation composition and structure across landscapes (Gottfried et al. 1998, Ohmann and Gregory 2002, Hudak et al. 2008, Tomppo et al 2008). Predictive mapping can represent the full range of variability in field data, mapping multiple attributes that vary continuously. This is especially attractive for the FTE, since it could provide landscape-level estimates of tree age structure not possible with field data alone, while reducing problems associated with mixed composition pixels that can confound traditional "hard" classification in remote sensing of ecotones. Published attempts to predictively map vegetation composition and structure in the FTE do not currently exist, but it has the potential to dramatically improve spatial characterization of FTE vegetation composition and structure.

Predictive mapping generally utilizes multi-spectral satellite imagery and digital elevation models, but relatively few studies have utilized airborne Light Detection and Ranging (LiDAR) (although see Hudak et al 2008). LiDAR generates high resolution three dimensional characterizations of terrain and vegetation structure, enabling examination of landscape patterns not previously possible (Lefsky et al. 2002, Vierling et al. 2008). LiDAR data can improve vegetation classification accuracy, and both characterize and predict forest vegetation structural attributes (Lefsky et al. 1999, Zimble et al. 2003, Chust et al. 2008). Applications of LiDAR to mapping the FTE are current lacking, but LiDAR may be especially useful in providing fine scale topographic data; whose patterns can influence microclimate, vegetation composition, and tree establishment at the FTE (Barry 1981, Körner 2003, Holtmeier 2003). Vegetation structure derived from LiDAR may also provide landscape-level estimates and spatial characterization of tree establishment patterns (via tree height age relationships), over long time periods not possible using field data or time series remote sensing imagery. LiDAR has only recently become available for ecological and FTE research, so it is unclear to what degree LiDAR data may improve predictions of vegetation composition and structure, and what explanatory variables derived from LiDAR will be most important.

The study has three objectives: (1) characterize spatial patterns of tree invasion via tree ages, vegetation composition, and vegetation structure in a FTE landscape in the Oregon Cascades using predictive mapping, (2) determine how vegetation composition and structure were associated with gradients of environmental factors derived from multispectral satellite imagery and LiDAR, and (3) determine if predictive mapping characterizations of tree ages, vegetation composition, and vegetation structure were improved by the inclusion of LiDAR data.

METHODS

Study Area Description

The study was conducted in Jefferson Park (44°42’ N 121°48’ W, 1693 – 1814 m asl), an approximately 260 ha subalpine basin in the Mount Jefferson Wilderness, Willamette National Forest, within the Oregon High Cascades ecoregion (Figure 2.1). The climate is intermediate between Mediterranean and maritime temperate with dry warm summers and significant winter precipitation (Csb/Cfb) under the Köppen Climate Classification System (Peel et al. 2007). The nearest weather station within the region at an elevation similar to Jefferson Park (Government Camp Station, National Weather Service Cooperative Network #353402, 45°18’ N 121°145’ W, 1213 m asl), reported annual average maximum and minimum temperatures of 10.2° C and 1.1° C. Annual precipitation averaged 217 cm, snow fall occurred predominantly between December and April, and annual snow fall averaged 682 cm during the 1951 to 2008 time period.

Jefferson Park geomorphology has been strongly shaped by volcanism and glaciation. Mount Jefferson is a Pleistocene stratovolcano of rhyolitic/basaltic origin above a broad plateau of older shield volcanoes (Walder et al. 1999). During the most recent glacial maxima of the Holocene Epoch, the Jefferson Park glacial advance and retreat deposited outwash, basal till and ablation till within the study area (Scott 1977). Since the mid-19th century, Cascade Range alpine glacier extent has substantially decreased (O'Connor and Costa 1993, McDonald 1995, Dyurgerov and Meier 2000). Glacial retreat, combined with steep slopes and loose parent materials, result in the Cascade Range having the highest concentration of neoglacial lakes in the conterminous United States (O'Connor et al. 2001). On August 21st, 1934, a small (~4,000 m^2) moraine dammed neoglacial lake breached on Mount Jefferson, covering 320,000 m^2 of eastern Jefferson Park with debris 0.3 to 2.4 m deep (The Oregonian Daily Journal, October 19th, 1934). Field reconnaissance during 2006 discovered a smaller undocumented debris flow in north Jefferson Park of older but indeterminate age. Soils of the study area are poorly documented, consisting of either rubble derived from ice, colluvium and residuum weathered from sedimentary rock with influences of volcanic ash; or Typic Vitricryands formed in residuum and colluvium from pyroclastic ash flows, andesite, and volcanic ash (MacDonald 1998).

Jefferson Park is within the lower FTE, the transition zone between the upper limit of closed montane forest (i.e. timberline) and the beginning of the alpine zone (sensu Körner 2003). Jefferson Park is within the mountain hemlock (*Tsuga mertensiana*) vegetation zone (Franklin and Dyrness 1988). Mountain hemlock and Pacific silver fir (*Abies amabilis*) are the dominant tree species, found in both single species and mixed-species stands. Most of these stands are "islands" of variable size and shape surrounded by meadow vegetation. The oldest trees in these forest islands are at least 200 years old, and can exceed 400 years of age. Subalpine fir (*Abies lasiocarpa*), whitebark pine (*Pinus albicaulis*), lodgepole pine (*Pinus contorta*), and Alaska yellow-cedar (*Callitropsis nootkatensis*) are also present, but in greatly reduced amounts and more restricted spatial distributions. Six vegetation groups were identified within the study area (see Appendix A for details regarding development of vegetation groups). Vegetation groups are generally consistent with prior studies of subalpine parklands in the Oregon Cascades (Campbell 1973, Halpern et al. 1984). A dry forb group on well-drained sites (Group 1) was characterized by *Arenaria capillaris*, *Lupinus arcticus*, *Eriogonum umbellatum*, and *Polygonum newberyi*. Important species in the pink mountain-heather type (Group 2) included *Phyllodoce empetriformis*, *Luetkia pectinata*, and *Lycopodium sitchensis*. The wet sedge meadow type (Group 3) was characterized by *Carex nigricans* and *Juncus drummondi*. The wet low forb type (Group 4) included *Aster alpiginus*, *Castelija parviflora*, *Festuca sp.*, *Gentian calycosa*, and *Kalmia microphylla*. The white mountain-heather type (Group 5) was characterized by *Cassiope mertensiana* and *Microseris alpestris*. The mountain-ash tall shrub type (Group 6) included *Sorbus sitchensis, Rubus lasiococcus, Vaccinium deliciosum, Ligustrum gracilis, Epibolium alpinum, Dodecatheon jeffreyi*, and *Veratrum viride*.

In addition to debris flows, Jefferson Park may have experienced other disturbance events such as livestock grazing. Sheep grazing occurred in what became the Willamette National Forest beginning in the 1890's, and largely ceased by the 1940's (Coville 1898, Kuhns 1917, Rakestraw & Rakestraw 1991). Historical records are scarce, so it is unclear if sustained heavy grazing occurred in meadows of Jefferson Park, although overgrazing at similar elevations and meadow vegetation types resulted in soil erosion and reduced plant cover (Kuhns 1917). Grazing was often more sustained and intense in close proximity to driveways (areas designated for sheep movement), and one of these driveways (the Skyline Trail) provided direct access to Jefferson Park (Oregon Tourist and Information Bureau 1921, Rakestraw & Rakestraw 1991). The long travel distances associated with its remote location and conflicts with recreational use discouraged livestock grazing in the study area, and livestock access to Jefferson Park via the Skyline Trail was closed in 1937 (Rakestraw & Rakestraw 1991). Low intensity pack animal grazing has continued within the study area to the present. Heavy livestock grazing of subalpine vegetation may either facilitate tree establishment via reduced vegetation competition and exposure of mineral soil, or inhibit tree establishment via direct browsing and trampling of seedlings. Direct experiments are lacking, but prior research has inferred grazing suppresses tree establishment at treeline and subalpine meadows, and a pulse of increased tree establishment often follows grazing cessation (Miller and Halpern 1998, Didier 2001, Gehring-Fasel et al. 2007). Fires are infrequent in the subalpine ecosystems of the region, with fire return intervals in the mountain hemlock zone ranging from centuries to several millennia (Lertzman and Krebs 1991, Hallett et al 2003). Intensive surveys of the study area for past fires were not conducted, but qualitative observations during field plot establishment found no evidence of charred tree boles or biological legacies indicative of past wildfires. Some whitebark pines displayed needle spots and cankers indicative of white pine blister rust (*Cronartium ribicola*), but observations suggest there has not been recent significant tree mortality due to blister rust or other pests and pathogens within the study area.

Overall Sampling Design

The study area was delineated by topography and vegetation, bounded on the east and west by steep declines in elevation coinciding with increased closed canopy forest and plant species typical of lower elevation montane forests, and bounded on the north and south by the steep slopes of Mount Jefferson, Park Butte, and Park Ridge (Figure 2.1). Vegetation composition and structure data was collected on 98 geo-referenced forest inventory subplots located in a randomized clustered design. Summary measures of vegetation species occurrence, tree age, basal area, diameter, stand density, and regeneration density were calculated for each plot. Values for landform type (glacial or debris flow), SPOT5 multi-spectral satellite imagery, LIDAR-derived topography, and LIDAR-derived vegetation structure explanatory variables were assigned to each geo-referenced plot in a Geographic Information System (GIS).

Field Plot Data

In the summers of 2007 and 2008, vegetation composition and structure data were collected on 98 circular plots (7.32 m radius) located in a randomized clustered design within Jefferson Park. Plot footprints were similar to those used by the U.S. Forest Service Forest Inventory and Analysis Program (FIA), consisting of a central 7.32 m radius subplot, and three equally sized subplots 36.6 m distance from the central subplot at 120°, 240°, and 360° degrees (Bechtold and Patterson 2005). Each of the four subplots within a cluster is a sample unit, and is referred to as a plot hereafter. Unlike Locations for 30 central plots were determined using the random point generator in Hawth's Tools version 3.24 (Beyer 2004). From each central plot, the centers of three additional plots in each cluster were calculated, resulting in a total of 120 plot coordinates in a random clustered design. This was believed to be the maximum number of plots which could be located and measured in the time permitted, while providing adequate sample numbers for analysis (later confirmed by species accumulation curves). Plots were located using GIS determined coordinates with a sub-meter accuracy GPS unit (Leica GS20 with an external pole antenna, Leica Geosystems AG, St. Gallen, Switzerland). At least ten GPS coordinates with positional errors less than 2 m were averaged for each plot center to improve positional accuracy (Wing and Karsky 2006). GPS subplot coordinates were post-processed using GIS DataPro software (Leica Geosystems AG, St. Gallen, Switzerland) and plot horizontal positional accuracy averaged 0.71 m (0.27 – 1.17 m 95% CI). Plots in lakes or high-use recreation areas (such as campsites or trails) were excluded, as was a single plot located within a fragile spring/seepage vegetation community that would have been excessively damaged by sampling activity. The early onset of winter snow storms in 2008 resulted in measurement of only 98 plots, with reduced plot density on the east and west sides of the study area (Figure 2.1).

Within each plot, all trees taller than breast height (1.3 m) were identified by species, and measured for diameter at breast height (DBH) and tree height. Stand density, basal area, and quadratic mean diameter were summarized by plot and species. On each plot, a subsample of trees was cored proportional to plot-level species and height distributions. Trees were cored at the root collar, or at the minimum height at which the increment borer could be used (5 – 40 cm depending on increment borer length). Tree cores were aged to generate maximum (stand initiation) and mean plot ages. Height age regressions were used to estimate the number of missing rings on cores collected above the root collar. Tree regeneration (i.e. trees shorter than breast height) was tallied by species and size class (5 - 50 cm, 50 - 130 cm tall) on two 2.07 m radius micro plots established 3.66 m from plot center at 90° and 270°. Regeneration density by plot, species, and size class calculated. The percent cover of overstory, understory, and ground cover vascular plants was recorded by species (Table 2.1). One of six vegetation groups was assigned to each plot as shown by the dendrogram in Appendix A.

SPOT 5 Imagery

Eight data layers were developed from bands 1-4 of SPOT 5 HRG imagery (Table 2.2). The study area fell within a single SPOT 5 scene taken on July 20, 2005 (ID 55262600507201912152J). Data layers were pan-sharpened to a 5 m pixel resolution. Plot sizes in this study are small (four 10 m pixels of imagery overlay a plot), although the number of pixels overlaying a plot can vary depending on plot to image alignment. SPOT 5 imagery has a global horizontal standard deviation of 50 m with level 2a processing for geometric distortions (SPOT Image Corp 2008), inadequate for extracting subplot-level spectral attributes. To address this, SPOT 5 imagery was co-registered to LiDAR data collected for the study area, which had extremely high positional accuracy. The panchromatic band of SPOT 5 imagery was co-registered to a LiDAR-derived vegetation height model using the program ITPFind, an automated, area-based technique for identifying image tie points used in image co-registration (Kennedy and Cohen 2003). ITPFind was run using a 100 * 100 pixel window and a 0.35 threshold minimum steepness value. Automatically designated tie points between SPOT 5 and LiDAR images were visually assessed, and 127 were retained to geo-rectify the SPOT 5 image using ERDAS Image version 9.2 (Leica Geosystems Geospatial Imaging, LLC). Geo-rectification used a 1st order polynomial model, which resulted in a combined root mean squared error (RMSE) of 3.45 m. SPOT 5 bands were resampled using nearest neighbor interpolation during geo-rectification.

LiDAR Data

Discrete return airborne LiDAR data was collected on September 3-4, 2007 by Watershed Sciences, Inc (Corvallis, Oregon USA) using a Leica ALS50 Phase II laser system flown on a fixed-wing aircraft approximately 2000 m above ground level. LiDAR data was collected with a 59 kHz pulse rate, capturing scan angle of ±11°, and scan swath $\geq$ 50%. Point density exceeded 10 points/m^2 within the study area. Based on known real-time kinematic ground survey points collected 8 km west of the study area, LiDAR data had a combined horizontal and vertical accuracy of 0.04 m. The LiDAR point cloud was converted into three grids with 1m pixel resolution: a digital elevation model (DEM) of bare earth ground elevation, a vegetation elevation model (VEM), and a vegetation height model (VHM) calculated by subtracting the DEM from the VEM. The three above mentioned grids were then resampled to 5 m pixel size. VHM grid was used to co-register the SPOT 5 imagery, eight topographic variables were derived from the DEM (Table 2.2), and fourteen vegetation structure variables were derived from the raw LiDAR point cloud first returns using the Grid Metrics function in FUSION version 2.61 (McGaughey 2007).

Additional Mapped Data and Plot-Level Data Extraction

Mapped data delineating landform types (glacial and debris flow landforms) was created by manually interpreting aerial photographs, LiDAR data, and field notes. The debris flow from 1934 was easily discernable in historical aerial photographs from 1949, where the lack of vegetation made it stand out from the much older surrounding glacial landforms. The older debris flow along the northern boundary of the study area was easily discernable using surface roughness maps derived from the LiDAR data. Both debris flows were confirmed by qualitative field examination of deposited surface material. Glacial landforms dominated the rest of the study area (Hodge 1925, Scott 1977). Shapefiles of the two landform types were manually traced as polygons, and then converted to grids in ArcGIS. To assign values from mapped environmental variable grids to plots, each plot was represented as a template of 0.5 m pixels approximating the plot's ground footprint, centered on its X and Y coordinates. Plot templates were overlain on each environmental variable grid using a GIS macro, and mean values of explanatory variables associated with each plot were extracted.

Predictive Mapping Method

Predictive mapping closely followed the gradient nearest neighbor (GNN) method described by Ohmann and Gregory (2002), and was conducted in four steps:

(1) A stepwise canonical correspondence analysis (CCA) was run to develop a model quantifying relationships between field (response) data and mapped (explanatory) data (ter Braak 1986, ter Braak and Prentice 1988).

(2) For each mapped 5 m pixel, scores were predicted for the first eight CCA axes by applying model coefficients from step 1 to the mapped values for explanatory variables.

(3) For each mapped pixel, the single and second nearest plots in eight-dimensional gradient space were identified. The distance metric is Euclidean, and axis scores were weighed by their respective eigenvalues.

4) The field attributes of the nearest plot were imputed into the mapped pixel. Maps were then constructed for vegetation attributes measured in the plots.

CCA is an ordination technique where the ordination of composition or structural data is constrained by a multiple linear regression of explanatory data. CCA can suffer from multicollinearity, poor retention of community structure in response to noisy environment data, and is best suited to data with unimodal responses to underlying environmental gradients (Neter et al. 1996, McCune 1997, McCune and Grace 2002). CCA also relies on the chi-square distance measure, which can give high weight to data with low total values or abundance, and deemphasize data with high total values or abundance (Minchin 1987). However there are few viable alternatives to CCA when associating community structure to environmental gradient data. Generalized Linear Models (GLMs), General Additive Models (GAMs), and Non-parametric Multiplicative Regressions (NPMR) can model complex surfaces of single dependent variables in relation to explanatory variables (Wimberly and Spies 2001, Guisan et al. 2002, McCune 2006). However, GAMs are constrained by the additive nature of model terms and limited functional forms, while requiring modeling of single response variables individually (McCune 2006). Single species models ignore important information found in species co-occurrence, and compiling many single species models can result in unrealistic predicted combinations of species co-occurrence (Mouer and Stage 1995). For these reasons, it was felt that despite its potential limitations, CCA was the best approach for realistic multi-species mapping.

Species composition and vegetation structure (including tree ages) were modeled separately in relation to mapped explanatory variables. Response variables in the species composition matrix included species presence/absence for all species listed in Table 2.1. Tree species presence/absence was divided into overstory trees and understory trees (which were defined as either occurring directly underneath overstory trees, or being open grown and under 8 m tall). Vegetation groups were included in the species composition models, coded as mutually exclusive binary indicator variables. Response variables in the vegetation structure matrix included: maximum and mean plot-level tree age, stand density (trees/ha), basal area (m^2/ha), quadratic mean diameter (cm), and regeneration density (trees less 1.3 m tall/ha) both separately by species and summed across species. To determine if LiDAR-derived data (both topographic and vegetation structure) improved GNN model predictions, nine different CCA models were developed with different subsets of mapped explanatory data (Table 2.3).

Composition and structure data were each modeled separately in relation to these nine combinations of mapped explanatory variables using CCA.

CCA models were developed using the package vegan for R with a Euclidean distance metric (Oksanen et al. 2008, R Development Core Team 2008). A forward stepwise procedure was used to retain variables describing the most variation in the vegetation data. Mapped explanatory variables were added in order of greatest additional variance described, and added only if they were significant ($P < 0.05$), as determined by Monte Carlo tests with 99 permutations. X and Y coordinates were excluded from stepwise CCA model development, but included in all final models to include geographic location in selection of nearest-neighbor plots. After CCA model development, first and second nearest plot neighbors ($k=2$) were imputed using the program yaImput in R version 2.8.1 (Crookston et al. 2007, R Core Development Team 2009). Following imputation (which assigns plot identifications to pixels), plot-level field attributes were joined to associated pixels, and maps constructed for vegetation attributes.

Model Evaluation and Accuracy Assessment

GNN predictions of vegetation composition and structure were evaluated at the study area and plot levels in a manner similar to that described by Ohmann and Gregory (2002). At the study area level, relative proportions of vegetation composition predicted by GNN were compared to relative proportions from the field plots. Means and variability of GNN vegetation structure predictions were compared to means and variability from field plots. Plot-level accuracy was assessed by comparing GNN predictions to observed (field plot) values for the 98 plot locations. This was accomplished by a leave-one-plot-out cross-validation approach. A 10-fold cross-validation was also generated, which produced similar results (not presented). Accuracy of vegetation composition predictions was assessed by calculating overall classification accuracy and kappa coefficients of agreement (Cohen 1960). Accuracy of vegetation structure predictions in relation to observed values were assessed with root mean square differences (RMSD). RMSD is computationally similar to root mean squared error (RSME), but divided by the standard deviation of the observed data. The spatial distribution of prediction accuracy was assessed by mapping nearest-neighbor distances. Nearest neighbor distances indicate potential spatial distribution of error in model predictions, with shorter distances indicating greater confidence in results (Ohmann and Gregory 2002). This approach to spatial uncertainty of model predictions allows for visualization of uncertainty across the landscape, as opposed to mapping prediction residuals versus observations only at plot locations as done by Ohmann and Spies (1998).

RESULTS

Gradients in Species Composition and Vegetation Structure

Species composition was most strongly associated with gradients of SPOT 5 and LiDAR-derived topography variables, with LiDAR-derived vegetation structure and landform variables describing much less variation in composition data (Table 2.4). The highest proportion of variance described in the composition data occurred for the model containing all types of mapped variables (i.e. SPOT 5, landform, topography, and vegetation structure). The primary gradient (diagonal across CCA axes 1 and 2) in vegetation composition was associated with reduced reflectance of the SPOT 5 mid IR and green bands, topographic position, slope, elevation, and vegetation height (Figure 2.2a-b). Along this primary gradient, trees, tall shrubs, and species associated with forest understory were found on drier sites and higher elevations on the right, while shorter stature and wet site species were found on the left. A weaker perpendicular gradient with red and near IR bands of SPOT5 imagery and landform type had species on well-drained and rocky sites in the lower left portion of the ordination. Gradients of vegetation structure were strongly associated with LiDAR-derived vegetation structure variables (Table 2.4). Adding topography, SPOT5, and landform variables during model development did little to improve the proportion of variance described in the vegetation structure data. The primary gradient (CCA axis 1) of vegetation structure was associated with percentiles of vegetation height, although potential relative radiation (RAD) was also strongly associated with variance in the vegetation structure ordination (Figure 2.2c).

Overall Prediction Accuracy

Predicted proportions of the study area occupied by different tree species and vegetation types generally matched field plot observations (Figure 2.3). The GNN model over-predicted overall overstory cover, as well as the overstory cover of Pacific silver fir and yellow-cedar, while closely matching overstory cover of mountain hemlock and subalpine fir.

GNN predictions for understory tree cover closely matched observations, over-predicted the proportion of the landscape in the tall shrub and dry forb vegetation groups, while underestimating the other four vegetation groups. Predicted means and standard deviations of vegetation structural attributes closely matched observed values, although prediction means tended to be greater than observed values (Table 2.5). Based on field observations, the overall geographic patterns of GNN predictions for individual species appear reasonable (Figure 2.4). Predictions appear excessive for the dry forb vegetation group (which should be more constrained to debris flows), and this over prediction appears to come largely at the expense of the mountain heather and tall shrub groups, especially along the heavily forested eastern edge of the study area (Figure 2.5). Spatial patterns of stand age appear reasonable, predicting no trees in large meadows, young trees in the debris flows where extensive tree regeneration has occurred, and recent tree establishment on glacial landforms clustered around older trees (Figure 2.5). Predicted initial tree establishment age over time was slightly higher overall than observed (Figure 2.6). Tree establishment occurred at a fairly low and constant rate from 1600 to 1925, increased beginning around 1925, and higher rates of establishment continued until around 1990. Spatial patterns of nearest neighbor distances for composition and structure models (Figure 2.7) suggest greatest potential uncertainty on the eastern edge of the study area, which also has the lowest plot density. Nearest neighbor distances in gradient space were positively correlated to geographic distances of pixels from field plots (Pearson product moment correlation coefficient = 0.282).

Plot-Level Predictive Accuracy

Classification accuracy was not calculated for all species at once at the plot level, since species occurrence was not mutually exclusive of another species. Instead overall classification accuracy and improvement from chance agreement (Kappa statistic, κ, Cohen 1960) were calculated for each species. Overall accuracy of predicted species presences ranged from 53% – 99%, were -12 – 79% better than expected by chance for individual species, and 19 – 38% better than chance for vegetation types (Table 2.6). Species with very low Kappa values either had low sample sizes, such as *Callitropsis nootkatensis* and *Veratrum viride* (both had n = 1), or were consistently present but had low or variable percent cover values within plots (e.g. *Carex nigricans*, and *Luetkea pectinata*). Based on kappa statistics and discounting extremely rare species, GNN predictions were highest for overstory trees, intermediate for tree regeneration, shrubs, and vegetation types, intermediate but variable for forbs, and lowest for graminoids. Overall mean vegetation structure values tended to be over predicted by 13 to 42 percent, but variation around mean values was comparable between predictions and observed data (Table 2.5). Plot-level GNN predictions were most accurate for mean and maximum stand age, but generally poor for basal area, stand density, regeneration density, and quadratic mean diameter (Figure 2.8).

DISCUSSION

The GNN model based on field plots, multi-spectral satellite imagery, and LIDAR, produced high-resolution maps rich in predicted ecological data such as tree invasion ages, vegetation composition, and vegetation structure. GNN map accuracy was highest for tree ages and species composition, providing both a long-term retrospective record of tree invasion across the FTE, and fine-scale projections of species distributions. Both vegetation composition and vegetation structure were strongly associated with gradients of topography and vegetation heights derived from LiDAR, but in different ways. Vegetation composition was strongly associated with LiDAR-derived topography and multi-spectral imagery, while vegetation structure was most strongly associated with LiDAR-derived vegetation height metrics. Inclusion of LIDAR data clearly improved predictions of vegetation composition and tree ages, but vegetation structural attributes (i.e. stand density, basal area, and quadratic mean diameter) had very low prediction accuracy. Results of this study suggest potential limitations of LiDAR data and predictive mapping methods for characterizing vegetation structure and specific species and vegetation communities in the FTE and other heterogeneous landscapes. Model patterns, the value of LiDAR data in predictive mapping, and limitations of predictive mapping are discussed below with respect to predictions of tree invasion, vegetation composition, and vegetation structure. In addition, spatial patterns of prediction uncertainty are discussed in relation to the spatial arrangement of field plots, which as implications for using existing and future plot networks to develop fine-scale predictive maps across landscapes for monitoring and inventory purposes.

Retrospective Predictions and Prediction Limitations of Tree Invasion Over Time

An objective of this study was to determine if predictive mapping could quantify spatiotemporal patterns of tree invasion in the FTE. Maximum and mean tree age were the only structural variables with high prediction accuracy, providing landscape-level estimates and spatial distributions of tree invasion in the FTE over time. Models of maximum tree age are inferred to represent initial dates of establishment, which are consistent with plot-level tree invasion. Jefferson Park basin was largely devoid of trees four hundred years ago, and tree establishment was gradual for approximately 300 years, with the landscape still dominated by non-tree vegetation until the early 1900's. The time period dominated by non-forest vegetation and low levels of tree invasion corresponds to cooler reconstructed temperatures in the Northern Hemisphere (Figure 2.6, Jansen et al. 2007), and regional glacial advances during the late Little Ice Age interval (Luckman 2000, Larocque and Smith 2003, Lewis and Smith 2004). Predicted and observed tree ages indicate increased tree establishment beginning in the 1920's, roughly corresponding to Northern Hemisphere warming. Increased tree establishment at the FTE in Jefferson Park was earlier than previous observations of subalpine meadow invasion in the Oregon Cascades, but similar to that found in the Olympic Mountains and Mount Rainer in Washington (Franklin et al. 1971, Woodward et al. 1995, Rochefort and Peterson 1996, Miller and Halpern 1998). High rates of tree establishment continued until approximately 1990 (17 years ago). Model predictions provide a landscape area estimate of current meadow extent, suggesting trees are absent from only 20 percent of the pixels in the study area, down from over 60 percent in 1900.

The greatest limitation of GNN stand age predictions is the lack of tree establishment since 1990 (Figure 2.6). Zald (2010) found high rates of tree invasion during the 1990's, suggesting the seventeen year period without predicted tree establishment may be an artifact of sampling and GNN methodology. Plot sampling used methods similar to the U.S. Forest Inventory and Analysis program, where trees below 1.3 m in height were counted but not aged on micro plots, eliminating young trees ages from the sample. The GNN approach retains the range and variability of plot-level data, so predictions of stand age preserve this aspect of the plot-level data, highlighting the potential limitation of using traditional forest inventory data collection methods (specifically limited collection and aging of small trees and regeneration data) in the FTE.

Predictions of Vegetation Structure and its Limitations within a Predictive Mapping Framework

GNN predictions of vegetation structure were strongly associated with LiDAR derived vegetation height variables, while SPOT5 spectral variables and LiDAR-derived topography variables added much less to the proportion of variance described in the vegetation structure matrix. With the exception of maximum and mean tree age, the GNN model of vegetation structure attributes (tree density, basal area, quadratic mean diameter, etc.) had very low prediction accuracy. Low prediction accuracy of these structural attributes may occur because of asynchronous patterns of vegetation structural development over time which manifest as high horizontal and vertical structural variability.

Trends in stand density, diameter, and volume were variable in relation to stand age (Figure 2.9). In the absence of secondary disturbance, field and remote sensed metrics of forest structure (such as basal area, stand density, tree diameters, canopy vertical distribution, spectral signatures, canopy volume, etc.) often display consistent trends associated with stand age (Bormann and Likens 1979, Spies and Franklin 1991, Jakubauskas 1996, Oliver and Larson 1996., Lesfky et al. 1999, Franklin et al. 2002). Developmental trends of forest structure which are generally synchronous over time following stand replacing disturbance are largely inferred from lower elevation forests with high productivity, canopy closure, and species of varying levels of shade tolerance. With the exception of stand height (which was strongly associated with age), stands in the study area do not display synchronous trends for many structural attributes over time. This may result from low productivity, which may attenuate stand structural development (Larson et al. 2008). Tree islands of variable size and shape are within a matrix of lower height vegetation which may result in increased penetration of photosynthetically active radiation (PAR) compared to forests with high canopy closure. Increased PAR in discontinuous and clustered forest canopy may promote higher densities of lower strata trees (North et al. 2004). Mountain hemlock and Pacific silver fir (the dominant trees in the study area) are very shade tolerant and can persistent as suppressed individuals in stands for up to 100 years (Kranjina 1969, Minore 1979, Packee et al. 1981). Higher PAR and species with high sub-canopy persistence may result in reduced aboveground competition over time compared to closed canopy forests of the region were light competition typically exerts strong controls on tree mortality, growth, canopy stratification which often are strongly correlated to tree height and canopy position (Rudnicki and Chen 2000, Ishi et al. 2000, North et al. 2004). Since GNN predictions are both constrained by and preserve the range of variability in field attributes using nearest-neighbor plots in multi-dimensional gradient space for imputation, prediction of vegetation structure attributes besides tree age may not be possible in ecotones or patchy landscapes where traditional trends of structural development over time are not apparent or obscured by high plot-level variability.

Intra-pixel variability and scale incompatibility between vegetation patterns, plot size, and plot spatial locations may also contribute to poor predictions of vegetation structure. Forest islands vary in size and shape, but generally have high edge to area ratios. Many of the community types and forest age cohorts in the study area can occur in patches and inter-patch lengths of less than 10 m (Figure 2.10), while plots were 7.32 m in radius. Edgy forest stands, combined with random location of plots, can result in overlap of forest and non-forest vegetation types with plots that would increase structural variability regardless of stand age, confounding patterns of structural development over time. This would suggest higher prediction accuracy could be achieved using either small plots, or recording intra-plot variability in vegetation composition and structure (i.e. stem and condition class mapping).

Unlike other structural attributes, tree height was strongly related to tree age. Curiously, maximum and 95th percentile height were not selected as explanatory variables in CCA models of the vegetation structure matrix, even though they would likely improve prediction accuracy of plot-level maximum and mean age. This may be a consequence of modeling multiple vegetation attributes at once using CCA (rather than modeling tree age in relation to height independently), since other attributes such as basal area or stand density may not be associated with maximum vegetation height and stand age. Modeling stand age or other structural attributes as single variables could yield superior predictions, yet single variable models lose information about co-occurrence of multiple variables within samples (Mouer and Stage 1995, Gottfried et al. 1998). While this loss of information is often in reference to single versus multiple species, it is likely that vegetation structural attributes also lose co-occurrence information when analyzed separately. This study suggests it may not be possible to accurately map tree establishment history and other metrics of vegetation structure within the same modeling framework, and separate mapping approaches may be needed to optimizing prediction accuracy for different variables, questions, and a given variable or question of interest.

Gradients of Vegetation Composition and Prediction Accuracy

GNN predictions of species composition varied by growth form, with high accuracy for tree species, moderate accuracy for shrubs, variable accuracy for forbs, and low accuracy for graminoids. Species gradients were largely associated with spectral variables from SPOT5 imagery and LiDAR-derived topographic variables, but LiDAR-derived variables of vegetation structure were important as well. Previous research has demonstrated the value of LiDAR derived topographic variables in vegetation and habitat classification (Gottfried et al. 1998, Chust et al. 2008). This study shows vegetation height data can be important in mapping species occurrence in heterogeneous landscapes, but it is the combination of LiDAR-derived topography variables describing species geographic niche, spectral data from satellite imagery differentiating species by their foliar absorption and reflectance, and LiDAR-derived vegetation height data differentiating species by growth form which provides the greatest predictive accuracy.

GNN predictions of understory and non-forest vegetation groups were moderately successful, but over predicted dry forb communities in areas likely to be wet sedge, low forb, mountain-heather, and tall shrub groups. Potential causes of poor classification include: scale incompatibilities between vegetation patterns and data sources like those mentioned for predicting vegetation structure, mapped variable co-registration problems, the use of presence/absence data, mixed pixel composition, and plot arrangement in the landscape. SPOT5 bands 1-3 were pan-sharpened from 10 m pixels and the mid IR band 4 was pan-sharpened from 20 m, so much of the spectral information is in fact at 10 and 20 m resolutions. Vegetation groups in the study area can occur in patches and inter-patch lengths of less than 10 m, resulting in pixels of mixed category identification, which can confound ecotone mapping (Hill et al 2007). Predictions of species used presence-absence data in the CCA, rather than the percent cover of species in each plot. Many species such as *Vaccinium deliciosum*, *Carex nigricans*, and *Cassiope mertensiana* were ubiquitous across the landscape, but varied greatly in their abundance. Commonly present species with highly variable cover may drive vegetation type misclassification, because presence-absence data is less useful for detecting more subtle differences between groups or sites (Lesica et al. 1991). Vegetation type prediction could potentially be improved within a predictive mapping approach by fuzzy classification (Gopal et al. 1999), or post-hoc development of vegetation types from joint occurrences of predicted percent cover for individual species (Martin et al. 2003), since the GNN method conserves species data at the plot level. Despite limitations of vegetation type classification, the species mapping presented in this study is a great improvement over traditional landcover classification which would classify the study area vegetation as forest, shrubs, grassland, and rock land cover. Predictive mapping can therefore provide a more complete picture of species abundance and distributions across landscapes such as the FTE, yet because it relies on field plot data to input into maps, it still requires field sampling, which can be costly in remote and mountainous FTE landscapes.

Implications for Monitoring and Inventory Methodology of the FTE

Integrating field inventories with remotely sensed imagery is increasingly used to improve inventories and monitoring of natural resources at multiple spatial scales. Predictive mapping of vegetation composition and structure has proven valuable for spatially extrapolating plot-based inventories across large regions (Ohmann and Gregory 2002, Tomppo 2006). This study found predictive mapping methods utilizing LiDAR data can also be applied with mixed success at fine scales to inventory and quantify change in heterogeneous and potentially sensitive landscapes such as the FTE. Spatial characterizations of tree establishment from predictive mapping can quantify the rates and extent of treeline movement and subalpine meadow invasion, potentially improving our understanding of meadow encroachment and treeline movement in response to climate change, disturbance history, and land use change. Predictions of species distributions could improve biological data used to model how species distributions and biodiversity may change in the future due to climate change. However, the use of predictive mapping at fine spatial scales is relatively unproven, so potential limitations of fine-scale predictive mapping products and the field data used in them need to be understood.

Limitations of fine-scale FTE predictive mapping which relies on plot data included a lack of recent tree establishment, and low accuracy predictions of many metrics of vegetation structure such as stand density and basal area, which likely result from asynchronous vegetation development over time and scale incompatibility between plot data and vegetation patterns. Predictive mapping accuracy may also be uniquely influenced by sample design strategies of field data. The GNN method preserves the range of variability in field data used in imputation, so missing or incomplete data (in this study tree regeneration was recorded but not aged) can be propagated as errors in predicted maps that may not be apparent to the end user without an understanding of the data these maps are derived from. Predictive mapping generates landscape-level estimates and also can be used for pattern detection of FTE change over time, in contrast to most ecological research, natural resource inventories, and environmental monitoring which are often singularly interested in either pattern detection or reducing error variance in parameter estimates. Predictive mapping may be especially attractive in the FTE and other habitat types traditional inventory programs may under sample due to their small and discontinuous land cover, yet are important biodiversity hotspots, potentially sensitive to the effects of climate change, or are high value recreation areas.

Sample design strategy (location, sample size, and plot size) will influence pattern detection and parameter estimates, and an optimal design for pattern detection can be suboptimal for parameter estimation (Kenkel et al. 1989), while field sampling design can be additionally constrained by non-statistical considerations such as financial costs and other logistic and historic considerations (Frayer and Furnival 1999). The value of mapping is to make inferences at scales where plot density is low, and characterize spatial patterns of ecological or resource attributes. These issues may be compounded for fine-scale predictive mapping, which may have to rely on limited subsets of existing inventories or new inventories with limited sample size; in contrast to predictive mapping at large spatial scales which can rely on very large plot numbers (Tomppo 1991, Ohmann and Gregory 2002, Tomppo et al. 2008).

Effects of sample size were not specifically addressed in this study, but relatively small increases in species detected occurred with over 40 plots, suggesting the sample size of this study was adequate to capture species richness within the study area (Figure 2.11). It is less certain if sample size was adequate to capture spatial patterns of all response variables, which may be especially important when response variables are spatially autocorrelated (Fortin et al. 1989). Prediction uncertainty was associated with increased geographic distance to field plots, suggesting the GNN predictions may also be influenced by the spatial arrangement of plots on the landscape. Mapping accuracy in landscapes with spatially autocorrelated vegetation patterns can be sensitive to the spatial distribution of plots, with clustered and random plot distributions more capable of detecting spatial patterns then systematic samples (Fortin et al. 1989). This suggests a potential conflict between improved detection of spatial structure provided by clustered and randomized sampling, versus improved geographic representation from systematic and stratified sampling approaches (Scott et al. 2005). Stratification can be more cost effective means of estimating parameters compared to random or clustered sampling, but can propagate new spatial errors by incorrectly stratifying along a low number of explanatory gradients, result in unbiased parameter estimates, risk circular logic when using vegetation strata when predictions are also vegetation types, and serious hamper the ability to detect change in the attributes of interest (Orlóci 1978, Kenkel et al. 1989, Fortin and Legendre 1989). Systematic sampling has traditionally been viewed as easier and most cost effective to establish than randomized plots, but recent widespread availability of inexpensive GIS and GPS systems can enable easy assignment and location of randomized plot coordinates. A potential compromise between random clustered sampling and systematic and stratified sampling in data for predictive mapping would be to cluster plots in a geographically stratified randomized design (where clusters of plots are randomly places within systematic geographic subsets of the study area). This approach may avoid bias and circularity problems associated with stratified and systematic sampling, improve geographic distribution of plots compared to random sampling, while still retain the clustered design for detection of auto correlated vegetation pattern and randomization for unbiased parameter estimation. In national inventory programs such as the USDA Forest Service Forest Inventory and Analysis Program, this is a key component of plot location (Bechtold and Patterson 2005). However local scale inventories rarely consider plot spatial distribution. Further investigation of the roles sample design and sample density have on fine scale predictive mapping accuracy could optimize costly field data placement if inventory and monitoring programs intend to utilize predictive mapping approaches in the future.

Acknowledgements

Funding for this research was provided by the USDA Forest Service, Pacific Northwest Research Station, Forest Inventory and Analysis Program; The Native Plant Society of Oregon, and the Hoener Memorial Fellowship program at the College of Forestry, Oregon State University. Special thanks to Dan Irvine for field data collection and tree core dating, Emilie Grossman and Matt Gregory for assistance with GNN computer code, and Keith Olsen for additional GIS assistance.

LITERATURE CITIED

Allen, T.R., and Walsh, S.J. 1996. Spatial and compositional pattern of alpine treeline, Glacier National Park, Montana. Photogrammetric Engineering and Remote Sensing 62: 1261-1268.

Araújo, M.B., and Guisan, A. 2006. Five (or so) challenges for species distribution modeling. Journal of Biogeography 33: 1677-1688.

Baker, B.B., Moseley, R.K. 2007. Advancing treeline and retreating glaciers: implications for conservation in Yunnan, P.R. China. Arctic, Antarctic, and Alpine Research 39: 200-209.

Barry, R.G. 1981. Mountain weather and climate. Methuen, London.

Bechtold, W.A., and Patterson, P.L. [eds]. 2005. The enhanced forest inventory and analysis program – National sampling design and estimation procedures. General Technical Report SRS-80. U.S.D.A Forest Service, Southern Research Station, Ashville, NC.

Bekker, M.F. 2005. Positive feedback between tree establishment and patterns of subalpine forest advancement, Glacial National Park, Montana, U.S.A. Arctic, Antarctic, and Alpine Research 37: 97-107.

Beyer, H. L. 2004. Hawth's Analysis Tools for ArcGIS. Available at http://www.spatialecology.com/htools.

Bonan, G.B., Pollard, D., and Thompson, S.L. 1992. Effects of boreal forest vegetation on global climate. Nature 359: 716-718.

Bormann, F.H., and Likens, G.E. 1979. Pattern and process in a forested ecosystem. Spring, New York, 253 pp.

Brown, D.G. 1994. Predicting vegetation types at treeline using topography and biophysical disturbance variables. Journal of Vegetation Science 5: 641-656.

Cannone, N., Sgorbati, S., and Guglielmin, M. 2007. Unexpected impacts of climate change on alpine vegetation. Frontiers in Ecology and Evolution 5: 360-364.

Campbell, A.G. 1973. Vegetative ecology of Hunt’s Cove, Mt. Jefferson, Oregon. Master’s Thesis, Oregon State University. pp 89.

CEC. 1994. CORINE land cover. Technical guide. Luxembourg (Office for Official Publications of European Communities).

Chuby, M.S., Franklin, S.E., and Wulder, M.A. 2006. Object-based analysis of Ikonos-2 imagery for extraction of forest inventory parameters. Photogrammetric Engineering and Remote Sensing. 72: 383-394.

Chust, G., Galparoso, I., Borja, A., Franco, J., and Uriarte, A. 2008. Coastal and estuarine habitat mapping, using LIDAR height and intensity and multi-spectral imagery. Estuarine, Coastal and Shelf Science 78: 633-643.

Cohen, J. 1960. A coefficient of agreement for nominal scales. Educational and Psychological Measurement 20: 37-36.

Coville, F. 1898. Forest growth and sheep grazing in theCascade Mountains of Oregon. USDA Division of Forestry Bulletin 15, Washington, DC.

Crookston, N.L., Finley, A.O. 2007. yaImpute: An R package for k-NN imputation. Journal of Statistical Software 23: 1-16.

Daniels, L.D., and Veblen, T.T. 2006. Spatiotemporal influences of climate on altitudinal treeline in Northern Patagonia. Ecology 85: 1284-1296.

Dearden, P., and Seawell, W.R.D. 1983. From gloom to glory and beyond: The North American mountain recreation experience. Bayfield, N.G., and Aitken, R. (eds). In: The ecological impacts of outdoor recreation on mountain areas in Europe and North America. Recreation Ecology Research Group Report No. 9. Wye, UK.

Devi, N., Hagedorn, F., Moiseev, P., Bugmann, H., Shiyatov, S., Mazepa, V., Rigling, A. 2008. Expanding forests and changing growth forms of Siberian larch at the polar Urals treeline during the 20th century. Global Change Biology 14: 1581-1591.

Didier, L. 2001. Invasion patterns of European larch and Swiss stone pine in subalpine pastures in the French Alps. Forest Ecology and Management 145: 67-77.

Dirnböck, T., Dullinger, S., and Grabherr, G. 2003. A regional impact assessment of climate and land-use change on alpine vegetation. Journal of Biogeography 30:
401-417.

Dufrene, M., and Legendre, P. 1997. Species assemblages and indicator species: the need for a flexible asymmetrical approach. Ecological Monographs 67: 345-366.

Dullinger, S., Dirnbock, T., and Grabherr, G. 2004. Modeling climate change-driven treeline shifts: relative effects of temperature increase, dispersal and invisibility. Journal of Ecology 92: 241-252.

Dyurgerov, M.B., and Meier, M.F. 2002. Twentieth century climate change: evidence from small glaciers. Proceeding of the National Academy of Sciences 97: 1406-1411.

Foley, J.A., Levis, S., Costa, M.H., Cramer, W., and Pollard, D. 2000. Incorporating dynamic vegetation cover within global climate models. Ecological Applications 10: 1620-1632.

Fortin, M-J. Drapeau, P., and Legendre, P. 1989. Spatial autocorrelation and sampling design in plant ecology. Vegatatio 83: 209-222.

Franklin, J.F., Moir, W.H., Douglas, G.W., and Wiberg, C. 1971. Invasion of subalpine meadows by trees in the Cascade Range, Washington and Oregon. Arctic, Antarctic, and Alpine Research 3: 215-224.

Franklin, J.F., and Dyrness, C.T. 1988. Natural vegetation of Oregon and Washington. Oregon State University Press, Corvallis, Oregon, USA.

Franklin, J.F., Spies, T.A., Van Pelt, R., Carey, A.B., Thornburgh, D.A., Rae Berg, D., Lindenmayer, D.B., Harmon, M.E., Keeton, W.S., Shaw, D.C., Bible, K., and Chen, J. 2002. Disturbances and structural development of natural forest ecosystems with silvicultural implications, using Douglas-fir forests as an example. Forest Ecology and Management 155: 399-423.

Frayer, W.E., and Furnival, G.M. 1999. Forest survey sampling designs: a history. Journal of Forestry 97: 4-10.

Guisan, A., Edwards, T.C., and Hastie, T. 2002. Generalized linear and generalized additive models in studies of species distributions: setting the scene. Ecological Modeling 157: 89-100.

Gamache, I., Payette, S. 2005. Latitudinal response of subarctic tree lines to recent climate change in eastern Canada. Journal of Biogeography 32: 849-862.

Gehrig-Fasel, J., Guisan, A., and Zimmerman, N.E. 2007. Tree line shifts in the Swiss Alps: climate change or land abandonment? Journal of Vegetation Science 18: 571-582.

Germino, M.J., Smith, W.K., and Resor, A.C. 2002. Conifer seedling distribution and survival in an alpine-treeline ecotone. Plant Ecology 162: 157-168.

Gopal, S., Woodcock, C.E., and Strahler, A.H. 1999. Fussy neural network classification of global land cover from the 1° AVHHRR data set. Remote Sensing of Environment 67: 230-243.

Gottfried, M., Pauli, H.P., Reiter, K., and Grabherr, G. 1998. A fine-scaled predictive model for changes in species distribution patterns of high mountain plants induced by climate warming. Diversity and Distributions 5: 241-251.

Grace, J. 1989. Tree Lines. Philosophical Transactions of the Royal Society of London. Series B, Biological Sciences 324(1223): 233-243.

Hallett, D.J., Lepofsky, D.S., Mathewes, R.W., and Lertzman, K.P. 2003. 11000 years of fire history and climate in the mountain hemlock rain forests of southwestern British Columbia based on sedimentary charcoal. Canadian Journal of Forest Research 33: 292-312.

Halloy, S.R.P., and Mark, A.F. 2003. Climate-change effects on alpine plant biodiversity: A New Zealand perspective on quantifying the threat. Arctic, Antarctic, and Alpine Research 35: 248-254.

Halpern, C.B., Smith, B.G., and Franklin, J.F. 1984. Composition, structure, and distribution of the ecosystems of the Three Sisters Biosphere Reserve/Wilderness Area. A final report of the United States Department of Agriculture.

Hansen, M.C., Defries, R.S., Townshend, J.R.G., and Sohlberg, R. 2000. Global land cover classification at 1 km spatial resolution using a classification tree approach. International Journal of Remote Sensing 21: 1331-1364.

Hardt, R.A., and Forman, R.T.T. 1989. Boundary form effects on woody colonization of reclaimed surface mines. Ecology 70: 1252-1260.

Harsch, M.A., Hulme, P.E., McGlone, M.S., and Duncan, R.P. 2009. Are treelines advancing? A global meta-analysis of treeline response to climate warming. Ecology Letters 12: 1040-1049.

Hill, R., Granica, K., Smith, G.M., Schardt, M. 2007. Representation of an alpine treeline ecotone in SPOT 5 HRG data. Remote Sensing of Environment 110: 458-467.

Hodge, E.T. 1925. Geology of Mt. Jefferson. Mazama 7: 25-58.

Holtmeier, F.K. 2003. Mountain timberlines: ecology, patchiness, and dynamics. Kluwer Academic Publishers.

Holtmeier, F.K., and Broll, G. 2005. Sensitivity and response of northern hemisphere altitudinal and polar treelines to environment change at landscape and local scales. Global Ecology and Biogeography 14: 395-410.

Homer, C., Huang, C., Yang, L., Wylie, B., and Coan, M. 2004. Development of a 2001 national land-cover database for the United States. Photogrammetric Engineering and Remote Sensing 70: 829-840.

Homer, C., Dewitz, J., Fry, J., Coan, M., Hossain, N., Larson, C., Herold, N., McKerrow, A., VanDriel, J.N., and Wickham, J. 2007. Completion of the 2001 national land cover database for the conterminous United States. Photogrammetric Engineering and Remote Sensing 73: 337-341.

Hudak, A.T., Crookston, N.L., Evans, J.S., Hall, D.E., and Falkowski, M.J. 2008. Nearest neighbor imputation of species-level, plot-scale forest structure attributes from LiDAR data. Remote Sensing of Environment 112: 2232-2245.

Ishii, H., Reynolds, J.H., Ford, E.D., and Shaw, D. 2000. Height growth and vertical development of an old-growth Pseudotsuga-Tsuga forest in southwestern Washington Stata, U.S.A. Canadian Journal of Forest Research 30: 17-24.

Jakubauskas, M.A. 1996. Thematic mapper characterization of lodgepole pine seral stages in Yellowstone National Park, USA. Remote Sensing of Environment 56: 118-132.

Jansen, E., Overpeck, J., Briffa, K.R., Duplessy, J.C., Joos, F., Masson-Delmotte, V., Olago, D., Otto-Bliesner, B., Peltier, W.R., Rahmstorf, S., Ramesh, R., Raynaud, D., Rind, D., Solomina, O., Villalba, R., and Zhang, D. 2007. Palaeoclimate. In: Climate change 2007: The physical science basis. Contribution of working group 1 to the Fourth Assessment Report of the Intergovernmental Panel on Climate Change [Solomon, S., D. Qin, M. Manning, Z. Chen, M. Marquis, K.B. Averyt, M. Tignor, and H.L. Miller (eds.)]. Cambridge University Press, United Kingdom and New York, NY, USA.

Jobbágy, E.G., Jackson, R.B. 2000. Global controls of forest line elevation in the northern and southern hemispheres. Global Ecology and Biogeography 9: 253-268.

Johnston, C.A., and Bonde, J. 1989. Quantitative analysis of ecotones using a geographic information system. Photogrammetric Engineering and Remote Sensing 55: 1643-1647.

Kadmon, R., Farber, O., and Danin, A. 2003. A systematic analysis of factors affecting the performance of climatic envelope models. Ecological Applications 13: 853-867.

Kenkel, N.C., Juhász-Nagy, P., and Podani, J. 1989. On sampling procedures in population and community ecology. Vegetatio 83: 195-207.

Kennedy, R.E., and Cohen, W.B. 2003. Automated designation of tie-points for image-to-image coregistration. International Journal of Remote Sensing. 24: 3467-3490.

Kennedy, R.E., Cohen, W.B., Schroeder, T.A. 2007. Trajectory-based change detection for automated characterization of forest disturbance dynamics. Remote Sensing of Environment 110: 370-386.

Körner, C. 1998. A re-assessment of high elevation treeline positions and their explanation. *Oecologia* 115: 445-459.

Körner, C. 2000. Biosphere responses to CO2 enrichment. *Ecological Applications,* 10: 1590-1619.

Körner, C. 2003. Alpine plant life: Functional plant ecology of high mountain ecosystems, 2nd ed. Springer, Berlin.

Krajina, V. J. 1969. Ecology of forest trees in British Columbia. *In* Ecology of western North America. vol. 2. p. 1-147. V. J. Krajina, ed. University of British Columbia, Department of Biology. Vancouver, BC.

Kuhns, J.C. 1917. G-Reconnaissance-Cascade. Report to theForest Supervisor. Supervisor's Office, Willamette National Forest, Eugene, OR.

Kuramoto, R.T., and Bliss, L.C. 1970. Ecology of subalpine meadows in the Olympic Mountains, Washington. Ecological Monographs 40: 317-347.

Lafleur, P.M., Griffis, T.J., and Rouse, W.R. 2001. Interannual variability in net ecosystem CO 2 exchange at the arctic treeline. Arctic, Antarctic, and Alpine Research. 33: 149-157.

Larocque, S.J., and Smith, D.J. 2003. Little Ice Age glacial activity in the Mt. Waddington area, British Columbia Coast Mountains, Canada. Canadian Journal of Earth Science 40: 1413-1436.

Larson, A.J., Lutz, J.A., Gersonde, R.F., Franklin, J.F., and Hietpas, F.F. 2008. Potential site productivity influences the rate of forest structural development. Ecological Applications 18: 899-910.

Lefsky, M.A., Cohen, W.B., Acker, S.A., Parker, G.G., Spies, T.A., and Harding, D. 1999. Lidar remote sensing of the canopy structure and biophysical properties of Douglas-fir western hemlock forests. Remote Sensing and Environment 70: 339-361.

Lefsky, M.A., Cohen, W.B., Parker, G.G., Harding, D.J. 2002. Lidar remote sensing for ecosystem studies. Bioscience 52: 19-30.

Lesica, P., McCune, B., Cooper, S.V., and Hong, W.S. 1991. Differences in lichen and bryophyte communities between old-growth and managed second-growth forests in the Swan Valley, Montana. Canadian Journal of Botany 69: 1745-1755.

Lertzman, K.P., and Krebs, C.J. 1991. Gap-phase structure of a subalpine old-growth forest. Canadian Journal of Forest Research 21: 1730-1741.

Lewis, D.H., and Smith, D.J. 2004. Little Ice Age glacial activity in Strathcona Provincial Park, Vancouver Island, British Columbia, Canada. Canadian Journal of Earth Science 41: 285-297.

Lloyd, A.H., and Graumlich, L.J. 1997. Holocene dynamics of treeline forests in the Sierra Nevada. Ecology 78: 1199-1210.

Luckman, B.H. 2000. The Little Ice Age in the Canadian Rockies. Geomorphology 32: 357-384.

Maher, E.L., Germino, M.J., Hasselquist, N.L. 2005. Interactive effects of tree and herb cover on survivorship, physiology, and microclimate of conifer seedlings at the alpine tree-line ecotone. Canadian Journal of Forest Research 35: 567-574.

Martin, K., Chytry, M., and Tichy, L. 2003. Formalized reproduction of an expert-based phytosociological classification: A case study of subalpine tall-forb vegetation. Journal of Vegetation Science 14: 601-610.

Martínez-Meyer, E. 2006. Climate change and biodiversity: Some considerations in forecasting shifts in species potential distributions. Biodiversity Informatics 2: 42-55.

Masek, J.G. 2001. Stability of boreal forest stands during recent climate change: evidence from Landsat satellite imagery. Journal of Biogeography 28: 967-976.

McCune, B. 1997. Influence of noisy environmental data on canonical correspondence analysis. Ecology 78: 2617-2623.

McCune, B. 2006. Non-parametric habitat models with automatic interactions. Journal of Vegetation Science 17: 819-830.

McCune, B., and Grace, J.B. 2002. Analysis of ecological communities. MjM Software, Gleneden Beach, Oregon.

McDonald, G.D. 1995. Changes in mass of Collier Glacier, Oregon, 1910-1994. M.S. Thesis, Oregon State University, Corvallis, OR.

McDonald, G.D. 1998. Soil survey of Warm Springs Indian Reservation, Oregon. U.S. Department of Agriculture and Natural Resources Conservation Service. Washington, D.C.

McGaughey, R.J. 2007. FUSION/LDV: Software for LIDAR data analysis and visualization. U.S. Department of Agriculture, Forest Service, Pacific Northwest Research Station.

Mihai, B., Savulescu, I., and Sandric, I. 2007. Change detection (1986-2002) of the vegetation cover in Romania. Mountain Research and Development 27: 250-258.

Miller, E.A. and Halpern, C.B. 1998. Effects of environment and grazing disturbance on tree establishment in meadows of the central Cascade Range, Oregon, USA. Journal of Vegetation Science 9: 265-282.

Minchin, P.R. 1987. An evaluation of the relative robustness of techniques for ecological ordination. Vegatatio 69: 89-107.

Minore, D. 1979. Comparative autecological characteristics of northwestern tree species—a literature review. USDA For. Serv. Gen. Tech. Rep. PNW-87. 72 p.

Mouer, M. and Stage, A.R. 1995. Most similar neighbor: an improved sampling inference procedure for natural resource planning. Forest Science 41: 337-359.

Neter, J., Kutner, M.H., Nachtsheim, C.J., and Wasserman, W. 1996. Applied linear statistical models, 4th edition. WCB McGraw-Hill. Boston.

North, M., Chen, J., Oakley, B., Song, B., Rudnicki, M., Gray, A., and Innes, J. 2004. Forest stand structure and patterns of old-growth western hemlock/douglas-fir and mixed conifer forests. Forest Science 50: 299-311.

O'Connor, J.E., and Costa, J.E. 1993. Geologic and hydrologic hazards in glacierized basins in North America reslting from 19th and 20th century global warming. Natural Hazards 8: 121-140.

O’Connor, J.E., Hardison, J.H. III, and Costa, J.E. 2001. Debris flows from failures of neoglacial-age moraine damns in the Three Sisters and Mount Jefferson Wilderness Areas, Oregon. U.S. Geoligcal Survey Profession Paper 1606.

Ohmann, J.L., and Gregory, M.J. 2002. Predictive mapping of forest composition and structure with direct gradient analysis and nearest-neighbor imputation in coastal Oregon, U.S.A. Canadian Journal of Forest Research 32: 725-741.

Ohmann, J.L., and Spies, T.A. 1998. Regional gradient analysis and spatial pattern of woody plant communities of Oregon forests. Ecological Monographs 68: 151-182.

Oksanen, J., Kindt, R., Legendre, P., O’Hara, B., Simpson, G.L., Solymos, P., Stevens, M.H.H., and Wagner, H. 2008. vegan: Community ecology package. R package version 1.15-1. http://cran.r-project.org/

Oliver, C.D., and Larson, B.C. 1996. Forest stand dynamics. John Wiley & Sons, New York.

Oregon Tourist and Information Bureau. 1921. Oregon Skyline Trail: Mt. Hood to Crater Lake [map]. Scale not given. Portland, OR: Oregon Tourist and Information Bureau.

Orloci, L. 1978. Multivariate analysis in vegetation research 2nd ed. Dr. W. Junk B.V., The Hague

Packee, E.C., Oliver, C.D., and Crawford, P.D. 1981. Ecology of pacific silver fir. *In* Proceedings of the Biology and Management of True Fir in the Pacific Northwest Symposium. p. 19-34. C.D. Oliver and R.M. Kenady , eds. University of Washington, College of Forest Resources, U.S.D.A. Forest Service, Pacific Northwest Forest and Range Experiment Station (Seattle, WA, Portland, OR)

Peel, M.C., Finlayson, B.L., amd McMahon, T.A. 2007. Updated world map of the Köppen-Geiger climate classification. Hydrology and Earth System Sciences Discussions 4: 439-473.

Price, M.F. 1985. Impacts of recreational activities on alpine vegetation in western North America. Mountain Research and Development 5: 263-277.

Prichard, S.J., Peterson, D.L., Hammer, R.D. 2000. Carbon distribution in subalpine forests and meadows of the Olympic Mountains, Washington. Soil Science Society of America Journal 64: 1834-1845.

R Development Core Team. 2009. R: A language and environment for statistical computing. R Foundation for Statistical Computing. Vienna, Austria.

Rakestraw, L., Rakestraw, M. 1991. History of the Willamette National Forest. USDA Willamette National Forest, Eugene, OR.

Rochefort, M.R., and Peterson, D.L. 1996. Temporal and spatial distribution of trees in subalpine meadows of Mount Rainier National Park, Washington, U.S.A. Arctic and Alpine Research 28: 52-59.

Roland, J., and Matter, S.F. 2007. Encroaching forests decouple alpine butterfly population dynamics. Proceedings of the National Academy of Sciences of the United States of America. 104: 13702-13704.

Rudnicki, M., and Chen, J. 2000. Relations of climate and radial increment of western hemlock in an old-growth Douglas-fir forest in southern Washington. Northwest Science 74: 57-68.

Scott, W.E. 1977. Quaternary glaciation and volcanism, Metolius river area, Oregon. Geological Society of America Bulletin 88: 113-124.

Scott, C.T., Bechtold, W.A., Reams, G.A., Smith, W.D., Westfall, J.A., Hansen, M.H., and Moisen, G.G. 2005. Sample-based estimators used by the forest inventory and analysis national information management system. *In:* Bechtold, W.A. and Patterson, P.L. (eds). The enhanced forest inventory and analysis program – National sampling design and estimation procedures. General Technical Report SRS-80, Southern Research Station, USDA Forest Service. Accessed on December 2, 2009 at http://www.treesearch.fs.fed.us/pubs/20371

Solomon, A.M. and Kirilenko, A.P. 1997. Climate change and terrestrial biomass: What if the trees do not migrate. Global Ecology and Biogeochemical Letters 6: 139-148.

Spies, T.A., Franklin, J.F. 1991. The structure of natural young,mature, and old-growth Douglas-fir forests. In: Ruggiero, L.F., Aubry, K.B., Carey, A.B., Huff, M.H. (Eds.), Wildlife and Vegetation of Unmanaged Douglas-fir Forests. USDA Forest Service General Technical Report PNW-GTR-285, pp. 91–110.

Spot Image Corp 2008. Preprocessing levels and location accuracy. Accessed on September 14, 2008 at http://www.spotimage.com/web/en/224-technical-information.php

ter Braak, C.J.F. 1986. Canonical correspondence analysis: a new eigenvector technique for multivariate direct gradient analysis. Ecology 67: 1167-1179.

ter Braak, C.J.F., and Prentice, I.C. 1988. A theory of gradient analysis. Advances in Ecological Research 18: 271-313.

Tolvanen, A., Forbes, B., Wall, S., and Norokorpi, Y. 2005. Recreation at treeline and interactions with other land-use activities. In: Wielgolaski, F.E., Karlsson, P.S., Neuvonene, S.S., and Thannheiser, D. (eds). Plant ecology, herbivory, and human impact in Nordic mountain birch forests. Ecological studies Vol. 180. Springer-Verlag, Berlin. 203-217.

Tomppo, E. 1991. Satellite image based national forest inventory of Finland. International Archives of Photogrammetry and Remote Sensing 28: 419-424.

Tomppo, E. 2006. The Finnish multi-source National Forest Inventory – small area estimation and map production. In: Kangas, A. & Maltamo, M. (eds.). Forest inventory. Methodology and applications. Managing Forest Ecosystems. Vol 10. Springer, Dordrecht. P. 195-224.

Tomppo, E., Olson, H., Ståhl, G., Nilsson, M., Hagner, O., and Katila, M. 2008. Combining national forest inventory field plots and remote sensing data for forest databases. Remote Sensing of Environment 112: 1982-1999.

Tranquillini, W. 1979. Physiological ecology of the alpine timberline: tree existence at high altitudes with special reference to the European Alps. Springer-Verlag, New York.

Turner, M.G., Baker, W.L., Peterson, C.J., and Peet, R.K. 1998. Factors influencing succession: lessons from large, infrequent natural disturbances. Ecosystems 1: 511-523.

Urban, D., Goslee, S., Pierce, K., and Lookingbill, T. 2002. Extending community ecology to landscapes. Ecoscience 9: 200-212

Vierling, K.T., Vierling, L.A., Gould, W.A., Martinuzzi, S., Clawges, R.M. 2008. Lidar: shedding new light on habitat characterization and modeling. Frontiers in Ecology and Environment 6: 90-98.

Vogelmann, J.E., S.M. Howard, L. Yang, C. R. Larson, B. K. Wylie, and J. N. Van Driel, 2001, Completion of the 1990's National Land Cover Data Set for the conterminous United States, Photogrammetric Engineering and Remote Sensing 67:650-662.

Walder, J.S., Gardner, C.A., Conrey, R.M., Fisher, B.J., Schilling, S.P. 1999. Volcano hazards in the Mount Jefferson region, Oregon. U.S. Geological Survey Open-File Report 99-24.

Wallentin, G., Tappeiner, U., Strobl, J., and Tasser, E. 2008. Understanding alpine tree line dynamics: an individual-based model. Ecological Modelling 218: 235-246.

Wardle, P, and Coleman, M.C. 1992. Evidence for rising upper limits of four native New Zealand forest trees. New Zealand Journal of Botany 30: 303-314.

Wing, M.G., Karsky, R. 2006. Standard and real-time accuracy and reliability of a mapping-grade GPS in a coniferous western Oregon forest. Western Journal of Applied Forestry 21: 222-227.

Wimberly, M.C., and Spies, T.A. 2001. Modeling landscape patterns of understory tree regeneration in the Pacific Northwest, USA. Applied Vegetation Science 4: 277-286.

Woodward, A., Schreiner, E.G., and Silsbee, D.G. 1995. Climate, geography, and tree establishment in subalpine meadows of the Olympic Mountains, Washington, U.S.A. Arctic and Alpine Research 27:217-225.

Zald, H.S.J. 2008. Extent and spatial patterns of grass bald land cover change (1948 – 2000), Oregon Coast Range, USA. Plant Ecology 201: 517-529

Zald, H.S.J. 2010. Seedling establishment in a subalpine parkland landscape controlled by interactions of topography, seed source, disturbance and climate, oregon cascades, USA. In: Patterns of Tree Establishment and Vegetation Composition in a Subalpine Meadow Landscape, Jefferson Park, Oregon, USA. Ph.D. Dissertation, Oregon State University, Corvallis, OR.

Zimble, D.A., Evans, D.L., Carlson, G.C., Parker, R.C., Grado, S.C., and Gerard, P.D. 2003. Characterizing vertical forest structure using small-footprint airborne LiDAR. Remote Sensing of Environment 87: 171-182.

Table 2.1. Tree, shrub, forb, and graminoid species recorded on plots, their species codes, and frequency.

Growth form	Scientific Name	Code	Frequency (n=98)	Growth form	Scientific Name	Code	Frequency (n=98)
Tree	*Abies amabilis*	ABAM	66	Forb	*Antennaria alpina*	ANAL	22
	Abies concolor	ABCO	8		*Arenaria capillaris*	ARCA	16
	Abies lasiocarpa	ABLA	4		*Aster alpigenus*	ASAL	85
	Callitropsis nootkatensis	CANO	4		*Aster foliaceus*	ASFO	2
	Pinus albicaulis	PIAL	25		*Caltha leptosepala*	CALE	6
	Pinus contorta	PICO	3		*Castilleja parviflora orepola*	CAPA	64
	Tsuga mertensiana	TSME	86		*Dodecatheon jefferyi*	DOJE	23
					Epilobium alpinum	EPAL	13
Shrub	*Cassiope mertensiana*	CAME	70		*Epilobium angustifolium*	EPAN	2
	Kalmia microphylla	KAMI	32		*Eriogonum umbellatum*	ERUM	5
	Phyllodoce empetriformis	PHEM	86		*Gentiana calycosa*	GECA	34
	Rhododendron albiflorum	RHAL	3		*Hieracium gracile*	HIGR	53
	Rubus lasiococcus	RULA	2		*Hypericum anagalloides*	HYAN	2
	Salix commutata	SACO	2		*Ligusticum grayi*	LIGR	55
	Sorbus sitchensis	SOSI	37		*Lupinus arcticus*	LUAR	17
	Vaccinium deliciosum	VADE	81		*Luetkea pectinata*	LUPE	84
	Vaccinium membranaceum	VAME	25		*Lycopodium sitchense*	LYSI	33
					Microseris alpestris	MIAL	8
Graminoid	*Carex aquatilis*	CAAQ	10		*Microseris borealis*	MIBO	7
	Carex nigricans	CANI	89		*Pedicularis bracteosa*	PEBR	2
	Carex spectabilis	CASP	57		*Plantanthera stricta*	PLST	2
	Festuca sp.	FESTU	10		*Potentilla flabellifolia*	POFL	11
	Juncus drummondii	JUDR	55		*Polygonum newberryi*	PONE	8
	Juncus mertensianus	JUME	9		*Saxifraga ferruginea*	SAFE	9
	Luzula sp.	LUZUL	3		*Saxifraga tolmiei*	SATO	6
	Poa sp.	POA	9		*Senecio triangularis*	SETR	4
					Tofieldia glutinosa	TOGL	2
					Veratrum vIride	VEVI	6
					Veronica wormskjoldii	VEWO	2
					Xerophyllum tenax	XETE	3

Table 2.2. Mapped explanatory variables used in the gradient nearest neighbor method.

Variable class and code	Definition
Topography derived from LiDAR	
ELEV	Elevation (m), from 5 m digital elevation model (DEM)
SLOPE	Slope (percent), from 5 m DEM
ASPECT	Cosine transformation of aspect (degrees) (Beers et al. 1966) 0.0 (southwest) to 2.0 (northeast), from 5 m DEM
RAD	Growing season Potential Relative Radiation (Pierce et al. 2005) June - September, from 5 m DEM
TOPO300	Topographic position index, difference between sample elevation and mean elevation 150 - 300 m from the sample
TOPO100	Topographic position index, 50 - 100 m from sample
TOPO30	Topographic position index, 15 - 30 m from sample
TOPO10	Topographic position index, 5 - 10 m from sample
Vegetation Structure derived from LiDAR	
VMAX	Maximum vegetation height (m)
VMIN	Minimum vegetation height (m)
VMEAN	Mean vegetation height (m)
VSTDEV	Standard deviation of vegetation height (m)
VCV	Coefficient of variation of vegetation height (m)
VRNG	Range of vegetation hieght (m)
VCOV	Percent vegetation cover greater than 3 m tall
VP05	5th percentile of vegetation height (m)
VP10	10th percentile of vegetation height (m)
VP25	25th percentile of vegetation height (m)
VP50	50th percentile (median) of vegetation height (m)
VP75	75th percentile of vegetation height (m)
VP90	90th percentile of vegetation height (m)
VP95	95th percentile of vegetation height (m)
SPOT 5 HRG Satellite Imagery	
PAN	Panchromatic band (0.48 - 0.71 µm), 5 m spatial resolution
B1	Band 1 (green, 0.50 - 0.59 µm), 10 m spatial resoution (pan-sharpened to 5 m)
B2	Band 2 (red, 0.61 - 0.68 µm), 10 m spatial resoution (pan-sharpened to 5 m)
B3	Band 3 (near-infrared, 0.79 - 0.89 µm), 10 m spatial resoution (pan-sharpened to 5 m)
B4	Band 4 (mid-infrared, 1.58 - 1.75 µm), 20 m spatial resoution (pan-sharpened to 5 m)
R32	Ratio of B3 to B2, pan-sharpened to 5 m
VI	Vegetation Index (B3 - B2), pan-sharpened to 5 m
NDVI	Normalized Difference Vegetation Index (B3 - B2) / (B3 + B2), pan-sharpened to 5 m
Geomorphology	
LANDFORM	Binary, with debris flow (1) and glacial (0) landforms
Location	
X	Easting in UTM NAD83 Zone 10N (m)
Y	Northing in UTM NAD83 Zone 10N (m)

Table 2.3. Explanatory variable subsets used in canonical correspondence analysis of species composition and vegetation structure.

Subsets of explanatory variables	Explanatory variable type			
	SPOT5 imagery	LiDAR-derived topography	LiDAR-derived vegetation structure	Landform type
1	X			
2		X		
3			X	
4				X
5	X			X
6	X	X		X
7	X		X	X
8		X	X	X
9	X	X	X	X

Note: Mapped explanatory variables described in Table 2.2.

Table 2.4. Amount of variation in response data described by the environmental variables (percent of total inertia), and number of explanatory variables selected, by subsets of explanatory variables in stepwise canonical correspondence analysis of species composition and vegetation structure.

	Proportion of total inertia			
Subset of explantory variables	compostion	nvars	structure	nvars
SPOT5	20.1	4	13.6	2
LiDAR-derived topography	20.2	6	18.8	8
LiDAR-derived vegetation structure	9.9	2	37.5	6
landform	6.8	1	3.7	1
SPOT 5 + landform	21.8	5	13.6	2
SPOT 5 + landform + LiDAR-derived topography	34.4	11	22.2	4
SPOT 5 + landform + LiDAR-derived veg structure	32.2	9	37.5	6
landform + LiDAR-derived topography + LiDAR-derived veg structure	28.4	7	39.5	6
All explantory variable subsets combined	38.6	12	39.5	6

Table 2.5. Descriptive statistics comparing observed (n = 98 plots) and predicted vegetation structure attributes

Vegetation attribute	Mean	Range	SD
Total basal area (m2/ha)			
Observed	3.89	0 - 70.34	9.84
Predicted	4.56	0 - 70.34	9.11
Stand density (trees/ha)			
Observed	147.58	0 - 1130.52	231.60
Predicted	167.13	0 - 1130.52	261.06
Quadratic mean diameter (cm)			
Observed	8.63	0 - 110.48	15.19
Predicted	10.18	0 - 110.48	14.27
Regeneration density (trees/ha)			
Observed	1818.89	0 - 16358.34	2664.92
Predicted	2193.07	0 - 16358.34	3297.47
Age of stand initiation (years)			
Observed	99.92	0 - 411	100.41
Predicted	129.01	0 - 411	124.00
Stand mean age (years)			
Observed	63.10	0 - 239.5	55.86
Predicted	75.41	0 - 239.5	62.90

Table 2.6. Plot-level overall classification accuracy, kappa statistic (K) and assympotic errors of kappa for GNN mapped species predictions.

Vegetation Type	Species	Species Code	Overall accuracy	K	ASE	Vegetation Type	Species	Species Code	Overall accuracy	K	ASE
Overstory	*All*	O_ALL	0.81	0.52	0.10	Forbs	*Antennaria alpina*	ANAL	0.77	0.36	0.12
trees	*Tsuga mertensiana*	O_TSME	0.84	0.57	0.10		*Arenaria capillaris*	ARCA	0.78	0.22	0.15
	Abies amabilis	O_ABAM	0.88	0.53	0.13		*Aster alpigenous*	ASAL	0.88	0.47	0.14
	Abies lasiocarpa	O_ABLA	0.97	-0.01	0.58		*Aster foliaceus*	ASFO	0.98	0.00	0.70
	Callitropsis nootkatensis	O_CANO	0.99	0.00	0.99		*Caltha leptosepala*	CALE	0.98	0.79	0.15
							Castilleja parviflora	CAPA	0.68	0.28	0.11
Tree	*All*	U_ALL	0.85	0.39	0.14		*Dodecatheon jeffreyii*	DOJE	0.73	0.30	0.12
regeneration	*Tsuga mertensiana*	U_TSME	0.86	0.45	0.14		*Epilobium alpinum*	EPAL	0.79	0.04	0.19
	Abies amabilis	U_ABAM	0.70	0.37	0.10		*Epilobium angustifolium*	EPAN	0.96	-0.02	0.50
	Abies lasiocarpa	U_ABLA	0.81	-0.10	0.23		*Eriogonum umbellatum*	ERUM	0.98	0.79	0.15
	Callitropsis nootkatensis	U_CANO	0.93	0.33	0.24		*Gentian calycosa*	GECA	0.67	0.30	0.10
	Pinus albicaulis	U_PIAL	0.70	0.14	0.13		*Hieracium gracile*	HIGR	0.57	0.15	0.10
	Pinuc contorta	U_PICO	0.95	-0.03	0.45		*Hypericum anagalloides*	HYAN	0.99	0.79	0.20
							Ligusticum grayii	LIGR	0.62	0.22	0.10
Shrubs	*Cassiope mertensiana*	CAME	0.78	0.44	0.11		*Lupinus arcticus*	LUAR	0.92	0.69	0.11
	Kalmia microphylla	KAMI	0.79	0.52	0.09		*Luetkea pectinata*	LUPE	0.77	0.01	0.18
	Phyllodoce empetriformis	PHEM	0.87	0.31	0.18		*Lycopodium sitchensis*	LYSI	0.56	0.05	0.11
	Rhododendron albiflorum	RHAL	0.94	-0.03	0.41		*Microseris alpestris*	MIAL	0.89	0.21	0.23
	Rubus lasiococcus	RULA	0.98	0.49	0.36		*Microseris borealis*	MIBO	0.92	0.29	0.24
	Salix commutata	SACO	0.97	-0.01	0.58		*Pedicularis bracteosa*	PEBR	0.98	0.49	0.36
	Sorbus sitchensis	SOSI	0.70	0.37	0.10		*Plantanthera stricta*	PLST	0.99	0.79	0.20
	Vaccinium deliciosum	VADE	0.82	0.29	0.15		*Potentilla flabellifolia*	POFL	0.85	0.26	0.18
	Vaccinium membranaceum	VAME	0.86	0.61	0.10		*Polygonum newberryi*	PONE	0.94	0.59	0.16
							Saxifraga ferruginea	SAFE	0.94	0.54	0.18
Graminoids	*Carex aquatilis*	CAAQ	0.81	0.07	0.19		*Saxifraga tolmeii*	SATO	0.97	0.71	0.16
	Carex nigricans	CANI	0.86	0.05	0.24		*Senecio triangularis*	SETR	0.97	0.56	0.25
	Carex spectabilis	CASP	0.53	0.07	0.10		*Tofieldia glutinosa*	TOGL	0.99	0.79	0.20
	Festuca sp.	FESTU	0.79	-0.12	0.22		*Veratrum viride*	VEVI	0.93	-0.04	0.38
	Juncus drummondii	JUDR	0.62	0.23	0.10		*Veronica wormskjoldii*	VEWO	0.99	0.79	0.20
	Juncus mertensianus	JUME	0.93	0.55	0.16		*Xerophyllum tenax*	XETE	0.98	0.66	0.24
	Luzula sp.	LUZUL	0.92	-0.04	0.35						
	Poa sp.	POA	0.78	-0.12	0.21	Vegetation	well drained sparse forbs	GRP1	0.71	0.33	0.11
						groups	low wet forbs	GRP2	0.84	0.24	0.17
							pink mountain-heather shrub	GRP3	0.78	0.38	0.12
							white mountain-heather shrub	GRP4	0.89	0.29	0.20
							tall mountain-ash shrub	GRP5	0.93	0.19	0.30
							wet sedge meadow	GRP6	0.78	0.31	0.13

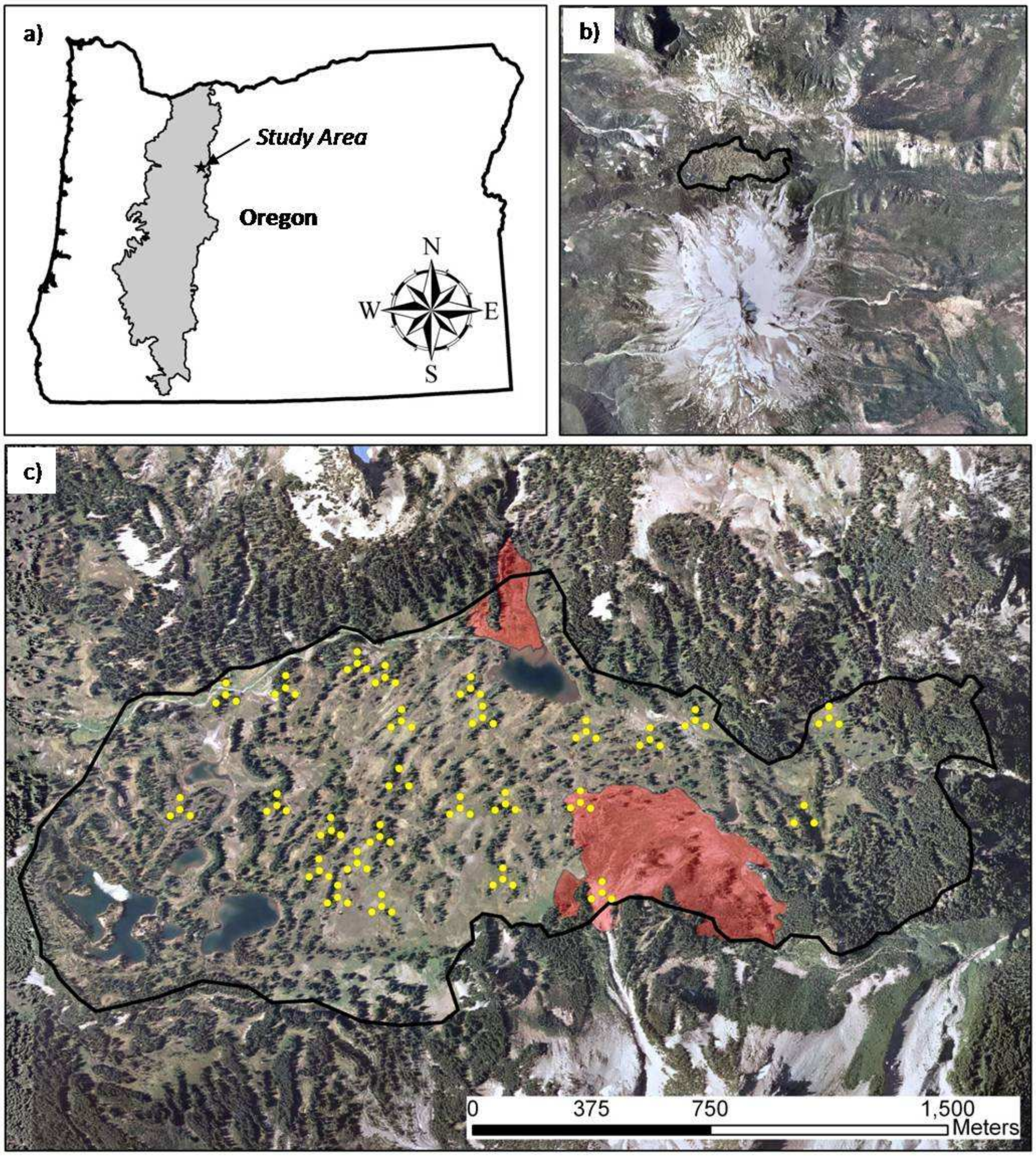

Figure 2.1. The study area location within the State of Oregon (a), with the Oregon Cascades ecoregion shaded in gray. The study area outlined in black in relation to Mount Jefferson (b). An enlarged image of the study area (c), with plot locations as yellow circles and debris flow landforms shaded red.

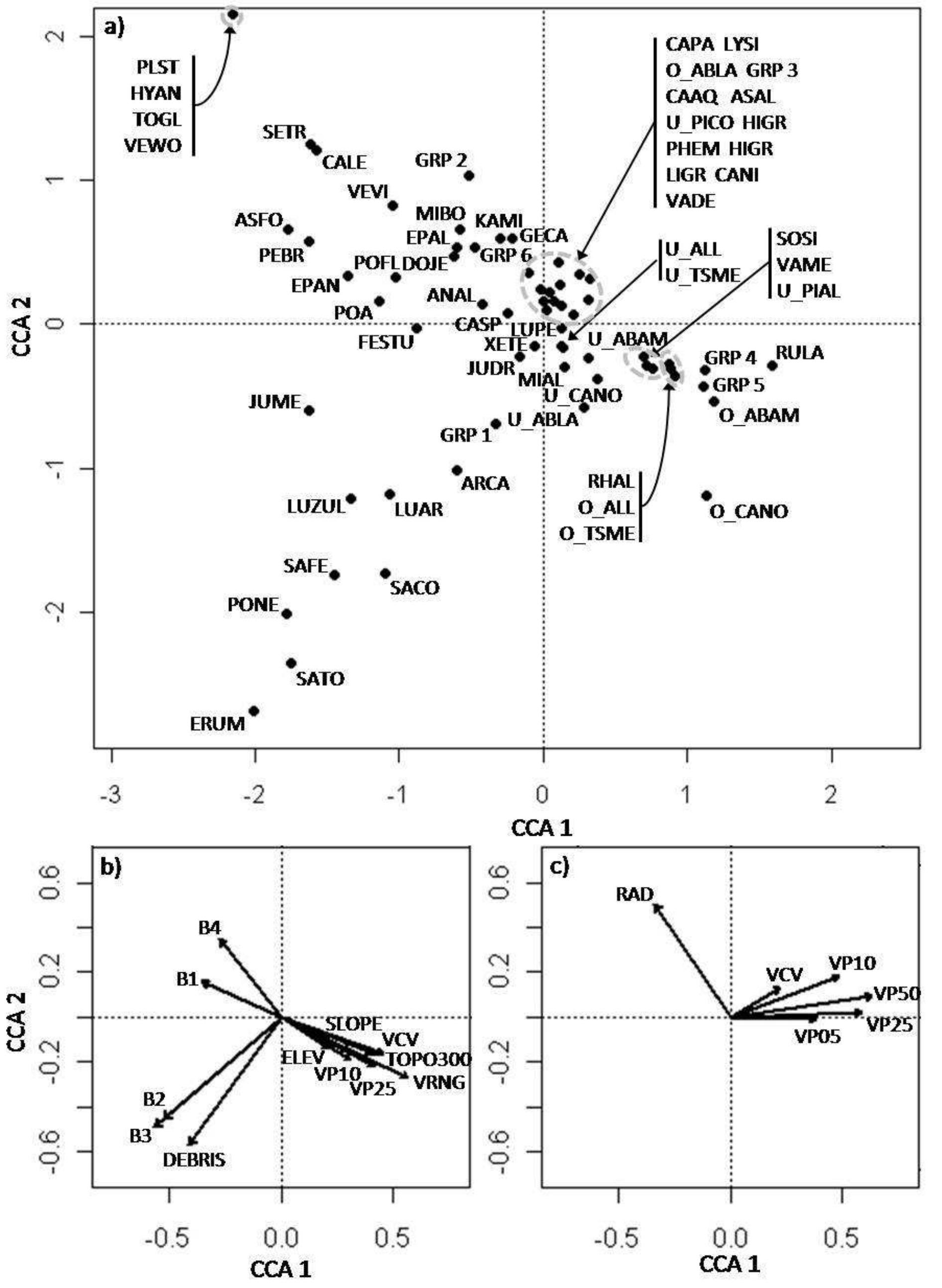

Figure 2.2. Biplots and ordinations showing associations between vegetation and explanatory variables from canonical correspondence analysis (CCA). (a) Species centroids in relation to the CCA axes and explanatory variables. (b) Explanatory variable biplot for species composition ordination (see Table 2.2 for variable definitions). (c) Explanatory biplot for vegetation structure ordination, centroids of vegetation structure variables were not plotted since structure variables were not categorical. Vector length and position in biplots indicates the strength and direction of correlation between explanatory variables and CCA axes.

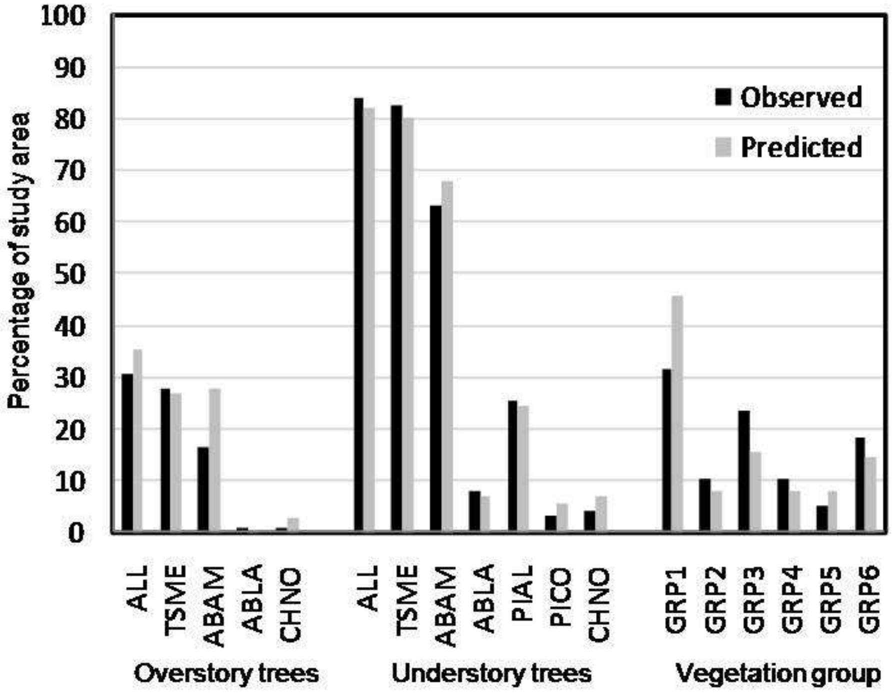

Figure 2.3. Predicted versus observed proportions of the study by overstory species, understory species, and vegetation groups. Overstory , understory, and vegetation group proportions are not mutually exclusive. See the study area description or Appendix A for descriptions of vegetation groups.

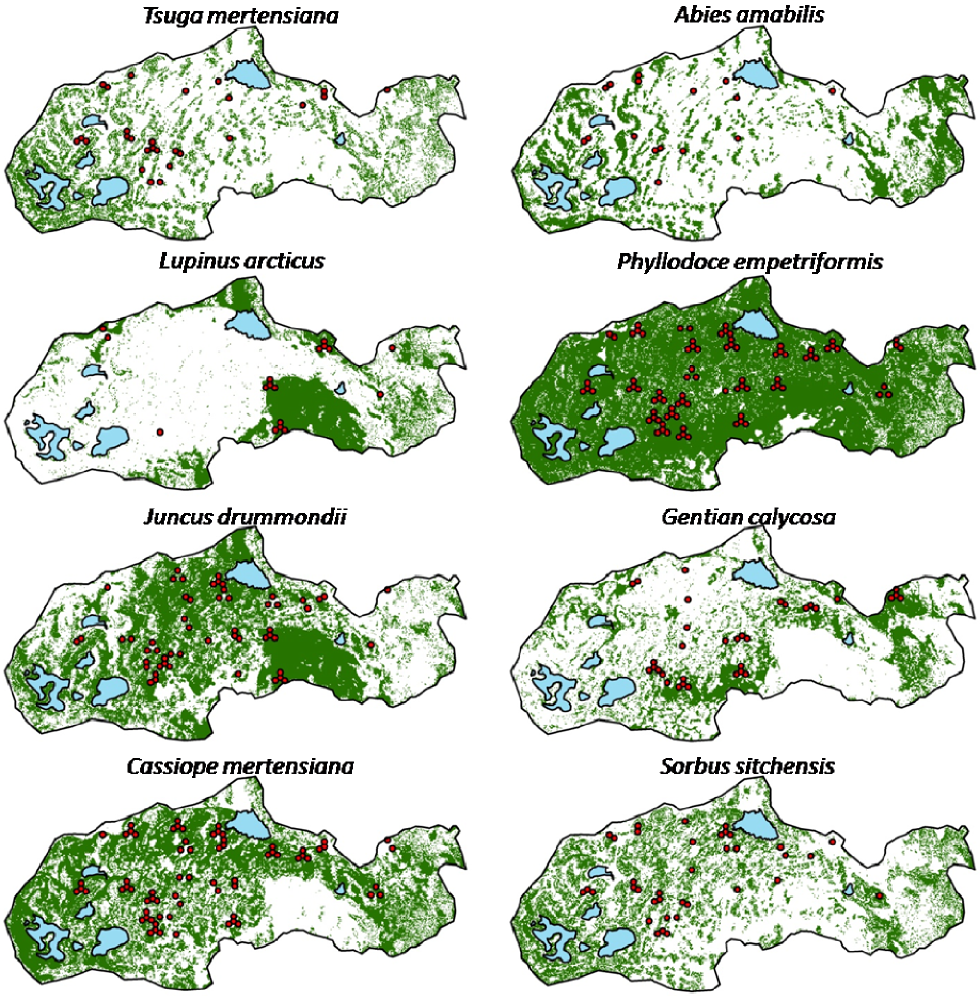

Figure 2.4. Predicted occurrence of selected species (shaded in green). Red circles are field plots where the species was observed. Lakes are light blue.

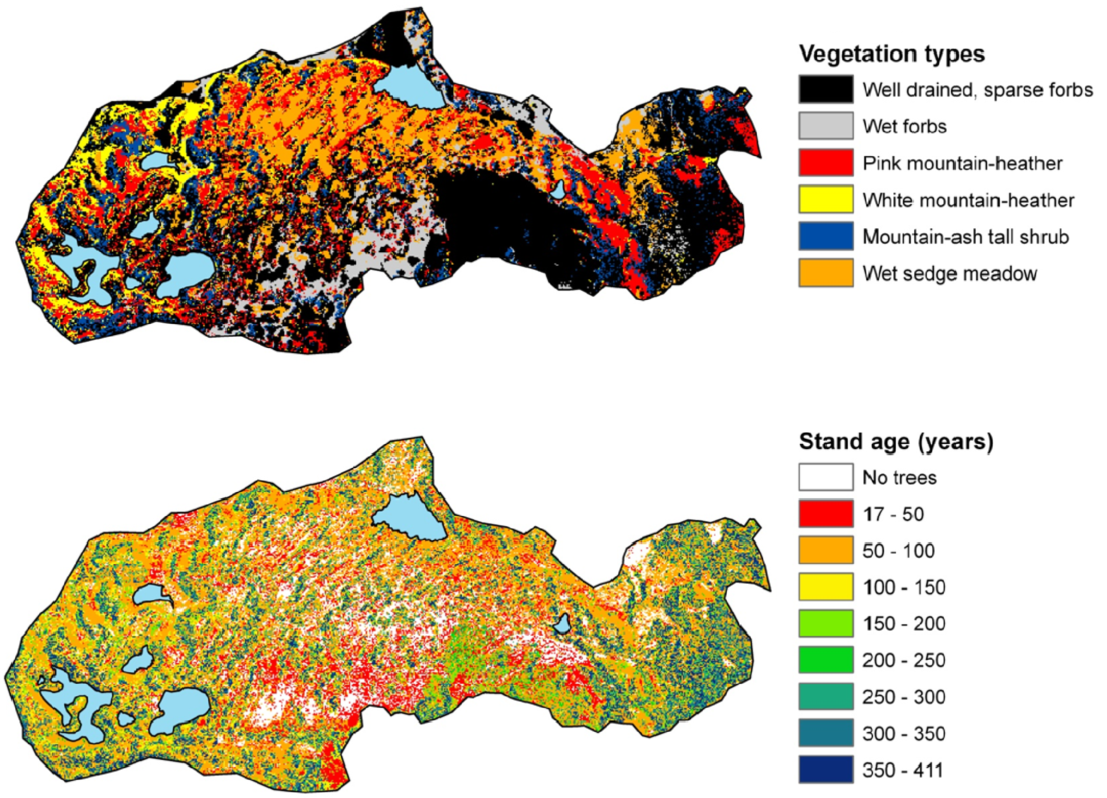

Figure 2.5. GNN predictions of vegetation groups (top) and stand initiation age (bottom). Lakes are light blue.

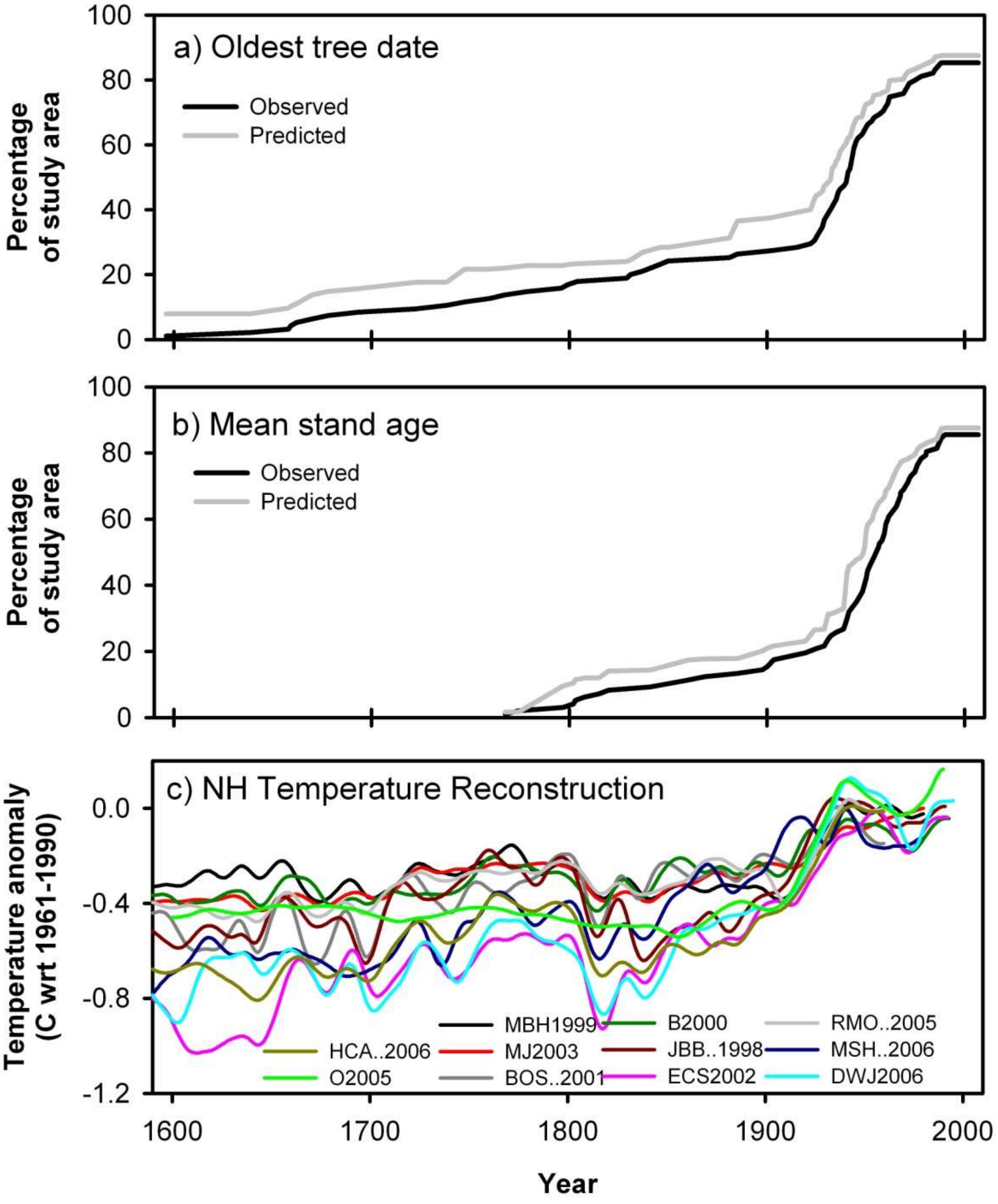

Figure 2.6. The predicted versus observed proportion of the study area occupied by (a) oldest tree age, and (b) mean tree age in relation to long term Northern Hemisphere temperature proxy reconstruction anomalies (c). Temperature reconstructions modified from Jansen et al. (2007), Figure 6.10.

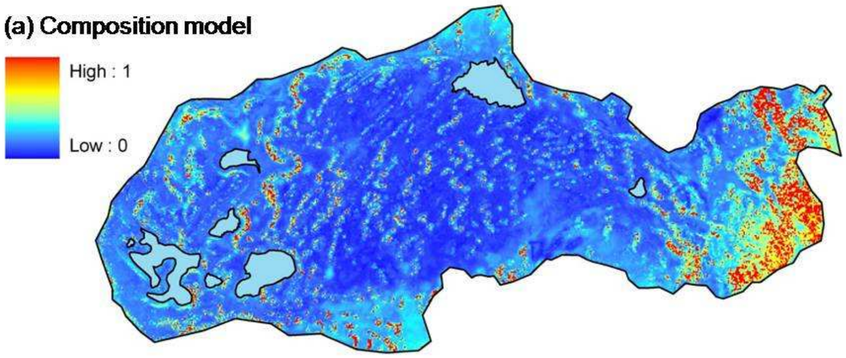

(a) Composition model

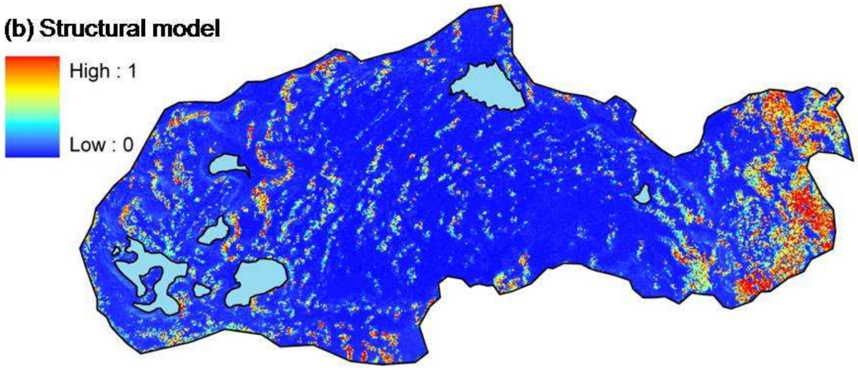

(b) Structural model

Figure 2.7. Nearest-neighbor distances for the (a) composition model and (b) structure model. Distances are Euclidean in eight-dimensional gradient space based on the first eight axes in the canonical correspondence analyses. Distance to each axis is weighted by its eigenvalue. Nearest neighbor distances are a proxy for prediction uncertainty, higher nearest neighbor distances indicating increased prediction uncertainty.

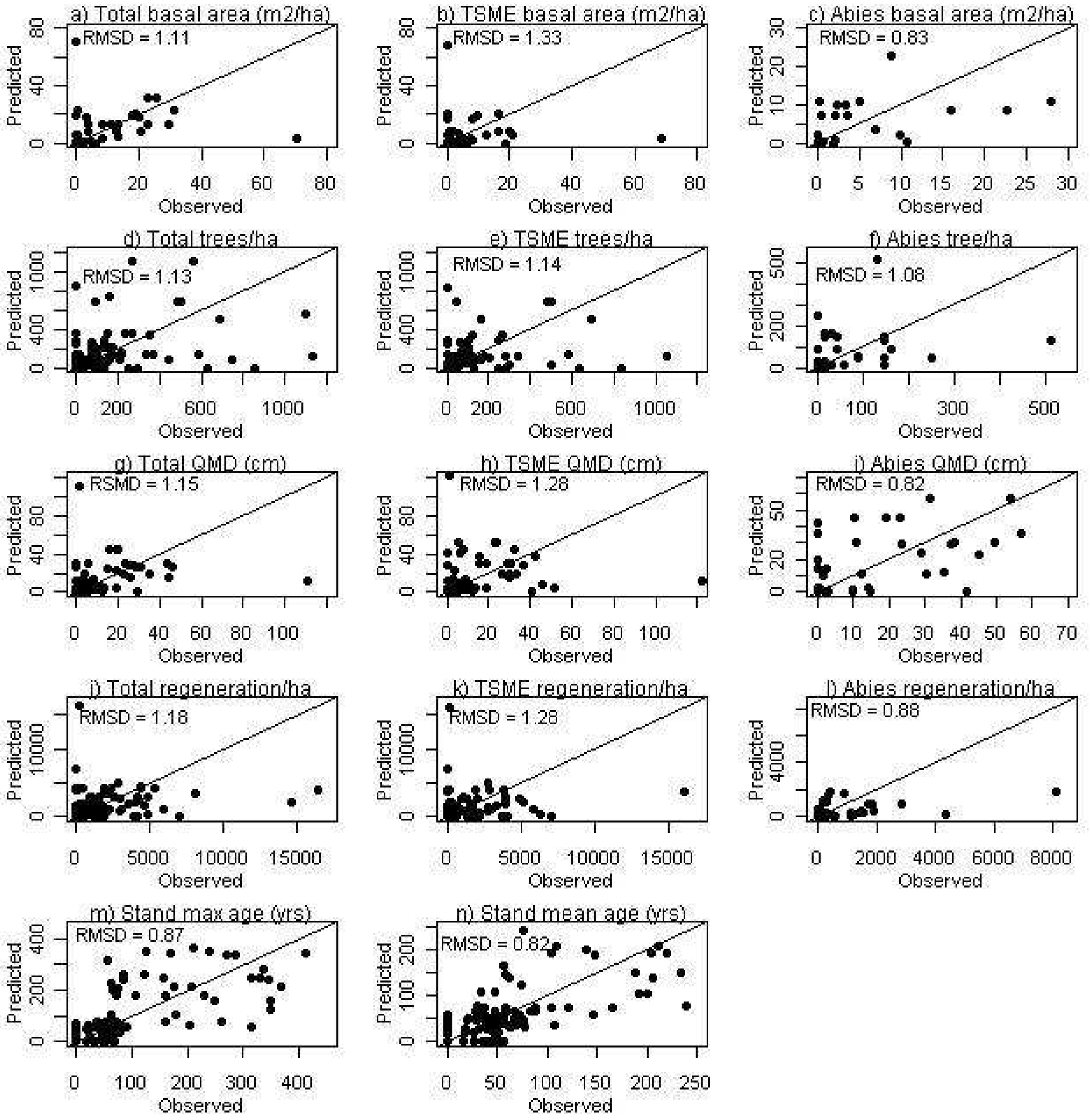

Figure 2.8. Comparison of predictions to plot observations of vegetation structure variables on n = 98 field plots. (a -c) Total, hemlock, and fir tree basal area (m2/ha) .(d –f) Total, hemlock, and fir stand density (trees/ha). (g – i) Total, hemlock, and fir tree quadratic mean diameter (QMD, cm). (j – l) Total, hemlock, and fir regeneration density (trees/ha). (m – n) Maximum and mean stand age in years.

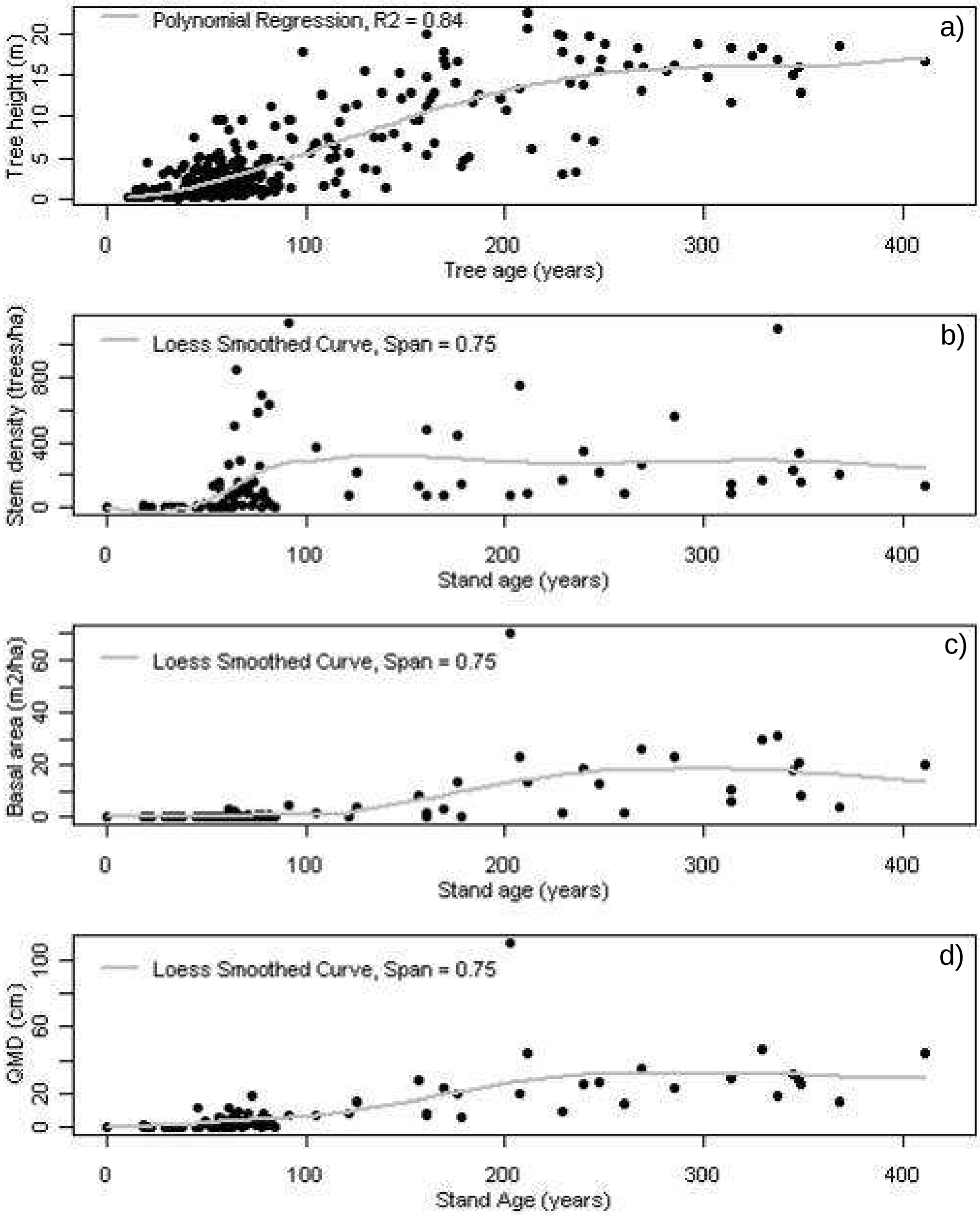

Figure 2.9. Comparison of (a) tree height, (b) stand density, (c) basal area, and (d) quadratic mean diameter (QMD) in relation to years since stand initiation. Gray lines of structural attributes in relation to stand age are fitted values for a third order polynomial regression in (a), and fitted LOESS regression curves for (b-d).

Figure 2.10. Photo within the Jefferson Park study area showing fine-scale patterns of vegetation groups. From left to right, vegetation grades from wet sedge meadow to pink mountain-heather shrub, to a mountain hemlock (Tsuga mertensiana) dominated tree island. Foreground scale is approximately 10 m across the image. Photo facing southwest, Mount Jefferson is in the background.

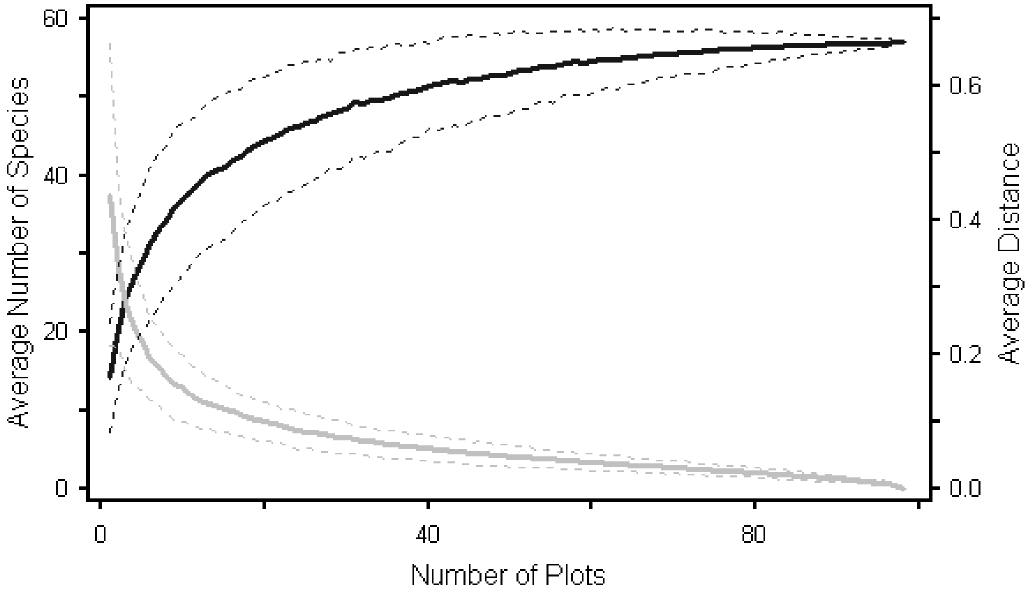

Figure 2.11. Species-area curve (solid black line) used to assess sample adequacy based of repeated subsampling of 98 plots and 57 species. Dotted black lines represent ± 1 standard deviation. The distance curve (solid gray line) describes the average Sorensen distance between subsamples and the whole sample, as a function of subsample size.

CHAPTER 3: SEEDLING ESTABLISHMENT IN A SUBALPINE PARKLAND LANDSCAPE CONTROLLED BY INTERACTIONS OF TOPOGRAPHY, SEED SOURCE, DISTURBANCE AND CLIMATE, OREGON CASCADES, USA.

ABSTRACT

Over the past five decades, FTE movement and tree invasion into alpine and subalpine meadows has been documented at many locations throughout the Northern Hemisphere. Relationships between temperature and FTE position suggest regional to global treeline shifts in response to climate change. However, treeline movement and meadow invasion are driven by tree regeneration processes, which are influenced by climatic, physical and biological factors at multiple spatial scales. This study utilized airborne Light Detection and Ranging (LiDAR), geo-referenced field plots, and tree establishment reconstructions to quantify spatiotemporal patterns of tree invasion in relation to landform types, fine-scale topographic variability, late season snow persistence, distances from potential seed sources, and climate variation in a subalpine parkland landscape in the Oregon Cascades, USA. The number of sites occupied by trees increased from 7.75% of the study area in 1950 to 34.7% in 2007. Landform types and finer-scale patterns of topography and vegetation structure nested within landforms influenced summer snow depth, which influenced temporal and spatial patterns of tree establishment. The rate of tree invasion was higher on the debris flow landform which has lower summer snow depth, suggesting potentially rapid treeline responses to disturbance events. Tree invasion rates were strongly associated with reduced annual snow fall on glacial landforms, but not on debris flows. Tree establishment was spatially constrained to micro sites with high topographic positions and close proximity to overstory canopy associated with low summer snow depth. Seed source limitations placed an additional species-specific spatial constraint on where trees invaded meadows. Climate and topography had an interactive effect, with trees establishing on higher topographic positions during both high snow/low temperature and low snow/high temperature periods, but had greater than expected establishment on lower topographic positions during low snow/high temperature periods. Within the context of lerger landform types, topography, and proximity to overstory trees placed constraints on where trees established in the meadows, even during favorable climate periods. Results of this study suggest large scale climate-driven models of vegetation change

may overestimate treeline movement and meadow invasion because they do not account for biophysical controls limiting tree establishment at multiple spatial scales.

INTRODUCTION

Subalpine parklands and treelines (also referred to as the forest-tundra ecotone, or FTE) are transitional areas between forested and alpine ecosystems. FTE positions are globally associated with thermal deficiencies limiting plant growth, implying that increased temperatures will result in FTE movement (Grace 1989, Körner 1998, Jobbágy and Jackson 2000). Contemporary FTE movement has been variable, but has occurred across a diverse range of geographic locations, climatic zones, and taxonomic groups, suggesting a global ecological phenomenon in response to climate change (Harsch et al. 2009). Changes in FTE positions and reductions of alpine and arctic vegetation may impacts surface radiation balance, ecosystem productivity and carbon sequestration, species distributions, and biodiversity (Bonan et al. 1992, Solomon et al. 1997, Foley et al. 2000, Körner 2000, Prichard et al. 2000, Halloy and Mark 2003, Dirnböck et al. 2003, Cannone et al. 2007). The magnitude of these varied ecological effects will be heavily influenced by temporal rates and spatial extent of FTE movement, which is fundamentally determined by seed-based regeneration processes (Lescop-Sinclair and Payette 1995, Smith et al. 2003).

Although often referred to as a “line”, the FTE is often a transitional area whose complexity increases from global to local spatial scales, resulting in landscape mosaics containing elements of both forest and tundra ecosystems (Holtmeier and Broll 2005). FTE positions may be thermally limited globally, but a variety of biophysical factors become important at finer scales (Körner 1998), emphasizing the importance of spatial scale in detecting patterns and determining driving factors in ecosystems (Wiens 1989, Levin 1992). FTE position and movement have largely been studied in relation to global and regional factors such as climate and land use change (Körner 1998, Gehring-Fasel et al. 2007, Batllori and Gutiérrez 2008); or local biophysical factors such as topography, regeneration ecology, seed source dispersal, competition, autogenic site modification, and disturbance (Germino et al. 2002, Bekker 2005, Dovčiak et al. 2008, Stueve et al. 2009). However the interactive effects of large-scale climate and local-scale biophysical factors on tree establishment in the FTE have received much less attention and are poorly understood (although see Kupfer and Cairns 1996, Daniels and Veblen 2004).

It is important to understand FTE dynamics in terms of both large-scale climate and local-scale biophysical factors, because vegetation change often results from interactions among climate, topography, biotic interactions, and disturbance (Turner et al. 1989, Urban et al. 2002, Holtmeier and Broll 2005). For example, snow pack depth and late season snow persistence have been observed to control FTE tree establishment in the Pacific Northwest region of North America (Fonda and Bliss 1969, Franklin et al. 1974). Snow pack in the Pacific Northwest is driven by large-scale temperature and circulation patterns (Mote 2003, Mote et al. 2005), but regional topography and climate interact, modifying snow pack depth and persistence, resulting in different patterns an temporal patterns of FTE tree establishment during different climatic regimes (Woodward et al. 1995, Rochefort and Peterson 1996, Miller and Halpern 1998). In addition to climate and topographic factors, seed source, vegetation structure (as modifier of snow depth) and disturbance can strongly influence patterns of FTE tree establishment (Arseneault and Payette 1992, Holtmeier and Broll 1992, Daniels and Veblen 2003, Dovčiak et al. 2008). However, the relative influences and interactions of climate, topography, disturbance, seed sources, and other biophysical controls on FTE dynamics is not well understood.

Heterogeneous FTE landscapes can confound attempts to untangle the multiple climatic and biophysical controls of FTE dynamics, while also making it difficult to estimate the landscape-level extent of FTE movement over time. Ecological research generally focuses on either pattern detection or estimating population parameters, and both sampling decisions and scope of inference often differ between these two objectives (Kenkel et al. 1989). Our understanding of how climate and biophysical drivers influence FTE dynamics has largely been inferred from observational research with pattern detection objectives, with quantification of FTE movement inferred from observations on transects or plots subjectively positioned in relation to a limited number of explanatory variable gradients such as elevation or aspect (Rochefort and Peterson 1996, Lloyd and Graumlich 1997). Since spatial patterns of vegetation are often shaped by multiple drivers and their interactions at varying spatial and temporal scales, observational data collected along a low number of environmental gradients may miss factors important to tree establishment at the FTE, which could result in incorrect inferences of processes from observed patterns . This suggests observations from subjective placement of transects or plots typically cannot be “scaled-up” to make landscape-level estimates of FTE movement or meadow invasion.

The study had two objectives: (1) to characterize changes in landscape pattern of tree establishment in a subalpine meadow complex over time, and (2) to determine how climate and biophysical characteristics interactively control the temporal and spatial patterns of tree establishment in a subalpine parkland landscape at multiple spatial scales. Five major hypotheses were developed:

[1] The areal extent of tree establishment has increased over the past fifty years.

[2] Variation in late season (summer) snow depth is associated with abiotic variables (microtopography and larger-scale landforms), biotic variables (distance to overstory tree canopy), and their interactions.

[3] Spatial patterns of tree establishment, like snow depth, are associated with microtopography, larger-scale landforms, and distance to overstory canopy, as well as distance from potential parent trees (i.e. seed source).

[4] Tree establishment is positively associated with years of low snowfall and increased temperature.

[5] Tree establishment is a function of interactions between regional climate factors and biophysical factors that operate at landscape and local spatial scales. For example, tree establishment will occur during cool and snowy regional climate periods on ridgetops and upper slopes, and on sites with greater potential snow depth (valleys and depressions) during warm and less snowy regional climate periods.

METHODS

Study Area Description

The study was conducted in 260 ha of Jefferson Park (44°42’ N 121°48’ W, 1693 – 1814 m), a subalpine parkland in the Mount Jefferson Wilderness, Willamette National Forest, Oregon, USA (Figure 3.1). The climate is intermediate between Mediterranean and maritime temperate, with dry warm summers and significant winter precipitation (Csb/Cfb) under the Köppen Climate Classification System (Peel et al. 2007). The nearest weather station above 1000 m (Government Camp Station, National Weather Service Cooperative Network #353402, 45°18’ N 121°145’ W, 1213 m, 1951 to 2008 time period), reported annual average maximum and minimum temperatures of 10.2° C and 1.1° C. Annual precipitation averaged 217 cm, the major of which fell as snow between December and April. Comparisons to climate data from three nearby weather stations (Marion Forks, 44°36’N 121°57’W 813 m; Santiam Junction 44°26’N 121°158’W, 1230 m; and Belknap Spring, 44°18’N 122°02’W, 705 m) suggests similar annual variation of temperature and precipitation across the region (Figure 3.2), but Jefferson Park is likely to be colder and have higher snowfall because of its higher elevation.

Jefferson Park contains landforms derived from glacial activity, as well as debris flows originating on the flanks of Mount Jefferson (3,199 m) and Park Butte (2,139 m). During the most recent glacial maxima of the Holocene Epoch, glacial advance and retreat deposited outwash, basal till and ablation till in the study area (Scott 1977). Since the mid-19th century, Cascade Range alpine glacier extent has substantially decreased (O’Connor and Costa 1993, Dyurgerov and Meier 2000). Glacial retreat, combined with steep slopes and loose parent materials, result in the Cascade Range having the highest concentration of neoglacial lakes in the conterminous United States (O’Connor et al. 2001). On August 21st, 1934, a small (~4,000 m^2) moraine dammed lake breached on Mount Jefferson, covering roughly 320,000 m^2 of Jefferson Park with debris 0.3 to 2.4 m deep (O’Connor et al. 2001). Field reconnaissance during 2006 discovered a smaller undocumented debris flow in north Jefferson Park of older but indeterminate age. Soils of the study area are poorly documented, consisting of either rubble derived from ice, colluvium and residuum weathered from sedimentary rock with influences of volcanic ash; or Typic Vitricryands formed in residuum and colluvium from pyroclastic ash flows, andesite, and volcanic ash (MacDonald 1998).

Jefferson Park is within the lower FTE, the transition zone between the upper limit of closed subalpine forest (i.e. timberline) and the beginning of the alpine zone (sensu Körner 2003). Jefferson Park is in the mountain hemlock (*Tsuga mertensiana*) vegetation zone (Franklin and Dyrness 1988). Mountain hemlock and Pacific silver fir (*Abies amabilis*) are the dominant tree species, found in both single species and mixed-species stands. Most of these stands are “islands” of variable size and shape surrounded by meadow vegetation. The oldest trees in these islands date to the 1600’s, and the majority of mature trees are at least 150 years old (Zald 2010a). Subalpine fir (*Abies lasiocarpa*), whitebark pine (*Pinus albicaulis*), lodgepole pine (*Pinus contorta*), and Alaska yellow-cedar (*Callitropsis nootkatensis*) are also present, but in greatly reduced amounts and more restricted spatial distributions. Six vegetation groups were previously identified within the study area (Zald 2010a), and are generally consistent with prior studies of subalpine parklands in the Oregon Cascades (Campbell 1973, Halpern et al. 1984). A dry forb group on well-drained sites (Group 1) was characterized by *Arenaria capillaris*, *Lupinus arcticus*, *Eriogonum umbellatum*, and *Polygonum newberyi*. The pink mountain-heather type (Group 2) included *Phyllodoce empetriformis*, *Luetkia pectinata*, and *Lycopodium sitchensis*. The wet sedge meadow type (Group 3) was characterized by *Carex nigricans* and *Juncus drummondi*. The wet low forb type (Group 4) included *Aster alpiginus*, *Castelija parviflora*, *Festuca sp.*, *Gentian calycosa*, and *Kalmia microphylla*. The white mountain-heather type (Group 5) was characterized by *Cassiope mertensiana* and *Microseris alpestris*. The mountain-ash tall shrub type (Group 6) included *Sorbus sitchensis, Rubus lasiococcus, Vaccinium deliciosum, Ligustrum gracilis, Epibolium alpinum*, *Dodecatheon jeffreyi*, and *Veratrum viride*.

In addition to debris flows livestock grazing may have occurred, although historical records are scarce so it is unclear if sustained heavy grazing occurred in Jefferson Park. Overgrazing in the region at similar elevations and vegetation types can result in soil erosion and reduced plant cover (Kuhns 1917). Grazing was more sustained and of higher intensity in close proximity to driveways (areas designated for sheep movement), and the Skyline Trail driveway was near Jefferson Park (Rakestraw & Rakestraw 1991). Long travel distances and conflicts with recreational users discouraged livestock grazing in Jefferson Park, and access to Jefferson Park via the Skyline Trail was closed to livestock in 1937 (Rakestraw & Rakestraw 1991). Low intensity grazing by recreational pack animals has continued at Jefferson Park to the present. Heavy livestock grazing of FTE and meadow vegetation may either facilitate tree establishment via reduced vegetation competition and exposure of mineral soil, or inhibit tree establishment via direct browsing and trampling of seedlings. Direct experiments are lacking, but prior research suggests grazing suppresses tree establishment at the FTE, and a pulse of increased tree establishment often follows grazing cessation (Miller and Halpern 1998, Didier 2001, Gehring-Fasel et al. 2007). Fire are another potential disturbance in high elevation ecosystems of the region, but are infrequent with fire return intervals in the mountain hemlock zone ranging from centuries to several millennia (Lertzman and Krebs 1991, Hallett et al 2003). Qualitative observations during field plot establishment found no evidence of charred tree boles or biological legacies indicative of past wildfires. Some whitebark pines showed symptoms of white pine blister rust (*Cronartium ribicola*), but otherwise qualitative observations did not find significant tree mortality due to pests or pathogens.

Sampling Design Overview

My previous observations of the study area in 2006 suggest distance to overstory canopy and microtopography influenced late summer snow persistence and tree establishment. However multiple topographic variables (elevation, topographic position, etc.) and overstory canopy trees were spatially autocorrelated, potentially complicating statistical analyses of individual and interactive effects of biophysical characteristics on tree establishment. Spatial autocorrelation would be likely to persist in traditional transect sampling, while transect sampling would also prohibit accurate estimation of landscape-level tree establishment. To overcome these problems, airborne discrete return Light Detection and Ranging (LiDAR) was used to map micro site scale (1 m) topography and vegetation structure on glacial and debris flow landforms throughout 260 ha of Jefferson Park defined in Zald (2010a). Maps of LiDAR-derived microtopography and distance to overstory canopy were entered into a Geographic Information System (GIS) to select geo-referenced sites in a spatially constrained stratified random sampling design. By stratifying in relation to microtopography and distance from overstory canopy, spatial correlation between variables could removed, individual and interactive variable effects could be quantified, and landscape-level estimates of tree establishment calculated, since the proportional distribution of each strata within the study area was known. Five hundred sites in the spatially clustered stratified random sample were located in the field using a high precision global positioning system (GPS), and a 2 m diameter plot was established at each site. Spatial constraints placed on sampling stratification allowed LiDAR data of overstory trees to be combined with field observations to calculate the distance of each plot to the nearest overstory canopy of each tree species present, providing a metric of potential seed source distances at each plot. At each plot, snow depth, vegetation type and cover, and substrate cover were measured, the abundance and sizes of trees were recorded by species, and a sample of these trees was either cored or cross-sectioned to obtain tree ages.

LiDAR-derived Microtopography and Overstory Canopy Data

Fine scale patterns of microtopography and vegetation structure were characterized using LiDAR data collected on September 3-4, 2007 by Watershed Sciences, Inc (Corvallis, Oregon USA). LiDAR was collected from approximately 2000 m above ground level using a Leica ALS50 Phase II laser with a 59 kHz pulse rate, capturing scan angle of ±11°, and scan swath overlap of at least 50%. LiDAR point density exceeded 10 points/m^2 within the study area. Because there was no road access to the study area, 523 real-time kinematic (RTK) ground survey points were collected eight kilometers west of the study area, and LiDAR data was collected over these survey points at the same time as the study area. The root mean squared error between coordinates of LiDAR data and RTK survey points was 0.04 m. LiDAR point data was converted into three grids with 1m pixel resolution to characterize microtopography and vegetation structure: 1) a digital terrain model of bare earth ground elevation, 2) a top of vegetation canopy elevation model, and 3) a vegetation height model calculated by subtracting the digital terrain model from the vegetation canopy elevation model.

Topographic position index (TOPO) and potential relative radiation (RAD) were calculated from the digital terrain model (Figure 3.3a-b). These two microtopography variables were believed most likely to influence late season snow depth and persistence, since snow melts fastest at higher radiation, is often blown off ridge tops, and accumulates in depressions (Marks and Dozier 1992, Lapen and Martz 1996). TOPO was calculated from the digital terrain model as the difference between a pixel’s elevation and mean elevation of an annulus spanning 5-10 m from that pixel. TOPO was also evaluated using annuli ranging from 2 to 50 m, but the 5-10 m annulus most effectively delineated small ridges and depressions that characterize the study area. RAD (Pierce et al. 2005) is an integrative potential relative radiation index which accounts for temporal variability in radiation by summing hourly estimates of clear-sky radiation for a given day, and then summing daily values over the growing season. RAD accounts for topographic shading of surrounding landscape features by incorporating the digital terrain model in point radiation estimates. RAD was calculated for the growing season (June through September). To reduced the number of sampling strata, RAD and TOPO were combined into a single ecological exposure index (EEI) representing the physical micro site gradient, calculated by relativizing RAD and

TOPO by their respective standard deviates and then averaging the relativized variables together (Figure 3.3c).

The second sampling stratum was distance from overstory canopy (CANDIST), selected because overstory canopy can reduce snow depth and persistence via interception, sloughing, and enhanced incident thermal radiation (Faria et al., 2000, Sicart et al. 2004). Overstory canopy was defined as any vegetation equal or greater than 8 m in height. Assigning a single height value to define “overstoryness” may oversimplify the influence vegetation structure has on snow melt. However, prior field reconnaissance found the 8 m threshold excluded all non-tree vegetation, while still included trees that influenced light and vegetation conditions underneath them. Trees greater than 8 m tall were also observed to be producing the vast majority of cones, making them the most likely seed sources in the study area. CANDIST was calculated as the nearest Euclidean distance of each 1 m grid pixel in the study area to the nearest pixel with vegetation over 8 m tall (Figure 3.3d). CANDIST also defined the population of interest (i.e. meadows) by excluding areas occupied by mature trees.

Stratification, Plot Selection, and Plot Location

Grids of EEI and CANDIST with continuous values were converted into grids with 5 classes each, and these two classified grids were the strata for sampling. Continuous values of EEI ranged from -8.08 to 6.79 and were classified into five quantiles (-8.08 to -0.33, -0.33 to 0.02, 0.02 to 0.26, 0.26 to 0.55, and 0.55 to 6.79). Continuous values of CANDIST ranged from 0 to 91.9 m, and were classified based on observed and modeled seed dispersal rates for the two dominant tree genera *Abies* and *Tsuga* (Franklin and Smith 1974, Carklin et al. 1978, LePage et al. 2000). The five distance classes (in meters) for CANDIST were 0 to 5, 5 to 10, 10 to 20, 20 to 30, and 30 to 91.9. Grids of classified EEI and CANDIST were then combined with a matrix function to produce a single grid of 25 strata representing all potential combination of the two 5 class grids (Figure 3.3e).

Plots were spatially constrained in 100 x 100 m clusters to reduce time needed for mapping overstory vegetation by species, which was used as a proxy for distance to potential seed sources. A moving window analysis found 23 non-overlapping 100 x 100 m clusters containing all 25 sampling strata. One cluster was excluded due to its location in sensitive habitat, another was excluded because it was partially located in water, and a third was randomly excluded resulting in twenty clusters selected for data collection (Figure 3.3f). Using Hawth's tools version 3.24 (Beyer 2004), twenty five points were located in a stratified random design within each of the 20 cluster (500 total plots, Figures 3.3g-h). Additionally, points had to be at least 4 m apart from each other and at least 2 m away from a stratum different from the one occupied. These additional constraints reduced the likelihood that GPS positional errors could result in 2 m diameter plots centered on points overlapping each other or strata. Spatial constraints had the additional benefit of removing potential short distance spatial autocorrelation for snow depth, RAD, TOPO, EEI, and CANIDST, the absence of which was confirmed by empirical semivariogram analyses (results not shown).

Plots were located in July of 2008 using a sub-meter GPS receiver (Leica GS20 with an external pole antenna, Leica Geosystems AG, St. Gallen, Switzerland). Plot coordinates from the GIS sample design were loaded into the GPS as waypoints, and field located. At least 10 GPS coordinates with a positional error less than 1 m were averaged for each plot center to improve positional accuracy (Wing and Karsky 2006). GPS coordinates were post-processed using GIS DataPro software (Leica Geosystems AG, St. Gallen, Switzerland), and horizontal positional accuracy averaged 0.28 m (0.26 - 0.29 m 95% CI). One hundred and nine plots (from six different clusters) were located in debris flow landforms, three hundred and ninety plots were located in older glacial landforms, and one plot was discarded because it lay at the intersection of debris and glacial landforms.

Distance to Potential Seed Sources

LiDAR-derived overstory canopy was combined with detailed field observations to spatially delineate overstory canopies by species, and the distance of each plot to the nearest overstory canopy of each species was calculated the distance to potential seed sources. A grid of LiDAR-derived overstory canopy (> 8m tall) was overlaid on a geo-referenced high resolution (1 m pixel) color aerial photograph to produce digital overstory canopy maps of the 100 x 100 m clusters, plus a 50 m horizontal buffer around each cluster. Overstory canopy maps were printed and taken to the field, every overstory tree within each map was visited, identified to species, and its canopy outline drawn. Canopy outlines drawn in the field on canopy maps were manually traced to GIS polygon shapefiles in ArcGIS (Environmental Systems Research Institute, Redlands, California). Canopy polygons were compared against the raw LiDAR point cloud to correct for any geographic offsets using the 3D visualization software FUSION version 2.61 (McGaughey 2007). Canopy polygons were converted to a 1 m pixel resolution grid of species-specific overstory canopy for each of the 20 clusters plus their 50 m buffers. The Euclidean distance from each plot to the nearest overstory canopy of each species present within the cluster and its buffer was calculated (i.e. TSMEDIST for mountain hemlock, and ABAMDIST for Pacific silver fir). Distances to overstory canopy exceeding 50 m were converted to 50 m (the maximum buffer distance). The direction to the nearest overstory canopy of any species (CANDIRECT) was also calculated, since the position of trees in relation to prevailing winds may be importance for snow redistribution (Holtmeier and Broll 1992, Hiemstra et al. 2002).

Plot-level Data Collection

Minimum, maximum, and plot center snow depth was measured on all plots between July 29 and August 1, 2008. Snow depth was measured to the nearest 0.05 m with a 2.5 m long metal probe. The snow year preceding data collection (September 2007 to April 2008) was above the 90th percentile for the 1951-2008 time period for the Government Camp weather station, and snow covered approximately 75 percent of the study area on July 29, 2008. On each plot, all trees 5 cm to 8 m tall were tallied by species and height class (5-10 cm, 10-50 cm, 50-130 cm, 130-800 cm). The 5 cm minimum height cutoff eliminated the more temporally variable pool of first year germinants. The tallest and shortest trees of each species on each plot had their diameters (either at breast height or basal if under 1.3 m tall) and height measured, and were classified as being initial or secondary establishment. Initial establishment was defined as a tree which established without the canopy of another tree above it, and no evidence the site was previously occupied by a taller tree that died. Secondary establishment was defined as being underneath the canopy of another tree of any size. The tallest and shortest tree of each species on each plot were cored or cross sectioned at the root/shoot boundary. Cores and cross sections were sanded and rings counted using a microscope to determine tree ages. Cross-dating methods as described by Yamaguchi (1991) and marker years were used to accurately assign calendar year of establishment for each sample. One of the six vegetation types defined in the study area description was assigned to each plot in the field, and the percent cover of vegetation, bare soil, rock, litter, coarse woody debris, moss, and lichen tallied by 5 percent cover classes.

Statistical Analyses

FTE movement and meadow invasion are often inferred by reconstructing tree demographics from tree rings of living and/or dead individuals (Arseneault and Payette 1992, Lloyd and Graumlich 1997, Didier 2001). These reconstructions are often presented as tree counts which may describe increases in tree density or changes in growth form over time, rather than tree establishment on previously unoccupied sites (Lescop-Sinclair and Payette 1995). For this reason I graphically present the number of aged trees established, but only site occupancy (proportion of plots occupied by trees, weighted by the proportion of the study area in the sampling strata associated with each occupied plot) over time was analyzed in relation to climate variables. Partial F tests were used to determine if rates of tree establishment (i.e. linear regression slopes of cumulative site occupancy over time) were different between landform (glacial versus debris flow) and establishment types (initial versus secondary establishment).

Relationships between site occupancy rates and individual climate variables on different landforms were assessed using Pearson product moment correlations. Rates of site occupancy were calculated as three-year bins rather than annual data, since: (1) many individual years lacked establishment on new sites, (2) mortality of conifer germinants in the FTE and subalpine forest environments is often high during the first year, but declines during the second or third years of growth (Rochefort and Peterson 1996, Brang 1998, Germino et al. 2002), and (3) cross-dating techniques were applied to tree cores and cross sections, but extremely small and distorted rings, missing rings, or false rings could lead to incorrectly aged trees by ± 1 year. Rates of site occupancy were correlated to mean, minimum, and maximum snowfall within three-year bins for two periods: annual (ANN_S, ANN_S_{min}, ANN_S_{max}), and "spring" (April through June: AJ_S, AJ_S_{min}, AJ_S_{max}) and mean, minimum, and maximum temperatures for three periods: annual (ANN_T, ANN_T_{min}, and ANN_T_{max}); spring (AJ_T, AJ_T_{min}, AJ_T_{max}); and "summer" (July through September: JS_T, JS_T_{min}, JS_T_{max}). Spring snowfall, spring temperature, and summer temperature were included because climate warming is generally expected to increase temperatures and reduce the overall and spring snow pack (Mote 2003), while subalpine tree growth in the region is sensitive to summer temperatures (Peterson and Peterson 1994). Summer snowfall does not result in measureable accumulation and was not included in analyses.

The relationships between biophysical variables and measured snow depth were assessed with nonparametric multiplicative regression (NPMR) using Hyperniche version 1.39 (McCune and Medford 2004). Snow depth was modeled in response to TOPO, RAD, CANDIST, Elevation, and CANDIRECT. The EEI variable enabled sampling to occur in a relatively simple two-stratum design with CANDIST, but inhibited analysis of the relative importance of TOPO and RAD individually on snow depth. TOPO and RAD could be individually assessed by decomposing the simple unweighted EEI into its two components (RAD and TOPO) for statistical analyses. This was possible since RAD and TOPO were not correlated in 499 sampled plots (Pearson correlation coefficient = 0.099), and distributions of both variables in samples did not differ from their distributions in the overall study area (randomization chi-squared tests with 100,000 randomizations, $p=0.238$ for RAD, and $p = 0.063$ for TOPO).

Separate models were developed for the 109 debris flow and 390 glacial landform plots. NPMR was run using a local mean, Gaussian weighting, and minimum average neighborhood size was set at five percent of sample units (4.45 and 19.5 for debris flow and glacial plots respectively). Variables were retained in the final model if they improved model fit by at least five percent. The best fit model was evaluated by a leave-one-out cross-validated statistic (xR^2). The relative importance of each predictor variable within the final models was evaluated by sensitivity analysis, nudging each explanatory variable value one at a time by ±5% throughout its range. Sensitivity was calculated as the average absolute value of the differences induced by nudging the predictor. A sensitivity value of one indicates that nudging a predictor resulted in a change in response of equal magnitude, while a sensitivity of zero would occur if nudging a predictor has no detectable effect on the response. Monte Carlo procedures were conducted for each model with 200 runs of randomized data to assess the null hypothesis that model fit was no better than obtained by chance alone. Differences between plot observations of snow depth, vegetation, bare ground, and rock cover on glacial versus debris flow landforms were assessed using Satterthwaite t tests for samples with unequal variances. Differences of RAD, TOPO, CANDIST, elevation, and vegetation height between landforms were compared for all grid cells within the study (i.e. complete census rather than population samples), therefore no statistical tests for differences of means or variances were performed.

Limited sample sizes restricted analyses of the relationships between tree abundance and biophysical variables to mountain hemlock and Pacific silver fir. Tree abundance in relation to microtopographic variables (TOPO, RAD, and elevation) and biotic variables (CANDIST, TSMEDIST, ABAMDIST and CANDIRECT) were modeled using generalized linear mixed models (GLMMs). GLMM was applied to tree count and biophysical data using the GLMMIX procedure in SAS version 9.2 (SAS Institute 2008). Tree counts were assumed to have a Poisson probability distribution, and plot clusters were treated as a G-side random effect (an element of the random effects vector). Laplace integral method was used to approximate marginal likelihood, allowing for information criteria model selection which would be otherwise biased when using default pseudo-likelihood estimates in GLMMIX (Schabenberger 2007). Tree counts were modeled by species and landform as a function of all possible combinations of explanatory variables (RAD, TOPO, CANDIST, CANDIRECT, elevation, and TSMEDIST or ABAMDIST). All 31 possible combinations of these variables (plus a null model) were compared using an information criterion approach to make inferences regarding the relative importance of biophysical variables on tree abundance. Model selection used the small-sample Akaike's Information Criterion (AIC_c), AIC_c differences (Δ_i) were calculated, a model was estimated to be best if $\Delta_i = 0$, considered to have substantial empirical support if Δ_i was between 0-2, moderate empirical support if Δ_i was between 2-4, and not empirically supported if Δ_i was greater than 4 (Hurvuch and Tsai 1989, Burnham and Anderson 2002).

Interactions between climate, micro site conditions, and tree establishment were analyzed by splitting the climate record into two regimes (cool and snowy years versus warm and low snow years), and testing for differences in the micro site conditions trees established on during the two climate regimes. Climate in a given year was considered cool and snowy if annual snowfall was greater than the mean for the 56 year climate record and either annual or summer mean temperature was below the mean. Twenty one years were considered cool and snowy (1953-1956, 1960-1975, and 2007). Thirty five years with conditions opposite from those described above were considered warm with low snowfall (1952, 1957-1959, and 1976-2006). Aged trees were assigned to climate regimes based on year of establishment, and the microsites occupied by trees in these two climate regimes were tested for differences with Wilcoxon-Mann-Whitney tests using the NPAR1WAY procedure in SAS version 9.2 (SAS Institute 2008). In addition, contingency tables were developed to test if tree establishment was more or less abundant than expected on microsites with high and low topographic position during high and low snow fall periods. Because of low sample sizes in contingency tables, Fisher's exact test was used to test if the relative proportions of observed tree establishment were independent of the expected number of trees established in each climate category. Expected numbers assumed equal proportions of trees established when accounting for different number of years (21 and 35 years) in each climate category.

RESULTS

Temporal Patterns of Tree Establishment and Correlates with Climate

Four hundred and ninety cores and cross sections (out of 505 collected) were successfully aged, 374 on glacial landforms, and 116 on debris flows. On glacial landforms, tree establishment in meadows began in the 1920's, was variable but generally increased until 1984, then increased dramatically until declining in 2005 (Figure 3.4a). Temporal patterns of tree establishment on debris flows were similar to those on glacial landforms, except tree establishment on debris flows was greatest during the 1963 to 1968 and 1988 to 1992 time periods, and invasion was low since 1998 (Figure 3.4b). Five trees established on the northern debris flow prior to the 1934, suggesting it predates the documented 1934 debris flow but is still young compared to glacial landforms. Sixty three percent of aged trees on glacial landforms were initial establishment, of which eighty two percent were mountain hemlock. Seventy six percent of Pacific silver fir established underneath existing trees. Sixty five percent of aged trees on debris flows were initial establishment, and the majority of these (sixty six percent) were mountain hemlock. Overall initial site occupancy across all landforms was 7.75% in 1950, and increased at an average rate of 0.49% yr^{-1}, with 34.71% site occupancy by 2008. In 1950, site occupancy was greater on glacial versus debris flow landforms (9.06% versus 2.55%), but occupancy rates (i.e. mean annual rate over time) were greater on debris flows from 1950 to 2008 (0.76% yr^{-1}. ±0.02 SE versus 0.42% yr^{-1} ±0.01 SE, a difference of 0.34% yr^{-1}, F value = 248.49, $p < 0.0001$). This resulted in greater site occupancy on debris flow landforms by 1974, and by 2008 site occupancy was 33.68% and 38.82% on glacial and debris flow landforms respectively.

Correlations between three-year occupancy rates and climate variables varied by landform, and somewhat establishment type (Figure 3.5a-b). Correlations between occupancy rates and climate variables were generally stronger on glacial landforms than debris flows. On glacial landforms, occupancy rates for both initial and secondary establishment were negatively correlated with annual maximum snow fall, and had non- significant negative correlations with mean and minimum annual snowfall. Initial occupancy rates were not correlated to temperate variables on glacial landforms, but secondary establishment rates were positively correlated to annual minimum and summer minimum temperatures. In contrast, occupancy rates on debris flow landforms were not correlated to annual snow variables, but had positive correlations with spring minimum snowfall, and no significant correlations for either establishment type with any temperature variables.

Snow Depth and Correlates with Landforms and Biophysical Variables

Snow depth was deeper on glacial (0.67 m, 0.59-0.75 m 95% CI) versus debris flow (0.21 m, 0.14-0.28 95%CI) landforms (t value = 8.87, df=387, $p < 0.0001$). Glacial landforms had closer proximity to overstory trees and rougher bare earth and vegetation surfaces compared to debris flow landforms (Table 3.1). Glacial landforms also had greater vegetation cover, less surface occupied by bare soil, and more rock cover than debris flow landforms.

NPMR models of snow depth in relation to explanatory variables differed between glacial and debris flow landforms (Figure 3.6). The snow model for glacial landforms had a final $xR^2 = 0.274$, and was a better fit than 200 runs of randomized data ($p = 0.0049$). Sensitivity analysis (SA) found snow depth on glacial landforms was most sensitive to elevation (SA = 0.596), followed by TOPO (0.425) and CANDIST (0.332), and was insensitive to RAD (0.020) and CANDIRECT (0.021). Snow depth declined with increased elevation, was lower on ridges (high TOPO values), and was lower in close proximity to overstory canopy (low CANDIST). Elevation, TOPO, and CANDIST had nonlinear interactive associations with snow depth. At high elevation, snow depth declined with increased TOPO in a linear manner. However at lower elevations, snow depth increased slowly from ridges to midslopes (TOPO from 1 to 0), but increased rapidly from mid slopes to depressions (TOPO from 0 to -1). At high elevations, snow depth initially increased and then declined with distance from overstory canopy, but at lower elevations displayed a more linear increase in snow depth with increased distance from overstory canopy. The snow model for debris flow landforms had a lower model fit ($xR^2 = 0.116$) compared to glacial landforms, although still better than expected by chance ($p = 0.0099$). Snow depth on debris flow landforms was most sensitive to RAD (SA = 2.235), followed by much lower sensitivity for CANDIST (0.162), and insensitive to elevation (0.060) and TOPO (0.047). CDIRECT was not included in the model for debris flows because it did not meet the 5% improvement criterion in model development. In addition to lower overall snow depth, lower variance described by biophysical variables, and different sensitivity to those variables, debris flow landforms had reduced interaction between explanatory variables and snow depth as inferred from the more linear response surfaces (Figure 3.6).

Tree Establishment and Correlates with Landforms and Biophysical Variables

In total, 1620 trees less than 8 m tall (835 mountain hemlock, 758 Pacific silver fir, 12 whitebark pine, 8 Alaska yellow-cedar , and 7 lodgepole pine) were observed in the plots. Only mountain hemlock and Pacific silver fir were analyzed. Tree abundance was highly variable, but did not differ between landform types for mountain hemlock (Satterthwaite T test with unequal variances: df=170, t=-0.46, p=0.6445) or Pacific silver fir (df=288, t=0.89, p=0.3722).

The relationships between tree abundance and biophysical variables in empirically supported GLMMs varied by species and landform type (Tables 3.2-3.3). The best model describing mountain hemlock abundance on glacial landforms included: RAD, TOPO, elevation, CANDIST, and TSMEDIST. One other model for mountain hemlock on glacial landforms had substantial empirical support; no models had moderate empirical support, there was a large Δ_i for the null model. On glacial landforms, mountain hemlock abundance increased with higher topographic position, decreased radiation, decreased distance to overstory canopy, and increased distance to hemlock overstory canopy. The same explanatory variables (except elevation) describing mountain hemlock abundance on the glacial landforms were present in the best debris flow model. In contrast to models of mountain hemlock abundance on glacial landforms, there were more alternative models, and a much smaller Δ_i for the null model of mountain hemlock on debris flow landforms. This was interpreted as evidence of strong associations between mountain hemlock abundance and explanatory variables on glacial landforms, but much weaker associations on debris flows. In the best model for mountain hemlock model on debris flow landforms, hemlock was more abundant with increased TOPO, decreased RAD and CANDIST, and increased TSMEDIST. For mountain hemlock on both landforms, TOPO had the strongest fixed effects.

For Pacific silver fir on glacial landforms, the best model of abundance included: RAD, TOPO, CANDIST, and ABAMDIST. Two other models had substantial empirical support, two had moderate support, and there was a large Δ_i for the null model. Pacific silver fir abundance on glacial landforms increased with reduced ABAMDIST and RAD, and high TOPO. There were multiple models of Pacific silver fir on debris flow landforms with substantial and moderate empirical support, along with a small Δ_i for the null model. This is interpreted as the presence of strong associations between Pacific silver fir abundance and explanatory variables on glacial landforms, and much weaker associations on debris flows. On debris flow landforms, Pacific silver fir abundance increased with higher TOPO and decreased ABAMDIST. ABAMDIST had the strongest fixed effects on glacial landforms, while TOPO had the largest fixed effects on debris flow landforms.

Interactive Effects of Climate and Microtopography on Tree Establishment

Sufficient sample numbers were only available to test interactive effects of climate and microtopography on mountain hemlock initial establishment on both landforms, and mountain hemlock secondary establishment on glacial landforms. From the 56 years of climate data, 21 were categorized as high snowfall and low temperatures, and 35 years as low snowfall and high temperatures. Initial establishment of mountain hemlock on glacial landforms occurred on high topographic positions during years of high snowfall and low temperatures, and on lower topographic positions during years with reduced snowfall and increased temperatures (Table 3.4). Establishment during low snow periods occurred on topographic positions with values around zero (approximately mid slope). Secondary establishment on glacial landforms did not occur on micro sites with different TOPO or elevation values during different climate periods. On debris flow landforms, initial establishment of mountain hemlock occurred at higher elevations during years of increased snowfall and reduced temperatures. On glacial landforms, observed abundance of initial establishment on high topographic positions or elevation was not different than expected during high or low snow periods (Table 3.5). However at low topographic positions, observed abundance of initial establishment was greater than expected during low snow periods. This suggests micro sites likely to have greater snow persistence require low snow periods for tree establishment, and tree establishment continues during these low snow periods on sites likely to have reduced snow persistence. On debris flow landforms, both initial and secondary establishment was not different than expected on high or low topographic and elevations positions during low or high snow periods.

DISCUSSION

This study provided a unique opportunity to examine the spatial and temporal patterns of tree establishment within the FTE at landscape to micro site scales. Previous studies have documented FTE movement and increased tree establishment in subalpine meadows (Lloyd and Graumlich 1997, Miller and Halpern 1998, Didier 2001), but methodological constraints prevented them from explicitly separating increases in tree density from landscape-level FTE movement and meadow invasion. In contrast, this study found large increases in the proportion of the Jefferson Park landscape occupied by trees over the past 50 years. The results of this study suggest tree invasion has been temporally and spatially constrained over time by a multi-scale hierarchy of climatic, landform, microtopographic, and biotic controls (Figure 3.7). I propose that the effects of regional drivers (e.g. snow fall) are modified by landscape-level patterns of microtopography and vegetation structure. These interactions are the primary controls of tree establishment, while differences in species seed sources and regeneration ecology additionally constrain micro site favorability. Finally, interactions between climate, landform, and microtopography not only influenced spatial patterns of tree establishment, but also influenced establishment rates, and resulted in complex establishment responses to climate conditions over time. Patterns and controls of tree establishment are discussed below within a framework of increasing complexity with decreasing spatial scale; focusing on regional patterns of snow persistence and tree establishment, how landforms and microtopography influenced snow and tree establishment, the role of biotic factors such as vegetation structure and regeneration ecology, and how climate and physical factors interactively generate complex tree establishment responses across the studied landscape.

Snow Persistence and Tree Establishment

Previous studies have hypothesized snow depth and seasonal persistence are the primary spatial and temporal controls of FTE movement and invasion of meadows in the Pacific Northwest region (Franklin et al. 1971 Woodward et al. 1995, Miller and Halpern 1998). These studies correlated temporal patterns of tree establishment with regional climate data, but did not co-measure tree establishment and snow depth on the same sites across topographic or other environmental gradients. Consequently, these previous studies provided relatively weak inference regarding the role of snow as the primary driver of temporal and spatial patterns of FTE tree establishment. Consistent with these past studies, I found correlations between tree establishment and regional annual snowfall. I also found early summer snow depth and tree abundance were associated with both landform and microtopographic variables, supporting the hypothesis that snow depth and persistence exert temporal and spatial controls on tree establishment in the FTE. It should be noted that associations between snow depth and tree establishment in the Pacific Northwest region contrasts with patterns documented in other climate regimes. For example, in the more arid and windy continental climate of the Rocky Mountains, increased snow depth facilitates tree establishment by increasing soil moisture; reducing wind desiccation, and moderating temperature extremes (Holtmeier 2003, Geddes et al. 2005, Hiemstra et al. 2006) , although very deep snow can still inhibit establishment (Hättenschwiler and Smith 1999, Maher et al. 2005). This highlights how tree establishment in the FTE can have contrasting responses to regional climate.

Landform and Microtopographic Controls of Snow Persistence and Tree Establishment

Landforms, and microtopographic gradients nested within them serve as the physical template which modifies spatial patterns of late season snow persistence, and therefore tree establishment. Snow depth was greatly reduced on debris flows versus glacial landforms, despite plot data with similar distributions of microtopography and distance to overstory canopy. LiDAR provides a synoptic view of larger landscape patterns that influence snow depth. Debris flows had more uniform ground elevations, lower and less variable vegetation heights, and increased distances to overstory canopy, resulting in a smoother surface compared to glacial landforms. Smoother surfaces have fewer depressions for snow deposition and higher surface wind speeds, which can increase wind redistribution of snow (Marks et al. 2002, Litaor et al. 2008). I propose that wind redistribution on debris flows partially results from a lack of control by surface structure, which is more strongly developed on glacial landforms, resulting in different scales controlling of snow distribution (sensu Trujillo et al 2007). Differences in surface radiation balance between the two landform types may result in different snow melt rates, since the cover of soil and different vegetation types which vary by landform have different albedos (Eugster et al. 2000). However, albedo differences between landforms is unlikely to cause landform-level differences in snow depth observed. Different land cover types have overlapping albedo values, and sparsely vegetated mineral soil can have a higher albedo than alpine vegetation and conifers, not less as would be needed to increase melting on the more sparsely vegetated debris flows (Goodin and Isard 1989).

Temporal and spatial patterns of tree establishment appear to have been driven by differences in snow persistence associated with landforms and microtopography within landforms. Rates of establishment have been greater on debris flows, where reduced snow depth and persistence increase growing season length by altering surface radiation balance (Ling and Zhand 2005). Relationships between tree abundance and microtopography are much weaker on debris flows versus glacial landforms, consistent with landform-scale wind redistribution of snow. Debris flows have been more favorable for tree establishment than glacial landforms, although substrate factors unrelated to snow persistence may contribute to this. Although glacial landforms had a high percentage of rock cover, debris flow substrate has a large component of exposed coarse gravel and cobble, fine scale heterogeneity which may facilitate seed trapping and provide safe sites for plant establishment (Jompponen et al 1999). Compared to glacial landforms, debris flows had three times greater mineral soil and reduced vegetation cover, which are generally thought to promote germination and establishment of many conifer species (Smith et al. 1997). This would suggest reduced snow cover at the landform-scale resulted in higher rates of tree establishment on debris flows, although additional factors such as substrate and vegetation competition may also facilitate increased tree establishment.

In addition to fundamentally altering the biophysical controls of snow persistence, debris flows are also high-severity disturbance events, burying almost all organic matter and vegetation, after which primary succession was initiated. Studies of FTE tree establishment in response to disturbances have primarily focused on lower-severity disturbances such as wildfire and/or grazing (Debenedetti & Parson 1979, Vale 1981, Butler 1986, Stueve et al. 2009). Prior research suggests deterministic successional pathways (Henderson 1973, Chapin et al. 1995) and long time periods for trees to establish at high elevations and latitudes post-disturbance (Agee and Smith 1984, Arseneault and Payette 1992, Coop and Schoettle 2009). In this study debris flow landforms were rapidly colonized by trees and rates of tree establishment were greater than on glacial landforms, suggesting more rapid post-disturbance tree establishment is possible at high elevations if the disturbance results in favorable site conditions and seed sources are available. Counter to more deterministic concepts of succession, rapid development of a young mountain hemlock forest on debris flows suggests there are multiple successional pathways, which can be a function of landscape context, seed availability, and stochastic events (Fastie et al. 1995, del Moral et al. 1995).

Biotic Controls of Snow Persistence and Tree Establishment

Vegetation structure was another important influence on both snow persistence and tree establishment. Proximity to overstory canopy was associated with reduced snow depth, consistent with the “tree well” pattern of reduced snow accumulation and increased snowmelt under canopy, resulting from interception, sloughing, and enhanced incident thermal radiation (Faria et al., 2000, Sicart et al. 2004). This is in contrast to studies in more arid and windy regions, were extensive wind redistribution causes snow to accumulate within and to the lee side of trees and taller vegetation (Holtmeier 2003, Geddes et al. 2005, Hiemstra et al. 2006). Compared these drier and windier regions, wind redistribution in the Pacific Northwest is likely to be less significant as a result of lower wind speeds and greater snow densities (Elliot et al. 1987, Mizukami and Perica 2008). The absence of flagged and krummholz trees also indicates relatively lower wind speeds within the study area. Tree wells form on glacial landforms where fine scale structures exert strong controls on snow distribution. However, on debris flows, they are less likely to form given the greater importance of wind and reduced influence of fine scale topography and vegetation structure.

Spatial and temporal patterns of tree invasion were also strongly influenced by the autoecology of the tree species present. Distance from con-specific overstory (potential seed sources) was the most important biophysical variable associated with Pacific silver fir abundance, with increased establishment associated with closer proximity to potential seed sources, but this relationship was much weaker and less consistent for mountain hemlock. The seeds of both species are wind dispersed, but the seeds of Pacific silver fir are 9 to 22 times heavier, resulting in shorter dispersal distances (Bonner and Karrfalt 2008). Pacific silver fir is also a poor seed producer and its cones can suffer high predation from insects and rodents (Owens and Molder 1997, Bonner and Karrfalt 2008). Short dispersal distances, poor seed production, and high potential seed predation suggest tree invasion into meadows may be more spatially restricted for Pacific silver fir than mountain hemlock due to recruitment limitations, even when suitable micro sites exist. It should be noted that separating the influences of all overstory on snow depth versus potential seed source limitation for mountain hemlock was complicated by the species dominance in the overstory (63% of overstory canopy area), possibly resulting in multi-collinearity confounding statistical models of mountain hemlock abundance. Despite these confounding factors evidence supports seed limitation for Pacific silver fir, with inconclusive evidence of seed limitation for mountain hemlock.

Trees may also facilitate secondary tree establishment underneath them via species differences in shade tolerance and other autogenic modifications of site conditions. Mountain hemlock was the dominant tree species initially establishing on both glacial and debris flow landforms, while Pacific silver fir was more restricted to establishing underneath hemlocks. Mountain hemlock and Pacific silver fir are very shade tolerant and can persistent as suppressed individuals in stands for up to 100 years (Kranjina 1969, Minore 1979, Packee et al. 1981). However Pacific silver fir is believed to be slightly more shade tolerant and slower growing when young (Kranjina 1969, Crawford and Oliver 1990), and mountain hemlock hemlocks grow best in partial shade (Means 1990). Correlations between site occupancy and annual climate variables were not weaker for secondary versus initial establishment, suggesting initially establishing trees do not weaken climatic controls of tree establishment over time via autogenic site modification as suggested by Miller and Halpern (1998). However, initial establishment of mountain hemlock on glacial landforms occurred on different topographic conditions during high and low snow climate periods, but secondary establishment did not. This would suggest some weakening of climate and topographic controls on secondary establishment, which may result from autogenic modification of site conditions. In combination, biotic factors may place spatial constraints on tree establishment because of species-specific recruitment limitation, and may facilitate tree establishment in the future via both overstory effects on snow depth and autogenic weakening of scale-dependent climate-site-establishment interactions.

Interactive Responses of Tree Establishment to Climate, Landform Type, and Microtopography

Multi-scale interactions of snow depth, landform type, microtopography, and vegetation structure not only influenced the spatial patterns of tree establishment, but also resulted in complex establishment responses to climate. Glacial landforms had slower rates of tree establishment which were positively associated with reduced annual snow fall. On debris flow landforms, tree establishment was more rapid, decoupled from annual snowfall, and was even associated with increased spring snow fall. Given the low snow depths and coarse well-drained substrate, tree establishment on debris flow landforms may be somewhat moisture, rather than thermally limited. This is counter to the belief that tree establishment in subalpine forests and the alpine FTE is thermally limited. However, moisture limitation of tree growth has been documented in the boreal forests and arctic FTE (Barber et al. 2000, Wilmking et al. 2002). This study suggests that both thermal limitation (via snow persistence) and moisture limitation may occur for tree establishment, depending on the landforms and substrate within the study area.

Regional snow fall was associated with rates of mountain tree establishment on glacial landforms over time, while micro site biophysical conditions (i.e. microtopography, elevation, overstory modified snow depth, and distance to potential seed sources) appear to control the spatial pattern of tree establishment. This study found evidence of climate and micro site variables interactively controlling both the spatial distribution and temporal rates of tree establishment in the FTE, which has implications for FTE sensitivity to future climate change. During years with high snow fall, initial hemlock establishment was restricted to ridge tops and upper elevations. During years with low snow fall, initial hemlock establishment continued on high topographic positions, but also occurred at lower topographic positions and lower elevations. Increased establishment occurred on lower positions on glacial landforms, but not on debris flows. Similar climate-site-establishment interactions have been observed within the Pacific Northwest region at much larger spatial scales of entire mountain ranges and across much larger gradients in topographic and edaphic factors (Woodward et al. 1995, Rochefort and Peterson 1996, Miller and Halpern 1998). However, in these regional-scale studies, tree establishment declined on sites with lower average snow depth during low snow periods. This study suggests climate-site-tree establishment interactions may be both scale dependent (varying in strength when going from regional to individual meadow/micro site spatial scales), and also landscape context dependent (in this case the influence of landforms on microtopographic features nested within them).

Study Limitations and Uncertainty

Inferences made in this study about the spatial and temporal patterns of tree establishment, and the underlying controls of these patterns are drawn from retrospective and observational data from one landscape. As such, interpretations and inferences drawn from this study have various limitations and uncertainty associated with them. Inference regarding spatial patterns of snow in relation to biophysical factors was based on snow depth measurements taken at a single point in time (late July of 2008). Biophysical variables did not explain a large amount of the spatial variation in snow depth. Similar studies within the region are lacking, but in an agricultural setting Lapen and Martz (1996) found similar variance of snow depth explained by topographic variables at comparable spatial scales (10 m pixel versus 2 m in this study). This suggests a high degree of stochastic variability in fine-scale spatial patterns of snow depth, but still demonstrates general patterns in relative snow depth are related to microtopography, and vegetation structure. Inter-annual spatial variation of snow depth likely occurs, and might be reflected in relatively low variance in snow depth described by biophysical controls. Despite the likely temporal variation in spatial patterns of snow depth, general patterns of relative snow depth likely persist at both intra- and inter-annual time scales (Heegaard 2002, Williams et al. 2009), suggesting general patterns of snow are generally valid beyond the single year of data collection.

This study was unable to determine the role of livestock grazing and its cessation on tree invasion in the meadows. It is unlikely grazing or its cessation have played a role in rapid tree invasion of the 1934 debris flow, since there would not have been significant forage for livestock due to the burial of almost all vegetation. On glacial landforms increased rates of tree establishment do appear to coincide with possible cessation of sheep grazing. However grazing history for the study area is qualitative and regional in nature, and cannot be used to quantify the timing or intensity of grazing within the Jefferson Park study area.

One objective of this study was to quantify tree establishment in relation to regional climate records. Consequently, sampling focused on younger trees, preventing detailed examination of trees established prior to the 1920's. Retrospective studies such as this one cannot detect tree establishment which may have since disappeared due mortality events. This has been the case on the debris flows, where trees that previously occupied those sites were either buried or transported off site in 1934. This limitation was addressed by restricting the temporal scope of inference for this study to not predate 1934. There are no documented wildfires within the study area, nor are there any biological legacies such as large woody debris, stumps, snags, or remnant trees indicative of past disturbances (sensu Franklin et al. 2002). However, mortality events in prior decades caused by multiple extreme snow years or avalanches could have resulted in mortality of young seedlings which would not be detectable during field sampling. The lack of such extreme events within the historical or proxy climate records suggests such mortality events are unlikely within this studies temporal scope of inference, but would become more problematic if extended before 1940 when extreme mutli-year droughts may have been more common regionally (Gedalof et al. 2004).

Implications for Future FTE Movement and Subalpine Meadow Invasion

Tree establishment in this study was temporally associated with low snowfall and higher annual and spring temperatures. The strong control snowpack has had on tree establishment across the region over the past five decades is likely to continue in the future. Snowpack in large areas of the FTE in Oregon and Washington many be sensitive to increased temperatures, and regional snowpack may be declining (Mote 2003, Mote et al. 2005, Nolan and Daly 2006). Regional models suggest declines in snow water equivalency by 11 to 70 percent in the Pacific Northwest by 2050 (Salathé et al. 2008, Casola et al. 2009, Salathé et al. 2009). However, regional precipitation and snow scenarios are major shortcomings of climate models (Randal et al. 2007). Until regional snow models are improved to provide transient, spatially-explicit, and annual predictions of snow pack, scenarios of FTE change will be dependent on highly uncertain snowpack scenarios whose spatial and temporal scales are not compatible with the ecological patterns and processes of tree establishment observed in this study.

Even if future climate conditions are favorable for tree establishment, this research suggests FTE movement and meadow invasion will be highly variable, driven by multi-scale interactions of climate, landform type, microtopography, existing vegetation structure, seed source limitations for some species, and disturbance regimes. Tree establishment has largely occurred on high topographic positions, with much of the meadow landscape in low topographic positions displaying micro sites consistently unfavorable for tree establishment over the past fifty years. If these low topographic position microsites maintain late season snow persistence even during reduced regional snowfall, they will likely persist as unfavorable sites for tree establishment in the future. Additionally, seed dispersal limitations for some species (such as Pacific silver fir and the similar subalpine fir) may also constrain tree establishment and FTE movement where these species dominate. Counteracting micro site and seed dispersal constraints could be autogenic feedbacks of tree establishment, where trees influence micro site conditions making adjacent establishment more likely even under unfavorable climate conditions. The temporal and spatial extent of these feedbacks is largely unknown, but may play a large role in future tree invasion in meadows as favorable sites in the landscape are increasingly occupied and only low topographic meadows remain on the landscape. The results of this study suggest considerable limitations for regional and global simulation models attempting to project future FTE movement or meadow loss; estimating since multi-scale and multi-species responses of the FTE to climate change may not be possible by downscaling larger models of climate or using simple single species responses to climate.

Acknowledgements

Funding for this research was provided by the USDA Forest Service, Pacific Northwest Research Station, Forest Inventory and Analysis Program; The Native Plant Society of Oregon, and the Hoener Memorial Fellowship program at the College of Forestry, Oregon State University. Special thanks to Alex Gonsiewski for field data collection and tree core dating, Manuela Huso with sampling design and statistical analyses, and Keith Olsen for GIS assistance.

LITERATURE CITIED

Agee, J.K., and Smith, L. 1984. Subalpine tree reestablishment after fire in the Olympic Mountains, Washington. Ecology 65: 810-819.

Arseneault, D., and Payette, S. 1992. A postfire shift from lichen-spruce to lichen-tundra vegetation at tree line. Ecology 73: 1067-1081.

Barber, V.A., Juday, G.P., and Kinney, B.P. 2000. Reduced growth of Alaskan white spruce in the twentieth century from temperature-induced drought stress. Nature 405: 668-673.

Batllori, E., and Gutiérrez, E. 2008. Regional tree line dynamics in response to global change in the Pyrenees. Journal of Ecology 96: 1275-1288.

Bekker, M.F. 2005. Positive feedback between tree establishment and patterns of subalpine forest advancement, Glacier National Park, Montana, U.S.A. Arctic, Antarctic, and Alpine Research 37: 97-107.

Beyer, H.L. 2004. Hawth's Analysis Tools for ArcGIS. Available at http://www.spatialecology.com/htools.

Bonan, G.B., Pollard, D., and Thompson, S.L. 1992. Effects of boreal forest vegetation on global climate. Nature 359: 716-718.

Bonner, F.T., and Karrfalt, R.P. [eds]. 2008. Woody plant seed manual. U.S. Department of Agriculture, U.S. Forest Service Agricultural Handbook 727.

Brang, P. 1998. Early seedling establishment of *Picea abies* in small forest gaps in the Swiss Alps. Canadian Journal of Forest Research 28: 626-639.

Burnham, K.P., and Anderson, D.R. 2002. Model selection and multimodel inference: A practical information-theoretic approach, 2nd ed. Springer, New York, NY.

Butler, D.R. 1986. Conifer invasion of subalpine meadows, central Lemhi Mountains, Idaho. Northwest Science 60: 166-173.

Campbell, A.G. 1973. Vegetative ecology of Hunt’s Cove, Mt. Jefferson, Oregon. pp. 89.

Cannone, N., Sgorbati, S., and Guglielmin, M. 2007. Unexpected impacts of climate change on alpine vegetation. Frontiers in Ecology and Evolution 5: 360-364.

Casola, J.H., Cuo, L., Livneh, B., Lettenmaier, D.P., Stoelinga, M.T., Mote, P.W., and Wallace, J.M. 2009. Assessing the impacts of global warming on snowpack in the Washington Cascades. Journal of Climate 22: 2758-2772.

Carkin, R.E., Franklin, J.F., Booth, J., and Smith, C.E. 1978. Seeding habits of upper-slope tree species IV: Seed flight of noble fir and Pacific silver fir. USDA Forest Service Research Notes PNW-312.Pacific Northwest Forest and Range Experimental Station, Portland, OR.

Chapin, S.F., Walker, L.R., Fastie, C.L., and Sharman, L.C. 1995. Mechanisms of primary succession following deglaciation at Glacier Bay, Alaska. Ecological Monographs 64: 149-175.

Coop, J.D., and Schoettle, A.W. 2009. Regeneration of Rocky Mountain bristlecone pine (*Pinus aristata*) and limber pine (*Pinus flexilis*) three decades after stand-replacing fires. Forest Ecology and Management 257: 893-903.

Crawford, P.D., and Oliver, C.D. 1990. Pacific silver fir. In: Silvics of North America: 1. Conifers. Burns, R.M., and Honkala, B.H. (technical coordinators). U.S. Department of Agriculture, Forest Service, Washington, DC.

Daniels, L.D., and Veblen, T.T. 2003. Regional and local effects of disturbance and climate on altitudinal treelines in northern Patagonia. Journal of Vegetation Science. 14: 733-742.

Daniels, L.D., and Veblen, T.T. 2004. Spatiotemporal influences of climate on altitudinal treeline in northern Patagonia. Ecology 85: 1284-1296.

DeBenedetti, S.H., and Parsons, D.J. 1979. Natural fire in subalpine meadows: a case description from the Sierra Nevada. Journal of Forestry 77: 477-479.

del Moral, R., Titus, J.H., and Cook, A.M. 1995. Early primary succession on Mount St. Helens, Washington, USA. Journal of Vegetation Science 6: 107-120.

Didier, L. 2001. Invasion patterns of European larch and Swiss stone pine in subalpine pastures in the French Alps. Forest Ecology and Management 145: 67-77.

Dirnböck, T., Dullinger, S., and Grabherr, G. 2003. A regional impact assessment of climate and land-use change on alpine vegetation. Journal of Biogeography 30: 401-417.

Douglas, G.W. 1972. Subalpine plant communities of the western North Cascades, Washington. Arctic and Alpine Research 4: 147-166.

Dovčiak, M., Hrivnák, R., Ujházy, K., and Gömöry, D. 2008. Seed rain and environmental controls on invasion of *Picea abies* into grassland. Plant Ecology 194: 135-148.

Dyurgerov, M.B., and Meier, M.F. 2002. Twentieth century climate change: Evidence from small glaciers. Proceeding of the National Academy of Sciences 97: 1406-1411.

Elliott, D.L., Holladay, C.G., Barchet, W.R., Foote, H.P., and Sandusky, W.F. 1987. Wind energy resource atlas of the United States. U.S. Department of Energy, Pacific Northwest National Laboratory. Richland, WA.

Eugster, W., Rouse, W.R., Pielke, R.A., McFadden, J.P., Baldocchi, D.D., Kittel, T.G., Chapin, F.S., Liston, G.E., Vidale, P.L., Vaganov, E., and Chambers, S. 2000. Land-atmosphere energy exchange in Arctic tundra and boreal forest: available data and feedbacks to climate. Global Change Biology 6: 84-115.

Faria, D.A., Pomeroy, J.W., and Essery, R.L.H. 2000. Effect of covariance between ablation and snow water equivalent on depletion of snow-covered area in a forest. Hydrological Processes 14: 2683-2695.

Fastie, C.L. 1995. Causes and ecosystem consequences of multiple pathways of primary succession at Glacier Bay, Alaska. Ecology 76: 1899-1916.

Foley, J.A., Levis, S., Costa, M.H., Cramer, W., and Pollard, D. 2000. Incorporating dynamic vegetation cover within global climate models. Ecological Applications 10: 1620-1632.

Fonda , R.W., amd Bliss, L.C. 1969. Forest vegetation of the montane and subalpine zones, Olympic Mountains, Washington. Ecological Monographs 39: 271-301.

Franklin, J.F., Moir, W.H., Douglas, G.W., and Wiberg, C. 1971. Invasion of subalpine meadows by trees in the Cascade Range, Washington and Oregon. Arctic and Alpine Research 3: 215-224.

Franklin, J.F., and Smith, C.E. 1974. Seeding habits of upper-slope tree species II: Dispersal of a mountain hemlock seedcrop on a clearcut. USDA For. Serv. Res. Note PNW-214, 9p. Pacific Northwest Forest and Range Experimental Station, Portland, OR.

Franklin J.F., and Dyrness C.T. 1988. Natural Vegetation of Oregon and Washington. Oregon State University Press. Corvallis, OR.

Franklin, J.F., Spies, T.A., Van Pelt, R., Carey, A.B., Thornburgh, D.A., Rae Berg, D., Lindenmayer, D.B., Harmon, M.E., Keeton, W.S., Shaw, D.C., Bible, K., and Chen, J. 2002. Disturbances and structural development of natural forest ecosystems with silvicultural implications, using Douglas-fir as an example. Forest Ecology and Management 155: 399-423.

Gedalof, Z., Peterson, D.L., and Mantua, N.J. 2004. Columbia river flow and drought since 1750. Journal of the American Water Resources Association 40: 1579-1592.

Geddes, C.A., Brown, D.G., and Fagre, D.B. 2005. Topography and vegetation as predictors of snow water equivalent across the alpine treeline ecotone at Lee Ridge, Glacier National Park, Montana, U.S.A.. Arctic, Antarctic, and Alpine Research 37: 197-205.

Gehrig-Fasel, J., Guisan, A., and Zimmerman, N.E. 2007. Tree line shifts in the Swiss Alps: Climate change or land abandonment? Journal of Vegetation Science 18: 571-582.

Germino, M.J., Smith, W.K., and Resor, A.C. 2002. Conifer seedling distribution and survival in an alpine-treeline ecotone. Plant Ecology 162: 157-168.

Goodin, D.G., and Isard, S.A. 1989. Magnitude and sources of variation in albedo within an alpine tundra. Theoretical and Applied Climatology 40: 61-66.

Grace, J. 1989. Tree Lines. Philosophical Transactions of the Royal Society of London. Series B, Biological Sciences 324(1223): 233-243.

Halloy, S.R.P., and Mark, A.F. 2003. Climate-change effects on alpine plant biodiversity: A New Zealand perspective on quantifying the threat. Arctic, Antarctic, and Alpine Research 35: 248-254.

Halpern, C.B., Smith, B.G., and Franklin, J.F. 1984. Composition, structure, and distribution of the ecosystems of the Three Sisters Biosphere Reserve/Wilderness Area. Final report to the U.S. Department of Agriculture. Forestry Sciences Laboratory. Corvallis, OR.

Hallett, D.J., Lepofsky, D.S., Mathewes, R.W., and Lertzman, K.P. 2003. 11000 years of fire history and climate in the mountain hemlock rain forests of southwestern British Columbia based on sedimentary charcoal. Canadian Journal of Forest Research 33: 292-312.

Hättenschwiler, S., and Smith, W.K. 1999. Seedling occurrence in alpine treeline conifers: A case study from the central Rocky Mountains, USA. Acta Oecologica 20: 219-224.

Harsch, M.A., Hulme, P.E., McGlone, M.S., and Duncan, R.P. 2009. Are treelines advancing? A global meta-analysis of treeline response to climate warming. Ecology Letters 12: 1040-1049.

Heegaard, E. 2002. A model of alpine species distribution in relation to snowmelt time and altitude. Journal of Vegetation Science 13: 493-504.

Henderson, J.A. 1973. Composition, distribution, and succession of subalpine meadows in Mount Rainier National Park. Ph.D. thesis Oregon State University. Corvallis, OR.

Hiemstra, C.A., Liston, G.E., and Reiners, W.A. 2002. Snow redistribution by wind and interactions with vegetation at upper treeline in the Medicine Bow Mountains, Wyoming, U.S.A. Arctic, Antarctic, and Alpine Research 34: 262-273.

Hiemstra, C.A., Liston, G.E., and Reiners, W.A. 2006. Observing, modeling, and validating snow redistribution by wind in a Wyoming upper treeline landscape. Ecological Modelling 197: 35-51.

Holtmeier, F.K. 2003. Mountain timberlines: ecology, patchiness, and dynamics. Kluwer Academic Publishers. Dordrecht, The Netherlands.

Holtmeier, F.K., and Broll, G. 1992. The influence of tree islands and microtopography on pedoecological conditions in the forest-alpine tundra ecotone on Niwot Ridge, Colorado Front Range, U.S.A. Arctic, Antarctic, and Alpine Research 24: 216-228.

Holtmeier, F.K., and Broll, G. 2005. Sensitivity and response of northern hemisphere altitudinal and polar treelines to environment change at landscape and local scales. Global Ecology and Biogeography 14: 395-410.

Hurvich, C.M., and Tsai, C-L. 1989. Regression and time series model selection in small samples. Biometrika 76: 297-307.

Jobbágy, E.G., and Jackson, R.B. 2000. Global controls of forest line elevation in the northern and southern hemispheres. Global Ecology and Biogeography 9: 253-268.

Jompponen, A., Vare, H., Mattson, K.G., Ohtonen, R., and Trappe, J.M. 1999. Characterization of ‘safe sites’ for pioneers in primary succession on recently deglaciated terrain. Journal of Ecology 87: 98-105.

Kenkel, N.C., Juhász-Nagy, P., and Podani, J. 1989. On sampling procedures in population and community ecology. Vegetatio 83: 195-207.

Körner, C. 1998. A re-assessment of high elevation treeline positions and their explanation. Oecologia 115: 445-459.

Körner, C. 2000. Biosphere responses to CO2 enrichment. Ecological Applications, 10: 1590-1619.

Körner, C. 2003. Alpine plant life: Functional plant ecology of high mountain ecosystems, 2nd ed. Springer, Berlin.

Kuhns, J.C. 1917. G-Reconnaissance-Cascade. Report to the Forest Supervisor. Supervisor’s Office, Willamette National Forest, Eugene, Oregon.

Kupfer, J.A., and Cairns, D.M. 1996. The suitability of montane ecotones as indicators of global climate change. Progress in Physical Geography 20: 253-272.
Krajina, V.J. 1969. Ecology of forest trees in British Columbia. Ecology of Western North America 2(1): 1-146.

Lapen, D.R., and Martz, L.W. 1996. An investigation of the spatial association between snow depth and topography in a prairie agricultural landscape using digital terrain analysis. Journal of Hydrology 184: 277-298.

LePage, P.T., Canham, C.D., Coates, K.D., and Bartemucci, P. 2000. Seed abundance versus substrate limitation of seedling recruitment in northern temperate forests of British Columbia. Canadian Journal of Forest Research 30: 415-417.

Levin, S.A. 1992. The problem of pattern and scale in ecology. Ecology 73: 1943-1967.

Lertzman, K.P., and Krebs, C.J. 1991. Gap-phase structure of a subalpine old-growth forest. Canadian Journal of Forest Research 21: 1730-1741.

Lescop-Sinclair, K., and Payette, S. 1995. Recent advance of the arctic treeline along the eastern coast of Hudson Bay. Journal of Ecology 83: 929-936.

Ling, F., and Zhang, T. 2005. Modeling the effect of variations in snowpack-disappearance date on surface-energy balance in the Alaskan North Slope. Arctic, Antarctic, and Alpine Research 37: 483-489.

Litaor, M.I., Williams, M., and Seastedt, T.R. 2008. Topographic controls on snow distribution, soil moisture, and species diversity of herbaceous alpine vegetation, Niwot Ridge, Colorado. Journal of Geophysical Research 113, doi:10.1029/2007JG000419.

Lloyd, A.H., and Graumlich, L.J. 1997. Holocene dynamics of treeline forests in the Sierra Nevada. Ecology 78: 1199-1210.

Maher, E.L., Germino, M.J., and Hasselquist, N.L. 2005. Interactive effects of tree and herb cover on survivorship, physiology, and microclimate of conifer seedlings at the alpine tree-line ecotone. Canadian Journal of Forest Research 35: 567-574.

Marks, D., and Dozier, J. 1992. Climate and energy exchange at the snow surface in the alpine region of the Sierra Nevada 2: Snow cover energy balance. Water Resources Research 28: 3043-3054.

Marks, D., Winstral, A., Seyfried, M. 2002. Simulation of terrain and forest shelter effects on patterns of snow deposition, snowmelt, and runoff over a semi-arid mountain catchment. Hydrological Processes 16: 3605-3626.

McCune, B. 2006. Non-parametric habitat models with automatic interactions. Journal of Vegetation Science 17: 819-830.

McCune, B., and Mefford, M.J. 2004. Hyperniche nonparametric multiplicative habitat modeling. Version 1.39. MjM Software, Gleneden Beach, Oregon.

McDonald, G.D. 1998. Soil survey of Warm Springs Indian Reservation, Oregon. U.S. Department of Agriculture and Natural Resources Conservation Service. Washington, D.C.

McGaughey, R.J. 2007. FUSION/LDV: Software for LIDAR data analysis and visualization. U.S. Department of Agriculture, Forest Service, Pacific Northwest Research Station. Available at http://www.fe.fed.us/eng/rsac/fusion/

Means, J.E. 1990. Mountain hemlock. In: Silvics of North America: 1. Conifers. Burns, R.M., and Honkala, B.H. (technical coordinators). U.S. Department of Agriculture, Forest Service, Washington, DC.

Miller, E.A. and Halpern, C.B. 1998. Effects of environment and grazing disturbance on tree establishment in meadows of the central Cascade Range, Oregon, USA. Journal of Vegetation Science 9: 265-282.

Minore, D. 1979. 1979. Comparative autecological characteristics of northwestern tree species: a literature review. U.S. Department of Agriculture, Forest Service, Pacific Northwest Forest and Range Experiment Station General. Technical Report PNW-87.

Mizukami, N., and Perica, S. 2008. Spatiotemporal characteristics of snowpack density in the mountainous regions of the western United States. Journal of Hydrometeorology 9: 1416-1426.

Mote, P.W., 2003. Trends in snow water equivalent in the Pacific Northwest and their climatic causes. Geophysical Research Letter 30: 1-4.

Mote, P.W., Hamlet, A.F., Clark, M.P., and Lettenmaier, D.P. 2005. Declining mountain snowpack in western North American. Bulletin of the American Meterological Association 86: 39-49.

Nolan, A.W., and Daly, C. 2006. Mapping “at risk” snow in the Pacific Northwest. Journal of Hydrometeorology 7: 1164-1171.

O’Connor, J.E., and Costa, J.E. 1993. Geologic and hydrologic hazards in glacierized basins in North America resulting from 19th and 20th century global warming. Natural Hazards 8: 121-140.

O’Connor, J.E., Hardison, J.H. III, and Costa, J.E. 2001. Debris flows from failures of neoglacial-age moraine damns in the Three Sisters and Mount Jefferson Wilderness Areas, Oregon. U.S. Geological Survey Professional Paper 1606.

Oke, T.R. 1987. Boundary layer climates. Methuen, London.

Owens, J.N., and Molder, M. 1977. Sexual reproduction of Abies amabilis. Canadian Journal of Botany 55: 2653-2667.

Packee, E.C., Oliver, C.D., and Crawford, P.D. 1981. Ecology of Pacific silver fir. In: Proceedings of the biology and management of true fir in the pacific northwest symposium. Oliver, C.D., and Kenday, R.M. (eds). University of Washington, College of Forest Resources, U.S. Department of Agriculture, Forest Service, Pacific Northwest Forest and Range Experiment Station Seattle, WA, Portland, OR.

Peel, M.C., Finlayson, B.L., and McMahon, T.A. 2007. Updated world map of the Köppen-Geiger climate classification. Hydrology and Earth System Sciences Discussions 4: 439-473.

Peterson, D.W., and Peterson, D.L. 1994. Effects of climate on radial growth of subalpine conifers in the North Cascade Mountains. Canadian Journal of Forest Research 34: 1921-1932.

Pierce, K.B., Lookingbill, T., and Urban, D. 2005. A simple method for estimating potential relative radiation (PRR) for landscape-scale vegetation analysis. Landscape Ecology 20: 137-147.
Prichard, S.J., Peterson, D.L., and Hammer, R.D. 2000. Carbon distribution in subalpine forests and meadows of the Olympic Mountains, Washington. Soil Science Society of America Journal 64: 1834-1845.

Rakestraw, L., and Rakestraw, M. 1991. History of the Willamette National Forest. USDA Willamette National Forest, Eugene, OR.

Randall, D.A., Wood, R.A., Bony, S., Colman, R., Fichefet, T., Fyfe, J., Kattsov, V., Pitman, A., Shukla, J., Srinivasan, J., Stouffer, R.J., Sumi, A., and Taylor, K.E. 2007. Climate models and their evaluation. In: Climate Change 2007: The physical science Basis. Contributions of the Working Group I to the fourth assessment report of the Intergovernmental Panel on Climate Change. Solomon, S., Qin, D., Manning, M., Chen, Z., Marquis M., Averyt, K.B., Tignor, M, and Miller, H.L. (eds.) Cambridge University Press, United Kingdom and New York, NY, USA.

Rochefort, M.R., and Peterson, D.L. 1996. Temporal and spatial distribution of trees in subalpine meadows of Mount Rainier National Park, Washington, U.S.A. Arctic and Alpine Research 28: 52-59.

SAS Institute Inc. 2008. SAS/STAT User’s Guide. Version 9.2. SAS Institute, Cary, NC.

Salathé, E.P., Steed, R., Mass, C.F., and Zahn, P.H. 2008. A high-resolution climate model of the U.S. Pacific Northwest: Mesoscale feedbacks and local responses to climate change. Journal of Climate 21: 5708-5726.

Salathé, E.P., L.R. Leung, Y. Qian, and Y. Zhang. 2009. Regional climate model projections for the State of Washington. Chapter 2 In: The Washington climate change impacts assessment: Evaluating Washington's future in a changing climate, Climate Impacts Group, University of Washington, Seattle, Washington.

Schabenberger, O. 2007. Growing up fast: SAS 9.2 enhancements to the GLIMMIX procedure. SAS Global Forum. Paper 177-2007.

Scott, W.E. 1977. Quaternary glaciation and volcanism, Metolius river area, Oregon. Geological Society of America Bulletin 88: 113-124.

Sicart, J.E., Pomeroy, J.W., Essery, R.L.H., Hardy, J., Link, T., and Marks, D. 2004. A sensitivity study of daytime net radiation during snowmelt to forest canopy and atmospheric conditions. Journal of Hydrometeorology 5: 774-784.

Smith, D.M., Larson, B.C., Kelty, M.J., and Ashton, P.M.S. 1997. The Practice of Silviculture: Applied forest ecology (9th edition). John Wiley and Sons, Inc. New York, NY, USA.

Smith, W.K., Germino, M.J., Hanocock, T.E., and Johnson, D.M. 2003. Another perspective on altitudinal limits of alpine timberlines. Tree Physiology 23: 1101-1112.

Solomon, A.M. and Kirilenko, A.P. 1997. Climate change and terrestrial biomass: What if the trees do not migrate. Global Ecology and Biogeochemical Letters 6: 139-148.

Stueve, K.M., Cerny, D.L., Rochefort, R.M., and Kurth, L.L. 2009. Post-fire tree establishment patterns at the alpine treeline Ecotone: Mount Rainer National Park, Washington, USA. Journal of Vegetation Sciences 20: 107-120.

Turner, M.G., Baker, W.L., Peterson, C.J., and Peet, R.K. 1989. Factors influencing succession: lesions from large, infrequent natural disturbances. Ecosystems 1: 511-523.

Trujillo, E., Ramirez, J.A., and Elder, K.J. 2007. Topographic, meteorologic, and canopy controls on the scaling characterstics of the spatial distribution of snow depth fields. Water Resources Research 43: W07409: doi:10.1029/2006WR005317.

Urban, D., Goslee, S., Pierce, K., and Lookingbill, T. 2002. Extending community ecology to landscapes. Ecoscience 9: 200-212.

Vale, T.R. 1981. Tree invasion of montane meadows in Oregon. American Midland Naturalist 105: 61-69.

Wiens, J.A. 1989. Spatial scaling in ecology. Functional Ecology 3: 385-397.

Williams, C.J., McNamara, J.P., and Chandler, D.G. 2009. Controls on the temporal and spatial variability of soil moisture in a mountainous landscape: the signature of snow and complex terrain. Hydrology and Earth Systems Sciences 13: 1325-1336.

Wilmking, M., Juday, G.P., Barber, V.A., Zald, H.S.J. 2004. Recent climate warming forces constrasting growth responses of white spruce at treeline in Alaska through temperature thresholds. Global Change Biology 10: 1724-1736.

Wing, M.G., and Karsky, R. 2006. Standard and real-time accuracy and reliability of a mapping-grade GPS in a coniferous western Oregon forest. Western Journal of Applied Forestry 21: 222-227.

Woodward, A., Schreiner, E.G., and Silsbee, D.G. 1995. Climate, geography, and tree establishment in subalpine meadows of the Olympic Mountains, Washington, U.S.A. Arctic and Alpine Research 27: 217-225.

Yamaguchi, D.K. 1991. A simple method for cross-dating increment cores from living trees. Canadian Journal of Forest Research 21: 414-416.

Zald, H.S.J. 2010a. Integrating LiDAR, satellite imagery, and forest inventory data to spatially characterize tree invasion, vegetation composition, and vegetation Structure in a subalpine meadow landscape, Oregon Cascades, USA. In: Patterns of Tree Establishment and Vegetation Composition in a Subalpine Meadow Landscape, Jefferson Park, Oregon, USA. Ph.D. Dissertation, Oregon State University.

Table 3.1. Biophysical characteristics of landforms based on field plots and LiDAR measurements.

	Glacial landforms		Debris flow landforms				
Plot variables (percent cover)	**mean**	**sd**	**mean**	**sd**	**df**	**t value**	**p**
Vegetation	53.31	25.38	47.04	25.24	283.45	2.54	0.0116
Bare Soil	5.20	13.03	18.21	24.22	187.05	-6.21	0.0000
Rock	10.78	16.92	7.31	12.89	365.09	2.50	0.0128
Litter	14.53	18.98	16.57	18.09	294.65	-1.14	0.2570
Coarse Wood Debris	0.70	3.67	1.21	3.98	262.68	-1.33	0.1859
Moss	12.73	15.09	8.07	12.60	334.59	3.57	0.0004
Lichen	1.09	2.29	0.31	1.30	461.23	4.82	0.0000
LiDAR-derived variables	**mean**	**sd**	**mean**	**sd**			
Elevation (m)	1790.49	6.47	1783.51	5.38			
CANDIST (m)	12.26	11.28	25.22	18.95			
RAD	3820.02	178.46	3836.05	85.32			
TOPO	-0.01	0.30	-0.02	0.19			
Vegetation Height	2.24	4.52	1.12	2.27			

Note: CANDIST is the distance to overstory canopy, RAD is potential relative radiation, and TOPO is the topographic position index. Differences between variables collected on field plots were assessed using Satterthwaite t tests assuming unequal variances. LiDAR-derived variables are a complete census of entire study area, so no statistical tests for differences between landform types were conducted.

Table 3.2. Selected, supported, and null models of tree abundance by species and landform type in relationship to biophysical explanatory variables.

Species	Landform	Explanatory variables in model	AIC_C	Δ_i
mountain hemlock	glacial	RAD TOPO ELEV CANDIST TSMEDIST	1865.56	0.00
		RAD TOPO CANDIST TSMEDIST	1866.67	1.11
		NULL	2106.47	240.91
mountain hemlock	debris flow	RAD TOPO CANDIST TSMEDIST	603.16	0.00
		RAD TOPO TSMEDIST	604.55	1.40
		TOPO CANDIST TSMEDIST	605.00	1.84
		RAD TOPO ELEV CANDIST TSMEDIST	605.71	2.55
		RAD TOPO	605.82	2.67
		RAD TOPO CANDIST	606.28	3.12
		TOPO TSMEDIST	606.80	3.64
		RAD TOPO ELEV CANDIST TSMEDIST	606.88	3.73
		TOPO ELEV CANDIST TSMEDIST	607.04	3.89
		NULL	612.14	8.99
Pacific silver fir	glacial	RAD TOPO CANDIST ABAMDIST	1868.33	0.00
		RAD TOPO ABAMDIST	1868.95	0.62
		RAD TOPO ELEV CANDIST ABAMDIST	1870.39	2.06
		RAD TOPO ELEV ABAMDIST	1870.99	2.66
		NULL	2245.46	377.13
Pacific silver fir	debris flow	TOPO ABAMDIST	438.44	0.00
		TOPO ELEV ABAMDIST	439.08	0.64
		TOPO CANDIST ABAMDIST	439.17	0.73
		TOPO ELEV CANDIST ABAMDIST	439.93	1.48
		RAD TOPO ABAMDIST	440.60	2.15
		RAD TOPO ELEV ABAMDIST	441.20	2.76
		RAD TOPO CANDIST ABAMDIST	441.38	2.94
		RAD TOPO ELEV CANDIST ABAMDIST	442.12	3.68
		NULL	483.18	44.74

Note: Akiake Information Criterion for small sample sizes (AIC_c), and delta AIC_c (Δ_i) values. Determination of empirically supported model in AIC model selection follows recommendation of Burnham and Anderson (2002). Explanatory variable are: potential relative radiation (RAD), topographic position index (TOPO), elevation (ELEV), distance to overstory canopy (CANDIST), distance to mountain hemlock overstory (TSMEDIST), and distance to Pacific silver fir overstory (ABAMDIST) in meters.

Table 3.3. Fixed effects of explanatory variables in the best empirically supported models ($\Delta_i = 0$) of tree abundance by species and landform type.

			Fixed effects solutions				Type III fixed effects		
Species	**Landform**	**Explanatory variable**	**estimate**	**se**	**lclm**	**uclm**	**df**	**f value**	**p**
mountain hemlock	glacial	RAD	-0.0023	0.0003	-0.0030	-0.0016	1, 368	46.5574	0.0000
		TOPO	1.5975	0.1224	1.3568	1.8382	1, 368	170.3093	0.0000
		ELEV	0.0232	0.0132	-0.0027	0.0491	1, 368	3.0953	0.0794
		CANDIST	0.1318	0.0249	0.0828	0.1808	1, 368	27.9603	0.0000
		TSMEDIST	-0.1229	0.0250	-0.1721	-0.0736	1, 368	24.0736	0.0000
mountain hemlock	debris flow	RAD	-0.0022	0.0010	-0.0042	-0.0003	1, 99	5.4005	0.0222
		TOPO	0.8314	0.2564	0.3226	1.3403	1, 99	10.5122	0.0016
		CANDIST	-0.0386	0.0194	-0.0771	0.0000	1, 99	3.9436	0.0498
		TSMEDIST	0.0468	0.0191	0.0089	0.0846	1, 99	6.0144	0.0159
Pacific silver fir	glacial	RAD	-0.0017	0.0003	-0.0023	-0.0010	1, 369	25.4059	0.0000
		TOPO	0.5289	0.1312	0.2709	0.7869	1, 369	16.2488	0.0001
		CANDIST	0.0133	0.0082	-0.0029	0.0295	1, 369	2.5898	0.1084
		ABAMDIST	-0.0636	0.0073	-0.0778	-0.0493	1, 369	76.8308	0.0000
Pacific silver fir	debris flow	TOPO	1.5349	0.2817	0.9762	2.0937	1, 101	29.6962	0.0000
		ABAMDIST	-0.0289	0.0068	-0.0424	-0.0155	1, 101	18.1728	0.0000

Note: Explanatory variable codes as defined in the methods section and Table 2.2.

Table 3.4. Mean (with 95% confidence intervals) of topographic position (TOPO) and elevation (ELEV) on micro sites where mountain hemlock trees established during periods of high snowfall with low temperature (HSLT), and low snowfall with high temperatures (LSHT) regimes.

Establishment Type	**Landform Type**	**Topographic Variable**	**Climate Regime**		**Z value**	**p**
			HSLT	**LSHT**		
initial	glacial		41 trees	99 trees		
		ELEV	1791.68 (1790.01, 1793.35)	1791.07 (1790.04, 1792.1)	0.7419	0.4594
		TOPO	0.24 (0.16, 0.33)	0.09 (0.02, 0.16)	2.5941	0.0105
initial	debris flow		23 trees	28 trees		
		ELEV	1782.61 (1781.92, 1783.3)	1781.06 (1780.05, 1782.07)	2.1209	0.0389
		TOPO	0.05 (-0.05, 0.15)	-0.04 (-0.14, 0.07)	1.0036	0.3204
secondary	glacial		11 trees	14 trees		
		ELEV	1790.01 (1786.09, 1793.92)	1793.25 (1790.1, 1796.41)	-1.5066	0.1450
		TOPO	0.26 (0.05, 0.48)	0.05 (-0.1, 0.21)	1.5066	0.1450

Note: Differences between HSLT and LSHT periods were assessed using Wilcoxon-Mann-Whitney tests. Climate variable codes as described in the methods section. Micro site variable codes as described in the methods section and Table 2.2.

Table 3.5. Observed versus expected tree establish for mountain hemlock by landform and establishment type, on micro sites with high and low topographic positions and elevations during high snow low temperature (HSLT) and low snow high temperature (LSHT) climate periods.

Landform Type	Topographic Variable	Topographic position		Climate Regime		p
				HSLT	LSHT	
glacial	TOPO	high	observed	28	41	
			expected	26	43	0.8616
glacial	TOPO	low	observed	13	61	
			expected	28	46	0.0009
debris	TOPO	high	observed	9	8	
			expected	6	11	0.4905
debris	TOPO	low	observed	15	21	
			expected	13.5	22.5	1.0000
glacial	ELEV	high	observed	22	47	
			expected	26	43	0.5921
glacial	ELEV	low	observed	18	56	
			expected	28	46	0.1094
debris	ELEV	high	observed	15	11	
			expected	10	16	0.2668
debris	ELEV	low	observed	7	17	
			expected	9	15	0.7601

Note: p values are from Fisher’s exact test. Expected values are the observed row totals multiplied by the percent of years in the climate record within HSLT and LSHT climate periods.

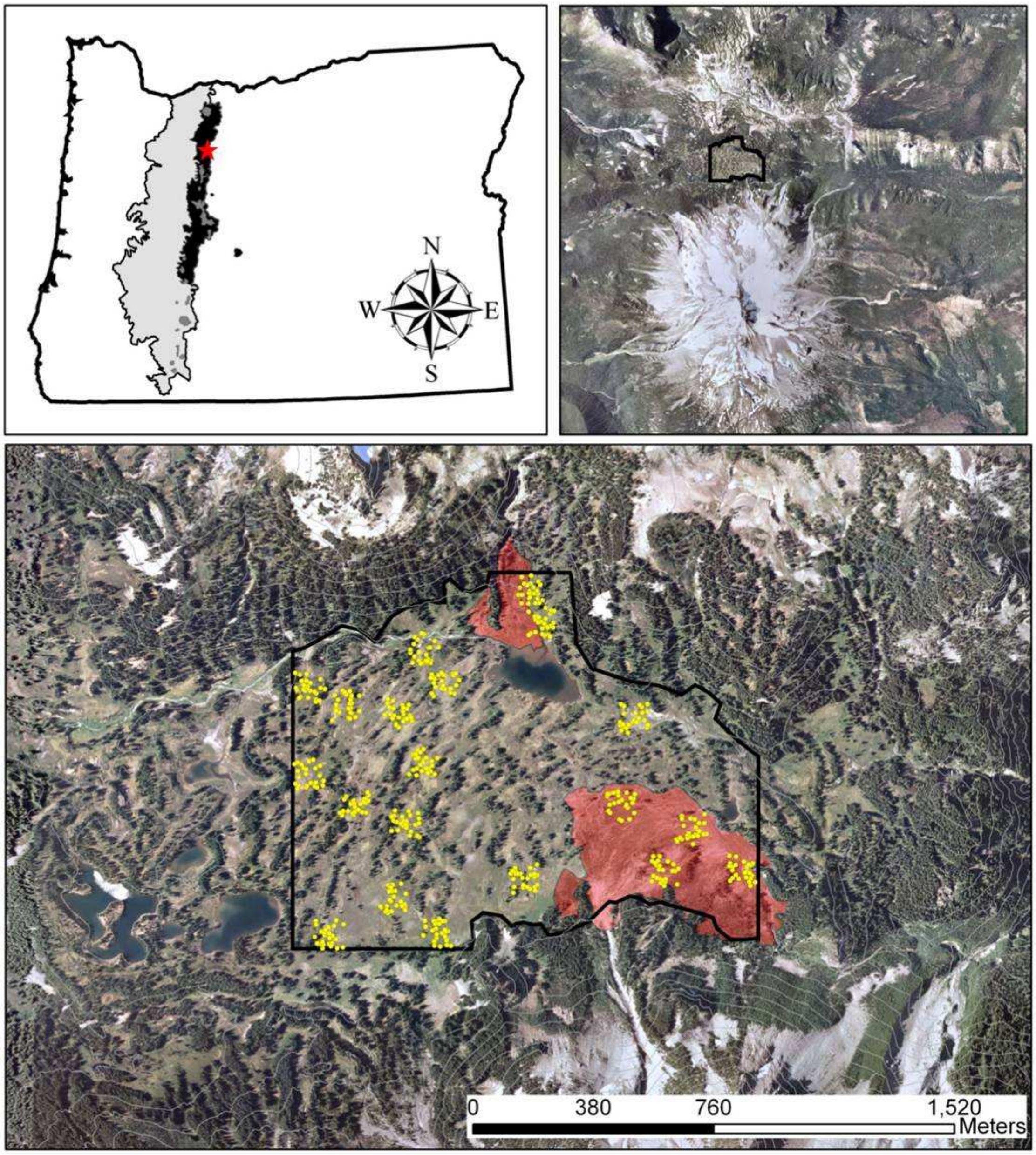

Figure 3.1. Study area location. (a) State of Oregon with the Cascades ecoregion in gray, the Cascades crest and montane zone in black, and subalpine and alpine areas in dark gray. The Jefferson Park study area (red star). (b) shows the study area (black outline) in relation to Mountain Jefferson. (c) close up image of the study area, plots (light yellow circles) , and debris flows (shaded red). Light grey lines are 25 m contour intervals.

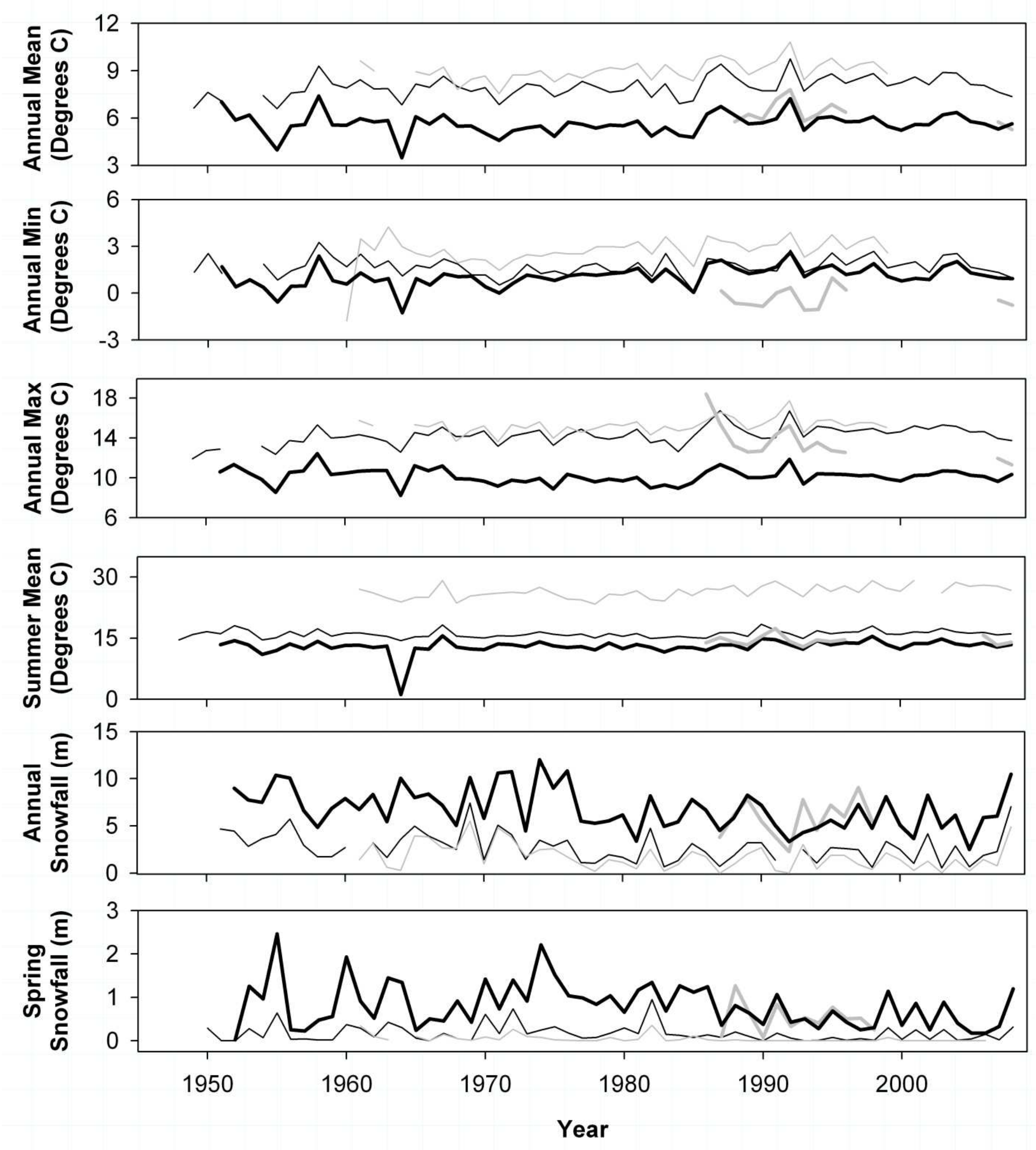

Figure 3.2. Regional snow fall and temperature from selected climate stations during the 1951 to 2008 time period. Annual minimum, maximum, and mean temperature, annual snowfall, and spring (April thru June) snowfall for the Government Camp (▬), Santiam Junction (▬), Marion Forks (—), and Belknap Springs (—) stations.

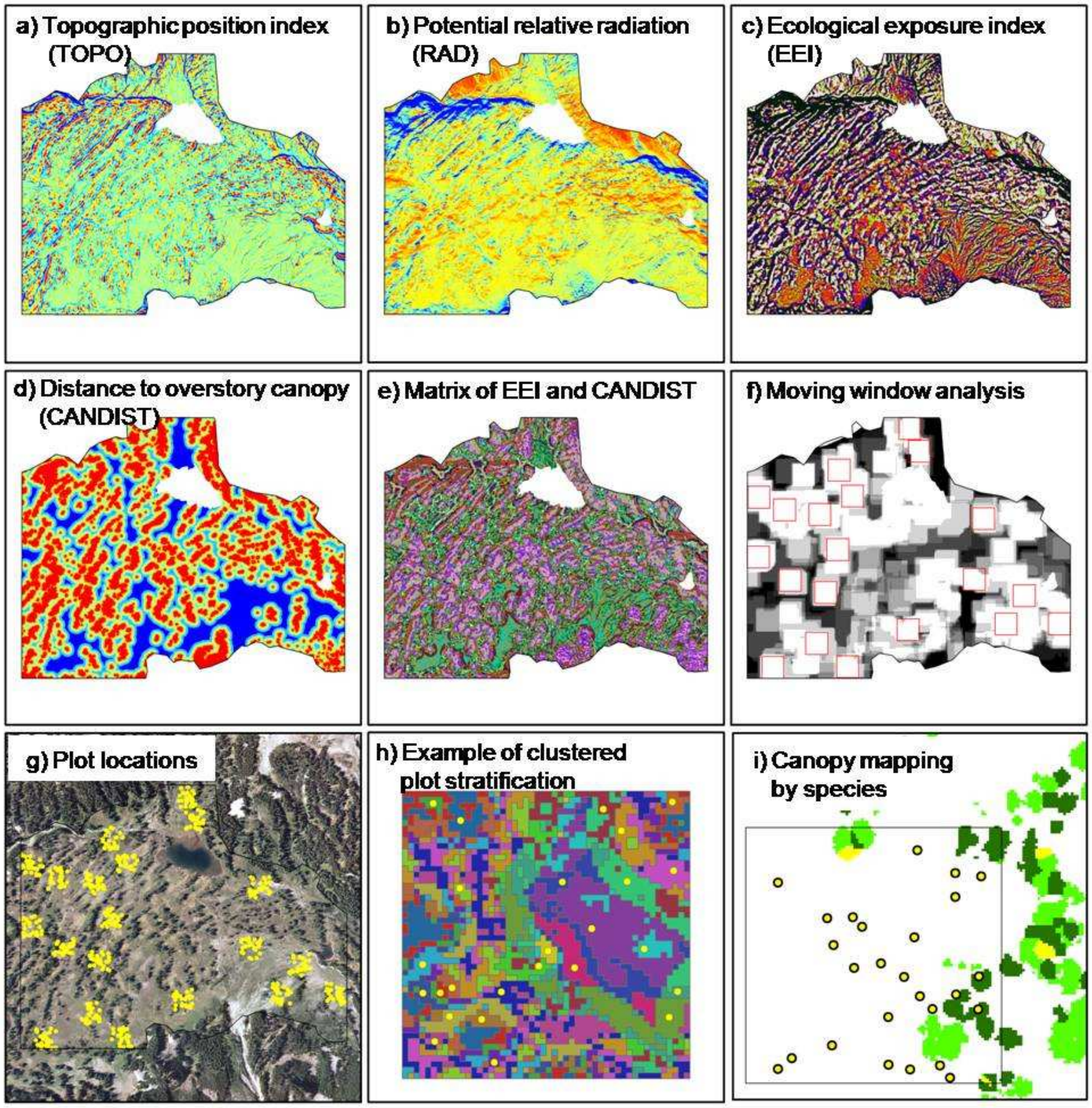

Figure 3.3. Constrained stratified random sampling design steps: a) TOPO explanatory variable grid, b) RAD explanatory variable grid, c) TOPO and RAD are relativized by their respective standard deviates and averaged to generate the EEI grid, d) distance to overstory canopy (vegetation greater than 8 m tall), e) 25 class matrix of all combinations of EEI and CANDIST, f) moving window analysis to find 100 * 100 m areas with all 25 class combinations of EEI and CD_ALL. Areas with all 25 strata are shown as red squares, g) final locations of 500 field plots shown as yellow dots, h) example 25 plot cluster stratified random sampling in relation to 25 strata. Plots are yellow dots, pixels are colored by the 25 sampling strata, i) example of overstory canopy maps by species in relation to a 100 * 100 m cluster showing mountain hemlock (dark green), Pacific silver fir (light green), and Alaska yellow-cedar (yellow) overstory canopy.

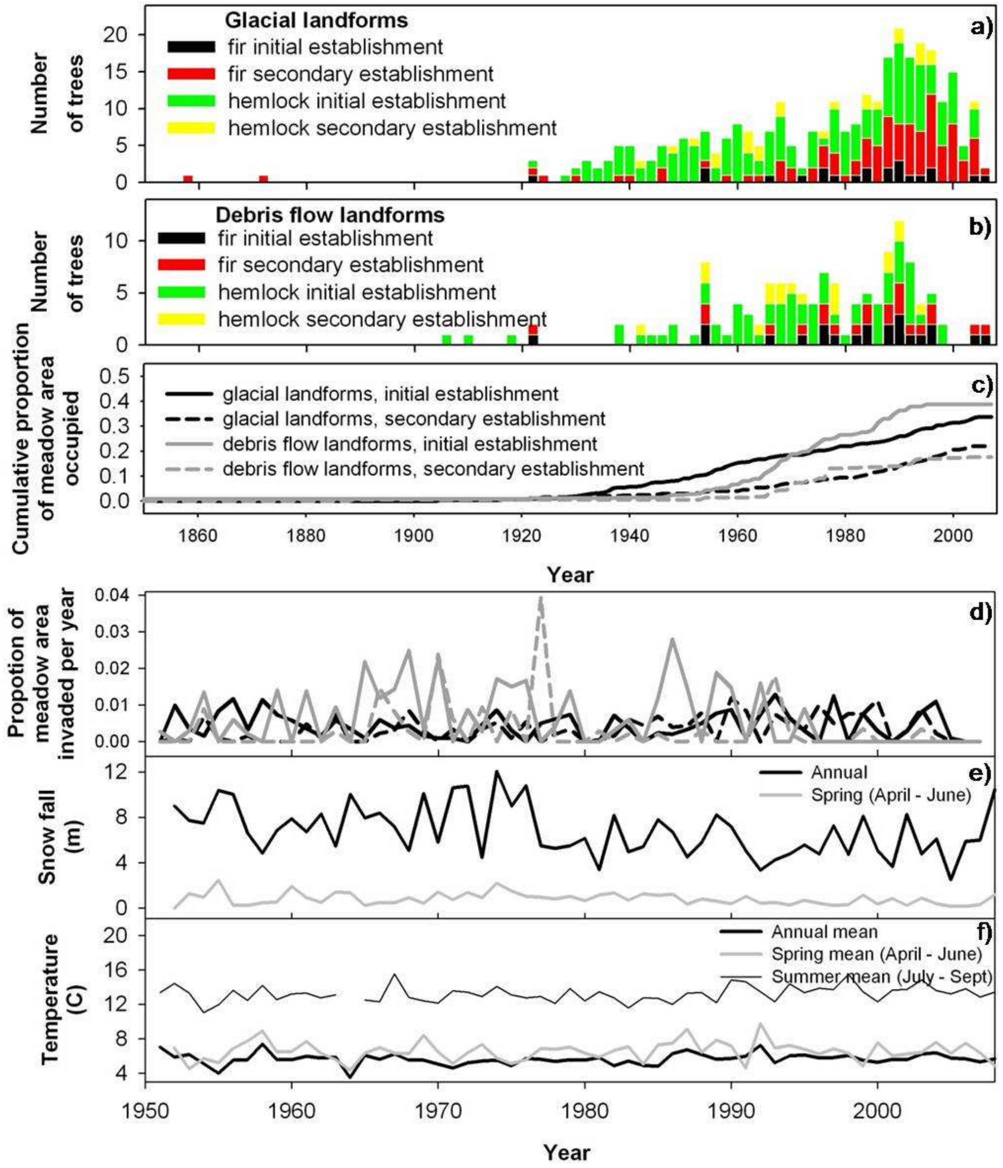

Figure 3.4. Count of trees less than 8 m tall on glacial (a) and debris flow (b) landforms, cumulative proportion of sites occupied by trees by landform and establishment type (c), and annual rates of site occupancy (d) in relation to selected regional snow fall (e) and temperature variables (f).

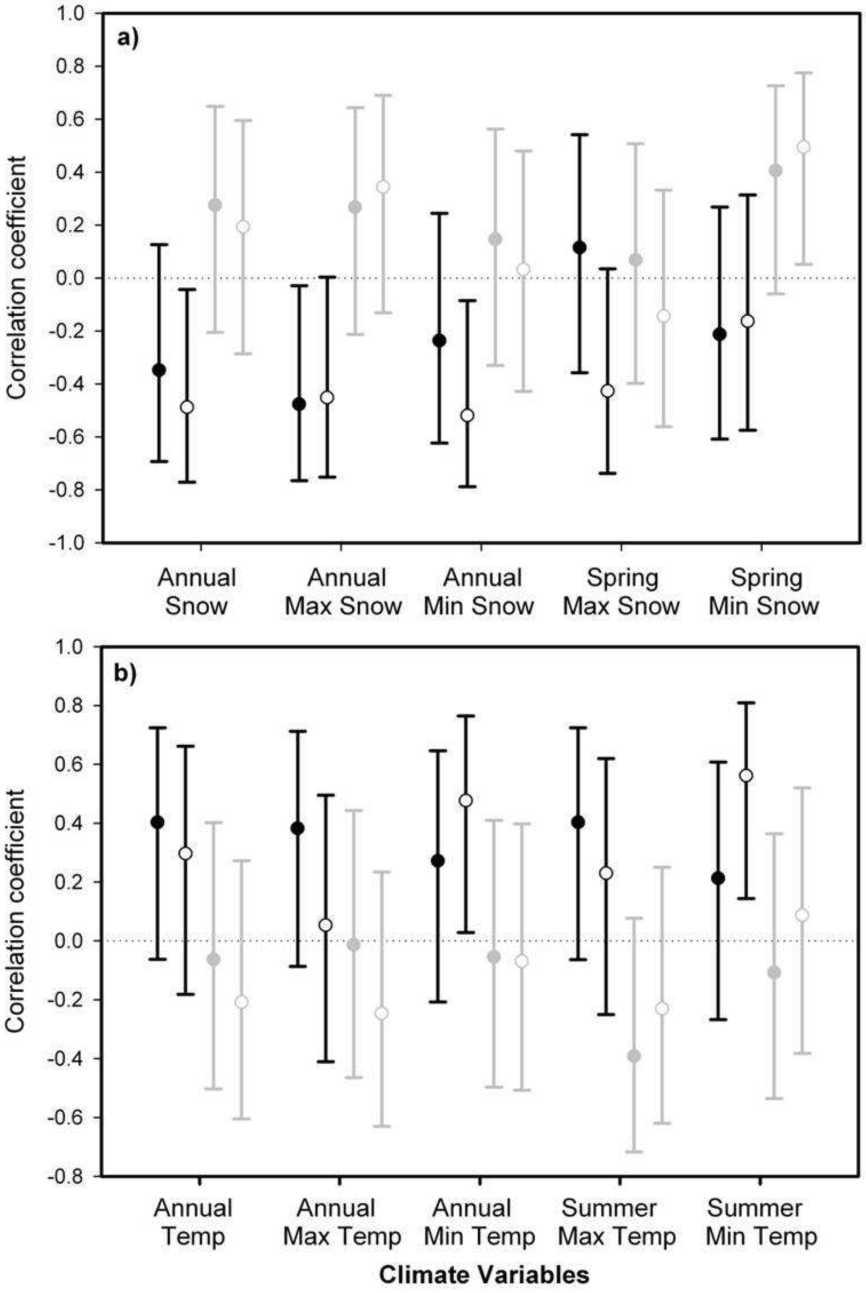

Figure 3.5. Pearson correlation coefficients between rates of site occupancy and climate variables for: a) snowfall, and b) temperature. Occupancy rates and climate variable data are for 3 year periods. Solid circle are for initial establishment, hollow circles are for secondary establishment, glacial landforms are shown in black, and debris flows are shown in gray. Error bars are the upper and lower 95% confidence limits of correlation coefficients. Correlations are significant at the 0.05 level if error bars do not intersect zero (highlighted with an asterisk above the bar).

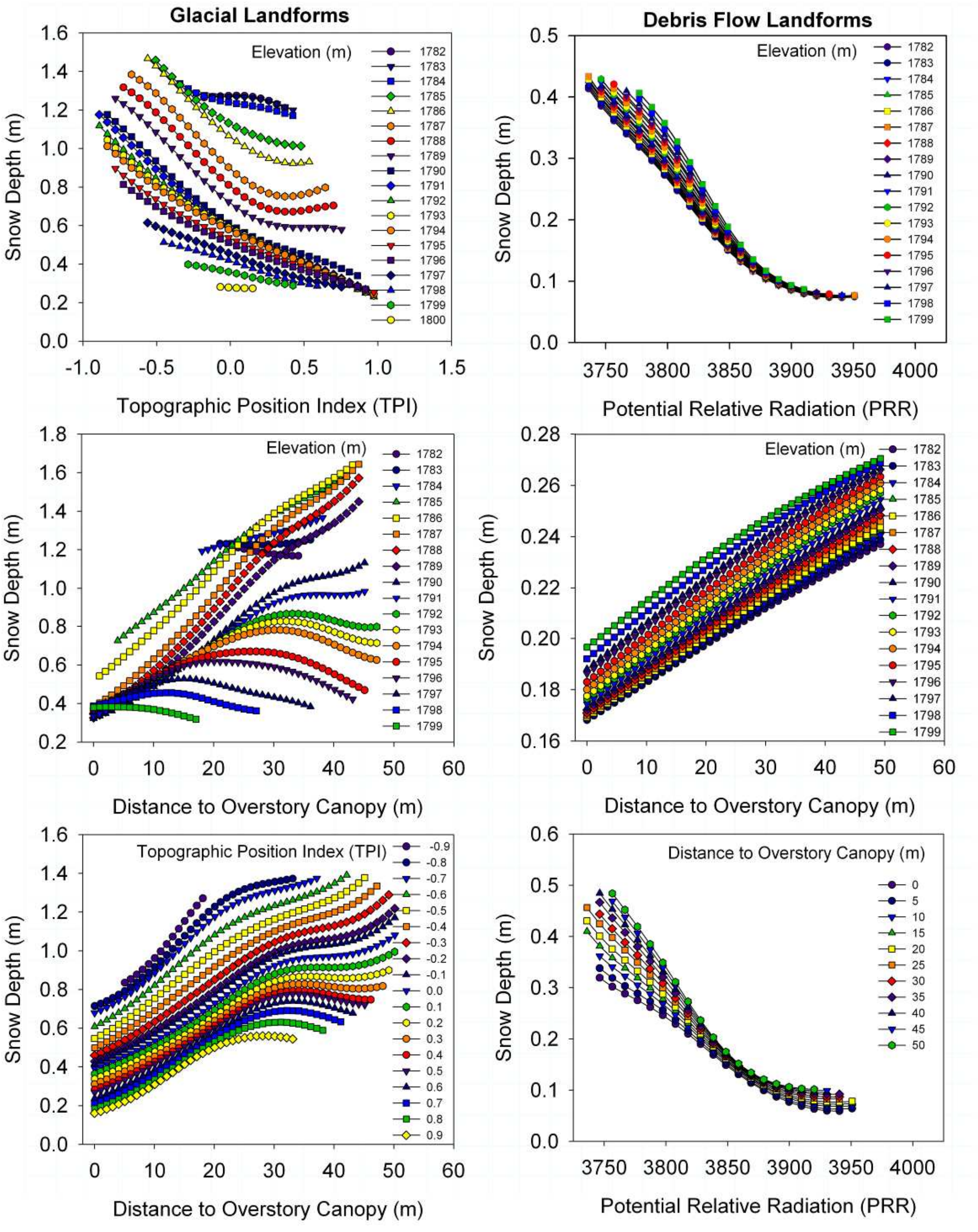

Figure 3.6. Modeled relationships between snow depth, microtopographic variables, and distance to overstory canopy by landform type (glacial landforms on the left three panels). Note the scale differences in modeled snow depth between landform types.

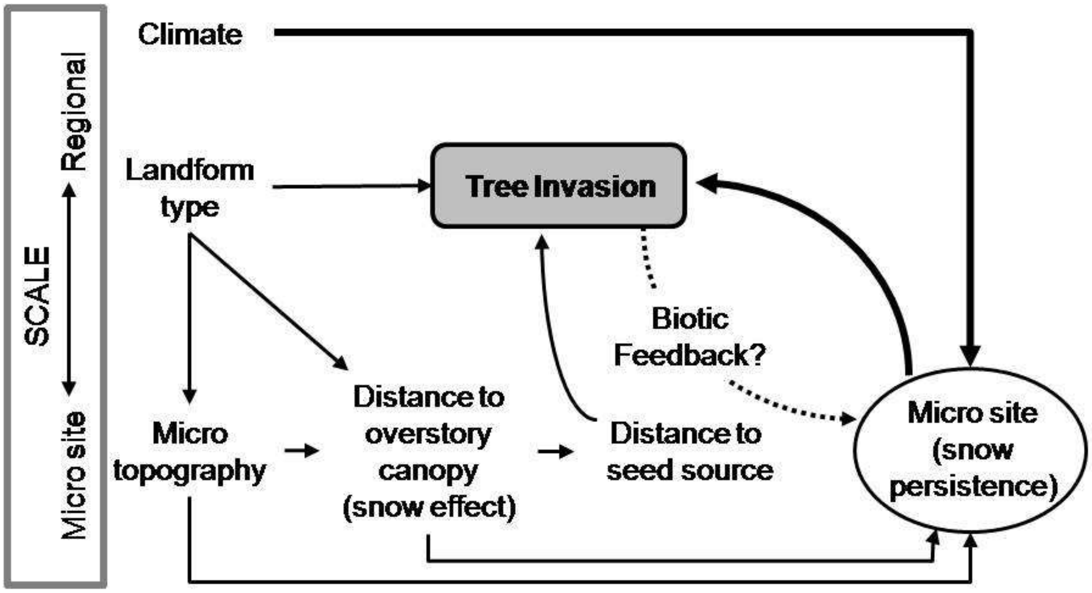

Figure 3.7. Conceptual model of interactions between climate and biophysical controls of recent tree establishment in the meadows at Jefferson Park.

CHAPTER 4: MODELING TREE INVASION OF A SUBALPINE MEADOW LANDSCAPE, OREGON CASCADES, USA.

ABSTACT

Climate-driven treeline movement and invasion of subalpine meadows have been documented across wide ranges of geographic locations and controlling factors. Treeline movement can in turn influence temperature feedbacks, carbon sequestration, and biodiversity at multiple spatial scales. Large-scale species distribution models (SDMs) suggest climate change will shifts species distributions and biomes and reduce biodiversity. Local scale SDMs incorporating downscaled climate models suggest local high-elevation persistence of species habitat, but do not specifically model plant regeneration in relation to the many non-climatic biophysical parameters important for treeline establishment (i.e. dispersal limitations, micro sites, biotic interactions, and disturbances). This study developed a fine-scale (2 m pixel size) spatially explicit statistical model of tree invasion into a subalpine meadow landscape in the Oregon Cascades, simulating historical tree invasion from 1950 to 2007, and potential future invasion from 2007 to 2064. The model incorporated temporal data from regional climate and tree-ring establishment reconstructions, and used Light Detection and Ranging (LiDAR) data to characterize micro sites, biotic interactions based on vegetation structure, and a historical debris flow disturbance event. From 2007 to 2064 tree invasion was modeled under six different annual snowfall scenarios with three levels of snowfall declines from historical means (0, 25, and 50 percent declines), crossed with two levels of forcing persistent three year periods of extreme high or low snowfall (forcing and no forcing). From 1950 to 2007, simulated historical meadow area declined from 82% to 65% of the study area. Model outputs of historical area, spatial distributions, and spatial clustering of tree invasion generally agreed with independent validation, and suggest biotic interactions due to young tree establishment facilitation are only important on glacial landforms. Simulations indicate meadows may decline by 36-43% from 2007 to 2064. Meadows area declined with reduced annual snow fall. Under all scenarios there were persistent areas of meadow without tree invasion in 2064. This model suggests subalpine meadows may significantly decline in relation to climate, but unfavorable micro sites and recruitment limitations may be equally or more important factors in meadow decline and persistence, while also suggesting local high-elevation persistence of subalpine meadows under future climate warming.

INTRODUCTION

The boundary between forests and alpine/arctic vegetation (referred to as treeline, subalpine parklands, or the forest-tundra ecotone, FTE), is a conspicuous feature of mountain and high latitude landscapes throughout the world. FTE positions are globally associated with thermal deficiencies limiting plant growth (Körner 1998, Jobbágy and Jackson 2000). Arctic and mountain ecosystems are believed to be sensitive to climate change (Christensen et al. 2007, Fischlin et al. 2007), while varying degrees of climate-driven FTE movement have been documented across a wide range of climatic regimes, forest types, and land use histories (Harsch et al. 2009). Climate-driven FTE movement may have numerous ecological effects including: temperature feedbacks resulting from altered surface energy balances (Bonan et al. 1992, Beringer et al. 2005), changes in ecosystem carbon storage (Prichard et al. 2000, Wilmking et al. 2006), and the loss of alpine biodiversity (Dirnbock et al. 2003, Halloy and Mark 2003, Thuiller et al. 2005). The magnitude of these ecological effects will in part be determined by the extent and rates of FTE movement. However the sensitivity of FTE movement and alpine/subalpine meadow invasion to climate can be dependent on numerous non-climatic biophysical factors (Miller and Halpern 1998, Daniels and Veblen 2004, Holtmeier and Broll 2005, Zald 2010b), making it difficult to quantify FTE movement and associated ecological effects in response to climate change. Simulation models have the potential to improve our understanding of FTE movement under future climate scenarios. At global to regional scales, simulation models have been used to project large geographic shifts in biomes, species distributions, and biodiversity in response to future climate scenarios (Bachelet et al 2001, Thuiller et al 2005, Rehfeldt et al. 2009). However, global and regional models of species and vegetation distributions are unlikely to generate realistic scenarios of future FTE movement, because they do not model at the spatial resolution at which FTE movement often occurs, and they tend to exclude many non-climatic factors which influence tree regeneration at the FTE.

Species distributions models (SDMs) are the most commonly used approach for simulating future species distributions and diversity in response to potential climate change (Guisan and Zimmerman 2000, Guisan and Thuiller 2005,). SDMs relate multiple abiotic habitat characteristics with observed occurrences of a species, fitting a bioclimatic envelope or realized niche. Climate change scenarios can then be applied to a species fitted bioclimatic envelope to simulate how the potential spatial distribution of a species (or biodiversity in the case of many species envelopes) may change in the future. However, global climate models (and regional models generated by statistical downscaling) used in SDMs may not realistically simulate the effects of meso-scale topography and landscape context on temperature and precipitation in mountainous landscapes (Salathé et al. 2008). This suggests scale incompatibilities between existing climate models and species observations (Guisan and Thuiller 2005, Randin et al. 2009). Scale incompatibilities may be especially problematic at the FTE, because climatic and non-climatic biophysical factors can control patterns of tree establishment at regional to micro site spatial scales (Rochefort and Peterson 1996, Holtmeier and Broll 2005, Zald 2010b). Coarse-resolution climate data also obscures fine-scale climate variability in mountain landscapes, and localized persistence of favorable thermal habitat conditions may allow species to persist in spite of climate change (Randin et al. 2009).

Another limitation of SDMs is their reliance on bioclimatic envelopes correlated to species occurrences, but tree migration and FTE movement are fundamentally determined by seed-based regeneration (Lescop-Sinclair and Payette 1995, Smith et al. 2003). SDMs are criticized for not incorporating many non-climatic factors (such as dispersal limitations, biotic interactions, and disturbance) important in determining species distributions (Woodward and Beerling 1997, Davis et al. 1998). Regeneration dynamics are not only problematic for SDMs, but also difficult to accurately simulate in a variety of forest dynamics, succession, and growth models (Price et al. 2001, Larocque et al. 2006, Pabst et al. 2008), suggesting many existing modeling frameworks are poorly suited to simulating regeneration dynamics fundamental to the rates and extent of FTE movement. Process-oriented forest regeneration models explicitly parameterize resources levels, recruitment, growth, and mortality (Pacala et al. 1996, Wallentin et al. 2008), but these parameters are largely unknown for forests with marginal or non-existent wood products value. Realistic scenarios of future FTE movement and tree invasion of alpine/subalpine meadows will require: modeling at spatial resolutions comparable to the patterns and processes of tree establishment, and incorporation of tree regeneration dynamics which are often influenced by many non-climatic parameters (i.e. seed dispersal, disturbance, biotic interactions, etc.).

The primary objective of this study was to spatially project historical and near-term future (1950 to 2064) tree invasion of a subalpine meadow landscape in the Pacific Northwest region of North America. In contrast to SDMs which utilize bioclimatic envelopes and forest dynamics, succession, and growth models which parameterize processes such as fecundity, dispersal, and growth; I developed an empirically-derived statistical model to quantify tree invasion in relation to deterministic spatial patterns of tree invasion controlled by biophysical factors (microtopography, seed sources, overstory and young tree interactions, larger-scale landform types), and probabilistic temporal patterns of tree establishment in relation to climate (specifically snowfall). Spatial and temporal patterns of tree invasion were quantified from results of Zald (2010b), which combined spatially explicit tree establishment reconstructions from tree-ring dating, regional historical climate data, and spatial characterizations of microtopography and vegetation structure derived from Light Detection and Ranging (LiDAR) data. Specifically, this model was developed to address the following three questions: (1) can fine-scale (2m pixel size) patterns of historical tree invasion be accurately predicted? (2) how sensitive is future tree invasion (and therefore meadow persistence) to different future snowfall scenarios? and (3) are non-climatic factors such as landforms and biotic interactions associated with different spatial patterns of tree invasion?

METHODS

Study Area Description

The study was conducted in 132 hectares of Jefferson Park (44°42’ N 121°48’ W, 1693-1814 m asl), a subalpine parkland immediately north of Mount Jefferson in the Mount Jefferson Wilderness Area, Willamette National Forest, Oregon, USA. Jefferson Park is within the High Cascades physiographic province of the Pacific Northwest region (Franklin and Dyrness 1989). The climate is intermediate between Mediterranean and maritime temperate, with dry warm summers and significant winter precipitation largely falling as snow. The physiography of Jefferson Park is dominated by glacial and debris flow landforms. Glacial landforms consist of outwash and till deposited during the most recent glacial maxima of the Holocene Epoch (Scott 1977). One debris flow occurred in 1934, depositing debris 0.36-2.4 m deep across 320,000 m^2 of eastern Jefferson Park (O’Connor et al. 2001). A smaller undocumented debris flow in north Jefferson Park occurred at an indeterminate age prior to 1934. Soils of the study area are poorly documented, and consist of either rubble or soils derived from glacial material, sedimentary rock, pyroclastic ash flows, and volcanic ash (MacDonald 1998). Additional details regarding the climate, geology, and soils of the study area can be found in Zald (2010a).

Mountain hemlock (*Tsuga mertensiana*) is the dominant tree species, followed by Pacific silver fir (*Abies amabilis*), found in single species and mixed-species stands. Most of these stands are “islands” of variable size and shape surrounded by meadow vegetation. Mature trees in these islands are generally 150 to 250 years old, but can exceed 400 years of age (Zald 2010a). Results from Zald (2010a) indicate mountain hemlock has been the dominant species invading meadows for the past 150 to 250 years. Subalpine fir (*Abies lasiocarpa*), whitebark pine (*Pinus albicaulis*), lodgepole pine (*Pinus contorta*), and Alaska yellow-cedar (*Callitropsis nootkatensis*) are also present, but in greatly reduced amounts (less than two percent of recent tree establishment). Due to its dominance in both older and recently initiated stands, the models in this study focus exclusively on mountain hemlock establishment.

Modeling Overview

Mountain hemlock establishment was simulated using a spatially and temporally explicit empirically-derived statistical model, with both deterministic and probabilistic spatial and temporal components. The study area was simulated as a 595 x 737 grid of 2 m pixels encompassing 132 ha. Tree establishment was simulated across the study area during the 1950 to 2064 time period in 3-year time steps. Tree invasion of meadows was modeled as the presence- absence of trees represented as 2 m pixels, which was considered reasonable because the slow growth and narrowly conical crowns of mountain hemlock will be largely confined to the pixel size over the time period of simulation. The model is based on the spatial and temporal patterns of tree invasion in relation to landform type, microtopography, vegetation structure, and climate from field data and analyses in Zald (2010b). The starting spatial distribution of trees in 1950 was determined by combining LiDAR data of tree heights with age-height regressions of dated trees sampled in Zald (2010a and 2010b). The base model iterates each three-year time step from 1950 starting conditions to 2064 as follows (Figure. 4.1):

1. Pixels are selected as having the potential to be invaded by a tree if their spatial probability of occupancy ($\text{Prob}_{\text{spat}}$) is greater than a randomly generated value.
2. The temporal probability of occupancy ($\text{Prob}_{\text{temp}}$) determines what proportion of pixels in the landscape invaded at each time step, where selected pixels from step 1 having higher $\text{Prob}_{\text{spat}}$ values are more likely to be invaded.

For each time step from 1950 to 2007, $\text{Prob}_{\text{temp}}$ was calculated as the proportion of meadow area invaded by landform type (glacial versus debris flows), as reconstructed via tree-ring dating in Zald (2010b). For projecting into the future (2007 to 2064), $\text{Prob}_{\text{temp}}$ was calculated from the relationship between the proportion meadow area invaded by landforms type and maximum annual snowfall as determined in Zald (2010b). This relationship between tree invasion and snowfall was applied to six different future snowfall scenarios representing potential changes in the mean and temporal variability of annual snowfall. In addition to the base model described above, a second model (referred to as the facilitation model) was developed where the probability of any given pixel being invaded can increase because of a facilitation effect of young tree presence in adjacent cells ($\text{Prob}_{\text{facil}}$). Details of $\text{Prob}_{\text{spat}}$, $\text{Prob}_{\text{temp}}$, $\text{Prob}_{\text{facil}}$, starting configurations, and future snowfall scenarios are described below.

Spatial Probability of Mountain Hemlock Occupancy ($\text{Prob}_{\text{spat}}$)

The spatial probability of occupancy ($\text{Prob}_{\text{spat}}$) was calculated from field data on the biophysical controls of tree establishment in the study area (Zald 2010b). Tree establishment was recorded on 499 2 m plots (390 on glacial landforms and 109 of debris flow landforms), located in a stratified random design in relation to microtopography and distance to overstory canopy, both derived from airborne discrete return Light Detection and Ranging (LiDAR). Zald (2010b) found mountain hemlock establishment was spatially controlled by a multi-scale hierarchy of landform type, microtopographic variables, and distance to overstory. Biophysical variables were associated with variation of late summer snow depth, thought to influence spatiotemporal patterns of FTE tree establishment in the Pacific Northwest region of North America via control of growing season length (Fonda and Bliss 1969, Franklin et al. 1971, Zald 2010b). Since 1950, mountain hemlock invasion of meadows in the study area was greater on debris flows versus glacial landforms, and was greatest on micro sites with higher topographic position, potential relation radiation, and elevation, and in closer proximity to overstory canopy. For details regarding field sampling design, data collection, and statistical analyses of tree invasion in relation to biophysical controls within the study area, please refers to Zald (2010b).

Based on these previous findings of mountain hemlock invasion in relation to biophysical controls, an empirically-derived grid of the spatial probability of tree occupancy ($\mathrm{Prob}_{\mathrm{spat}}$) was developed for the study area. The probability of mountain hemlock presence was modeled in relation to seven biophysical variables (Table 4.1). Zald (2010b) analyzed tree establishment in relation to only one fine-scale topographic position index variable (TOPO1). However TOPO1 failed to account for larger-scale depressions and drainages where increased snow depth reduced the presence of mountain hemlock. To characterize larger-scale topographic features, four additional topographic position indices (TOPO2-5) were developed with annuli ranging from 10 to 300 m in size, but only TOPO2 and TOPO4 were selected in model below.

The probability of mountain hemlock presence was modeled in relation to biophysical variables with nonparametric multiplicative regression (NPMR) using Hyperniche version 1.39 (McCune and Medford 2004). Like linear regressions, NPMR quantifies the relationships between a response and explanatory variables. However, NPMR represents dependent variable responses to multiple explanatory variables based on kernel functions to weight observations, rather than generating regression coefficients for a model of fixed global form. NPMR can be applied to data with many explanatory dimensions, and multidimensionality is provided automatically and multiplicatively (rather than additively as in linear regressions), parsimoniously modeling the complex interactions among predictors (McCune 2006). Separate models were developed for plots on debris flow and glacial landforms. NPMR was run using a local mean with a Gaussian weighting function, binary response, and the minimum average neighborhood size was set at 5 percent of sample units. Variables were retained in the final model if they improved model fit by at least five percent. The best fit model was evaluated by the log 10 of the likelihood ratio (11.8 and 3.55 for glacial and debris landforms). The selected model of mountain hemlock presence on glacial landforms had five explanatory variables (CANDIST, TOPO1, TOPO2, RAD, and slope), while four variables were selected on debris flow landforms (CANDIST, elevation, TOPO1, and TOPO4). The sensitivity of tree presence to each predictor variable was evaluated by nudging each explanatory variable value one at a time by ±5% of its range throughout its range. Sensitivity was calculated as the average absolute value of the differences induced by nudging the predictor (Table 4.2). Mountain hemlock presence was most sensitive to CANDIST and TOPO2 on glacial landforms, and ELEV and SLOPE on debris flow landforms. Monte Carlo permutation procedures were conducted for each model with 200 runs ($p = 0.0040$ and $p = 0.0396$ for glacial and debris flow landforms), suggesting that model fit was better than could obtained by chance alone. Similar to Yost (2008), a grid of the probability of occupancy of each pixel ($\text{Prob}_{\text{spat}}$) in the study area was generated by applying the model response surfaces to a set of grids representing each explanatory variable in the model (Figure 4.2). $\text{Prob}_{\text{spat}}$ values ranged from 0.01 to 0.94, or a 1 to 94 percent chance of being occupied.

Temporal Probability of Mountain Hemlock Occupancy (Prob_{temp})

In the FTE of the Pacific Northwest region of North America, temporal patterns of tree establishment are strongly associated with annual variation of snow fall (Franklin et al. 1971, Woodward et al. 1995, Rochefort and Peterson 1995, Zald 2010b). Temporal probability of tree occupancy ($\text{Prob}_{\text{temp}}$) was calculated in 3 year time steps as the non-treed proportion of the study area by landform type occupied by trees in a given time step, as determined from tree establishment reconstruction using tree-ring dating in Zald (2010b). For the 1950 to 2007 time period, $\text{Prob}_{\text{temp}}$ is simply the reconstructed proportion of the study area invaded (without replacement of the area invaded in the previous time step) in three year time steps. $\text{Prob}_{\text{temp}}$ was calculated using three year bins rather than annually because: (1) a large number of individual years lacked new site invasion, (2) three year bins implicitly incorporate FTE germinant mortality which is often high during the first year, but declines during the second and third years of growth (Rochefort and Peterson 1996, Brang 1998, Germino et al. 2002), and (3) distorted and extremely small rings near the pith of dated trees could have led to incorrectly aged trees by ± 1 year in the tree invasion reconstruction in Zald (2010b). The rate of meadow invasion by trees (without area replacement) in the study area was negatively associated with annual maximum snowfall on glacial landforms (adjusted $R^2 = 0.2887$, $F_{1,17} =$

8.308, $p \leq 0.01034$), but this relationship was not significant on debris flows (adjusted R^2 = -0.0356, $F_{1,17} = 0.382$, $p = 0.545$) (Figure 4.3).

Future Snowfall Scenarios (2007 to 2064)

For the 2007 to 2064 time period, $Prob_{temp}$ was calculated by applying future snowfall scenarios to the regression coefficients and confidence intervals from the historical relationship between snowfall and tree invasion rates. There are currently no published scenarios of future snowfall in the region with an annual temporal resolution. I developed six future scenarios bounded by the most recent regional climate simulations which suggest future April snow water equivalency (SWE) will decline in the Oregon Cascades roughly 20-40% by 2050 (Salathe et al. 2008, Salathe et al. 2009). Annual snowfall and April SWE at the Marion Forks, Oregon weather station (44°36’N 121°57’W 813 m) are strongly correlated for the 1950 to 2007 time period (linear regression, $F_{1,55} = 173.6$, $P < 0.0001$, Adjusted $R^2 = 0.76$), suggesting changes in April SWE translate well to the annual snow fall data used in this study. Salathe et al. (2008, 2009) also suggest there will be increased snowfall variability and extreme events, which have been largely absent in the region for the past five centuries (Gedalof et al. 2004). Based on the information above, six scenarios of future annual snowfall were developed (Table 4.3) with three different annual snowfall means (historical base, twenty five percent reduction, and fifty percent reduction from historical base), and two different types of extreme event durations (same as the historical record, and extreme snowfall periods which persist for three consecutive years). Although comparisons between annual snowfall and April SWE were made using data from Marion Forks, snowfall data used to generation future snowfall scenarios come from the Government Camp weather station (45°18’ N 121°145’ W, 1213 m), believed to more closely reflect snowfall at Jefferson Park due to its higher elevation (Zald 2010b).

For scenarios without prolonged extreme snowfall years, it was assumed semi-decadal variation of future snowfall would be similar to the past 57 years of snow fall data. This was achieved by iteratively applying loess regressions with different span lengths to the historical snowfall data. Wavelet analysis (morlet wavelet number six, numbers of power of 2 = 9, significance level = 0.99) were conducted on each loess iteration, and a loess span = 0.2

resulted in wavelet power spectra that retained only semi-decadal variance in the loess curve and 2-4 year variation in the loess regression residuals. For each scenario a constant was subtracted from the loess regression residuals to achieve the appropriate mean for a given scenario (loess regression residuals have a mean approaching zero). For each scenario, one hundred iterations of 57 years were created by randomly assigning snowfall values within a normal distribution based on the scenario mean and standard deviation of loess regression residuals using the function rnorm in R version 2.91 (R Development Core Team 2009). The loess regression line was then added to the simulated residuals, resulting in 100 iterations for each of the six snow scenarios with the desired mean and variance, while retaining semi-decadal variability similar to the historical climate record (Figure 4.4).

Prolonged extreme snowfall periods were generated by first identifying all years within each snowfall iteration where snow fall was greater or less than one standard deviation from the mean. The following two years were then recalculated as randomly generated values within a normal distribution of the snowfall data subset greater or less than one standard deviation from the mean, dependent on if the initial extreme year was a high or low snowfall year. It is important to note these snowfall scenarios have not been developed as statistically-downscaled regional climate models, nor do they represent climate projections under different emissions scenarios, although they are based on snowfall scenarios from downscaled climate models that do. Instead they represent a range of potential scenarios bounded by reasonable estimates of future annual average snowfall and its temporal variability.

Facilitation of Tree Establishment by Existing Adjacent Young Trees ($Prob_{facil}$)

In addition to seed source and micro site effects of mature trees, young trees may facilitate tree establishment in their immediate vicinity by alteration of micro site conditions (Miller and Halpern 1998, Smith et al. 2003, Zald 2010b). To quantify facilitation effects from young trees (defined as trees less than eight meters tall), presence-absence data from field plots was analyzed to determine how probability of occupancy was associated with young tree presence in adjacent two meter pixels (eight-pixel neighborhood) when accounting for $Prob_{spat}$. Young tree presence in neighboring pixels was determined from a grid of vegetation height derived from LiDAR data. To avoid confusing young trees with non-tree vegetation, neighboring pixels were only considered to be occupied by young trees if LiDAR-derived vegetation height was greater than 0.4 m, the 95th percentile of non-tree vegetation height measured on all 499 plots. To avoid confusing young tree facilitation with that from overstory trees, plots within four meters of overstory canopy were removed, leaving 243 plots for analysis. Tree presence/absence on plots in response to the number of the eight neighboring pixels occupied by young trees was modeled using the logistic regression in SAS version 9.2 (SAS Institute 2008). Logistic regressions were run separately for each landform type. Maximum likelihood estimates were significant for the number of neighboring pixels occupied on both glacial and debris flow landforms ($p < 0.0001$ and $p= 0.0025$) when accounting for $Prob_{spat}$. Using logistic regression coefficients, point estimates were generated of the probability of occupancy due to young tree facilitation ($Prob_{facil}$) when accounting for $Prob_{spat}$:

[1] For glacial landforms:

$Prob_{facil} = 1-(1/(1+(\exp(-2.0128 + 2.4383*Prob_{spat} + 0.4724*Count))))$

[2] For debris flow landforms:

$Prob_{facil} = 1-(1/(1+(\exp(-4.265 + 5.5685*Prob_{spat} + 0.5007*Count))))$

Where count is the number of eight neighboring pixels occupied by young trees.

Starting Configuration and Model Runs (1950 to 2007)

The starting configuration for the year 1950 was established in three steps. First all cells containing vegetation greater than eight meters tall as defined by the LiDAR data were considered to be occupied by trees in 1950 (overstory trees in Figure 4.3). This was determined by height-age relationships from 398 mountain hemlocks collected in the study area (Zald 2010a). Tree height was related to age using a fourth order polynomial regression ($F_{4,394} = 528.8$, $p = < 0.0001$, Adjusted $R^2 = 0.84$), which found trees equal or greater than eight meters tall to have established on or before 1950 (95th percentile). Second, a conditional statement was applied where $Prob_{spat}$ pixel values were retained if they were greater than pixel values of a randomly generated grid of equal dimensions and value ranges. The purpose of this conditional statement was to generate stochastic variability in $Prob_{spat}$ values. This conditional statement was iterated 100 times, and the results of all 100 iterations averaged. By averaging many stochastic iterations of this $Prob_{spat}$ conditional statement, the number of unique values was greatly increased without altering its distribution. This was important for the third step, when the averaged pixels of the $\text{Prob}_{\text{spat}}$ conditional statements were divided into 1000 quantiles, with pixels in the top 9.058 and 2.551 percent of values assigned as occupied in 1950 on glacial and debris flow landforms respectively. These starting percentages are the proportions of the study area (excluding vegetation over 8 m tall) occupied by young trees in 1950 on both landform types (Zald 2010b). The starting configuration of pixels occupied was merged with the $\text{Prob}_{\text{spat}}$ grid to obtain the starting configuration grid for the model containing occupied cells (with cell values = 1) and values of $\text{Prob}_{\text{spat}}$ ranging from 0.01to 0.94.

From the starting configuration in 1950, three iterations of the condition statement $\text{Prob}_{\text{spat}}$ > random grid were run at each time step, where $\text{Prob}_{\text{spat}}$ cell values were retained if greater than the random generated grid cell values, and set to zero it they did not. The products of these three iterations were averaged, and then divided into 1000 quantiles. Grid cells in the quantile equal or greater than $\text{Prob}_{\text{temp}}$ (by landform type) were occupied at each time step. Note that from 1950 to 2007, $\text{Prob}_{\text{temp}}$ is deterministic (calculated from the proportion of meadows invaded by trees over time). Pixels not occupied in current or preceding time steps retained their $\text{Prob}_{\text{spat}}$ value. In the model variant with young tree facilitation, $\text{Prob}_{\text{facil}}$ was calculated for each grid pixel at the end of each time step.

Model Validation (1950 to 2007)

Models were validated using two different datasets: tree presence/absence data from field plots, and LiDAR-derived estimates of tree invasion. Plot-level accuracy assessment occurred for the 2007 model time by extracting model presence/absence data on pixels corresponding to field plots. Using tree presence/absence data from models (observed) and field plots (expected); overall accuracy, errors of commission and commission, and kappa statistics (Cohen 1960) were calculated. However, plot-based level accuracy assessments represent a small percentage of the landscape, and are not completely independent of data used to construct the $\text{Prob}_{\text{spat}}$ model parameter. To address these concerns, LiDAR data of vegetation height was used to independently validate model accuracy of tree presence across the entire study area. However, LiDAR data also has limitations for accuracy assessments of tree invasion. As noted in the description of $\text{Prob}_{\text{facil}}$, LiDAR-derived vegetation height had to be greater than 0.4 m to discriminate between tree and non-tree vegetation, which excludes the youngest trees. To determine the age threshold at which young trees could be detected (i.e. age of trees ≥ 0.4 m tall), the age and height of 287 mountain hemlocks from Zald (2010b) were regressed (third order Polynomial regression: adjusted $R^2 = 0.6$, $p < 0.0001$), in which trees less than 24 years old had a 95th percent chance of being less than 0.4 m tall. Based on this regression, LiDAR-based accuracy assessments were only applied to models at the time step associated with 1983. As with plot-based model validation, overall accuracy, errors of commission and commission, and kappa statistics were calculated. Error maps of the study area were also generated, comparing models in 1983 to LiDAR-derived observations of tree presence to assess spatial patterns of model accuracy.

In addition to traditional accuracy assessments, the spatial point patterns of the two models (with and without the facilitation effect of young trees) for the 1983 time step were compared against spatial point patterns of LiDAR-derived tree presence to determine if models accurately portrayed point patterns of tree establishment (i.e. clustered, random, or dispersed). Grids of model predictions and LiDAR-derived observations were converted to point data. L function second-moment point patterns for model predictions and LiDAR observations were calculated as described by Haase (1995). Computational limitations prevented the L function from being calculated for the entire study area. Instead, a randomly located four hectare square was selected from the model predictions and LiDAR observations in each landform type. Random plots had 1614, 1618, and 1698 treed points in the glacial landforms for the two model predictions and LiDAR observations; and 4136, 4157, and 4177 treed points in the debris flow landforms for model predictions and LiDAR observations respectively. L functions and 95% confidence envelopes (based on 100 Monte Carlo simulations) were calculated using the package spatstats in R version 2.9 (Baddeley and Turner 2005).

Model Runs 2007 to 2064

Model runs from 2007 to 2064 were run in a similar manner as from 1950 to 2007, but the temporal rate ($Prob_{temp}$) of invasion was probabilistic (rather than deterministic as during the 1950 to 2007 time period). $Prob_{temp}$ for 2007 to 2064 was derived by applying simulated snowfall datasets to the linear regressions of tree invasion rates in relation to snowfall. There were 100 iterations for each snowfall scenario, with the same mean and variance but different values for each individual year. Annual snowfall data in each iteration was converted to three year bins and the maximum snowfall in each bin determined. Three year maximum snowfall values were applied to the empirical climate-tree establishment rate regression coefficients and confidence intervals with the rnorm function in R version 2.9. This resulted in $Prob_{temp}$ values for each time step that reflected both the variation in snowfall scenarios, and the uncertainty in the relationships between snowfall and tree establishment. One hundred iterations of the model were run for each of the six climate scenarios. For each iteration, the total number of cells invaded was converted to the percentage of the total study area. Differences in the percentage of meadow area remaining by landform type in 2016, 2037, and 2064 were assessed with the Tukey Honest Significant Difference (HSD) method in R version 2.9.

RESULTS

Meadow Invasion and Model Validation (1950 to 2007)

Tree invasion of meadows in models with and without young tree facilitation closely matched plot-based invasion reconstructions, although invasion in the model with young tree facilitation was slightly higher (Table 4.4). Compared to field plots, overall accuracy of modeled tree invasion from 1950 to 2007 varied from 0.65 to 0.74 (1.0 being 100% accurate), which was 26% to 47% greater than expected by chance alone. Accuracy was higher on debris flow versus glacial landforms (Table 4.5). Error for all models and landforms was slightly biased towards predicting tree invasion were plots had no trees (commission error). For plot-based accuracy assessments, inclusion of young tree facilitation slightly reduced model accuracy (both overall accuracy and kappa statistic) on glacial landforms, but improved model accuracy on debris flows.

Compared to LiDAR-derived tree invasion, overall accuracy of modeled invasion from 1950 to 1983 varied from 0.61 to 0.74 (Table 4.5). Modeled tree invasion was 14 to 22% greater than expected by chance, lower than the plot-based accuracy assessment. Across all models and landforms, error was biased towards predicting no tree invasion when LiDAR-derived data indicated tree invasion (omission error). Omission error biases resulted from LiDAR-derived estimates of tree invasion for the 1950 to 1983 time period, which were greater than the plot-based invasion estimates used to derive $Prob_{temp}$. For LiDAR-based accuracy assessments, inclusion of young tree facilitation had little effect on model accuracy (both overall accuracy and kappa statistic) for either landform type. Prediction errors for both models in 1983 were most extensive in debris flows, with pronounced areas of omission error in the eastern half of the larger debris flows. Commission errors in both landform types were greatest in close proximity to both overstory trees and areas of correctly modeled invasion (Figure 4.5).

LiDAR-derived tree invasion displayed significant clustering on both landform types (Figure 4.6). On glacial landforms, the strength of clustering declined slightly at distances greater than 20 m, while clustering was largely constant at distances greater than 20 m for debris flow landforms. On glacial landforms, the model with young tree facilitation resulted in spatial patterns of tree invasion more comparable LiDAR-derived invasion across the range of distances. On debris flows, models resulted in patterns of predicted invasion that were more clustered across the wide range of distances than LiDAR-derived invasion patterns, but over-clustering was more pronounced with young tree facilitation. Although the accuracy assessments (plot and LiDAR-derived) showed little difference in modeling accuracy when including young tree facilitation, point pattern analyses suggested young tree facilitation better represented spatial patterns of tree invasion on glacial landforms. For these reasons, facilitation effects were only included on glacial landforms modeling future (2007 to 2064) tree invasion under the six different climate scenarios.

2007 to 2064 Tree Invasion

Based on the LiDAR estimates of overstory canopy and the field data (Zald 2010b), 82 percent of the study area (80 percent glacial and 94 percent debris flow) was subalpine meadow in 1950 (1950 baseline area). By 2007, predicted tree invasion in both models resulted in meadow area of 65.3, 66.3, and 61.2 percent of 1950 baseline, on all landforms, glacial, and debris flow landforms respectively. By 2016, median meadow area across all snow scenarios ranged from 61.3 to 62.5 percent of 1950 baseline across the study area, 61.8 to 63.4 percent on glacial landforms, and 58.1 to 58.9 percent on debris flow landforms (Figure 4.7). In 2016, meadow area (overall study area and meadows on glacial landforms) declined with reduced mean snowfall (scenarios A-C), declines in meadow area were not associated with increased persistence of extreme snowfall (scenarios D-F), but a 50 percent decline in snowfall (scenario C) resulted in the most meadow area remaining on debris flow landforms.

By 2037, median meadow area across all snow scenarios ranged from 52.4 to 56.1 percent of 1950 baseline area across the study area, 52.4 to 57.1 percent on glacial landforms, and 51.1 to 53.4 percent on debris flow landforms. For both the entire study area and glacial landforms, meadow area declined with reduced mean snowfall (scenarios A-C), while increased persistent extreme events combined with a 25 percent reduction in snowfall (scenario E) retained greater meadow area than 25 percent snowfall reductions alone (scenario B). On debris low landforms, meadow area generally declined with increased snowfall and increased persistence of extreme events, although there was considerable overlap between scenarios. A 50 percent decline in snowfall (scenario C) resulted in higher meadow area remaining on debris flow landforms

All scenarios resulted in a shift from a landscape dominated meadow matrix with patches of forests in 1950, to a roughly even split between meadows and trees in 2007, to a landscape dominated by forest with greatly reduced patches of meadow by 2064. By 2064, median meadow area across all snow scenarios ranged from 41.4 to 47.4 percent of 1950 baseline area across the study area, 40.3 to 47.9 percent on glacial landforms, and 43.9 to 47.6 percent on debris flow landforms. For both the entire study area and glacial landforms, 2064 reductions from 1950 baseline meadow area were greatest with reduced mean snowfall (scenarios A-C), while increased persistent extreme events combined with a 25 percent reduction in snowfall (scenario E) resulted in greater meadow area than 25 percent snowfall reductions alone (scenario B). On debris low landforms, meadow area declined with increased snowfall (scenarios A-C). Increased persistence of extreme events did not result in different proportions of meadow area remaining for a given mean snowfall scenario (for example scenarios A versus D), but did reduce differences between difference mean snowfall scenarios (for example scenarios D versus E). Spatial patterns of tree invasion were consistent across scenarios, but differed by landform type (Figure 4.8). On glacial landforms, a general enlargement of forest islands has occurred since, shifting the landscape from meadows that were largely interconnected in 1950, to meadows of varying shapes and sizes increasingly separated by stands of mountain hemlock in 2064. In contrast to island enlargement on glacial landforms, modeled tree invasion on the southern debris flow was spatially continuous, resulting in an extensive area of mountain hemlock forest.

DISCUSSION

The primary objective of this study was to spatially characterize historical (1950 to 2007) and project near-term future (2007 to 2064) tree invasion in the subalpine meadow landscape of Jefferson Park. Results of model runs and accuracy assessments from 1950 to 2007 suggest historical fine-scale patterns of tree invasion can be accurately predicted. Model runs from 2007 to 2064 indicate continued declines in meadow area, shifting the study area from meadow dominated land cover in 1950, to a mountain hemlock forest dominated landscape in 2064. Climate scenarios with different annual average snowfalls resulted in significant differences in the proportion of meadow land cover invaded by trees. However, differences in projected meadow area remaining were small (median values ranging from 41 to 48% of the landscape without tree invasion in 2064), suggesting landscape-level tree invasion may be relatively insensitive to large reductions in annual average snowfall across the time period of study. Insensitivity to reductions in snowfall, combined with spatially consistent areas lacking tree invasion across climate scenarios, suggests there will be persistent areas of meadow habitat in the future. The spatial pattern of tree invasion (and therefore remaining meadows) appears largely dependent on fine-scale patterns of microtopography and overstory canopy nested within larger-scale landform features, resulting in a mosaic of meadow and forest land cover on glacial landforms, and largely contiguous areas of mountain hemlock forests on debris flows. Young-tree facilitation appears to be an important landform-dependent factor in shaping spatial patterns of tree invasion, but the mechanism and extent of this control over space and time is unclear. Model accuracy, tree invasion sensitivity to climate and meadow persistence, and non-climatic influences on tree invasion are discussed in detail below; as are limitations associated with the conceptual framework of the model, and uncertainty regarding the field and climate data which drive it.

Accuracy of Modeled Historical Tree Invasion

Overall extent of predicted tree invasion during the historical period (1950 to 2007) was moderately accurate, but spatial patterns of model error varied by landform type.

Predicted invasion on glacial landforms closely matched LiDAR-derived estimates, independently validating model rates of tree invasion for the 1950 to 1983 time period. Spatially, the greatest prediction errors on glacial landforms were on sites with the highest probability of tree invasion (i.e. higher topographic positions and close proximity to overstory trees) (Zald 2010b). Stochastic variation in seed dispersal, germination, and mortality may result in favorable sites remaining unoccupied. A high degree of stochastic variation in tree invasion would not be surprising given the spatial resolution of this study, since fine-grained spatial scales generally increase variance in the pattern or process of interest (Wiens 1989). Spatial heterogeneity of site conditions can also influence the regeneration niche, and the 2 m resolution of this study may miss even finer scale environmental controls of regeneration success (Grubb 1977, Gray and Spies 1997).

Spatial patterns of prediction errors were very different on debris flows, occurring over larger contiguous areas compared to smaller clusters on glacial landforms. Spatial patterns of debris flow prediction errors likely result from some combination of: (1) longer and weaker gradients of site favorability; (2) gradients of site favorability; which may not be associated with available explanatory variables; (3) increased stochastic variability in tree establishment compared to glacial landforms; and (4) debris flow specific problems using LiDAR-derived estimates of tree invasion as validation data. The spatial probability of occupancy ($Prob_{spat}$) on debris flows occurs along a long declining gradient from west to east, resulting in extensive areas expected to be invaded. This gradient is also much weaker compared to glacial landforms, with tree abundance partially decoupled from many microtopographic and seed source controls which influence site favorability on glacial landforms (Zald 2010b). Microtopography and distance to potential seed sources may not characterize age, stability, and quality of substrate; which can be important determinants of tree establishment and vegetation composition on young depositional landforms (Yarie et al. 1998, Pabst and Spies 2001, Garbarino et al 2010). Debris flow landforms are also disturbance events, on which primary succession can be highly stochastic (del Moral et al.1995, del Moral et al. 2009). Finally, the LiDAR-derived accuracy assessment may have greater bias on debris flow landforms because of extensive areas containing the tall herbaceous perennial *Lupinus lepidus*, which is rare on glacial landforms (Zald 2010a). *L. lepidus* often grows taller than the 0.4 m, the height cutoff distinguishing small trees from shrubs and herbaceous plants. Field data used to establish this cutoff may have underrepresented *L. lepidus* on debris flows in Zald (2010b), resulting in an overestimation of LiDAR-derived tree invasion. This would explain why models of tree invasion closely match plot based estimates of tree invasion on glacial landforms, but have greater errors of omission in comparison to LiDAR-derived invasion estimates on debris flows.

Tree Invasion Sensitivity to Future Climate and Meadow Persistence

Sensitivity of projected tree invasion to future climate scenarios can be viewed from different perspectives. The projected amount of tree invasion from 2007 to 2064 is significantly different between scenarios with different mean annual snowfall, although differences are much weaker (and even reversed) on debris flow versus glacial landforms. Across all scenarios (including future projections of historical baseline) projected tree invasion results in a landscape matrix shift from a meadow to tree domination by 2064. Sensitivity analysis was not performed on the tree invasion in relation snowfall and its variability, since snow scenarios were bounded by a wide range of reasonable potential snow fall given current information (Salathé et al. 2008, Salathé 2009). Prolonged extreme snow fall scenarios were also realistic, given what is known about long-term snow pack variability in the region via tree-ring reconstructions (Gedalof et al. 2004). The empirical relationship between snow fall and tree establishment ($\mathrm{Prob}_{\mathrm{temp}}$) was also linear, suggesting sensitivity analysis would be unlikely to find a snowfall threshold important to invasion rates within the bounded snowfall scenarios employed.

If viewed from the scale of the entire study area, projected climate scenarios do not greatly influence the proportion of the study area landscape invaded, with approximately 50 to 36 percent of the study area remaining as meadow in 2064. Additionally, the areas remaining as meadow are consistent across scenarios, suggesting large areas of meadow persistence by 2064, even with large reductions in snowfall. This is consistent with the ‘local high-elevation habitat persistence hypothesis’ (LHP), where fine-grained topographic modification of climate results in suitable thermal habitat conditions, which would otherwise be perceived as unsuitable when related to climate change at coarser spatial scales (Randin et al. 2009). Randin et al. (2009) support this hypothesis using the SDM’s (i.e. bioclimatic envelopes). Species occurrences used in SDMs can be from any life history stage from recent germinants to mature individuals, although plant species identification is more definitive with mature specimens. Mature individuals and populations in treeline and alpine environments can survive under adverse climatic conditions for centuries to millennia (Steinger et al. 1996, Bettin et al. 2007, Salzer et al. 2009). In contrast, meadow persistence in this study is based on tree establishment which is spatially restricted in relation to landform, microtopography, and overstory canopy (biophysical modifiers of fine-scale snow depth and seasonal persistence), and temporally restricted by tree establishment rates in relation to regional climate records. This study provides additional support for the 'local high-elevation habitat persistence hypothesis' in part because it is based on species regeneration, which is most sensitive life history stage for individuals and populations (Grubb 1977).

It is important to recognize this study supports the LHP hypothesis by using tree invasion as a proxy for habitat loss of numerous alpine and subalpine species which occupy meadows, rather than aggregated persistence of thermal habitat for numerous individual species projected with SDMs. Projected persistence of individual meadow species was outside the scope of this study, so it is unclear any plant communities would be lost from the study area, or if plant communities with decline in area differently. However, species and community presence within the study area in relation to micro site conditions (Zald 2010a) suggests areas most likely to be invaded are currently dominated by Ericaceous shrubs on glacial landforms and well-drained forb communities on debris flows, while the hydrologic setting of wet sedge meadows (e.g. hydric soils, high water table) may be least likely to be invaded by trees. However, habitat for each species and/or community type is unlikely to remain static, and migration potential will depend not only on future climate conditions, but also propagule availability, competition, facilitation, disturbance regimes, etc.

Non-climatic Influences on Tree Invasion Spatial Patterns

Landforms, and the micro site conditions nested within them, play a significant role in where tree invasion occurs on the landscape. Landform type determined the degrees of variation in microtopography, as well has the distance to overstory canopy which modified snow depth and proximity to potential seed sources (Zald 2010b). Landforms and micro site conditions within them influence the association between tree invasion and climate on debris flows. This resulted in spatially constrained and clustered projected tree invasion on glacial landforms, and wide spread invasion on debris flows. Overstory trees play an important role in the spatial pattern of projected tree invasion by influencing snow depth and seed availability (Faria et al., 2000, Sicart et al. 2004, Dovčiak et al 2008).

Less clear is the role of neighboring young trees in facilitating tree invasion. Young tree facilitation effects were empirically derived by relating young tree presence in plots to LiDAR-derived young tree presence (0.4 m to 8 m vegetation height) in neighboring pixels. As previously discussed for model validation, LiDAR-derived estimates of neighboring young tree presence could have been overestimated by the abundance of tall *Lupinus lepidus* on debris flows. In addition, facilitation was quantified by the number of neighboring pixels occupied young trees, but alteration of micro site climatic conditions is likely to be influenced by other variables (i.e. percent cover or density of vegetation in different strata) that are difficult for even small footprint LiDAR to accuracy quantify at the spatial resolution of this study.

Model Limitations and Uncertainty

In addition to specific limitations already discussed above (i.e. limitations of LiDAR in model validation, scale issues with regeneration, young tree facilitation, etc.), it is important to view projected tree invasion in this study in relation to the conceptual limitations and uncertainty in the model framework itself. This model attempted to incorporate stochastic variability into empirically-parameterized tree invasion simulations. Both climate data and the climate-establishment relationships driving the temporal patterns of tree invasion are probabilistic. Snowfall scenarios each have a distribution with a mean and variance, as does the percentage of the landscape occupied in each time step as a function of climate. Both the spatial ($\text{Prob}_{\text{spat}}$) and young tree facilitation ($\text{Prob}_{\text{facil}}$) parameters were deterministic, although $\text{Prob}_{\text{spat}}$ had a stochastic element due to conditional statements involving random data. In reality $\text{Prob}_{\text{spat}}$ and $\text{Prob}_{\text{facil}}$ have an unknown amount of variance associated, and this variance varies spatially across the study landscape. If $\text{Prob}_{\text{spat}}$ and $\text{Prob}_{\text{facil}}$ parameters were probabilistic, it would have likely increased the confidence envelopes (increased uncertainty) of all scenario outputs.

It is also important to note that interactions between landform type, micro site conditions, and climate can result in contrasting spatial and temporal patterns of tree invasion, which were not incorporated into the model. Trees can invade lower topographic positions with low Prob_{spat} values during low snow years (Zald 2010b). This would suggest Prob_{spat} is not static, but rather has dynamic interactions with micro site favorability, climate conditions, and tree invasion. It was not possible to quantify this dynamic interaction, but the static nature of the Prob_{spat} grid may only be a minor limitation of this model. Contrasting spatial patterns of tree invasion may result from interactions with microtopography and climate, but the dominant signal was for trees to invade higher topographic positions in meadows, and invasion of these micro sites was greater during low snowfall years (Zald 2010b). Overstory trees also should in reality influence the probability of a micro site being invaded in a dynamic way over time, since young trees will eventually grow into overstory trees (defined as 8 m tall), influencing snow persistence and seed available. This model only projected 57 years into the future, approximately the time for a seedling to grow to 8 m (based on historical growth rates). Tree growth into the overstory was not incorporated into the model because it is unknown what size (and therefore age) trees begin to influence micro site probability of invasion, and what the strength and spatial extent of these effects may be in relation to tree size. The absence of this factor may bias predictions towards underestimating the probability of invasion over time,

Although using empirical relationships to parameterize these models had the benefit of incorporating realistic relationships and uncertainty in tree establishment-climate relationships, it also may have constrained the model conceptually. Tree establishment-climate relationships were restricted to the range of conditions observed in the historical period, and are essentially static relationships. When climate conditions were outside this range, predictions of tree establishment follow the regressions, and can go outside the statistical scope of inference of available data. These assumptions are major shortcomings of not only this model, but species distribution models as well (Zuller et al. 2009). This could be especially problematic if there is potential for novel ecosystem responses to changing climate and/or disturbance regimes (Rupp et al. 2000, Edwards et al. 2005). Limitations of static and equilibrium based models highlight the need for experiments which attempt to impose future climatic conditions on current ecosystems. Experiments modifying snow and/or temperature have occurred in a wide range of ecosystems, but not in the FTE (Beier et al. 2004, Hurteau and North 2008, Wipf et al. 2009). Our understanding of future FTE responses to climate change could be greatly improved with long-term studies examining tree establishment in response to manipulated snow depth and snowmelt timing. In addition to the impacts of manipulated snow and temperature on tree establishment, another dynamic response could be increased seed production by existing trees, since seed production is likely to vary in relation to temperature and drought stress (Mencuccini et al. 1995).

Despite these limitations, this study suggests continued loss of meadow habitat over the next five decades. Climate has a role in this process, but dominant controls of tree invasion appear to be topographic for the next few decades and constraints on establishment rates and the abundance of micro sites resistant to tree invasion will likely persist under a wide range of reduced snow scenarios. These remaining meadows will likely become smaller in size and less interconnected.

Acknowledgements

Funding for this research was provided by the USDA Forest Service, Pacific Northwest Research Station, Forest Inventory and Analysis Program; The Native Plant Society of Oregon, and the Hoener Memorial Fellowship program at the College of Forestry, Oregon State University. Special thanks to Alex Gonsiewski for field data collection and tree core dating, Manuela Huso with sampling design, Nick Som and Emile Grossman for computer programming advice, and Keith Olsen for GIS assistance.

LITERATURE CITED

Bachelet, D., Lenihan, J.M., Daly, C., Neilson, R.P., Ojima, D.S., and Parton, W.J. 2001. MC1: A dynamic vegetation model for estimating the disturbance of vegetation and associated ecosystem fluxes of carbon, nutrients, and water – technical documentation. Verson 1.0. Gen. Tech. Rep. PNW-GTR-508. Portland, OR: U.S. Department of Agriculture, Forest Service, Pacific Northwest Research Station. 95 p.

Baddeley, A., and Turner, R. 2005. Spatstat: an R package for analyzing spatial point patterns. Journal of Statistical Software 12: 1-42.

Beier, C., Emmett, B., Gundersen, P., Tietema, A., Penuelas, J., Estiarte, M., Gordon, C., Gorissen, A., Llorens, L., Roda, F., and Williams, D. 2004. Novel approaches to study climate change effects on terrestrial ecosystems in the field: drought and passive nighttime warming. Ecosystems 2004: 583-597.

Bettin, O., Cornejo, C., Edwards, P.J., and Holderegger, R. 2007. Phylogeography of the high alpine plant *Senecio halleri* (Asteraceae) in the European Alps: *in situ* glacial survival with postglacial stepwise dispersal in peripheral areas. Molecular Ecology 16: 2517-2524.

Bonan, G.B., Pollard, D., and Thompson, S.L. 1992. Effects of boreal forest vegetation on global climate. Nature 359: 716-718.

Brang, P. 1998. Early seedling establishment in Picea abies in small forest gaps in the Swiss Alps. Canadian Journal of Forest Research 28: 626-639.

Christensen, J.H., B. Hewitson, A. Busuioc, A. Chen, X. Gao, I. Held, R. Jones, R.K. Kolli, W.-T. Kwon, R. Laprise, V. Magaña Rueda, L. Mearns, C.G. Menéndez, J. Räisänen, A. Rinke, A. Sarr and P. Whetton, 2007: Regional Climate Projections. In: Climate Change 2007: The Physical Science Basis. Contribution of Working Group I to the Fourth Assessment Report of the Intergovernmental Panel on Climate Change [Solomon, S., D. Qin, M. Manning, Z. Chen, M. Marquis, K.B. Averyt, M. Tignor and H.L. Miller (eds.)]. Cambridge University Press, Cambridge, United Kingdom and New York, NY, USA.

Cohen, J. 1960. A coefficient of agreement for nominal scales. Educational and Psychological Measurement 20: 37-36.

Daniels, L.D., and Veblen, T.T. 2004. Spatiotemporal influences of climate on altitudinal treeline in Northern Patagonia. Ecology 85: 1284-1296.

Davis, A.J., Jenkinson, L.A., Lawton, J.H., Shorrocks, B., and Wood, S. 1998. Making mistakes when predicting shifts in species range in response to global warming. Nature 391: 783-786

Del Moral, R., Titus, J.H., and Cook, A.M. 1995. Early primary succession on Mount St. Helens, Washington, USA. Journal of Vegetation Science 6: 107-120.

Del Moral, R., Sandler, J.E., and Muerdter, C.P. 2009. Spatial factors affecting primary succession on the Muddy River Lahar, Mount St. Helens, Washington. Plant Ecology 202: 177-190.

Dirnböck, T., Dullinger, S., and Grabherr, G. 2003. A regional impact assessment of climate and land-use change on alpine vegetation. Journal of Biogeography 30: 401-417.

Dovčiak, M., Hrivnák, R., Ujházy, K., and Gömöry, D. 2008. Seed rain and environmental controls on invasion of *Picea abies* into grassland. Plant Ecology 194: 135-148.

Edwards, M.E., Brubaker, L.B., Lozhkin, A.V., and Anderson, P.M. 2005. Strucutrally noval biomes: a response to past warming in Beringia. Ecology 86: 1696-1703.

Faria, D.A., Pomeroy, J.W., and Essery, R.L.H. 2000. Effect of covariance between ablation and snow water equivalent on depletion of snow-covered area in a forest. Hydrological Processes 14: 2683-2695.

Fischlin, A., G.F. Midgley, J.T. Price, R. Leemans, B. Gopal, C. Turley, M.D.A. Rounsevell, O.P. Dube, J. Tarazona, A.A. Velichko, 2007: Ecosystems, their properties, goods, and services. Climate Change 2007: Impacts, Adaptation and Vulnerability. Contribution of Working Group II to the Fourth Assessment Report of the Intergovernmental Panel on Climate Change, M.L. Parry, O.F. Canziani, J.P. Palutikof, P.J. van der Linden and C.E. Hanson, Eds., Cambridge University Press, Cambridge, 211-272.

Franklin, J.F., Moir, W.H., Douglas, G.W., and Wiberg, C. 1971. Invasion of subalpine meadows by trees in the Cascade Range, Washington and Oregon. Journal of Arctic and Alpine Research 3:215-224.

Franklin, J.F., and Smith, C.E. 1974 Seeding habits of upper-slope tree species II: Dispersal of a mountain hemlock seedcrop on a clearcut. USDA Forest Service Research Note PNW-214. Pacific Northwest Forest and Range Experimental Station, Portland, OR.

Franklin, J.F., and Dyrness, C.T. 1988 Natural Vegetation of Oregon and Washington. Oregon State University Press. Corvallis, OR.

Garbarino, M., Lingua, E., Nagel, T.A., Godone, D., and Motta, R. 2010. Patterns of larch establishment following deglaciation of Ventina glacier, central Italian Alps. Forest Ecology and Management 259: 583590.

Gedalof, Z., Peterson, D.L., and Mantua, N.J. 2004. Columbia river flow and drought since 1750. Journal of the American Water Resources Association 40: 1579-1592.

Germino, M.J., Smith, W.K., and Resor, A.C. 2002. Conifer seedling distribution and survival in an alpine-treeline ecotone. Plant Ecology 162: 157-168.

Gray, A.N., and Spies, T.A. 1997. Microsite controls on tree seedling establishment in conifer forest canopy gaps. Ecology 78: 2458-2473.

Grubb, P.J. 1977. The maintenance of species-richness in plant communities: the importance of the regeneration niche. Biological Reviews 52: 107-145.

Guisan, A., and Zimmerman, N.E. Predictive habitat distribution models in ecology. Ecological Modelling 135: 147-186.

Guisan, A., and Thuiller, W. 2005. Predicting species distribution: offering more than simple habitat models. Ecology Letters 8: 993-1009.

Halloy, S.R.P., and Mark, A.F. 2003. Climate-change effects on alpine plant biodiversity: A New Zealand perspective on quantifying the threat. Arctic, Antarctic, and Alpine Research 35: 248-254.

Harsch, M.A., Hulme, P.E., McGlone, M.S., and Duncan, R.P. 2009. Are treelines advancing? A global meta-analysis of treeline response to climate warming. Ecology Letters 12: 1040-1049.

Haase, P. 1995. Spatial pattern analysis in ecology based on Ripley’s K-function: Introduction and methods of edge correction. Journal of Vegetation Science 6: 575-582.

Holtmeier, F.K., and Broll, G. 2005. Sensitivity and response of northern hemisphere altitudinal and polar treelines to environment change at landscape and local scales. Global Ecology and Biogeography 14: 395-410.

Hurteau, M. and North, M. 2008. Mixed-conifer understory response to climate change, nitrogen, and fire. Global Change Biology 14: 1543-1552.

Jobbágy, E.G., and Jackson, R.B. 2000. Global controls of forest line elevation in the northern and southern hemispheres. Global Ecology and Biogeography 9: 253-268.

Körner, C. 1998. A re-assessment of high elevation treeline positions and their explanation. Oecologia 115: 445-459.

Larocque, G.R., Archambault, L., and Delisle, C. 2006. Modelling forest succession in two southeastern Canadian mixedwood ecosystems types using the ZELIG model. Ecological Modelling 199: 350-362.

Lescop-Sinclair, K., and Payette, S. 1995. Recent advance of the arctic treeline along the eastern coast of Hudson Bay. Journal of Ecology 83: 929-936.

McDonald, G.D. 1998. Soil survey of Warm Springs Indian Reservation, Oregon. U.S. Department of Agriculture and Natural Resources Conservation Service. Washington, D.C.

McGill, R., Tukey, J., and Larsen, W.A. 1978. Variations of box plots. The American Statistician 32: 12-16.

McCune, B., Mefford, M.J. 2004. Hyperniche nonparametric multiplicative habitat modeling. Version 1.39. MjM Software, Gleneden Beach, Oregon.

McCune, B. 2006. Non-parametric habitat models with automatic interactions. Journal of Vegetation Science 17: 819-830.

Means, J. 1990. Mountain hemlock. In: Silvics of North America, Volume 1: Conifers. R.M. Burns and B.H. Honkala Technical Editors. Agricultural Handbook 271. U.S. Department of Agriculture, Forest Service. Washington, DC. Available via http://www.na.fs.fed.us/spfo/pubs/silvics_manual/table_of_contents.htm. Accessed 1 September, 2009.

Mencuccini, M., Piussi, P., Sulli, A.Z. 1995. Thirty years of seed production in a subalpine Norway spruce forest: patterns of temporal and spatial variation. Forest Ecology and Management 76: 109-125.

Miller, E.A. and Halpern, C.B. 1998. Effects of environment and grazing disturbance on tree establishment in meadows of the central Cascade Range, Oregon, USA. Journal of Vegetation Science 9: 265-282.

O’Connor, J.E., Hardison, J.H. III, and Costa, J.E. 2001. Debris flows from failures of neoglacial-age moraine damns in the Three Sisters and Mount Jefferson Wilderness Areas, Oregon. U.S. Geoligcal Survey Profession Paper 1606.

Pabst, R.J., and Spies, T.A. 2001. Ten years of vegetation succession on a debris-flow deposit in Oregon. Journal of the American Water Resources Association 37: 1693-1708.

Pabst, R.J., Goslin, M.N., Garman, S.L., and Spies, T.A. 2008. Calibrating and testing a gap model for simulating forest management in the Oregon Coast Range. Forest Ecology and Management 256: 958-972.

Pacala, S.W., Canham, C.D., Sapnara, J., Silander, J.A., Kobe, R.K., and Ribbens, E. 1996. Forest models defined by field measurements: Estimation, error analysis and dynamics. Ecological Monogrpahs 66: 1-43.

Pierce, K.B., Lookingbill, T., and Urban, D. 2005. A simple method for estimating potential relative radiation (PRR) for landscape-scale vegetation analysis. Landscape Ecology 20: 137-147.

Price, D.T., Zimmerman, N.E., Van Der Meer, P.J., Lexer, M.J., Leadley, P., Jorritsma, I.T.M., Schaber, J., Clark, D.F., Lasch, P, McNulty, S., Wu, J., and Smith, B. 2001. Regeneration in gap models: Priority issues for studying forest responses to climate change. Climatic Change 51: 475-508.

Prichard, S.J., Peterson, D.L., and Hammer, R.D. 2000. Carbon distribution in subalpine forests and meadows of the Olympic Mountains, Washington. Soil Science Society of America Journal 64: 1834-1845.

R Development Core Team. 2009. R: A language and environment for statistical computing. R Foundation for Statistical Computing. Vienna, Austria.

Randin, C.F., Engler, R., Normand, S., Zappa, M., Zimmerman, N., Pearman, P., Vittoz, P., Thuiller, W., and Guisan, A. 2009. Climate change and plant distribution: local models predict high-elevation persistence. Global Change Biology 15: 1557-1569.

Rehfeldt, G.E., Ferguson, D.E., and Crookston, N.L. 2009. Aspen, climate, and sudden decline in western USA. Forest Ecology and Management 258: 2353-2364.

Rochefort, M.R., and Peterson, D.L. 1996. Temporal and spatial distribution of trees in subalpine meadows of Mount Rainier National Park, Washington, U.S.A. Arctic and Alpine Research 28: 52-59.

Rupp, T.S., Chapin, S.T., and Starfield, A.M. 2000. Response of subarctic vegetation to transient climate change on the Seward Peninsula in north-west Alaska. Global Change Biology 6: 541-555.

SAS Institute Inc. 2008. SAS/STAT User’s Guide. Version 9.2. SAS Institute, Cary, NC.

Salathé, E.P., Steed, R., Mass, C.F., and Zahn, P.H. 2008. A high-resolution climate model of the U.S. Pacific Northwest: Mesoscale feedbacks and local responses to climate change. Jounral of Climate 21: 5708-5726.

Salathé, E.P., L.R. Leung, Y. Qian, and Y. Zhang. 2009. Regional climate model projections for the State of Washington. Chapter 2 In: The Washington Climate Change Impacts Assessment: Evaluating Washington's Future in a Changing Climate, Climate Impacts Group, University of Washington, Seattle, Washington.

Salzer, M.W., Hughes, M.K., Bunn, A.G., and Kipfmueller, K.F. 2009. Recent unprecedented tree-ring growth in bristlecone pine at the highest elevations and possible causes. Proceedings of the National Academy of Sciences of the United States of America 106: 20348-20353.

Scott, W.E. 1977. Quaternary glaciation and volcanism, Metolius river area, Oregon. Geological Society of America Bulletin 88: 113-124.

Sicart, J.E., Pomeroy, J.W., Essery, R.L.H., Hardy, J., Link, T., and Marks, D. 2004. A sensitivity study of daytime net radiation during snowmelt to forest canopy and atmospheric conditions. Journal of Hydrometeorology 5: 774-784.

Smith, W.K., Germino, M.J., Hanocock, T.E., and Johnson, D.M. 2003. Another perspective on altitudinal limits of alpine timberlines. Tree Physiology 23: 1101-1112.

Steinger, T., Korner, C., and Schmid, B. 1996. Long-term persistence in a changing climate: DNA analysis suggests very old ages of clones of alpine *Carex curvula*. Oecologia 105: 94-99.

Thuiller, W., Lavorel, S., Araujo, M.B., Sykes, M.T., and Prentice, I.C. 2005. Climate change threats to plant diversity in Europe. Proceedings of the National Academy of Sciences of the United States of America 102: 8245–8250.

Wallentin, G., Tappeiner, U., Strobl, J., and Tasser, E. 2008. Understanding alpine tree line dynamics: An individual-based model. Ecological Modelling 218: 235-246.

Wiens, J.A. 1989. Spatial scaling in ecology. Functional Ecology 3: 385-397.

Wilmking, M., Harden, J., and Tape, K. 2006. Effect of tree line advance on carbon storage in NW Alaska. Journal of Geophysical Research 111: G02023.1-G02023.10.

Wipf, S., Stoeckii, V., Bebi, P. 2009. Winter climate change in alpine tundra: plant responses to changes in snow depth and snowmelt timing. Climatic Change 94: 105-121.

Woodward, A., Schreiner, E.G., and Silsbee, D.G. 1995. Climate, geography, and tree establishment in subalpine meadows of the Olympic Mountains, Washington, U.S.A. Arctic and Alpine Research 27:217-225.

Woodward, F.I., and Beerling, D.J. 1997. The dynamics of vegetation change: Health warnings for equilibrium ‘dodo’ models. Global Ecology and Biogeography Letters 6: 413-418.

Yarie, J., Viereck, L., Van Cleve, K., and Adams, P. 1998. Flooding and ecosystem dynamics along the Tanana river. Bioscience. 48: 690-695.

Yost, A.C. 2008. Probabilistic modeling and mapping of plant indicator species in a Northeast Oregon industrial forest, USA. Ecological Indicators 8: 46-56.

Zald, H.S.J. 2010a. Integrating LiDAR, satellite imagery, and forest inventory data to spatially characterize tree invasion, vegetation composition, and vegetation structure in a subalpine meadow landscape, Oregon Cascades, USA. In: Patterns of Tree Establishment and Vegetation Composition in a Subalpine Meadow Landscape, Jefferson Park, Oregon, USA. Ph.D. Dissertation, Oregon State University, Corvallis, OR.

Zald, H.S.J. 2010b. Seedling establishment in a subalpine parkland landscape controlled by interactions of topography, seed source, disturbance and climate, oregon cascades, USA. In: Patterns of Tree Establishment and Vegetation Composition in a Subalpine Meadow Landscape, Jefferson Park, Oregon, USA. Ph.D. Dissertation, Oregon State University, Corvallis, OR.

Zuller, D., Jeltsch, F., Dormann, C.F., and Schröder, B. 2009. Static species distribution models in dynamically changing systems: how good can predictions really be? Ecography 32: 1-12.

Table 4.1. Codes and descriptions of biophysical variables selected in nonparametric multiplicative regression (NPMR) models used to generate probability of tree occupancy ($\text{Prob}_{\text{spat}}$) grids.

Variable Code	Description
ELEV	Elevation (in meters), from 1 m digital elevation model (DEM)
SLOPE	Slope (percent), from 1 m DEM
RAD	Growing season Potential Relative Radiation (Pierce et al. 2005) June - September, from 1 m DEM
TOPO1	Topographic position index, anulus 5 - 10 m from DEM
TOPO2	Topographic position index, anulus 10 - 15 m from DEM
TOPO4	Topographic position index, anulus 50 - 100 m from DEM
CANDIST	Distance from overstory canopy, in meters

Table 4.2. Monte carlo test p value, Log likelihood ratio (LogB), and sensitivity analysis results for nonparametric multiplicative regressions (NPMR) of mountain hemlock presence in relation to mapping explanatory variables.

Landform	P value	LogB	Explanatory Varible	Sensitivity
Glacial	0.0040	11.80	CANDIST	0.9640
			TOPO2	0.6777
			SLOPE	0.3537
			TOPO1	0.2525
			RAD	0.0863
Debris flow	0.0396	3.55	ELEV	1.1061
			TOPO4	1.0120
			TOPO1	0.2766
			CANDIST	0.0455

Note: See Table 4.1 for explanatory variable descriptions.

Table 4.3. Snowfall scenarios used in models, and their respective annual means, percent differences from historical means, and standard deviations.

Scenario	Change from mean	Prolonged extreme snow fall years	Annual snowfall mean (cm)	Annual snowfall stdev (cm)
A	historical (1950-2007)	historical	682	222
B	-25% historical	historical	511	213
C	-50% historical	historical	346	204
D	historical	three year	675	275
E	-25% historical	three year	509	280
F	-50% historical	three year	339	262

Table 4.4. Percentages of the study area occupied by trees (vegetation greater than 8 m tall excluded), by data type, and year.

		Year		
Data Type	Landform	1950	1983	2007
Lidar	All	-	0.241	-
Model 1	All	0.078	0.231	0.336
Model 2	All	0.078	0.240	0.342
Reconstructed	All	0.077	0.240	0.347
Lidar	Glacial	-	0.189	-
Model 1	Glacial	0.091	0.226	0.325
Model 2	Glacial	0.091	0.233	0.332
Reconstructed	Glacial	0.091	0.231	0.337
Lidar	Debris	-	0.409	-
Model 1	Debris	0.026	0.260	0.372
Model 2	Debris	0.026	0.267	0.380
Reconstructed	Debris	0.026	0.275	0.388

Table 4.5. Omission and commission error, overall accuracy and kappa statistics for model 1 (without young tree facilitation) and model 2(with young tree facilitation) by landform. Model predictions were compared to field plots over the 1950 – 2007 time period. Comparisons to LiDAR data occurred over the 1950 – 1983 time period (see validation section for details)

Ground Truth data type	Model	Landform	Overall accuracy	Omission error	Comission error	Kappa statistic
Field plots	1	All	0.67	0.34	0.47	**0.32**
Field plots	2	All	0.67	0.38	0.46	0.30
Field plots	1	Glacial	0.66	0.33	0.49	**0.30**
Field plots	2	Glacial	0.65	0.41	0.50	0.26
Field plots	1	Debris flows	0.71	0.37	0.37	0.39
Field plots	2	Debris flows	0.74	0.30	0.33	**0.47**
LiDAR	1	All	0.71	0.63	0.61	**0.19**
LiDAR	2	All	0.70	0.63	0.62	0.18
LiDAR	1	Glacial	0.74	0.58	0.65	**0.22**
LiDAR	2	Glacial	0.72	0.61	0.67	0.18
LiDAR	1	Debris flows	0.61	0.66	0.46	**0.15**
LiDAR	2	Debris flows	0.61	0.65	0.47	0.14

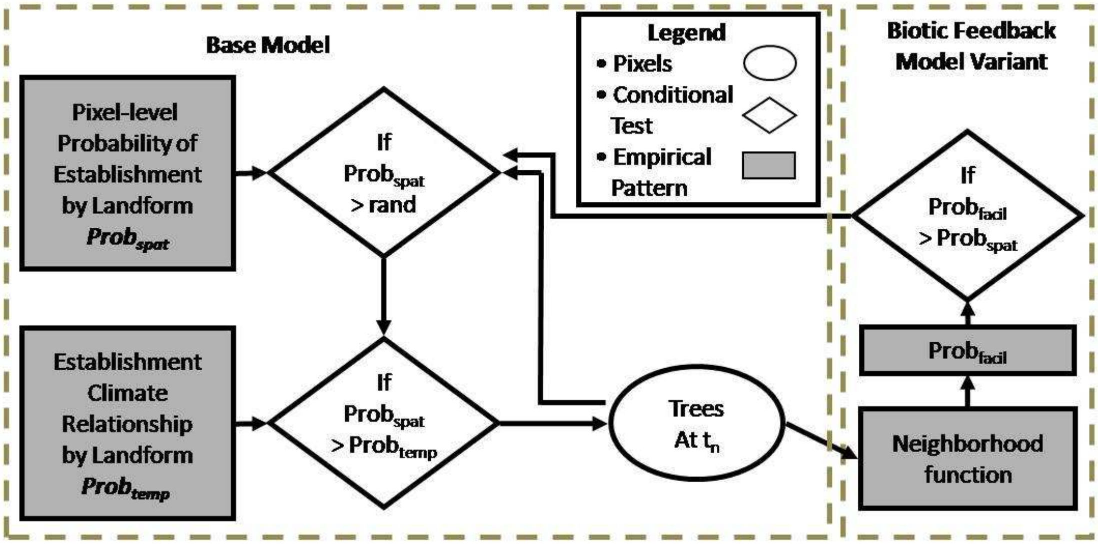

Figure 4.1. Model conceptual diagram. The base model iterates each three year time step through spatial and temporal probabilities of establishment. A tree establishes if the spatial probability of establishment ($\text{Prob}_{\text{spat}}$) is greater than both random (rand), and the temporal probability of establishment ($\text{Prob}_{\text{temp}}$) derived from tree establishment-climate reconstruction. The second model (with biotic feedback) also iteratively assesses how many neighboring pixels are occupied by young trees, and applies a probability of establishment with feedback ($\text{Prob}_{\text{facil}}$) which replaces $\text{Prob}_{\text{spat}}$.

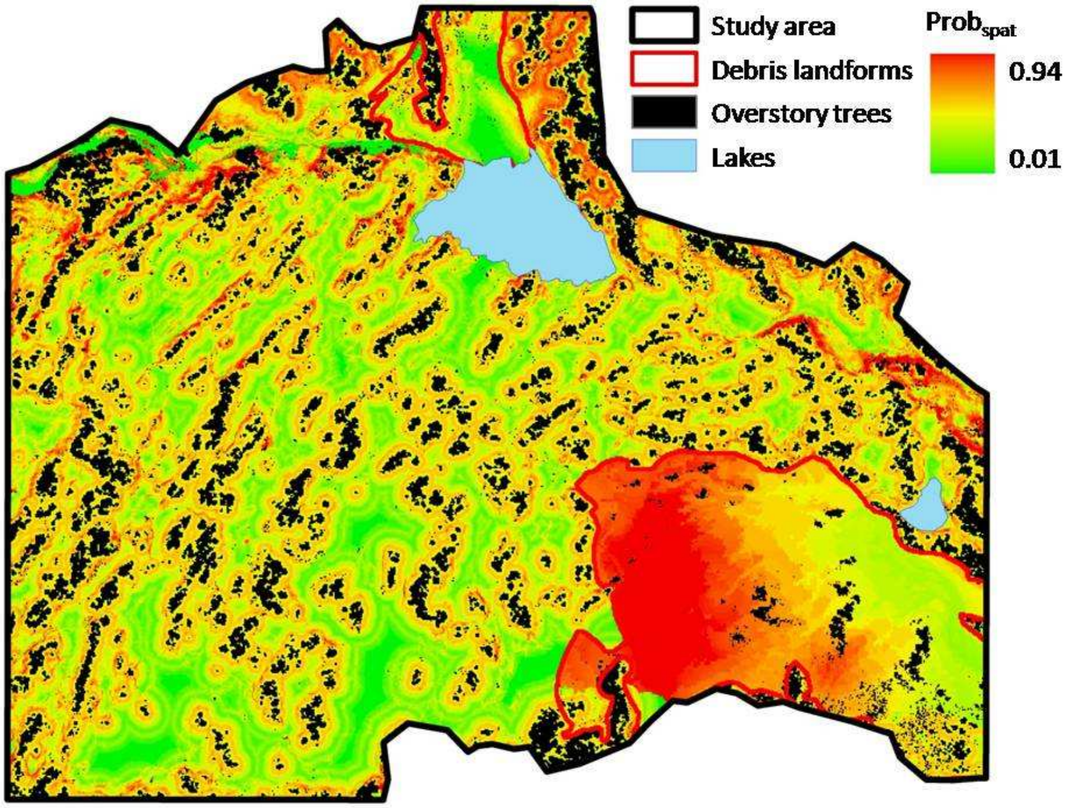

Figure 4.2. Spatial probability of tree invasion (Prob_{spat}) derived from nonparameteric multiplicative regression (NPMR). Prob_{spat} values are proportional in relation to a potential maximum of 1.

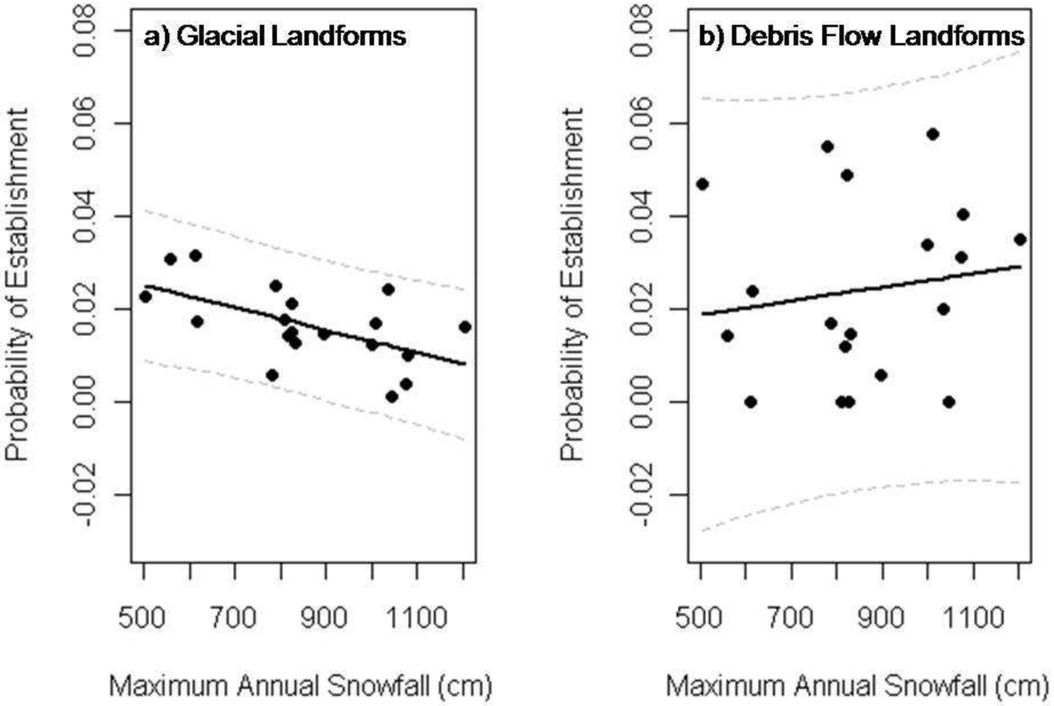

Figure 4.3. Linear regressions of the probability of establishment (Prob$_{temp}$) in relation to maximum annual snowfall for glacial and debris flow landforms. Fitted lines are in solid black, 95 percent confidence intervals are dotted gray.

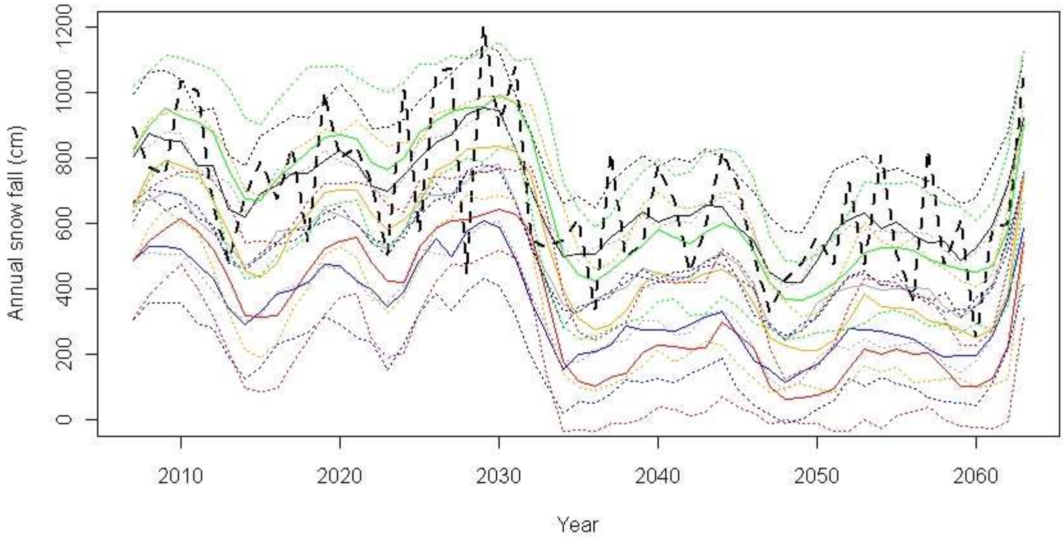

Figure 4.4. Median (solid lines) and 95 percent confidence envelopes (dotted lines) for the six snow scenarios. Lines are color coded by scenario: scenario A (black), scenario B (gray), scenario C (blue), scenario D (yellow), scenario E (orange), and scenario F (red). The historical snow record (thick black dashed line) is superimposed for reference.

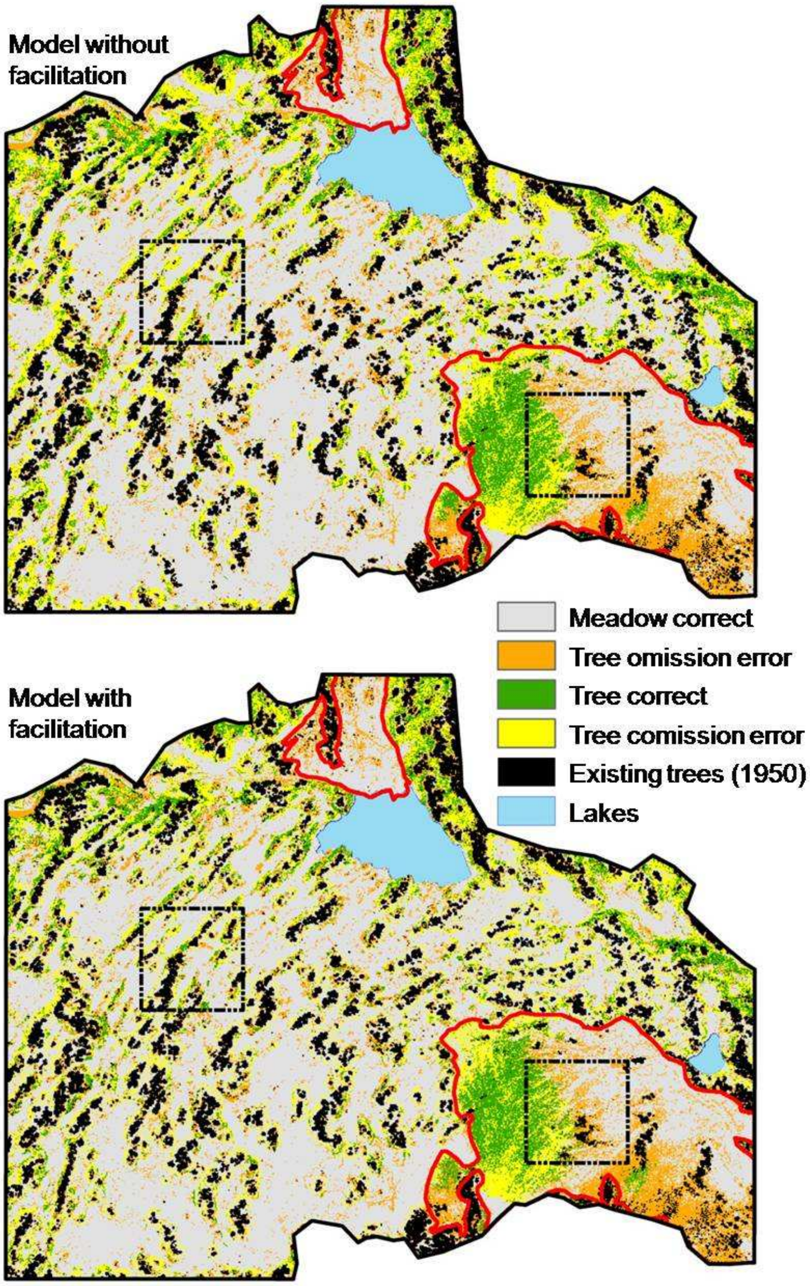

Figure 4.5. Error maps of study area predicted tree invasion from 1950 – 1983. Errors based on comparison of model predicted invasion to LiDAR observations. Areas outlined in red are debris flow landforms. Pixels in black are overstory trees. The two dashed black boxes are the locations of a subset of the model predictions and LiDAR observations used to assess spatial point patterns of tree invasion.

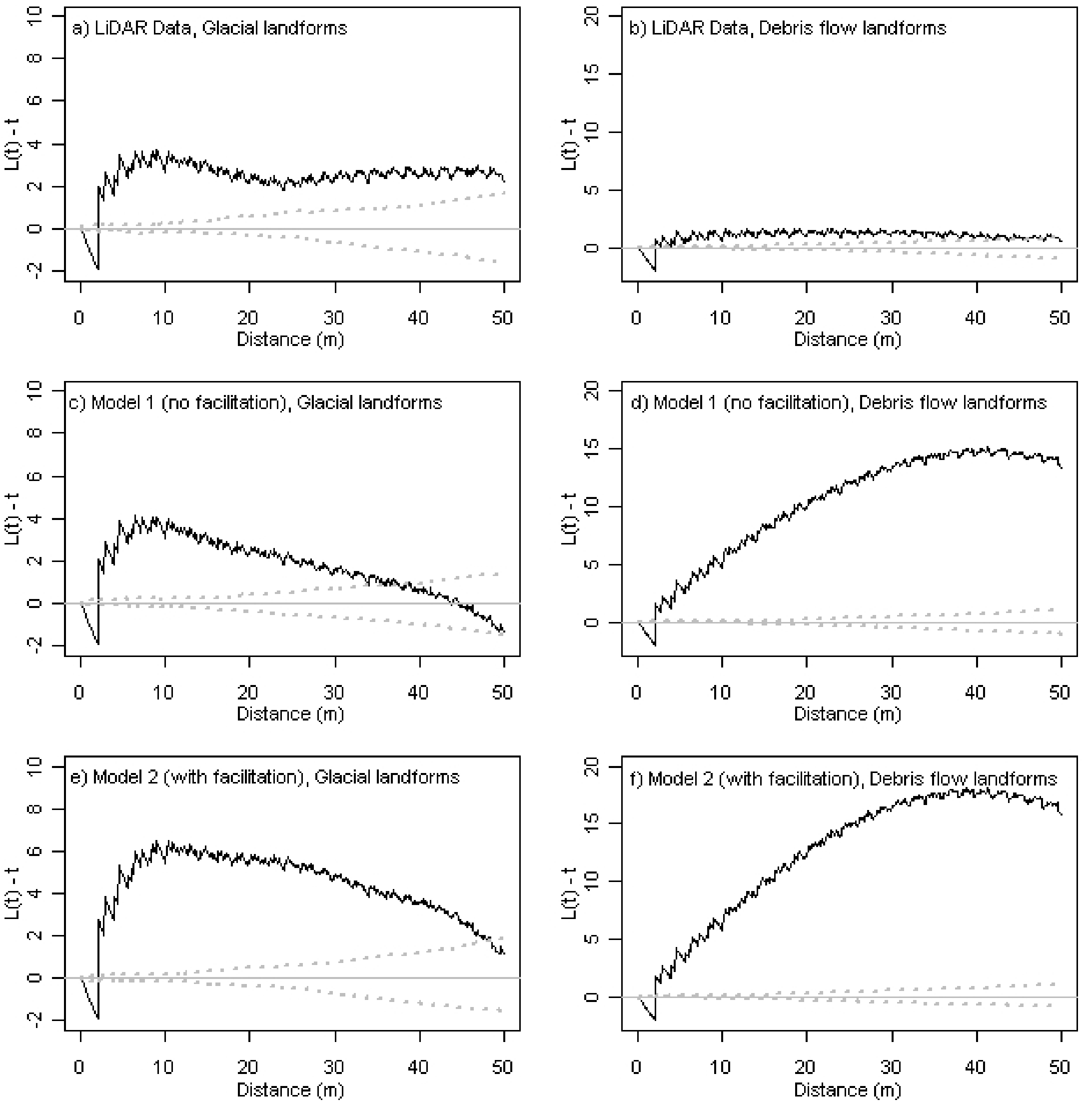

Figure 4.6. Spatial point patterns of LiDAR observed, model1 (without young tree facilitation), and model2 (with young tree facilitation) tree invasion by landform. The solid line denotes the spatial point patterns of tree invasion, and the two dashed lines denote the 95% confidence envelope. The spatial point pattern is considered clustered at distances (in meters) were the solid line is above the upper dashed line, randomly distributed if between the dashed lines, and dispersed if below both dashed lines.

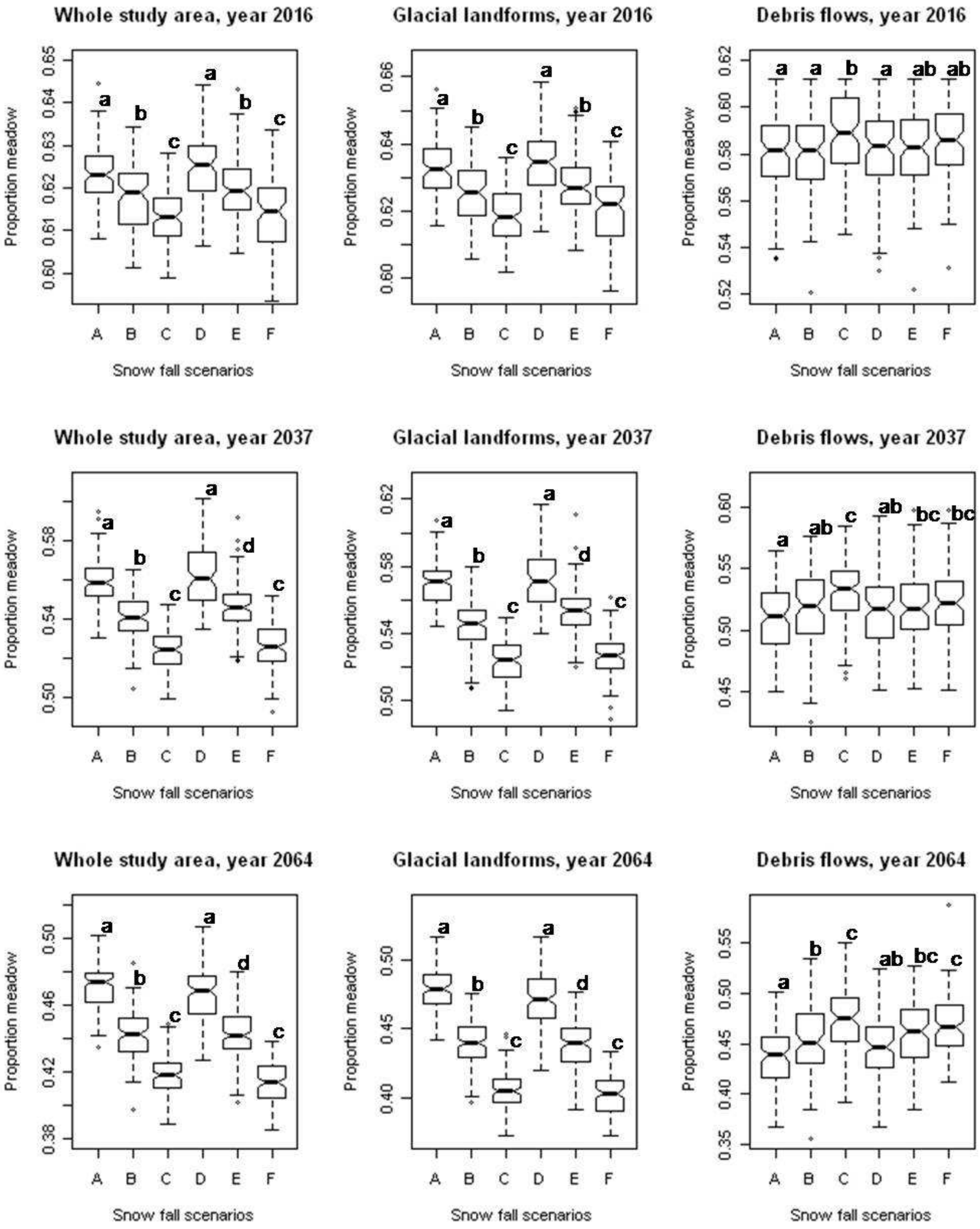

Figure 4.7. Notched box plots for the percent of the study area remaining as meadow separated by landform (panels left to right) at three times during the model (panels top to bottom) in relation to snowfall scenarios. Following McGill(1978), Non-overlapping notches imply significant differences in meadow remaining between snow fall scenarios. Different superscripts represent significantly different areas of meadow invaded from results of Tukey HSD tests. See Table 3 for descriptions of snow fall scenarios.

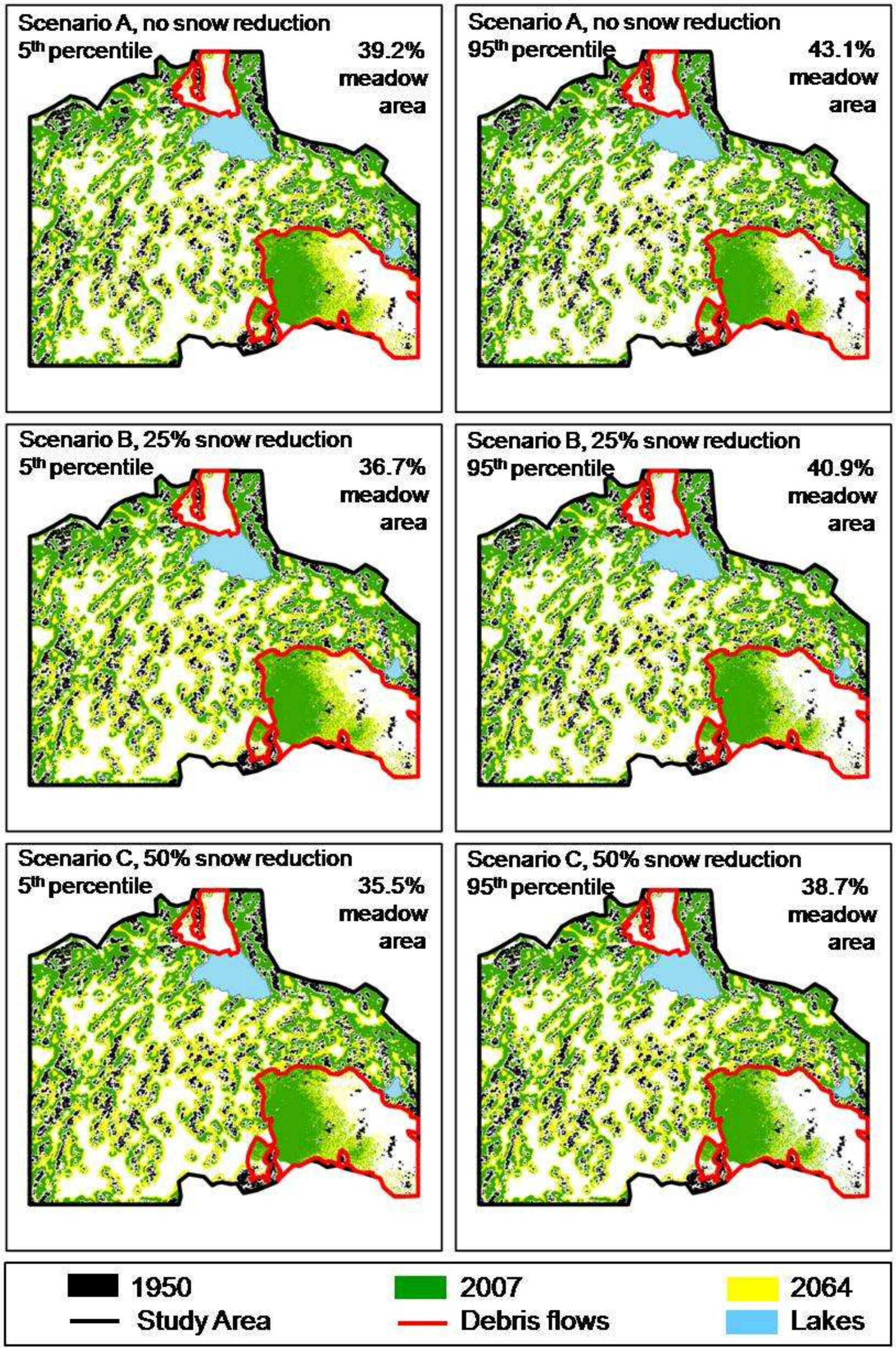

Figure 4.8. Maps of the 5th and 95th percentile iterations of simulated meadow invasion from 1950 to 2064. Colors represent trees in 1950 (black), 2007 (green), and 2064 (yellow). Blue areas are lakes, and the outlines of debris flows are in red.

CHAPTER 5: CONCLUSION

In this dissertation, I set out to understand past, present, and potential future FTE dynamics in Jefferson Park, Oregon from perceptive ranging from the entire study area landscape to individual micro sites. Within this overall past, present, and future perceptive, I directed my studies in relation to three central themes: combining pattern detection and population/landscape estimation, understanding FTE sensitivity to climate in relation to non-climatic biophysical controls, and integrating LiDAR and satellite imagery with field data in multiple ways to improve our understanding of FTE dynamics. I quantified the spatiotemporal patterns of tree establishment and the factors driving these patterns, as well as the spatial patterns of vegetation composition and structure, in the subalpine parkland of Jefferson Park, Oregon, with three overall goals: (1) to characterize fine-scale spatial patterns of current vegetation structure, species distributions, and tree ages, (2) to determine how climate and non-climate biophysical factors have influences patterns of tree invasion in subalpine meadows of the study area over the past five decades, and (3) through simulation models which incorporated climatic and biophysical controls, project tree invasion patterns within the study area over the next five decades under different future climate scenarios.

In chapter 2, I integrated field data on vegetation composition, vegetation structure, and tree ages with high-resolution multispectral satellite imagery, and discrete return Light Detection and Ranging (LiDAR) data to predictively map vegetation composition, structure and tree establishment within 260 ha of the subalpine parklands of Jefferson Park. The objectives of this study were to: (1) characterize spatial patterns of tree invasion via tree ages, vegetation composition, and vegetation structure in a FTE landscape in the Oregon Cascades using predictive mapping, (2) determine how vegetation composition and structure were associated with gradients of environmental factors derived from multispectral satellite imagery and LiDAR, and (3) determine if predictive mapping characterizations of tree ages, vegetation composition, and vegetation structure were improved by the inclusion of LiDAR data. Spatial predictions were accomplished using gradient analysis with nearest neighbor imputation; integrating field plots, multispectral SPOT 5 satellite imagery, and Light Detection and Ranging (LiDAR) data.

Vegetation composition was best described by SPOT 5 imagery and LiDAR-derived topography, while vegetation structure was best described by LiDAR-derived vegetation heights. Tree invasion was the most accurately predicted vegetation structure variable, and indicates the study area was largely un-forested in 1600, gradually invaded from 1600 to the 1920's, and rapid invasion by trees occurred from the 1920's to 1980. Other vegetation structural attributes (e.g. stand density, basal area, quadratic mean diameter) had very low prediction accuracy, which likely results from a combination of asynchronous development of forest structure over time, and within pixel fine-scale spatial heterogeneity of vegetation patches. Species occurrence predictions were most accurate for tree species, moderate for shrub species and vegetation groups, and highly variable for graminoid species.

This study suggests multispectral satellite imagery, LiDAR data, and field plots can be integrated to accurately predict fine-scale spatial characterizations of species distributions and tree invasion in the FTE. When integrated with tree age data, fine-scale predictive mapping can provide previously unavailable landscape estimates of FTE movement and invasion of alpine meadows. However, characterization of tree invasion in predictive mapping is constrained by the range of tree age data collected on field plots, which in this study failed to quantify tree invasion which has occurred in the last 17 years. Poor predictive mapping of vegetation structure suggests limitations to the applicability of LiDAR data for characterizing vegetation in landscapes where forest structure is highly variable, does not develop along consistent trajectories over time, and where spatial heterogeneity of structural attributes occurs at finer grains than field or remotely sensed data. Predictions of species occurrence suggest predictive mapping may be an effective means of generating species information in the FTE. This approach may also be applicable to other habitat types that are important biodiversity hotspots, potentially sensitive to the effects of climate change, or are high value recreation areas, yet may be under sampled by traditional inventory program s because of their small size and discontinuous land cover. This study also found the spatial arrange of field plots can strongly influence spatial variation in prediction accuracy, suggesting sample design could have implications for spatially extrapolating field data from natural resource inventory and monitoring programs. Predictive mapping using inventory data is increasingly being used to generate spatial characterizations of vegetation composition and structure as a decision support tool for natural resource management (Tomppo et al. 2008, Nationwide Forest

Imputation Study 2010). Despite increasing use of predictive mapping methods, the field inventory data which it is based on is not explicitly designed to address spatial patterns of predictive error, which will need to be further investigated in the future.

In chapter 3, I continued to focus on tree establishment in Jefferson Park, but turned my attention to spatial and temporal patterns of tree establish over the past five decades. This short time period of study enabled me to ask how tree invasion tree has occurred over time and space in relation to historical regional climate, in additional to non-climatic biophysical controls such as topography and seed sources at landscape to micro site spatial scales. This chapter had two objectives: (1) to characterize landscape patterns of tree establishment over time, and (2) to determine how climate and biophysical characteristics interactively control the temporal and spatial patterns of tree establishment in the Jefferson Park landscape at multiple spatial scales. This was accomplished utilized airborne Light Detection and Ranging (LiDAR) to establish geo-referenced field plots, and tree establishment reconstructions to quantify spatiotemporal patterns of tree invasion in relation to landform types, fine-scale topographic variability, late season snow persistence, distances from potential seed sources, and regional climate variation.

The percentage meadow area (represented as 2m pixels) occupied by trees increased from 7.75% of the study area in 1950 to 34.7% in 2007. Landform types and finer-scale patterns of topography and vegetation structure nested within landforms influenced summer snow depth, which in turn influenced temporal and spatial patterns of tree establishment. Rates of tree invasion were higher on debris flow landforms which have lower summer snow depth. Tree invasion rates on glacial landforms were strongly associated with reduced annual snow fall, but not on debris flows. High invasion rates not associated with snow fall on debris flows were surprising given conventional wisdom that vegetation recovery is slow and follows deterministic successional pathways at the FTE following disturbance (Agee and Smith 1984, Arsenault and Payette 1992, Coop and Schoettle 2009). The study indicates rapid post-disturbance tree establishment and alternative successional pathways are possible if the disturbance results in favorable micro sites conditions and seed sources are nearby. Tree establishment was spatially constrained to micro sites with high topographic positions and close proximity to overstory canopy associated with low summer snow depth. However seed source limitations placed additional species-specific spatial constraints on meadow invasion.

Climate and topography had an interactive effect, with trees establishing on higher topographic positions during both high snow/low temperature and low snow/high temperature periods, but had greater than expected establishment on lower topographic positions during low snow/high temperature periods. Strong biophysical controls of tree establishment at multiple spatial scales restricted the sites within meadows that trees establish on, even during favorable climate periods. Results of this study suggest large scale climate-driven models of vegetation change may overestimate treeline movement and meadow invasion because they do not account for biophysical controls limiting tree establishment at multiple spatial scales.

In chapter 4, I built on the previous chapter’s retrospective characterization of spatial and temporal patterns of tree establishment to develop a simulation model characterizing historical (1950 to 2007) tree establishment and near-term future (2007 to 2064) tree invasion in relation to six future climate scenarios (no change, 25%, and 50% reductions from historical annual snow fall crossed with forcing or not forcing three year periods of extreme high and low snow fall). I developed an empirically-derived statistical model to quantify tree invasion in relation to deterministic spatial patterns of tree invasion controlled by biophysical factors (microtopography, seed sources, overstory and young tree interactions, larger-scale landform types), and probabilistic temporal patterns of tree establishment in relation to climate (specifically snowfall). This is in contrast to species distribution models which utilize bioclimatic envelopes, and forest dynamics, succession, and growth models which parameterize processes such as fecundity, dispersal, and growth. Specifically, this model was developed to address the following three questions: (1) can fine-scale (2m pixel size) patterns of historical tree invasion be accurately predicted? (2) how sensitive is future tree invasion (and therefore meadow persistence) to different future snowfall scenarios? and (3) are non-climatic factors such as landforms and biotic interactions associated with different spatial patterns of tree invasion? From 1950 to 2007, simulated meadow area declined from 82% to 65% of the study area. Model outputs of historical area, spatial distributions, and spatial clustering of tree invasion generally agreed with independent validation. Model results indicate biotic interactions due to young tree establishment facilitation play an important role in the spatial pattern of tree establishment on glacial landforms but not debris flows. Simulations of future potential tree invasion resulted in declines of 36-43% of the study area remaining as meadows by 2064. Meadows area declined with reduced annual snow fall, but not under prolonged high and low snow fall periods. Under all scenarios there were persistence areas of meadows in 2064. Using species distribution modeling, Randin et al. (2009) suggest fine-scale climate variability in mountain landscapes may cause localized persistent favorable climatic conditions in spite of climate change, resulting in local high-elevation habitat persistence. Although my results suggest subalpine meadows may significantly decline in the future, also lend support to the hypothesis that high-elevation subalpine meadows will persist for the next several decades under climate warming.

Tree establishment in Jefferson Park has not just increased tree density; but tree invasion has reduced meadow land cover, especially over the past 50 years. Reductions in snow fall and increases in temperature promoting longer growing seasons for tree germination and establishment, which promote tree invasion. Temporal patterns of tree invasion are consistent with Northern Hemisphere observations of FTE movement in response to climate change (Harsch et al. 2009). However, biophysical factors such as topography, overstory vegetation, and potential seed sources exert strong controls (equal to and sometimes exceeding climatic controls) on the spatial and temporal patterns of tree establishment in the FTE, and these controls are nested within larger scale landforms, emphasizing the importance of landscape context in determining FTE sensitivity to climate change. These biophysical controls not only have constrained patterns of FTE movement and meadow invasion in the past, but are likely to do so in the future as well.

Despite their potential sensitivity to climate change, intrinsic values for biodiversity and recreation, and small proportions of the overall terrestrial landscape, species abundance and distributions are poorly quantified in the FTE. There are many remaining uncertainties as to how FTEs will respond to a changing climate. Attempts to understand biodiversity risks caused by climate-driven FTE movement are hampered by low resolution and incomplete species distribution information which the predictive mapping methods of chapter 2 may help alleviate. Chapters 2-4 demonstrate on a limited scale the power of integrating field inventories with remotely sensed data sources to improve not only our ability to detect changes in FTE dynamics, but characterize how these changes may occur across complex mountain landscapes. It is landscape characterization of species distributions and change that will allow us to move beyond highly speculative assessments of FTE movements ecological consequences, and begin to quantify what FTE movement will mean for biodiversity, ecosystem productivity, mountain snowmelt hydrology, etc. This dissertation also demonstrates the potential applications (and limitations) of using LiDAR data in FTE research. Of particular value, chapters 3 and 4 demonstrated how LiDAR data can be used not just as another variable for statistical analysis, but how it can be used to formula new research questions and sampling strategies previously difficult or not possible in complex heterogeneous landscapes.

However, more fundament questions and uncertainty remain to understand FTE movement and its potential impacts in a changing climate. Many projections of future change (both in this dissertation and in numerous other studies), are based on historical responses to climate or notions of steady state conditions (Zuller et al. 2009). These assumptions are unlikely to be correct, and may be especially problematic if there are novel ecosystem responses to climate and/or disturbance regimes in the future (Rupp et al. 2000, Edwards et al. 2005). Limitations of static and equilibrium based models highlight the need for experiments which attempt to impose future climatic conditions on current ecosystems. For example, experiments modifying snow and/or temperature have occurred in a wide range of ecosystems, but not in the FTE (Beier et al. 2004, Hurteau and North 2008, Wipf et al. 2009). Our understanding of future FTE responses to climate change could be greatly improved with long-term studies examining FTE dynamics in response to manipulated climate conditions.

BIBLIOGRAPHY

Agee, J.K., and Smith, L. 1984. Subalpine tree reestablishment after fire in the Olympic Mountains, Washington. Ecology 65: 810-819.

Allen, T.R., and Walsh, S.J. 1996. Spatial and compositional pattern of alpine treeline, Glacier National Park, Montana. Photogrammetric Engineering and Remote Sensing 62: 1261-1268.

Araújo, M.B., and Guisan, A. 2006. Five (or so) challenges for species distribution modeling. Journal of Biogeography 33: 1677-1688.

Arseneault, D., and Payette, S. 1992. A postfire shift from lichen-spruce to lichen-tundra vegetation at tree line. Ecology 73: 1067-1081.

Bachelet, D., Lenihan, J.M., Daly, C., Neilson, R.P., Ojima, D.S., and Parton, W.J. 2001. MC1: A dynamic vegetation model for estimating the disturbance of vegetation and associated ecosystem fluxes of carbon, nutrients, and water – technical documentation. Verson 1.0. Gen. Tech. Rep. PNW-GTR-508. Portland, OR: U.S. Department of Agriculture, Forest Service, Pacific Northwest Research Station. 95 p.

Baddeley, A., and Turner, R. 2005. Spatstat: an R package for analyzing spatial point patterns. Journal of Statistical Software 12: 1-42.

Baker, B.B., Moseley, R.K. 2007. Advancing treeline and retreating glaciers: implications for conservation in Yunnan, P.R. China. Arctic, Antarctic, and Alpine Research 39: 200-209.

Barber, V.A., Juday, G.P., and Kinney, B.P. 2000. Reduced growth of Alaskan white spruce in the twentieth century from temperature-induced drought stress. Nature 405: 668-673.

Barry, R.G. 1981. Mountain weather and climate. Methuen, London.

Batllori, E., and Gutiérrez, E. 2008. Regional tree line dynamics in response to global change in the Pyrenees. Journal of Ecology 96: 1275-1288.

Bechtold, W.A., and Patterson, P.L. (eds.). 2005. The enhanced forest inventory and analysis program – National sampling design and estimation procedures. General Technical Report SRS-80. U.S.D.A Forest Service, Southern Research Station, Ashville, NC.

Beier, C., Emmett, B., Gundersen, P., Tietema, A., Penuelas, J., Estiarte, M., Gordon, C., Gorissen, A., Llorens, L., Roda, F., and Williams, D. 2004. Novel approaches to study climate change effects on terrestrial ecosystems in the field: drought and passive nighttime warming. Ecosystems 2004: 583-597.

Bekker, M.F. 2005. Positive feedback between tree establishment and patterns of subalpine forest advancement, Glacial National Park, Montana, U.S.A. Arctic, Antarctic, and Alpine Research 37: 97-107.

Beniston, M., Diaz, H.F., and Bradley, R.S. 1997. Climatic change at high elevation sites: an overview. Climatic Change 36: 233-251.

Bettin, O., Cornejo, C., Edwards, P.J., and Holderegger, R. 2007. Phylogeography of the high alpine plant *Senecio halleri* (Asteraceae) in the European Alps: *in situ* glacial survival with postglacial stepwise dispersal in peripheral areas. Molecular Ecology 16: 2517-2524.

Beyer, H. L. 2004. Hawth's Analysis Tools for ArcGIS. Available at http://www.spatialecology.com/htools.

Bonan, G.B., Pollard, D., and Thompson, S.L. 1992. Effects of boreal forest vegetation on global climate. Nature 359: 716-718.

Bonner, F.T., and Karrfalt, R.P. [eds]. 2008. Woody plant seed manual. U.S. Department of Agriculture, U.S. Forest Service Agricultural Handbook 727.

Bormann, F.H., and Likens, G.E. 1979. Pattern and process in a forested ecosystem. Spring, New York, 253 pp.

Brang, P. 1998. Early seedling establishment of *Picea abies* in small forest gaps in the Swiss Alps. Canadian Journal of Forest Research 28: 626-639.

Brink, V.C. 1959. A direction change in the subalpine forest-heath ecotone in Garibaldi Park, Bristish Columbia. Ecology 40: 10-16.

Brown, D.G. 1994. Predicting vegetation types at treeline using topography and biophysical disturbance variables. Journal of Vegetation Science 5: 641-656.

Burnham, K.P., and Anderson, D.R. 2002. Model selection and multimodel inference: A practical information-theoretic approach, 2nd ed. Springer, New York, NY.

Butler, D.R. 1986. Conifer invasion of subalpine meadows, central Lemhi Mountains, Idaho. Northwest Science 60: 166-173.

Campbell, A.G. 1973. Vegetative ecology of Hunt’s Cove, Mt. Jefferson, Oregon. Master’s Thesis, Oregon State University. pp 89.

Cannone, N., Sgorbati, S., and Guglielmin, M. 2007. Unexpected impacts of climate change on alpine vegetation. Frontiers in Ecology and Evolution 5: 360-364.

Casola, J.H., Cuo, L., Livneh, B., Lettenmaier, D.P., Stoelinga, M.T., Mote, P.W., and Wallace, J.M. 2009. Assessing the impacts of global warming on snowpack in the Washington Cascades. Journal of Climate 22: 2758-2772.

Carkin, R.E., Franklin, J.F., Booth, J., and Smith, C.E. 1978. Seeding habits of upper-slope tree species IV: Seed flight of noble fir and Pacific silver fir. USDA Forest Service Research Notes PNW-312.Pacific Northwest Forest and Range Experimental Station, Portland, OR.

CEC. 1994. CORINE land cover. Technical guide. Luxembourg (Office for Official Publications of European Communities).
Chapin, S.F., Walker, L.R., Fastie, C.L., and Sharman, L.C. 1995. Mechanisms of primary succession following deglaciation at Glacier Bay, Alaska. Ecological Monographs 64: 149-175.

Christensen, J.H., B. Hewitson, A. Busuioc, A. Chen, X. Gao, I. Held, R. Jones, R.K. Kolli, W.-T. Kwon, R. Laprise, V. Magaña Rueda, L. Mearns, C.G. Menéndez, J. Räisänen, A. Rinke, A. Sarr and P. Whetton, 2007: Regional Climate Projections. In: Climate Change 2007: The Physical Science Basis. Contribution of Working Group I to the Fourth Assessment Report of the Intergovernmental Panel on Climate Change [Solomon, S., D. Qin, M. Manning, Z. Chen, M. Marquis, K.B. Averyt, M. Tignor and H.L. Miller (eds.)]. Cambridge University Press, Cambridge, United Kingdom and New York, NY, USA.

Chuby, M.S., Franklin, S.E., and Wulder, M.A. 2006. Object-based analysis of Ikonos-2 imagery for extraction of forest inventory parameters. Photogrammetric Engineering and Remote Sensing. 72: 383-394.

Chust, G., Galparoso, I., Borja, A., Franco, J., and Uriarte, A. 2008. Coastal and estuarine habitat mapping, using LIDAR height and intensity and multi-spectral imagery. Estuarine, Coastal and Shelf Science 78: 633-643.

Cohen, J. 1960. A coefficient of agreement for nominal scales. Educational and Psychological Measurement 20: 37-36.

Coop, J.D., and Schoettle, A.W. 2009. Regeneration of Rocky Mountain bristlecone pine (*Pinus aristata*) and limber pine (*Pinus flexilis*) three decades after stand-replacing fires. Forest Ecology and Management 257: 893-903.

Coville, F. 1898. Forest growth and sheep grazing in theCascade Mountains of Oregon. USDA Division of Forestry Bulletin 15, Washington, DC.

Crawford, P.D., and Oliver, C.D. 1990. Pacific silver fir. In: Silvics of North America: 1. Conifers. Burns, R.M., and Honkala, B.H. (technical coordinators). U.S. Department of Agriculture, Forest Service, Washington, DC.

Crookston, N.L., Finley, A.O. 2007. yaImpute: An R package for k-NN imputation. Journal of Statistical Software 23: 1-16.

Daniels, L.D., and Veblen, T.T. 2003. Regional and local effects of disturbance and climate on altitudinal treelines in northern Patagonia. Journal of Vegetation Science. 14: 733-742.

Daniels, L.D., and Veblen, T.T. 2004. Spatiotemporal influences of climate on altitudinal treeline in Northern Patagonia. Ecology 85: 1284-1296.

Davis, A.J., Jenkinson, L.A., Lawton, J.H., Shorrocks, B., and Wood, S. 1998. Making mistakes when predicting shifts in species range in response to global warming. Nature 391: 783-786

Dearden, P., and Seawell, W.R.D. 1983. From gloom to glory and beyond: The North American mountain recreation experience. Bayfield, N.G., and Aitken, R. (eds). In: The ecological impacts of outdoor recreation on mountain areas in Europe and North America. Recreation Ecology Research Group Report No. 9. Wye, UK.

DeBenedetti, S.H., and Parsons, D.J. 1979. Natural fire in subalpine meadows: a case description from the Sierra Nevada. Journal of Forestry 77: 477-479.

Del Moral, R., Titus, J.H., and Cook, A.M. 1995. Early primary succession on Mount St. Helens, Washington, USA. Journal of Vegetation Science 6: 107-120.

Del Moral, R., Sandler, J.E., and Muerdter, C.P. 2009. Spatial factors affecting primary succession on the Muddy River Lahar, Mount St. Helens, Washington. Plant Ecology 202: 177-190.

Devi, N., Hagedorn, F., Moiseev, P., Bugmann, H., Shiyatov, S., Mazepa, V., Rigling, A. 2008. Expanding forests and changing growth forms of Siberian larch at the polar Urals treeline during the 20th century. Global Change Biology 14: 1581-1591.

Didier, L. 2001. Invasion patterns of European larch and Swiss stone pine in subalpine pastures in the French Alps. Forest Ecology and Management 145: 67-77.

Dirnböck, T., Dullinger, S., and Grabherr, G. 2003. A regional impact assessment of climate and land-use change on alpine vegetation. Journal of Biogeography 30: 401-417.

Douglas, G.W. 1972. Subalpine plant communities of the western North Cascades, Washington. Arctic and Alpine Research 4: 147-166.

Dovčiak, M., Hrivnák, R., Ujházy, K., and Gömöry, D. 2008. Seed rain and environmental controls on invasion of *Picea abies* into grassland. Plant Ecology 194: 135-148.

Dufrene, M., and Legendre, P. 1997. Species assemblages and indicator species: the need for a flexible asymmetrical approach. Ecological Monographs 67: 345-366.

Dullinger, S., Dirnbock, T., and Grabherr, G. 2004. Modeling climate change-driven treeline shifts: relative effects of temperature increase, dispersal and invisibility. Journal of Ecology 92: 241-252.

Dyurgerov, M.B., and Meier, M.F. 2002. Twentieth century climate change: evidence from small glaciers. Proceeding of the National Academy of Sciences 97: 1406-1411.

Edwards, M.E., Brubaker, L.B., Lozhkin, A.V., and Anderson, P.M. 2005. Strucutrally noval biomes: a response to past warming in Beringia. Ecology 86: 1696-1703.

Elliott, D.L., Holladay, C.G., Barchet, W.R., Foote, H.P., and Sandusky, W.F. 1987. Wind energy resource atlas of the United States. U.S. Department of Energy, Pacific Northwest National Laboratory. Richland, WA.

Eugster, W., Rouse, W.R., Pielke, R.A., McFadden, J.P., Baldocchi, D.D., Kittel, T.G., Chapin, F.S., Liston, G.E., Vidale, P.L., Vaganov, E., and Chambers, S. 2000. Land-atmosphere energy exchange in Arctic tundra and boreal forest: available data and feedbacks to climate. Global Change Biology 6: 84-115.

Faria, D.A., Pomeroy, J.W., and Essery, R.L.H. 2000. Effect of covariance between ablation and snow water equivalent on depletion of snow-covered area in a forest. Hydrological Processes 14: 2683-2695.

Fastie, C.L. 1995. Causes and ecosystem consequences of multiple pathways of primary succession at Glacier Bay, Alaska. Ecology 76: 1899-1916.

Fischlin, A., G.F. Midgley, J.T. Price, R. Leemans, B. Gopal, C. Turley, M.D.A. Rounsevell, O.P. Dube, J. Tarazona, A.A. Velichko, 2007: Ecosystems, their properties, goods, and services. Climate Change 2007: Impacts, Adaptation and Vulnerability. Contribution of Working Group II to the Fourth Assessment Report of the Intergovernmental Panel on Climate Change, M.L. Parry, O.F. Canziani, J.P. Palutikof, P.J. van der Linden and C.E. Hanson, Eds., Cambridge University Press, Cambridge, 211-272.

Foley, J.A., Levis, S., Costa, M.H., Cramer, W., and Pollard, D. 2000. Incorporating dynamic vegetation cover within global climate models. Ecological Applications 10: 1620-1632.

Fonda , R.W., amd Bliss, L.C. 1969. Forest vegetation of the montane and subalpine zones, Olympic Mountains, Washington. Ecological Monographs 39: 271-301.

Fortin, M-J. Drapeau, P., and Legendre, P. 1989. Spatial autocorrelation and sampling design in plant ecology. Vegatatio 83: 209-222.

Franklin, J.F., Moir, W.H., Douglas, G.W., and Wiberg, C. 1971. Invasion of subalpine meadows by trees in the Cascade Range, Washington and Oregon. Arctic and Alpine Research 3: 215-224.

Franklin, J.F., and Smith, C.E. 1974. Seeding habits of upper-slope tree species II: Dispersal of a mountain hemlock seedcrop on a clearcut. USDA For. Serv. Res. Note PNW-214, 9p. Pacific Northwest Forest and Range Experimental Station, Portland, OR.

Franklin, J.F., and Dyrness, C.T. 1988. Natural vegetation of Oregon and Washington. Oregon State University Press, Corvallis, Oregon, USA.

Franklin, J.F., Spies, T.A., Van Pelt, R., Carey, A.B., Thornburgh, D.A., Rae Berg, D., Lindenmayer, D.B., Harmon, M.E., Keeton, W.S., Shaw, D.C., Bible, K., and Chen, J. 2002. Disturbances and structural development of natural forest ecosystems with silvicultural implications, using Douglas-fir forests as an example. Forest Ecology and Management 155: 399-423.

Frayer, W.E., and Furnival, G.M. 1999. Forest survey sampling designs: a history. Journal of Forestry 97: 4-10.

Gamache, I., Payette, S. 2005. Latitudinal response of subarctic tree lines to recent climate change in eastern Canada. Journal of Biogeography 32: 849-862.

Garbarino, M., Lingua, E., Nagel, T.A., Godone, D., and Motta, R. 2010. Patterns of larch establishment following deglaciation of Ventina glacier, central Italian Alps. Forest Ecology and Management 259: 583590.

Gedalof, Z., Peterson, D.L., and Mantua, N.J. 2004. Columbia river flow and drought since 1750. Journal of the American Water Resources Association 40: 1579-1592.

Geddes, C.A., Brown, D.G., and Fagre, D.B. 2005. Topography and vegetation as predictors of snow water equivalent across the alpine treeline ecotone at Lee Ridge, Glacier National Park, Montana, U.S.A.. Arctic, Antarctic, and Alpine Research 37: 197-205.

Gehrig-Fasel, J., Guisan, A., and Zimmerman, N.E. 2007. Tree line shifts in the Swiss Alps: climate change or land abandonment? Journal of Vegetation Science 18: 571-582.

Gopal, S., Woodcock, C.E., and Strahler, A.H. 1999. Fussy neural network classification of global land cover from the 1° AVHHRR data set. Remote Sensing of Environment 67: 230-243.

Goodin, D.G., and Isard, S.A. 1989. Magnitude and sources of variation in albedo within an alpine tundra. Theoretical and Applied Climatology 40: 61-66.

Gottfried, M., Pauli, H.P., Reiter, K., and Grabherr, G. 1998. A fine-scaled predictive model for changes in species distribution patterns of high mountain plants induced by climate warming. Diversity and Distributions 5: 241-251.

Grace, J. 1989. Tree Lines. Philosophical Transactions of the Royal Society of London. Series B, Biological Sciences 324(1223): 233-243.

Grace, J., Berninger, F., and Nagy, L. 2002. Impacts of climate change on the tree line. Annals of Botany 90: 537-544.

Gray, A.N., and Spies, T.A. 1997. Microsite controls on tree seedling establishment in conifer forest canopy gaps. Ecology 78: 2458-2473.

Griggs, R.F. 1934. The edge of the forest in Alaska and the reasons for its position. Ecology 15: 80-96.

Grubb, P.J. 1977. The maintenance of species-richness in plant communities: the importance of the regeneration niche. Biological Reviews 52: 107-145.

Guisan, A., Edwards, T.C., and Hastie, T. 2002. Generalized linear and generalized additive models in studies of species distributions: setting the scene. Ecological Modeling 157: 89-100.

Guisan, A., and Zimmerman, N.E. 2000. Predictive habitat distribution models in ecology. Ecological Modelling 135: 147-186.

Guisan, A., and Thuiller, W. 2005. Predicting species distribution: offering more than simple habitat models. Ecology Letters 8: 993-1009.

Haase, P. 1995. Spatial pattern analysis in ecology based on Ripley's K-function: Introduction and methods of edge correction. Journal of Vegetation Science 6: 575-582.

Hallett, D.J., Lepofsky, D.S., Mathewes, R.W., and Lertzman, K.P. 2003. 11000 years of fire history and climate in the mountain hemlock rain forests of southwestern British Columbia based on sedimentary charcoal. Canadian Journal of Forest Research 33: 292-312.

Halloy, S.R.P., and Mark, A.F. 2003. Climate-change effects on alpine plant biodiversity: A New Zealand perspective on quantifying the threat. Arctic, Antarctic, and Alpine Research 35: 248-254.

Halpern, C.B., Smith, B.G., and Franklin, J.F. 1984. Composition, structure, and distribution of the ecosystems of the Three Sisters Biosphere Reserve/Wilderness Area. A final report of the United States Department of Agriculture.

Hansen, M.C., Defries, R.S., Townshend, J.R.G., and Sohlberg, R. 2000. Global land cover classification at 1 km spatial resolution using a classification tree approach. International Journal of Remote Sensing 21: 1331-1364.

Hardt, R.A., and Forman, R.T.T. 1989. Boundary form effects on woody colonization of reclaimed surface mines. Ecology 70: 1252-1260.

Harsch, M.A., Hulme, P.E., McGlone, M.S., and Duncan, R.P. 2009. Are treelines advancing? A global meta-analysis of treeline response to climate warming. Ecology Letters 12: 1040-1049.

Hättenschwiler, S., and Smith, W.K. 1999. Seedling occurrence in alpine treeline conifers: A case study from the central Rocky Mountains, USA. Acta Oecologica 20: 219-224.

Heegaard, E. 2002. A model of alpine species distribution in relation to snowmelt time and altitude. Journal of Vegetation Science 13: 493-504.

Henderson, J.A. 1973. Composition, distribution, and succession of subalpine meadows in Mount Rainier National Park. Ph.D. thesis Oregon State University. Corvallis, OR.

Hermes, K. 1955. Die Lage der oberen Waldgrenze in den Gebirgen der Erde und ihr Abstand zur Schneegrenze. Kölner geographische Arbeiten, Heft 5. Geographisches Institut, University of Köln.

Hiemstra, C.A., Liston, G.E., and Reiners, W.A. 2002. Snow redistribution by wind and interactions with vegetation at upper treeline in the Medicine Bow Mountains, Wyoming, U.S.A. Arctic, Antarctic, and Alpine Research 34: 262-273.

Hiemstra, C.A., Liston, G.E., and Reiners, W.A. 2006. Observing, modeling, and validating snow redistribution by wind in a Wyoming upper treeline landscape. Ecological Modelling 197: 35-51.

Hill, R., Granica, K., Smith, G.M., Schardt, M. 2007. Representation of an alpine treeline ecotone in SPOT 5 HRG data. Remote Sensing of Environment 110: 458-467.

Holtmeier, F.K., and Broll, G. 1992. The influence of tree islands and microtopography on pedoecological conditions in the forest-alpine tundra ecotone on Niwot Ridge, Colorado Front Range, U.S.A. Arctic, Antarctic, and Alpine Research 24: 216-228.

Hodge, E.T. 1925. Geology of Mt. Jefferson. Mazama 7: 25-58.

Holtmeier, F.K. 2003. Mountain timberlines: ecology, patchiness, and dynamics. Kluwer Academic Publishers.

Holtmeier, F.K., and Broll, G. 2005. Sensitivity and response of northern hemisphere altitudinal and polar treelines to environment change at landscape and local scales. Global Ecology and Biogeography 14: 395-410.

Homer, C., Huang, C., Yang, L., Wylie, B., and Coan, M. 2004. Development of a 2001 national land-cover database for the United States. Photogrammetric Engineering and Remote Sensing 70: 829-840.

Homer, C., Dewitz, J., Fry, J., Coan, M., Hossain, N., Larson, C., Herold, N., McKerrow, A., VanDriel, J.N., and Wickham, J. 2007. Completion of the 2001 national land cover database for the conterminous United States. Photogrammetric Engineering and Remote Sensing 73: 337-341.

Hudak, A.T., Crookston, N.L., Evans, J.S., Hall, D.E., and Falkowski, M.J. 2008. Nearest neighbor imputation of species-level, plot-scale forest structure attributes from LiDAR data. Remote Sensing of Environment 112: 2232-2245.

Hurteau, M. and North, M. 2008. Mixed-conifer understory response to climate change, nitrogen, and fire. Global Change Biology 14: 1543-1552.

Hurvich, C.M., and Tsai, C-L. 1989. Regression and time series model selection in small samples. Biometrika 76: 297-307.

Ishii, H., Reynolds, J.H., Ford, E.D., and Shaw, D. 2000. Height growth and vertical development of an old-growth Pseudotsuga-Tsuga forest in southwestern Washington Stata, U.S.A. Canadian Journal of Forest Research 30: 17-24.

Jakubauskas, M.A. 1996. Thematic mapper characterization of lodgepole pine seral stages in Yellowstone National Park, USA. Remote Sensing of Environment 56: 118-132.

Jansen, E., Overpeck, J., Briffa, K.R., Duplessy, J.C., Joos, F., Masson-Delmotte, V., Olago, D., Otto-Bliesner, B., Peltier, W.R., Rahmstorf, S., Ramesh, R., Raynaud, D., Rind, D., Solomina, O., Villalba, R., and Zhang, D. 2007. Palaeoclimate. In: Climate change 2007: The physical science basis. Contribution of working group 1 to the Fourth Assessment Report of the Intergovernmental Panel on Climate Change [Solomon, S., D. Qin, M. Manning, Z. Chen, M. Marquis, K.B. Averyt, M. Tignor, and H.L. Miller (eds.)]. Cambridge University Press, United Kingdom and New York, NY, USA.

Jobbágy, E.G., Jackson, R.B. 2000. Global controls of forest line elevation in the northern and southern hemispheres. Global Ecology and Biogeography 9: 253-268.

Johnston, C.A., and Bonde, J. 1989. Quantitative analysis of ecotones using a geographic information system. Photogrammetric Engineering and Remote Sensing 55: 1643-1647.

Jompponen, A., Vare, H., Mattson, K.G., Ohtonen, R., and Trappe, J.M. 1999. Characterization of ‘safe sites’ for pioneers in primary succession on recently deglaciated terrain. Journal of Ecology 87: 98-105.

Kadmon, R., Farber, O., and Danin, A. 2003. A systematic analysis of factors affecting the performance of climatic envelope models. Ecological Applications 13: 853-867.

Kenkel, N.C., Juhász-Nagy, P., and Podani, J. 1989. On sampling procedures in population and community ecology. Vegetatio 83: 195-207.

Kennedy, R.E., and Cohen, W.B. 2003. Automated designation of tie-points for image-to-image coregistration. International Journal of Remote Sensing. 24: 3467-3490.

Kennedy, R.E., Cohen, W.B., Schroeder, T.A. 2007. Trajectory-based change detection for automated characterization of forest disturbance dynamics. Remote Sensing of Environment 110: 370-386.

Körner, C. 1995. Alpine plant diversity: a global survey and functional interpretation. In: Chapin F.S. III., Körner, C. (eds). Arctic and alpine biodiversity: patterns, causes, and ecosystem consequences. Ecological Studies, vol 113. Springer, New York, pp 45-62.

Körner, C. 1998. A re-assessment of high elevation treeline positions and their explanation. *Oecologia* 115: 445-459.

Körner, C. 2000. Biosphere responses to CO2 enrichment. *Ecological Applications,* 10: 1590-1619.

Körner, C., and Spehn, E.M. (eds). 2002. Mountain biodiversity. A global assessment. Parthenon, New York.

Körner, C. 2003. Alpine plant life: Functional plant ecology of high mountain ecosystems, 2nd ed. Springer, Berlin.

Krajina, V. J. 1969. Ecology of forest trees in British Columbia. *In* Ecology of western North America. vol. 2. p. 1-147. V. J. Krajina, ed. University of British Columbia, Department of Biology. Vancouver, BC.

Kuhns, J.C. 1917. G-Reconnaissance-Cascade. Report to theForest Supervisor. Supervisor's Office, Willamette National Forest, Eugene, OR.

Kupfer, J.A., and Cairns, D.M. 1996. The suitability of montane ecotones as indicators of global climate change. Progress in Physical Geography 20: 253-272.

Kuramoto, R.T., and Bliss, L.C. 1970. Ecology of subalpine meadows in the Olympic Mountains, Washington. Ecological Monographs 40: 317-347.

Lafleur, P.M., Griffis, T.J., and Rouse, W.R. 2001. Interannual variability in net ecosystem CO 2 exchange at the arctic treeline. Arctic, Antarctic, and Alpine Research. 33: 149-157.

Lapen, D.R., and Martz, L.W. 1996. An investigation of the spatial association between snow depth and topography in a prairie agricultural landscape using digital terrain analysis. Journal of Hydrology 184: 277-298.

Larocque, S.J., and Smith, D.J. 2003. Little Ice Age glacial activity in the Mt. Waddington area, British Columbia Coast Mountains, Canada. Canadian Journal of Earth Science 40: 1413-1436.

Larocque, G.R., Archambault, L., and Delisle, C. 2006. Modelling forest succession in two southeastern Canadian mixedwood ecosystems types using the ZELIG model. Ecological Modelling 199: 350-362.

Larson, A.J., Lutz, J.A., Gersonde, R.F., Franklin, J.F., and Hietpas, F.F. 2008. Potential site productivity influences the rate of forest structural development. Ecological Applications 18: 899-910.

Lefsky, M.A., Cohen, W.B., Acker, S.A., Parker, G.G., Spies, T.A., and Harding, D. 1999. Lidar remote sensing of the canopy structure and biophysical properties of Douglas-fir western hemlock forests. Remote Sensing and Environment 70: 339-361.

Lefsky, M.A., Cohen, W.B., Parker, G.G., Harding, D.J. 2002. Lidar remote sensing for ecosystem studies. Bioscience 52: 19-30.

LePage, P.T., Canham, C.D., Coates, K.D., and Bartemucci, P. 2000. Seed abundance versus substrate limitation of seedling recruitment in northern temperate forests of British Columbia. Canadian Journal of Forest Research 30: 415-417.

Lescop-Sinclair, K., and Payette, S. 1995. Recent advance of the arctic treeline along the eastern coast of Hudson Bay. Journal of Ecology 83: 929-936.

Lesica, P., McCune, B., Cooper, S.V., and Hong, W.S. 1991. Differences in lichen and bryophyte communities between old-growth and managed second-growth forests in the Swan Valley, Montana. Canadian Journal of Botany 69: 1745-1755.

Lertzman, K.P., and Krebs, C.J. 1991. Gap-phase structure of a subalpine old-growth forest. Canadian Journal of Forest Research 21: 1730-1741.

Levin, S.A. 1992. The problem of pattern and scale in ecology. Ecology 73: 1943-1967.

Lewis, D.H., and Smith, D.J. 2004. Little Ice Age glacial activity in Strathcona Provincial Park, Vancouver Island, British Columbia, Canada. Canadian Journal of Earth Science 41: 285-297.

Ling, F., and Zhang, T. 2005. Modeling the effect of variations in snowpack-disappearance date on surface-energy balance in the Alaskan North Slope. Arctic, Antarctic, and Alpine Research 37: 483-489.

Litaor, M.I., Williams, M., and Seastedt, T.R. 2008. Topographic controls on snow distribution, soil moisture, and species diversity of herbaceous alpine vegetation, Niwot Ridge, Colorado. Journal of Geophysical Research 113, doi:10.1029/2007JG000419.

Liu, X., and Chen, B. 2000. Climatic warming in the Tibetan Plateau during recent decades. International Journal of Climatology 20: 1729-1742.

Lloyd, A.H., and Graumlich, L.J. 1997. Holocene dynamics of treeline forests in the Sierra Nevada. Ecology 78: 1199-1210.

Luckman, B.H. 2000. The Little Ice Age in the Canadian Rockies. Geomorphology 32: 357-384.

Maher, E.L., Germino, M.J., Hasselquist, N.L. 2005. Interactive effects of tree and herb cover on survivorship, physiology, and microclimate of conifer seedlings at the alpine tree-line ecotone. Canadian Journal of Forest Research 35: 567-574.

Marks, D., and Dozier, J. 1992. Climate and energy exchange at the snow surface in the alpine region of the Sierra Nevada 2: Snow cover energy balance. Water Resources Research 28: 3043-3054.

Marks, D., Winstral, A., Seyfried, M. 2002. Simulation of terrain and forest shelter effects on patterns of snow deposition, snowmelt, and runoff over a semi-arid mountain catchment. Hydrological Processes 16: 3605-3626.

Martin, K., Chytry, M., and Tichy, L. 2003. Formalized reproduction of an expert-based phytosociological classification: A case study of subalpine tall-forb vegetation. Journal of Vegetation Science 14: 601-610.

Martínez-Meyer, E. 2006. Climate change and biodiversity: Some considerations in forecasting shifts in species potential distributions. Biodiversity Informatics 2: 42-55.

Masek, J.G. 2001. Stability of boreal forest stands during recent climate change: evidence from Landsat satellite imagery. Journal of Biogeography 28: 967-976.

McCune, B. 1997. Influence of noisy environmental data on canonical correspondence analysis. Ecology 78: 2617-2623.

McCune, B., and Grace, J.B. 2002. Analysis of ecological communities. MjM Software, Gleneden Beach, Oregon.

McCune, B., and Mefford, M.J. 2004. Hyperniche nonparametric multiplicative habitat modeling. Version 1.39. MjM Software, Gleneden Beach, Oregon.

McCune, B. 2006. Non-parametric habitat models with automatic interactions. Journal of Vegetation Science 17: 819-830.

McDonald, G.D. 1995. Changes in mass of Collier Glacier, Oregon, 1910-1994. M.S. Thesis, Oregon State University, Corvallis, OR.

McDonald, G.D. 1998. Soil survey of Warm Springs Indian Reservation, Oregon. U.S. Department of Agriculture and Natural Resources Conservation Service. Washington, D.C.

McGaughey, R.J. 2007. FUSION/LDV: Software for LIDAR data analysis and visualization. U.S. Department of Agriculture, Forest Service, Pacific Northwest Research Station. Available at http://www.fe.fed.us/eng/rsac/fusion/

McGill, R., Tukey, J., and Larsen, W.A. 1978. Variations of box plots. The American Statistician 32: 12-16.

Means, J. 1990. Mountain hemlock. In: Silvics of North America, Volume 1: Conifers. R.M. Burns and B.H. Honkala Technical Editors. Agricultural Handbook 271. U.S. Department of Agriculture, Forest Service. Washington, DC. Available via http://www.na.fs.fed.us/spfo/pubs/silvics_manual/table_of_contents.htm. Accessed 1 September, 2009.

Mencuccini, M., Piussi, P., Sulli, A.Z. 1995. Thirty years of seed production in a subalpine Norway spruce forest: patterns of temporal and spatial variation. Forest Ecology and Management 76: 109-125.

Mihai, B., Savulescu, I., and Sandric, I. 2007. Change detection (1986-2002) of the vegetation cover in Romania. Mountain Research and Development 27: 250-258.
Miller, E.A. and Halpern, C.B. 1998. Effects of environment and grazing disturbance on tree establishment in meadows of the central Cascade Range, Oregon, USA. Journal of Vegetation Science 9: 265-282.

Minchin, P.R. 1987. An evaluation of the relative robustness of techniques for ecological ordination. Vegatatio 69: 89-107.

Minore, D. 1979. Comparative autecological characteristics of northwestern tree species—a literature review. USDA For. Serv. Gen. Tech. Rep. PNW-87. 72 p.

Mizukami, N., and Perica, S. 2008. Spatiotemporal characteristics of snowpack density in the mountainous regions of the western United States. Journal of Hydrometeorology 9: 1416-1426.

Mote, P.W., 2003. Trends in snow water equivalent in the Pacific Northwest and their climatic causes. Geophysical Research Letter 30: 1-4.

Mote, P.W., Hamlet, A.F., Clark, M.P., and Lettenmaier, D.P. 2005. Declining mountain snowpack in western North American. Bulletin of the American Meterological Association 86: 39-49.

Mouer, M. and Stage, A.R. 1995. Most similar neighbor: an improved sampling inference procedure for natural resource planning. Forest Science 41: 337-359.

Nationwide Forest Imputation Study. 2010. Accessed online on February 22, 2010 at http://blue.for.msu.edu/NAFIS/index.html

Nielson , R.P. 1993. Transient Ecotone responses to climatic change: some conceptual and modeling approaches. Ecological Applications 3: 385-395.

Neter, J., Kutner, M.H., Nachtsheim, C.J., and Wasserman, W. 1996. Applied linear statistical models, 4th edition. WCB McGraw-Hill. Boston.

Nolan, A.W., and Daly, C. 2006. Mapping “at risk” snow in the Pacific Northwest. Journal of Hydrometeorology 7: 1164-1171.

North, M., Chen, J., Oakley, B., Song, B., Rudnicki, M., Gray, A., and Innes, J. 2004. Forest stand structure and patterns of old-growth western hemlock/douglas-fir and mixed conifer forests. Forest Science 50: 299-311.

O'Connor, J.E., and Costa, J.E. 1993. Geologic and hydrologic hazards in glacierized basins in North America reslting from 19th and 20th century global warming. Natural Hazards 8: 121-140.

O'Connor, J.E., Hardison, J.H. III, and Costa, J.E. 2001. Debris flows from failures of neoglacial-age moraine damns in the Three Sisters and Mount Jefferson Wilderness Areas, Oregon. U.S. Geoligcal Survey Profession Paper 1606.

Ohmann, J.L., and Gregory, M.J. 2002. Predictive mapping of forest composition and structure with direct gradient analysis and nearest-neighbor imputation in coastal Oregon, U.S.A. Canadian Journal of Forest Research 32: 725-741.

Ohmann, J.L., and Spies, T.A. 1998. Regional gradient analysis and spatial pattern of woody plant communities of Oregon forests. Ecological Monographs 68: 151-182.

Oke, T.R. 1987. Boundary layer climates. Methuen, London.

Oksanen, J., Kindt, R., Legendre, P., O'Hara, B., Simpson, G.L., Solymos, P., Stevens, M.H.H., and Wagner, H. 2008. vegan: Community ecology package. R package version 1.15-1. http://cran.r-project.org/

Oliver, C.D., and Larson, B.C. 1996. Forest stand dynamics. John Wiley & Sons, New York.

Oregon Tourist and Information Bureau. 1921. Oregon Skyline Trail: Mt. Hood to Crater Lake [map]. Scale not given. Portland, OR: Oregon Tourist and Information Bureau.

Orloci, L. 1978. Multivariate analysis in vegetation research 2nd ed. Dr. W. Junk B.V., The Hague

Owens, J.N., and Molder, M. 1977. Sexual reproduction of Abies amabilis. Canadian Journal of Botany 55: 2653-2667.

Pabst, R.J., and Spies, T.A. 2001. Ten years of vegetation succession on a debris-flow deposit in Oregon. Journal of the American Water Resources Association 37: 1693-1708.

Pabst, R.J., Goslin, M.N., Garman, S.L., and Spies, T.A. 2008. Calibrating and testing a gap model for simulating forest management in the Oregon Coast Range. Forest Ecology and Management 256: 958-972.

Pacala, S.W., Canham, C.D., Sapnara, J., Silander, J.A., Kobe, R.K., and Ribbens, E. 1996. Forest models defined by field measurements: Estimation, error analysis and dynamics. Ecological Monogrpahs 66: 1-43.

Packee, E.C., Oliver, C.D., and Crawford, P.D. 1981. Ecology of pacific silver fir. *In* Proceedings of the Biology and Management of True Fir in the Pacific Northwest Symposium. p. 19-34. C.D. Oliver and R.M. Kenady , eds. University of Washington, College of Forest Resources, U.S.D.A. Forest Service, Pacific Northwest Forest and Range Experiment Station (Seattle, WA, Portland, OR).

Peel, M.C., Finlayson, B.L., amd McMahon, T.A. 2007. Updated world map of the Köppen-Geiger climate classification. Hydrology and Earth System Sciences Discussions 4: 439-473.

Peterson, D.W., and Peterson, D.L. 1994. Effects of climate on radial growth of subalpine conifers in the North Cascade Mountains. Canadian Journal of Forest Research 34: 1921-1932.
Price, M.F. 1985. Impacts of recreational activities on alpine vegetation in western North America. Mountain Research and Development 5: 263-277.

Pierce, K.B., Lookingbill, T., and Urban, D. 2005. A simple method for estimating potential relative radiation (PRR) for landscape-scale vegetation analysis. Landscape Ecology 20: 137-147.

Price, D.T., Zimmerman, N.E., Van Der Meer, P.J., Lexer, M.J., Leadley, P., Jorritsma, I.T.M., Schaber, J., Clark, D.F., Lasch, P, McNulty, S., Wu, J., and Smith, B. 2001. Regeneration in gap models: Priority issues for studying forest responses to climate change. Climatic Change 51: 475-508.

Prichard, S.J., Peterson, D.L., Hammer, R.D. 2000. Carbon distribution in subalpine forests and meadows of the Olympic Mountains, Washington. Soil Science Society of America Journal 64: 1834-1845.

R Development Core Team. 2009. R: A language and environment for statistical computing. R Foundation for Statistical Computing. Vienna, Austria.

Rakestraw, L., Rakestraw, M. 1991. History of the Willamette National Forest. USDA Willamette National Forest, Eugene, OR.

Randall, D.A., Wood, R.A., Bony, S., Colman, R., Fichefet, T., Fyfe, J., Kattsov, V., Pitman, A., Shukla, J., Srinivasan, J., Stouffer, R.J., Sumi, A., and Taylor, K.E. 2007. Climate models and their evaluation. In: Climate Change 2007: The physical science Basis. Contributions of the Working Group I to the fourth assessment report of the Intergovernmental Panel on Climate Change. Solomon, S., Qin, D., Manning, M., Chen, Z., Marquis M., Averyt, K.B., Tignor, M, and Miller, H.L. (eds.) Cambridge University Press, United Kingdom and New York, NY, USA.

Randin, C.F., Engler, R., Normand, S., Zappa, M., Zimmerman, N., Pearman, P., Vittoz, P., Thuiller, W., and Guisan, A. 2009. Climate change and plant distribution: local models predict high-elevation persistence. Global Change Biology 15: 1557-1569.

Rehfeldt, G.E., Ferguson, D.E., and Crookston, N.L. 2009. Aspen, climate, and sudden decline in western USA. Forest Ecology and Management 258: 2353-2364.

Rochefort, M.R., and Peterson, D.L. 1996. Temporal and spatial distribution of trees in subalpine meadows of Mount Rainier National Park, Washington, U.S.A. Arctic and Alpine Research 28: 52-59.

Roland, J., and Matter, S.F. 2007. Encroaching forests decouple alpine butterfly population dynamics. Proceedings of the National Academy of Sciences of the United States of America. 104: 13702-13704.

Rudnicki, M., and Chen, J. 2000. Relations of climate and radial increment of western hemlock in an old-growth Douglas-fir forest in southern Washington. Northwest Science 74: 57-68.

Rupp, T.S., Chapin, S.T., and Starfield, A.M. 2000. Response of subarctic vegetation to transient climate change on the Seward Peninsula in north-west Alaska. Global Change Biology 6: 541-555.

SAS Institute Inc. 2008. SAS/STAT User’s Guide. Version 9.2. SAS Institute, Cary, NC.

Salathé, E.P., Steed, R., Mass, C.F., and Zahn, P.H. 2008. A high-resolution climate model of the U.S. Pacific Northwest: Mesoscale feedbacks and local responses to climate change. Journal of Climate 21: 5708-5726.

Salathé, E.P., L.R. Leung, Y. Qian, and Y. Zhang. 2009. Regional climate model projections for the State of Washington. Chapter 2 In: The Washington climate change impacts assessment: Evaluating Washington's future in a changing climate, Climate Impacts Group, University of Washington, Seattle, Washington.

Salzer, M.W., Hughes, M.K., Bunn, A.G., and Kipfmueller, K.F. 2009. Recent unprecedented tree-ring growth in bristlecone pine at the highest elevations and possible causes. Proceedings of the National Academy of Sciences of the United States of America 106: 20348-20353.

Schabenberger, O. 2007. Growing up fast: SAS 9.2 enhancements to the GLIMMIX procedure. SAS Global Forum. Paper 177-2007.

Scott, W.E. 1977. Quaternary glaciation and volcanism, Metolius river area, Oregon. Geological Society of America Bulletin 88: 113-124.

Scott, C.T., Bechtold, W.A., Reams, G.A., Smith, W.D., Westfall, J.A., Hansen, M.H., and Moisen, G.G. 2005. Sample-based estimators used by the forest inventory and analysis national information management system. *In:* Bechtold, W.A. and Patterson, P.L. (eds). The enhanced forest inventory and analysis program – National sampling design and estimation procedures. General Technical Report SRS-80, Southern Research Station, USDA Forest Service. Accessed on December 2, 2009 at http://www.treesearch.fs.fed.us/pubs/20371

Sicart, J.E., Pomeroy, J.W., Essery, R.L.H., Hardy, J., Link, T., and Marks, D. 2004. A sensitivity study of daytime net radiation during snowmelt to forest canopy and atmospheric conditions. Journal of Hydrometeorology 5: 774-784.

Smith, D.M., Larson, B.C., Kelty, M.J., and Ashton, P.M.S. 1997. The Practice of Silviculture: Applied forest ecology (9th edition). John Wiley and Sons, Inc. New York, NY, USA.

Smith, W.K., Germino, M.J., Hanocock, T.E., and Johnson, D.M. 2003. Another perspective on altitudinal limits of alpine timberlines. Tree Physiology 23: 1101-1112.

Solomon, A.M. and Kirilenko, A.P. 1997. Climate change and terrestrial biomass: What if the trees do not migrate. Global Ecology and Biogeochemical Letters 6: 139-148.

Spies, T.A., Franklin, J.F. 1991. The structure of natural young,mature, and old-growth Douglas-fir forests. In: Ruggiero, L.F., Aubry, K.B., Carey, A.B., Huff, M.H. (Eds.), Wildlife and Vegetation of Unmanaged Douglas-fir Forests. USDA Forest Service General Technical Report PNW-GTR-285, pp. 91–110.

Spot Image Corp 2008. Preprocessing levels and location accuracy. Accessed on September 14, 2008 at http://www.spotimage.com/web/en/224-technical-information.php

Steinger, T., Korner, C., and Schmid, B. 1996. Long-term persistence in a changing climate: DNA analysis suggests very old ages of clones of alpine *Carex curvula*. Oecologia 105: 94-99.

Stueve, K.M., Cerny, D.L., Rochefort, R.M., and Kurth, L.L. 2009. Post-fire tree establishment patterns at the alpine treeline Ecotone: Mount Rainer National Park, Washington, USA. Journal of Vegetation Sciences 20: 107-120.

ter Braak, C.J.F. 1986. Canonical correspondence analysis: a new eigenvector technique for multivariate direct gradient analysis. Ecology 67: 1167-1179.

ter Braak, C.J.F., and Prentice, I.C. 1988. A theory of gradient analysis. Advances in Ecological Research 18: 271-313.

Thuiller, W., Lavorel, S., Araujo, M.B., Sykes, M.T., and Prentice, I.C. 2005. Climate change threats to plant diversity in Europe. Proceedings of the National Academy of Sciences of the United States of America 102: 8245–8250.

Tolvanen, A., Forbes, B., Wall, S., and Norokorpi, Y. 2005. Recreation at treeline and interactions with other land-use activities. In: Wielgolaski, F.E., Karlsson, P.S., Neuvonene, S.S., and Thannheiser, D. (eds). Plant ecology, herbivory, and human impact in Nordic mountain birch forests. Ecological studies Vol. 180. Springer-Verlag, Berlin. 203-217.

Tomppo, E. 1991. Satellite image based national forest inventory of Finland. International Archives of Photogrammetry and Remote Sensing 28: 419-424.

Tomppo, E. 2006. The Finnish multi-source National Forest Inventory – small area estimation and map production. In: Kangas, A. & Maltamo, M. (eds.). Forest inventory. Methodology and applications. Managing Forest Ecosystems. Vol 10. Springer, Dordrecht. P. 195-224.

Tomppo, E., Olson, H., Ståhl, G., Nilsson, M., Hagner, O., and Katila, M. 2008. Combining national forest inventory field plots and remote sensing data for forest databases. Remote Sensing of Environment 112: 1982-1999.

Tranquillini, W. 1979. Physiological ecology of the alpine timberline: tree existence at high altitudes with special reference to the European Alps. Springer-Verlag, New York.
Troll, C. 1961. Klima und Pflanzenkleid der Erde in dreidimensionaler Sicht. Naturwissenschaften 9: 332-348.

Trujillo, E., Ramirez, J.A., and Elder, K.J. 2007. Topographic, meteorologic, and canopy controls on the scaling characterstics of the spatial distribution of snow depth fields. Water Resources Research 43: W07409: doi:10.1029/2006WR005317.

Turner, M.G., Baker, W.L., Peterson, C.J., and Peet, R.K. 1998. Factors influencing succession: lessons from large, infrequent natural disturbances. Ecosystems 1: 511-523.

Urban, D., Goslee, S., Pierce, K., and Lookingbill, T. 2002. Extending community ecology to landscapes. Ecoscience 9: 200-212

Vale, T.R. 1981. Tree invasion of montane meadows in Oregon. American Midland Naturalist 105: 61-69.

Vierling, K.T., Vierling, L.A., Gould, W.A., Martinuzzi, S., Clawges, R.M. 2008. Lidar: shedding new light on habitat characterization and modeling. Frontiers in Ecology and Environment 6: 90-98.

Vogelmann, J.E., S.M. Howard, L. Yang, C. R. Larson, B. K. Wylie, and J. N. Van Driel, 2001, Completion of the 1990's National Land Cover Data Set for the conterminous United States, Photogrammetric Engineering and Remote Sensing 67:650-662.

Walder, J.S., Gardner, C.A., Conrey, R.M., Fisher, B.J., Schilling, S.P. 1999. Volcano hazards in the Mount Jefferson region, Oregon. U.S. Geological Survey Open-File Report 99-24.

Wallentin, G., Tappeiner, U., Strobl, J., and Tasser, E. 2008. Understanding alpine tree line dynamics: an individual-based model. Ecological Modelling 218: 235-246.

Wardle, P, and Coleman, M.C. 1992. Evidence for rising upper limits of four native New Zealand forest trees. New Zealand Journal of Botany 30: 303-314.

Wiens, J.A. 1989. Spatial scaling in ecology. Functional Ecology 3: 385-397.

Williams, C.J., McNamara, J.P., and Chandler, D.G. 2009. Controls on the temporal and spatial variability of soil moisture in a mountainous landscape: the signature of snow and complex terrain. Hydrology and Earth Systems Sciences 13: 1325-1336.

Wilmking, M., Juday, G.P., Barber, V.A., Zald, H.S.J. 2004. Recent climate warming forces constrasting growth responses of white spruce at treeline in Alaska through temperature thresholds. Global Change Biology 10: 1724-1736.

Wilmking, M., Harden, J., and Tape, K. 2006. Effect of tree line advance on carbon storage in NW Alaska. Journal of Geophysical Research 111: G02023.1-G02023.10.

Wing, M.G., Karsky, R. 2006. Standard and real-time accuracy and reliability of a mapping-grade GPS in a coniferous western Oregon forest. Western Journal of Applied Forestry 21: 222-227.

Wimberly, M.C., and Spies, T.A. 2001. Modeling landscape patterns of understory tree regeneration in the Pacific Northwest, USA. Applied Vegetation Science 4: 277-286.

Wipf, S., Stoeckii, V., Bebi, P. 2009. Winter climate change in alpine tundra: plant responses to changes in snow depth and snowmelt timing. Climatic Change 94: 105-121.

Woodward, A., Schreiner, E.G., and Silsbee, D.G. 1995. Climate, geography, and tree establishment in subalpine meadows of the Olympic Mountains, Washington, U.S.A. Arctic and Alpine Research 27:217-225.

Woodward, F.I., and Beerling, D.J. 1997. The dynamics of vegetation change: Health warnings for equilibrium ‘dodo’ models. Global Ecology and Biogeography Letters 6: 413-418.

Yamaguchi, D.K. 1991. A simple method for cross-dating increment cores from living trees. Canadian Journal of Forest Research 21: 414-416.

Yarie, J., Viereck, L., Van Cleve, K., and Adams, P. 1998. Flooding and ecosystem dynamics along the Tanana river. Bioscience. 48: 690-695.

Yost, A.C. 2008. Probabilistic modeling and mapping of plant indicator species in a Northeast Oregon industrial forest, USA. Ecological Indicators 8: 46-56.

Zald, H. 2008. Extent and spatial patterns of grass bald land cover change (1948 – 2000), Oregon Coast Range, USA. Plant Ecology 201: 517-529

Zald, H.S.J. 2010a. Integrating LiDAR, satellite imagery, and forest inventory data to spatially characterize tree invasion, vegetation composition, and vegetation structure in a subalpine meadow landscape, Oregon Cascades, USA. In: Patterns of Tree Establishment and Vegetation Composition in a Subalpine Meadow Landscape, Jefferson Park, Oregon, USA. Ph.D. Dissertation, Oregon State University, Corvallis, OR.

Zald, H.S.J. 2010b. Seedling establishment in a subalpine parkland landscape controlled by interactions of topography, seed source, disturbance and climate, oregon cascades, USA. In: Patterns of Tree Establishment and Vegetation Composition in a Subalpine Meadow Landscape, Jefferson Park, Oregon, USA. Ph.D. Dissertation, Oregon State University, Corvallis, OR.

Zimble, D.A., Evans, D.L., Carlson, G.C., Parker, R.C., Grado, S.C., and Gerard, P.D. 2003. Characterizing vertical forest structure using small-footprint airborne LiDAR. Remote Sensing of Environment 87: 171-182.

Zuller, D., Jeltsch, F., Dormann, C.F., and Schröder, B. 2009. Static species distribution models in dynamically changing systems: how good can predictions really be? Ecography 32: 1-12.

APPENDIX A. VEGETATION GROUP CLASSIFICATION

VEGETATION DATA AND STATISTICAL ANALYSES

Vegetation data was collected on 98 plots as percent cover by species. Species cover data was only collected on vascular plants. Excluding tree species, 58 species were identified and assigned cover values. 11 species were found only in one plot each, and did not exceed one percent cover individually. These 11 species were excluded from the dataset, leaving 47 species for analysis. The development of vegetation types was accomplished by: 1) conducting a cluster analysis of the 47 species in 98 plots which assigned plots to groups, 2) assessing species within group agreement to groups assigned by cluster analysis to determine the most parsimonious number of vegetation groups, and 3) quantifying and assessing significance of species associated with each vegetation type. All analyses were conducted using PC-ORD version 5 (McCune and Mefford 1999).

Agglomerative cluster analysis was conducted on species percent cover values in plots using Euclidean distance measures and Ward's linkage method. Chaining was minimal at 3.6%, and the dendrogram of plots in species space shows a primary split of sedge meadow plots, followed by an additional split between forb and shrub dominated plots.

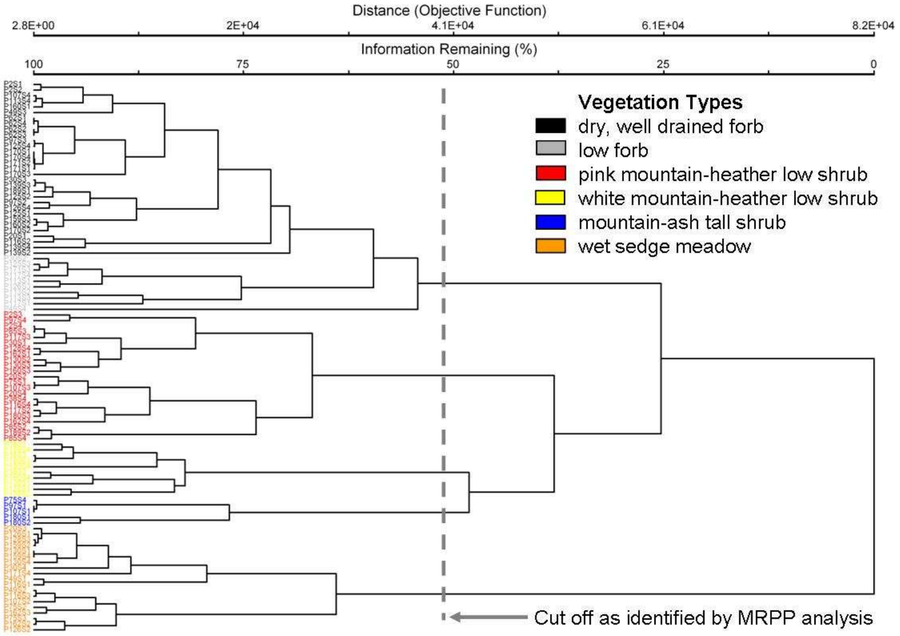

Dendrogram of plots in species space. Plots are color coded by species groups as defined by multi-response permutation procedures (MRPP), and Indicator species Analysis (ISA).

To determine the most parsimonious number of vegetation types, two to 97 groups were generated as identified by the cluster analysis, and species agreement within these groups assessed using Multi-response permutation procedures (MRPP). MRPP was run using Euclidean distance and natural weighting. The significance (p-value), chance-corrected within group agreement (A statistic), and improvement in A statistic with an additional group (Delta A) were calculated for clusters with two to 15 groups. Results are presented for only 2 – 15 groups since all numbers of groups were statistically significant ($p \leq 0.0001$) and chance-corrected within group agreement leveled out at approximately 10 groups (see figures below). The most parsimonious number of groups was defined as the fewest number of groups with the lowest improvement in agreement with the addition of that group. Six groups were selected, with a chance-corrected within group agreement of 0.37 ($p \leq 0.0001$).

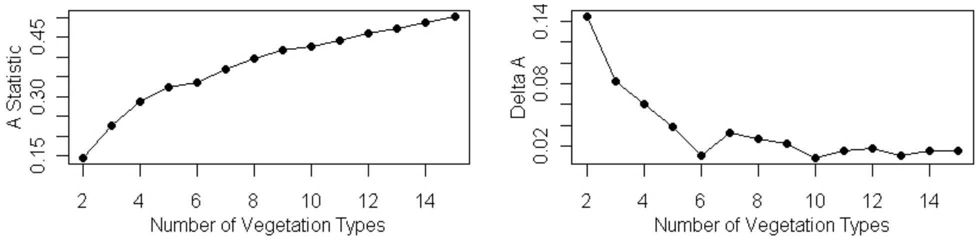

Chance corrected within group agreement (A statistic) and Delta A in relation to the number of groups generated in cluster analyses.

Indicator Species Analysis (ISA) was used to quantify and assign significance to species in association with the six vegetation groups (Dufrene and Legendre 1997). ISA uses species percent cover in each plot and the a priori groups of plots seen in the dendrogram as selected by the MRPP analysis. ISA is implemented in five steps: 1) the proportional abundance of each species in each vegetation group is calculated relative to each species abundance in all groups, 2) the proportional frequency of each species is calculated for each group, 3) proportional abundance and proportional frequency are multiplied, resulting in an indicator value (IV), which can be high only if a species is both commonly present in a group and has high relative abundance within that group, 4) the highest indicator value (IV_{max}) from each species across groups is saved, and 5) the statistical significance of IV_{max} is evaluated by a Monte Carlo approach with 4999 randomizations.

Indicator and significance values are presented in the table below. Gray shaded values in the table are the highest indictor value by group for species of at least suggestive importance ($p \leq 0.1$). Indicator values were considered significance if $p \leq 0.05$. Important species on well drained sites (Group 1) included: *Arenaria capillaris*, *Lupinus arcticus*, *Eriogonum umbellatum,* and *Polygonum newberyi*. Important species in the pink mountain-heather type (Group 2) are *Phyllodoce empetriformis*, *Luetkia pectinata*, and *Lycopodium sitchensis*. The wet sedge meadow type (Group 3) had high indicator values for *Carex nigricans* and *Juncus drummondi*. Species with high indicator values in the low forb type (Group 4) included: *Aster alpiginus*, *Castelija parviflora*, *Festuca sp.*, *Gentian calycosa*, and *Kalmia microphylla*. In the white mountain-heather type (Group 5), *Cassiope mertensiana* and *Microseris alpestris* had high indicator values. The mountain-ash tall shrub type (Group 6) has high IVs for *Sorbus sitchensis*, *Rubus lasiococcus*, *Vaccinium deliciosum*, *Ligustrum gracilis*, *Epibolium alpinum*, *Dodecatheon jeffreyi*, and *Veratrum viride*.

Indicator values of species by vegetation groups, observed and randomized indicator values by species, and p values from randomization procedures. Gray boxes associated with significant indicator species and the vegetation group in which they have the highest indicator value.

		Indicator Value by Vegetation Group						Observed Indicator Value (IV)	IV from randomized groups		
		1	2	3	4	5	6		Mean	SD	P*
Species	N Plots	31	23	19	9	10	5				
ANAL		19	1	3	7	0	0	18.8	14.7	7.25	0.2024
ARCA		33	0	0	0	1	0	32.9	10.7	5.41	0.0058*
ASAL		4	8	19	59	2	5	58.5	25.4	5.35	0.0002*
ASFO		6	0	0	0	0	0	6.5	7	4.78	0.4293
CAAQ		2	1	3	0	0	1	3.4	12.7	7.13	0.9836
CALE		3	0	5	0	0	0	5.2	8.8	5.61	0.7532
CAME		1	27	3	6	56	1	55.8	21.8	5.04	0.0002*
CANI		3	5	59	16	2	14	58.6	24.7	4.43	0.0002*
CAPA		5	21	13	33	2	3	33.2	18.6	3.91	0.0036*
CASP		16	3	28	12	1	4	28.5	23.3	7.52	0.1998
DOJE		1	0	1	9	0	30	30.1	15.2	7.57	0.0598
EPAL		0	1	6	4	0	20	20.2	9.7	5.5	0.0514
EPAN		1	0	3	0	0	0	3.3	7	4.63	0.7483
ERUM		16	0	0	0	0	0	16.1	8.1	5.24	0.0528
FESTU		2	0	0	47	0	0	47	9.3	5.55	0.001*
GECA		0	4	5	54	2	2	53.6	14.9	5.6	0.0004*
HIGR		5	19	16	4	14	2	18.8	17.4	4.45	0.3015
HYAN		0	0	5	0	0	0	5.3	6.3	4.28	0.4459
JUDR		19	10	39	0	2	0	38.6	19.7	5.88	0.0146*
JUME		6	0	6	1	0	0	6.3	8.9	5.48	0.6989
KAMI		3	18	4	32	0	0	32.3	16.3	6.75	0.0316*
LIGR		3	9	2	5	6	60	59.5	21	6.92	0.0014*
LUAR		42	0	0	1	0	0	42.1	12.6	6.54	0.005*
LUPE		6	35	13	3	26	9	35.4	23	4.28	0.0158*
LUZUL		1	0	7	0	0	0	6.5	7.4	4.83	0.4629
LYSI		0	29	4	6	14	0	29.2	17.1	7.08	0.0668
MIAL		0	0	0	0	20	0	19.5	10.8	6.48	0.073
MIBO		3	0	2	0	5	0	5	8.4	5.34	0.7101
PEBR		1	0	0	6	0	0	6.4	6.8	4.68	0.4969
PHEM		7	47	15	20	4	4	46.9	22.1	3.43	0.0002*
PLST		0	0	5	0	0	0	5.3	6.3	4.28	0.4459
POA		5	0	4	2	0	0	4.9	8.8	5.22	0.7884
POFL		3	0	11	1	0	4	10.8	9.7	5.84	0.2805
PONE		26	0	0	0	0	0	25.8	9.2	5.73	0.026*
RHAL		0	0	0	0	7	6	7	7.6	4.98	0.4621
RULA		0	0	0	0	0	17	17.2	7	4.64	0.0542
SAFE		14	1	1	0	0	0	13.8	9.1	5.47	0.1466
SACO		6	0	0	0	0	0	6.5	6.9	4.52	0.6049
SATO		13	1	0	0	0	0	12.7	8.3	5.4	0.1462
SETR		1	0	2	0	0	7	7.4	7.5	4.93	0.3651
SOSI		5	2	0	0	14	61	60.7	17	6.29	0.0002*
TOGL		0	0	5	0	0	0	5.3	6.3	4.28	0.4459
VADE		4	12	5	3	21	52	52.1	22.4	4.12	0.0002*
VAME		13	3	0	0	14	7	14.3	15.4	7.12	0.4537
VEVI		1	0	0	0	0	18	18.1	7.4	4.72	0.0338*
VEWO		0	0	5	0	0	0	5.3	6.3	4.28	0.4459
XETE		6	0	0	2	0	0	5.6	7.6	4.86	0.6635

*Indicator values considered significance if p ≤ 0.05. P values are the proportion of randomized trials with indicator value equal to or exceeding the observed indicator value.